

**Compound-specific isotope analysis to delineate  
the sources and fate of organic contaminants  
in complex aquifer systems**

Dissertation

zur Erlangung des Grades eines Doktors der Naturwissenschaften

der Geowissenschaftlichen Fakultät  
der Eberhard Karls Universität Tübingen

vorgelegt von  
Michaela Blessing  
aus Schwäbisch Gmünd

2008

Tag der mündlichen Prüfung: 08. August 2008

Dekan: Prof. Dr. Peter Grathwohl

1. Berichterstatter: Prof. Dr. Stefan Haderlein

2. Berichterstatter: Prof. Dr. Torsten Schmidt

Hiermit versichere ich, dass ich die vorliegende Arbeit selbständig verfasst, keine anderen als die angegebenen Quellen und Hilfsmittel benutzt und wörtlich oder inhaltlich übernommene Stellen als solche gekennzeichnet habe.

## Danksagung

Mein besonderer Dank gilt meinen Betreuern Torsten Schmidt und Stefan Haderlein für hilfreiche Diskussionen und konstruktive Kritik in allen Phasen meiner Arbeit. Danke für Rat und Tat, Motivation, organisatorische sowie finanzielle Unterstützung.

Bei den Mitarbeitern im ZAG, vor allem im Labor möchte ich mich für die angenehme Arbeitsatmosphäre und Hilfestellung bedanken. Ganz besonders möchte ich Maik hervorheben, der entscheidenden Anteil daran hatte, dass ich die Arbeit im Labor nicht gleich aufgegeben habe und der es geschafft hat, doch tatsächlich noch einen Mechaniker aus mir zu machen. Für besonders viel Spaß während der gemeinsamen Arbeit in Labor und Büro möchte ich Anke lobenswert erwähnen, Thomas für unzählige He-Flaschenwechsel, Bernd und Heiner für die EA/IRMS-Messungen, Erping und Satoshi für ihre Hilfe und Expertise bei den Sorptionsexperimenten, meinem Hiwi Lunliang für die Aufreinigung der Bodenextrakte, meinen beiden AEG-Studentinnen Oxana und Kathryn für ihre engagierte Arbeit zum einen an Sorptionsversuchen und zum anderen bei der reaktiven Transportmodellierung, deren Masterarbeiten einen wertvollen Beitrag geleistet haben.

Ferner möchte ich mich bei allen Projektpartnern für die gute Zusammenarbeit bei der Bearbeitung der kontaminierten Standorte bedanken, insbesondere bei Rainer Dinkel und Christian Kiffer von der UW Umweltwirtschaft GmbH, Anita Peter und Eugen Martac vom Tübinger Grundwasserforschungsinstitut, sowie den Herren Ufrecht, Wolff und Carle vom Amt für Umweltschutz der Stadt Stuttgart.

Nicht zuletzt bedanke ich mich bei der Deutschen Bundesstiftung Umwelt für die finanzielle Unterstützung sowie für die Organisation von abwechslungsreichen Stipendiatenseminaren und -veranstaltungen an ausgesprochen schönen Orten.

Guido, danke dafür, dass Du mich mit deiner stoischen Ruhe immer wieder schnell aus dem Wahnsinn zurückgeholt hast – auch mit der Anschaffung der zwei kleinen, gemütlichen Kater gleich zu Beginn meiner Promotionsphase hast Du einen wertvollen Beitrag geleistet.

Bei allen ehemaligen und aktuellen Leidensgenossen, insbesondere Anke, Florian, Iris, Katja, Katharina, Kerstin, Lihua, Maik, Michael, Nicole, Safi und Satoshi für die nötige Abwechslung zwischendurch. Die Abende mit den Ehemaligen vermisse ich bereits seit geraumer Zeit, alle anderen erholsamen und lustigen Freizeitaktivitäten mit Euch Aktuellen werde ich in Zukunft bestimmt schwer vermissen...

---

## **Compound-specific isotope analysis to delineate the sources and fate of organic contaminants in complex aquifer systems**

### **Abstract**

The extensive use of organic compounds has frequently caused soil and groundwater contamination. Volatile organic compounds, such as chlorinated and aromatic hydrocarbons and the semi-volatile polycyclic aromatic hydrocarbons are among the most widespread organic pollutants. The fate and behavior of such compounds in the subsurface depend on a number of physicochemical and biological processes, which may lead to 'natural attenuation'. For the consideration of these in-situ contaminant-reducing processes as a valid remedial approach, it is necessary to attain an appropriate understanding of the key processes occurring in natural aquifers. Compound-specific isotope analysis (CSIA) with on-line gas chromatography-isotope ratio mass spectrometry (GC/IRMS) offers a versatile tool for the characterization of origin and fate of organic contaminants in environmental analytical chemistry.

The aim of the present work was to evaluate and demonstrate the potential and limitations of CSIA for studying sources and fate of organic contaminants at heterogeneous and complex aquifer systems. One major drawback in the application of CSIA to field studies, is that current GC/IRMS systems are limited in their sensitivity. To overcome this limitation and to enhance method detection limits, various sample extraction and injection techniques were optimized and validated for their use in CSIA field studies. For volatile compounds, a commercially available purge-and-trap sample extractor has been technically improved to meet the specific requirements at real sites. The results obtained demonstrate the good performance of the sample preconcentration and extraction techniques applied for the compound-specific carbon isotope analysis of volatile compounds at trace concentrations. Applied to different field sites, the techniques helped to assess the potential for biodegradation according to the Rayleigh-equation. A new analytical approach, based on the injection of large sample volumes (large-volume injection, LVI) of organic extracts into a programmable temperature vaporizer (PTV) injector, has been developed and validated for the determination of compound-specific carbon isotope ratios. The PTV-LVI method was thoroughly optimized in terms of its accuracy, precision, linearity, reproducibility and limits of detection. It was shown that the technique allows to determine accurately and precisely  $\delta^{13}\text{C}$  values of semi-volatile organic contaminants at low

concentrations (1-3  $\mu\text{g/L}$  for aqueous or 10-20  $\mu\text{g/kg}$  for soil samples) and thus expands the applicability of CSIA considerably in environmental applications. The applicability of the method was verified for  $\delta^{13}\text{C}$  determination of individual PAHs and exemplified by a source apportionment study at a creosote-contaminated site.

So far, most field applications of CSIA have been limited to fairly homogeneous aquifers. To evaluate the applicability of the CSIA concept for studying the source and fate of organic contaminants and to quantify the rate of in-situ degradation in contaminant plumes even at highly complex conditions, extensive site investigations were performed at an urban, heterogeneous bedrock aquifer system. The study highlights the potential of using  $\delta^{13}\text{C}$  values of chlorinated hydrocarbons (tetrachloroethene and its transformation products) as a tracer for discriminating different contaminant sources even in the presence of biodegradation. It was shown that careful statistical evaluation and interpretation of highly precise compound specific isotope signatures, geochemical data and site-specific additional information may allow for a comprehensive site assessment under complex boundary conditions. In addition, for a plume in the southern part of this site, a reactive transport model-based analysis of concentration and isotope data was carried out to assess natural attenuation of the chlorinated ethenes in this part of the aquifer. The results provided strong evidence for the occurrence of aerobic TCE and DCE degradation. As PCE is recalcitrant at aerobic conditions, it could be used as a conservative tracer to estimate the extent of dilution. The dilution-corrected concentrations together with stable carbon isotope data allowed for the reliable assessment of the extent of *in-situ* biodegradation at the site. Finally, limitations of CSIA under natural field conditions and potential analytical pitfalls of the method are critically discussed and strategies to avoid possible sources of error are provided. The results of this work exemplify how CSIA can contribute for a reliable assessment of contaminated sites, even at complex contamination scenarios. Moreover, future work will significantly benefit from the method developments attained in this study.

# **Komponentenspezifische Isotopenanalyse zur Aufklärung der Herkunft und des Verbleibs von organischen Schadstoffen in komplexen Grundwasserleitern**

## **Kurzfassung**

Auf intensiv genutzten Industriestandorten kommt es oft zu einer hohen organischen Schadstoffbelastung in Grundwasser und Böden. Die flüchtigen chlorierten und aromatischen Kohlenwasserstoffverbindungen, sowie polyzyklische aromatische Kohlenwasserstoffe (PAK), gehören dabei zu den am häufigsten nachgewiesenen organischen Schadstoffen an kontaminierten Standorten. Physikalisch-chemische und biologische Abbau- und Rückhalteprozesse in der gesättigten und ungesättigten Bodenzone können dabei die Ausbreitung der Schadstoffe verlangsamen und unter günstigen Bedingungen zu einer Begrenzung der Schadstofffahne führen („Natural Attenuation“). *In-situ* Prozesse, die zu einer tatsächlichen Minimierung der Schadstofffrachten führen, stellen dabei eine alternative Sanierungsstrategie dar, deren Anwendung allerdings ein gutes Prozessverständnis des Transport- und Abbauverhaltens der Schadstoffe im Untergrund voraussetzen. Die substanzspezifische Isotopenanalyse (CSIA) mittels gekoppelter Gaschromatographie-Isotopenverhältnis-Massenspektrometrie (GC/IRMS) stellt in der Umweltanalytik eine wertvolle Methode dar, um solche Aussagen über die Herkunft und den Verbleib von organischen Schadstoffen zu ermöglichen.

Ziel der vorliegenden Arbeit war das Aufzeigen des Potentials und Grenzen der CSIA bei der Untersuchung der Herkunft und des Verbleibs von Schadstoffen an heterogenen und komplexen Feldstandorten. Die begrenzte Empfindlichkeit derzeitiger GC/IRMS-Systeme ist häufig der limitierende Faktor beim Einsatz der CSIA in Feldstudien. Um die Empfindlichkeit zu steigern im Sinne verbesserter Nachweisgrenzen, wurden verschiedene Probenextraktions- und Probenaufgabetechniken optimiert und für den Einsatz in der CSIA evaluiert. Für eine effizientere Extraktion flüchtiger Verbindungen konnte ein kommerziell erhältliches Purge&Trap-System im Rahmen dieser Arbeit für die speziellen Anforderungen optimiert werden. Die erhaltenen Ergebnisse zeigen, dass die hier eingesetzten Probenanreicherungs- und Extraktionstechniken effizient und zuverlässig in der substanzspezifischen Isotopenanalytik angewendet werden können. In den durchgeführten Studien konnte damit an unterschiedlichen Feldstandorten das biologische Abbaupotential anhand der Rayleigh-Gleichung abgeschätzt

werden. Für weniger flüchtige Verbindungen (z.B. PAK) wurde eine neue Methode evaluiert: PTV-LVI. Diese Technik basiert auf der Injektion größerer Probenmengen (large-volume injection; LVI) in einen speziellen, temperatursteuerbaren Injektor (PTV-Injektor). Für ihre Anwendung in der Isotopenanalytik wurde diese neue Technik auf Genauigkeit, Linearität, Präzision und Reproduzierbarkeit untersucht, sowie die methodenspezifische Nachweisgrenze ermittelt. Diese Injektionstechnik (PTV-LVI) ermöglicht jetzt auch für die bisher problematischen mittelflüchtigen organischen Verbindungen verlässliche  $\delta^{13}\text{C}$ -Bestimmungen im Spurenkonzentrationsbereich (1-3  $\mu\text{g/L}$  für wässrige Proben, bzw. 10-20  $\mu\text{g/kg}$ -Bereich für Bodenproben) und erweitert damit das mögliche Anwendungsspektrum der CSIA-Methode in der Umweltanalytik erheblich, wie am Beispiel eines Kreosot-kontaminierten Standorts gezeigt wird. Da bislang die Feldanwendung der CSIA auf relativ homogene Aquifer-Systeme beschränkt war, lag der Anwendungsschwerpunkt der Methoden auf Feldstandorten mit komplexen Bedingungen und Kontaminationsgeschichte. Dabei konnte gezeigt werden, dass die über CSIA ermittelten  $\delta^{13}\text{C}$  Werte von chlorierten Kohlenwasserstoffen, in diesem Fall Tetrachlorethen und seinen Abbauprodukten, zur Identifizierung von potentiellen Verursachern (Kontaminationsquellen) herangezogen werden können, auch wenn Bioabbau eine Rolle spielt. In einem komplexen Realfall können, wie in der Arbeit am Beispiel eines geklüfteten Festgesteinsaquifer dargelegt,  $\delta^{13}\text{C}$  Werte zusammen mit geochemischen und anderen standortspezifischen Informationen zuverlässig und mit hoher statistischer Aussagekraft interpretiert werden. In einer Schadstofffahne im südlichen Bereich des Standorts wurde zudem, durch die Integration der gemessenen Konzentrations- und Isotopendaten in ein reaktives Transportmodell, das NA-Potential in diesem Teil des Aquifers quantitativ erfasst. Die Resultate zeigen den biologischen Abbau von Tri- und *cis*-1,2-Dichlorethen unter aeroben Bedingung am Standort an. Tetrachlorethen wird unter aeroben Bedingungen nicht abgebaut, und kann daher als konservativer Tracer zur Abschätzung des Verdünnungsgrades dienen. Die um den so erhaltenen Verdünnungsfaktor korrigierten Konzentrationen ließen in Zusammenhang mit den Isotopendaten dann eine zuverlässige Abschätzung des Bioabbaus vor Ort zu. Ausgehend von den Ergebnissen der im Rahmen dieser Arbeit bearbeiteten Standorte werden die Beschränkungen und potentielle Fallgruben der CSIA unter Realbedingungen kritisch diskutiert und Strategien vorgeschlagen, mögliche Fehlerquellen zu vermeiden. Insgesamt verdeutlichen die hier erzielten Ergebnisse, wie CSIA-Methoden zu einer erfolgreichen Standortuntersuchung, auch für komplexe Schadensfälle, beitragen können. Zudem werden künftige Untersuchungen einen hohen Nutzen aus den hier verbesserten Methoden ziehen können.



---

## Content

Eidesstattliche Erklärung .....	iii
Danksagung .....	iv
Abstract .....	v
Kurzfassung .....	vii
Content .....	ix
1. General Introduction .....	1
1.1. Contaminated Site Evaluation and Management .....	1
1.2. Compound-Specific Isotope Ratio Analyses and Terminology .....	2
1.3. CSIA Applications in Environmental Analytical Chemistry .....	3
1.4. Physical Processes Controlling the Extent of Isotope Fractionation.....	5
1.5. Scope of the Present Study.....	8
1.6. References .....	9
2. Compound-Specific Isotope Analysis of Volatile Organic Compounds (VOCs) at Trace Levels .....	12
2.1. Introduction .....	12
2.2. Materials and Methods .....	14
2.3. Description of Field Sites .....	16
2.4. Results .....	18
2.4.1. P&T-analysis with enhanced purge volume and PEEK sample loop .....	18
2.4.2. Comparison of accuracy and reproducibility .....	21
2.4.3. Application to environmental field studies .....	22
2.5. References .....	29
2.6. Appendix .....	31
3. Semi-Volatile Contaminants at Trace Concentrations: Evaluation of a Large Volume Injection – GC/IRMS-Method .....	34
3.1. Introduction .....	34
3.2. Experimental Section .....	36
3.3. Results and Discussion.....	38
3.4. Conclusions .....	49
3.5. References .....	50
3.6. Appendix .....	53

---

4. Analytical Problems and Limitations in Compound-Specific Isotope Analysis of Environmental Samples.....	54
4.1. Introduction .....	54
4.2. Groundwater Sampling .....	55
4.3. Sensitivity and Linearity of CSIA.....	58
4.4. Problems Related to Chromatographic Resolution .....	64
4.5. CSIA of Non-Volatile Compounds.....	67
4.6. Uncertainties of Data Interpretation.....	68
4.7. References .....	69
5. Delineation of Multiple Chlorinated Ethene Sources in an Industrialized Area.....	73
5.1. Introduction .....	73
5.2. Material and Methods.....	74
5.3. Results and Discussion.....	77
5.4. References .....	87
5.5. Appendix .....	89
6. Quantitative Assessment of Aerobic Biodegradation of Chlorinated Ethenes in a Fractured Bedrock Aquifer.....	95
6.1. Introduction .....	95
6.2. Material and Methods.....	97
6.3. Results and Discussion.....	100
6.4. References .....	109
6.5. Appendix .....	111
7. General Conclusions and Outlook.....	117
List of Figures and Tables .....	120
List of Abbreviations .....	125
Curriculum Vitae .....	127

## 1. General Introduction

### 1.1. Contaminated Site Evaluation and Management

Organic contaminants deriving from industry, oil spills, improper disposal and/or leaking storage tanks, landfill leachates, household use, motor vehicle emissions as well as agricultural fertilizers and pesticides may pose a severe threat to soil and groundwater. Chlorinated solvents, polycyclic- and mono-aromatic hydrocarbons are among the most widespread environmental pollutants. Due to their toxic and carcinogenic potential they are of common concern (1). A variety of naturally occurring biological, chemical, and physical processes are capable to reduce the contaminant concentration in soil and groundwater over time. These self-induced *in-situ* processes are termed 'natural attenuation' (NA) and can be classified due to their either destructive or nondestructive nature. While biotic and abiotic degradation processes destroy or transform the compounds in general to minimize associated environmental risks, physical attenuation mechanisms including dispersion, diffusion, sorption, and volatilization only influence the transport of contaminants in groundwater. The consideration of these NA-processes in contaminated site management is defined by the US-EPA directive on monitored natural attenuation (MNA) as the 'reliance on natural attenuation processes – within the context of a carefully controlled and monitored site cleanup approach – to achieve site-specific remediation objectives within a time frame that is reasonable compared to that offered by other, more active methods' (2). For the concept of MNA to become a generally accepted remediation approach it is necessary to develop a mechanistic understanding of the key subsurface processes occurring in natural aquifers.

Approaches of determining the extent of *in-situ* degradation include indicators for microbial activity such as contaminant and electron acceptor concentrations supported by other geochemical parameters, concentrations of specific metabolites, and microbiological methods. However, conclusive evidence of *in-situ* degradation by traditional mass balance approaches are intricate, as other, nondestructive, processes can also reduce the contaminant concentration in the field and the detection of metabolites is often difficult. Hence, especially under complex site conditions, such measurements provide only limited or ambiguous data for the estimation of degradation rates (3,4). Microbiological techniques such as microcosm studies or molecular microbiology provide a direct evidence of microbial diversity in the field and are powerful qualitative tools for demonstrating degradation processes. However, the methods are straightforward to apply and interpret on homogeneous systems; in fact, physical and

geochemical heterogeneities within the aquifer may hamper the interpretation and extrapolation of laboratory-based biodegradation rates to the field scale situation (5). In some cases, microbiological assays might be misleading because only a subset of microbes are grown on the typical laboratory media and the real site conditions may not be reflected by laboratory-based parameters. Moreover, not the mere existence of microorganisms but rather the proof of their degradative activities is important, which requires molecular techniques that allow the determination of specific degradative enzymes (6). In the field of contaminant hydrology the analysis of stable isotope signatures of individual contaminants has gained raising attention as an approach to assess *in-situ* degradation of organic pollutants in aquifer systems. Within the past decade compound-specific isotope analysis (CSIA) with on-line gas chromatography-isotope ratio mass spectrometry (GC/IRMS) evolved as valuable tool for the characterization of origin and fate of organic contaminants in environmental analytical chemistry (7,8).

### 1.2. Compound-Specific Isotope Ratio Analyses and Terminology

**GC/IRMS System.** Analytical improvements of coupling gas chromatography (GC) to isotope ratio mass spectrometry (IRMS) in the early 90ies allowed to directly measure the isotope ratios of individual compounds of contaminant mixtures (9). In case of carbon isotope ratio measurements, the compounds eluting from the GC capillary are individually combusted to CO<sub>2</sub> and H<sub>2</sub>O in a combustion unit (CuO/NiO/Pt-oxidation reactor) operated at 940 °C. H<sub>2</sub>O is trapped within the interface unit on a Nafion membrane. Nitrogen oxides, that might result from the combustion can be reduced to N<sub>2</sub> in a reduction furnace maintained at 650 °C. CO<sub>2</sub> is then transferred (via open-split) to the IRMS where the ions with the different masses of CO<sub>2</sub> (*m/z* 44, 45 and 46) are continuously monitored on fixed collectors (Principle shown in Figure 1-1).

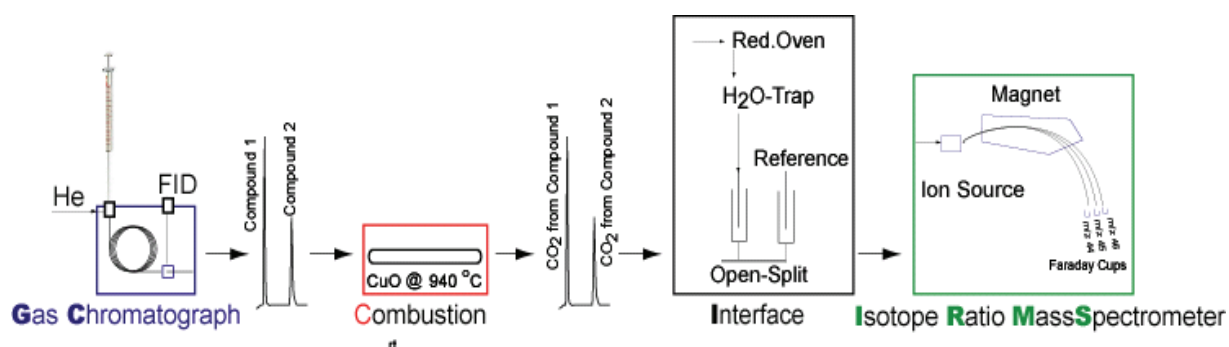


**Figure 1-1.** Set-up of GC/IRMS system for the determination of carbon isotope ratios of individual compounds, figure taken from Schmidt et al. (8).

**Terminology.** Stable carbon isotope analysis involves measurement of the two stable isotopes of carbon,  $^{12}\text{C}$  and  $^{13}\text{C}$ . Isotopic compositions are reported in per mill deviation (‰) relative to an international standard using the conventional  $\delta$ -notation ( $\delta^{13}\text{C}$ ):

$$\delta^{13}\text{C} = (R_{\text{sample}} / R_{\text{standard}} - 1) \times 1000$$

where  $R_{\text{sample}}$  and  $R_{\text{standard}}$  are the ratios of the heavy isotope to the light isotope ( $^{13}\text{C}/^{12}\text{C}$ ) of a compound and of the international standard. The standard reference material for carbon isotope analyses is VPDB (10). The relative changes in isotope signatures are expressed with the fractionation factor  $\alpha$ , defined as:

$$\alpha = R_{\text{product}}/R_{\text{reactant}}$$

For carbon isotope ratios  $R$  represents the ratio of the heavy to the light isotope ( $^{13}\text{C}/^{12}\text{C}$ ). Values of  $\alpha$  are derived from experimental results by using the simple form of the Rayleigh equation after Mariotti et al. (11):

$$R_t/R_0 = (C_t/C_0)^{(\alpha-1)} = f^{(\alpha-1)}$$

where  $\alpha$  is the isotope fractionation factor,  $R_t$  and  $R_0$  are the isotope ratios ( $^{13}\text{C}/^{12}\text{C}$ ) of the residual contaminant and the initial, unreacted compound, respectively and  $C_t/C_0$  is the fraction ( $f$ ) of compound remaining at time  $t$ . In the literature isotope changes are commonly expressed as the enrichment factor  $\epsilon$ , which can be easily rearranged using the equation  $\epsilon = (\alpha-1) \times 1000$ .

By substituting the Rayleigh equation, where  $R_t$  and  $R_0$  are the isotope ratios ( $^{13}\text{C}/^{12}\text{C}$ ) of the residual contaminant and the initial isotopic composition of the source, respectively, the percentage of biodegradation ( $B$ ) can be calculated:

$$R_t/R_0 = C_t/C_0^{(\alpha-1)} \quad \text{or} \quad R_t/R_0 = f^{(\alpha-1)}$$

$$\ln R_t/R_0 = \ln f^{(\alpha-1)}$$

$$f = \exp(\ln(\delta^{13}\text{C}_t/1000+1)/(\delta^{13}\text{C}_0/1000+1) / (\alpha-1))$$

$$B = (1-f) \times 100 \quad (\text{in } \%)$$

### **1.3. CSIA Applications in Environmental Analytical Chemistry**

The application of stable isotope analysis to evaluate and quantify intrinsic degradation relies on the fact that chemical and microbial transformation reactions are frequently associated with a shift in the isotopic composition of the compound being degraded (12-16). This kinetic isotope fractionation effect occurs since bonds formed by the lighter isotopes of an element (e.g.  $^{12}\text{C}$ - $^{12}\text{C}$ ) react faster than bonds formed by the heavy isotopes (e.g.  $^{12}\text{C}$ - $^{13}\text{C}$  bonds). As a consequence, the

lighter isotopologues are preferentially degraded, leading to a change in the isotopic composition of the parent compound and the product (17). The preferential degradation of molecules containing light isotopes, leads to a progressive enrichment of the heavy isotopologues in the remaining contaminant fraction (exemplarily shown in Figure 1-2), while the product becomes depleted in heavy isotopologues.

Isotope fractionation effects have been investigated mainly for aromatic hydrocarbons (e.g. benzene, toluene) (15,18-24), fuel oxygenates (methyl *tert*-butyl ether) (25-27) and chlorinated solvents (such as trichloroethene) (14,16,28-31) during aerobic and anaerobic biodegradation. Studies demonstrated that fractionation factors may change for various microbial cultures. For example, the aerobic degradation of toluene by an enrichment culture was not associated with carbon isotope fractionation (16), while pure strains showed significant isotope fractionation effects (22). Observed fractionation factors may be specific not only for the bacterial strains, but may also be characteristic for reaction mechanisms or degradation pathways (32). As microcosm experiments have been performed under different aquifer conditions, fractionation factors are available for a wide range of redox conditions (e.g. oxic, nitrate-reducing, sulphate-reducing, methanogenic). Fractionation of organic compounds was not only studied in laboratory batch systems but also tested under simulated aquifer conditions in flow-through column experiments (15,33,34). In addition, isotope fractionation factors of abiotic transformation reactions are available for some chlorinated hydrocarbons (33-36). More detailed information on environmental applications of CSIA, and various biochemical mechanisms and pathways involved in biodegradation reactions, are reviewed by Schmidt et al. (8) and Meckenstock et al. (7), where also an extensive compilation of various enrichment factors for aerobic and anaerobic degradation of important groundwater contaminants can be found.

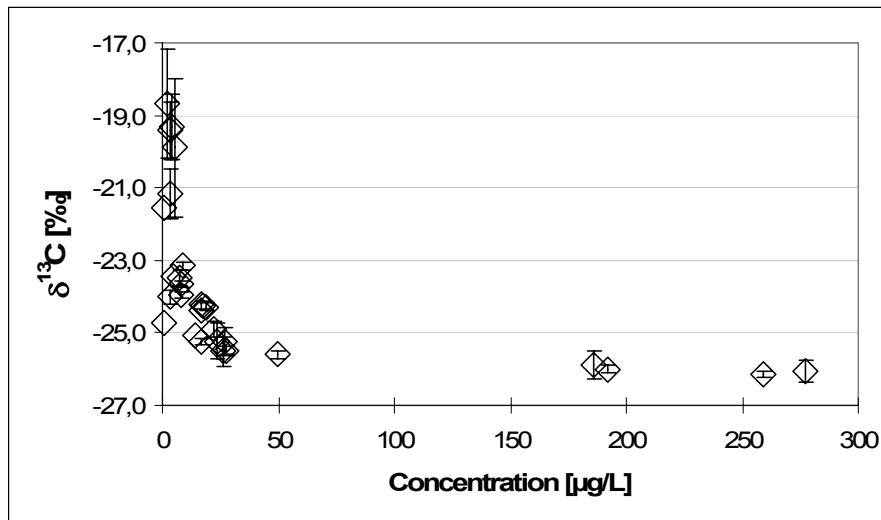


**Figure 1-2.** Decreasing concentration associated with enrichment of heavy isotopologues indicating biodegradation (exemplified for benzene degradation at the former military airfield Brand, site-specific details are given in Chapter 2).

In contrast, for some other organic compounds, especially high molecular weight compounds such as polycyclic aromatic hydrocarbons (PAHs) or long-chain *n*-alkanes, no significant fractionation has been documented (37,38). Isotopic signatures of individual compounds can thus be used as a possible tool to trace the origin of contaminants in the environment (37-39). Source apportionment of polycyclic aromatic hydrocarbons was successfully performed by determining  $\delta^{13}\text{C}$  values of individual PAHs in environmental samples (37,39-42). Several other chemicals such as benzene, toluene, ethylbenzene and xylenes (BTEX) (43), polychlorinated biphenyls (PCBs) (44,45) and fuel oxygenates such as methyl *tert*-butyl ether (MTBE) (46) show differences in their isotopic signatures depending on manufacturer, raw material used and route of synthesis. For pure-phase products of chlorinated solvents differences in stable isotope compositions between different manufacturers were observed (33,47-49). Hence, the technique of CSIA not only offers a useful tool to identify and quantify *in-situ* degradation reactions, moreover, it provides the potential to allocate individual contaminants to their sources.

#### **1.4. Physical Processes Controlling the Extent of Isotope Fractionation**

To attribute a change in isotope signatures to biodegradation processes, it must be certain that effects of other physical processes occurring in natural aquifers do not (or not significantly) alter the isotopic composition of the contaminants.

**Advective-Dispersive Transport (Including Diffusion).** Laboratory and field results evidence that  $\delta^{13}\text{C}$  values of dissolved solvents are not significantly different from those of the DNAPL causing the plume, source-near  $\delta^{13}\text{C}$  values may therefore be representative for the initial isotopic composition of the source (14,50,51). In plumes not affected by biodegradation, isotope values of dissolved chlorinated solvents remained unchanged along the groundwater flow path, indicating that the effect of dispersion, including diffusion, has no influence on the isotopic composition of organic compounds (48,50). Preferential diffusion of  $^{12}\text{C}$  molecules over  $^{13}\text{C}$  molecules could only be observed to a minor extent and only in the plume fringes where vertical concentration gradients were large (50). Hence, isotope fractionation effects associated with groundwater flow can be neglected.

**Volatilization.** Evaporation of organic compounds from aqueous solution was demonstrated to be a non-fractionating process (51), while small enrichments of  $^{13}\text{C}$  in the vapor phase were observed in experiments with vaporization of pure phase compounds (51-54). A significant isotope fractionation due to vaporization will only occur if a very high percentage of contaminant mass is lost through evaporation, and is less relevant in natural aquifer systems, where the loss due to vaporization is likely to be small (55). However, the observed isotope fractionation effects may be relevant for soil vapor extraction and air sparging techniques used in remediation processes (52).

**Sorption/Desorption.** The isotope effects of sorption have been characterized in several laboratory experiments. In single-step batch experiments, no significant isotope fractionation ( $\pm 0.5\%$ ) could be observed during equilibrium sorption on different carbonaceous sorbents (including activated carbon, graphite, lignite and lignite coke) even if very high amounts ( $>95\%$ ) of the compound has been sorbed (56,57).

In contrast, stable carbon isotope fractionation was observed to a certain extent for benzene and toluene in multi-step batch experiments with sorption on suspended humic acid under equilibrium conditions (58). The isotopic composition of both analytes evidenced that the lighter isotopologues are prone to sorption, resulting in a  $^{13}\text{C}$ -enrichment measured in the residual fractions. Similar observations were made for trichloroethene and toluene on peat and charcoal as sorption materials in multi-step batch experiments (59). Kopinke et al. proposed that, depending on aquifer properties together with plume source, length and variance with time, sorption based isotope fractionation might play a role and may be expressed in the isotopic composition of a migrating plume front (58). In HPLC column experiments with humic acid-coated silica performed under simulated non-equilibrium conditions, the observed shift in  $\delta^{13}\text{C}$  values between



the front and the tail of the peaks was up to 4‰ (benzene), 8‰ (2,4-dimethylphenol) and 13‰ (o-xylene), representing enrichment factors of 0.17, 0.35, and 0.92‰, respectively (58). These results suggest that in an expanding contaminant plume (under non-stationary aquifer conditions) the heavier isotopologues tend to move faster and fractionation factors tend to increase with increasing hydrophobicity of a compound (58). The fractionation effect was studied in an HPLC-experiment performed with an Eurosoil column and toluene, as illustrated in the chromatographic experiment shown in Figure 1-3.

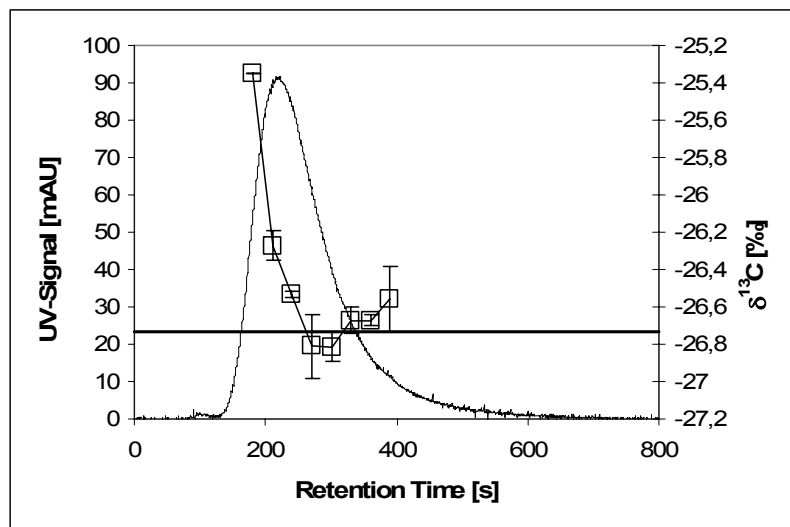


**Figure 1-3.** HPLC-chromatogram for toluene (column: Eurosoil 4; flow 0.1 mL/min) together with corresponding carbon isotope composition along the peak. The horizontal line represents the  $\delta^{13}\text{C}$  value of the non-fractionated toluene.

However, due to heterogeneities in natural aquifer systems, the effect of sorption will be masked as a result of mixing effects. The effect of sorption-induced isotope fractionation has not been observed under field conditions, even after a short contamination event, which represents non-stationary plume conditions (60). Thus, stable isotope analysis serves as a valuable technique to distinguish (bio)degradation from physical, nondegradative processes that also account for contaminant mass reduction. This possibility is of fundamental importance for the evaluation of remediation strategies that rely on the monitored natural and engineered attenuation of organic contaminants in soil and groundwater systems. Hence, CSIA offers an alternative method to assess *in-situ* degradation rates and to quantify the biodegradation independently of mass balances.

### **1.5. Scope of the Present Study**

The main aim of the present work is to evaluate and demonstrate the potential and limitations of CSIA for studying sources and fate of organic contaminants at heterogeneous and complex aquifer systems. The first chapters of this work deal with compound-specific isotope analysis (CSIA) with on-line gas chromatography-isotope ratio mass spectrometry (GC-C-IRMS) as an emerging technique with significant potential for tracing the origin of contaminants and elucidating the processes controlling their fate and transport in hydrogeologic environments. As the isotope changes are relatively independent of physical processes, CSIA has the potential for identification and quantification of key processes occurring in natural aquifers. However, in particular for field applications, a major drawback of CSIA is its rather poor sensitivity in terms of amount of compound required on column. This currently limits or even prevents the use of CSIA in some application areas such as fate studies of semi-volatile compounds, for example. To overcome this problem, various sample extraction and injection techniques, some of which are already well established in quantitative water analysis at trace levels will be optimized and validated within this work for their application in CSIA studies.

To date, most field studies are limited to homogeneous aquifer systems. As CSIA is gaining more and more popularity in the assessment of *in-situ* biodegradation of organic contaminants, an increasing number of authorities and environmental consulting offices are interested in the application of the method for contaminated site remediation. Therefore, the present work aims to demonstrate the potential of the method at site conditions, usually confronted with in practical contaminated site management. To this end, site investigations will focus on heterogeneous aquifer systems to validate the applicability of the methods under complex conditions. The performance of newly developed sample extraction and injection techniques will be tested at different sampling locations to cover the broad variety of contaminants, concentrations and hydrologic and geochemical conditions that are typically found at NA field investigation sites. Limitations associated with compound-specific isotope measurements of environmental samples will be studied and discussed. To validate the applicability of the CSIA concept for studying the fate and transport of organic contaminants and to reliably quantify the rate of *in-situ* degradation in contaminant plumes even at highly complex conditions, site investigations will be performed at an urban, heterogeneous bedrock aquifer system. To this end groundwater samples will be taken and isotope ratios of individual chlorinated hydrocarbons measured. Data interpretation will be performed in order to distinguish various potential sources of the contaminants within the

plume and to estimate the potential for natural attenuation in the investigated aquifer. One goal of this study will be to quantify natural degradation processes based on compound-specific carbon isotope data. A possible approach might be to incorporate information on isotope fractionation in a reactive transport model in order to maximize information from isotope data gained at this complex field site, in particular for the potential degradation intermediates. Further steps will be to apply and evaluate prospects and limitations of CSIA under field conditions and develop a guideline to make CSIA methods better accessible for stakeholders such as authorities and consultants.

## 1.6. References

- (1) U.S. Environmental Protection Agency. National primary drinking water regulations, list of drinking water contaminants & their MCLs, EPA 816-F-03-016. <http://www.epa.gov/safewater/consumer/pdf/mcl.pdf> **2003**.
- (2) U.S. Environmental Protection Agency. Use of Monitoring Natural Attenuation at Superfund, RCRA Corrective Action, and Underground Storage Tank Sites. *Office of Solid Waste and Emergency Response Directive 9200.4-17*. **1997**.
- (3) Madsen, E. L. Determining in-situ biodegradation - facts and challenges. *Environ. Sci. Technol.* **1991**, *25*, 1662-1673.
- (4) Aggarwal, P. K.; Fuller, M. E.; Gurgas, M. M.; Manning, J. F.; Dillon, M. A. Use of Stable Oxygen and Carbon Isotope Analyses for Monitoring the Pathways and Rates of Intrinsic and Enhanced in Situ Biodegradation. *Environ. Sci. Technol.* **1997**, *31*, 590-596.
- (5) Wiedemeier, T. H.; Swanson, M. A.; Moutoux, D. E.; Gordon, E. K.; Wilson, J. T.; Wilson, B. H.; Kampbell, D. H.; Haas, P. E.; Miller, R. N.; Hansen, J. E.; Chapelle, F. H. Technical Protocol for Evaluating Natural Attenuation of Chlorinated Solvents in Ground Water. *EPA/600/R-98/128 National Risk Management Research Laboratory, Office of Research and Development, U. S. ENVIRONMENTAL PROTECTION AGENCY; Cincinnati, Ohio* **1998**.
- (6) Stapleton, R. D.; Sayler, G. S.; Boggs, J. M.; Libelo, E. L.; Stauffer, T.; MacIntyre, W. G. Changes in Subsurface Catabolic Gene Frequencies during Natural Attenuation of Petroleum Hydrocarbons. *Environ. Sci. Technol.* **2000**, *34*, 1991-1999.
- (7) Meckenstock, R. U.; Morasch, B.; Griebler, C.; Richnow, H. H. Stable isotope fractionation analysis as a tool to monitor biodegradation in contaminated aquifers. *J. Contam. Hydrol.* **2004**, *75*, 215-255.
- (8) Schmidt, T. C.; Zwank, L.; Elsner, M.; Berg, M.; Meckenstock, R. U.; Haderlein, S. B. Compound-specific stable isotope analysis of organic contaminants in natural environments: a critical review of the state of the art, prospects, and future challenges. *Anal. Bioanal. Chem.* **2004**, *378*, 283-300.
- (9) Hayes, J. M.; Freeman, K. H.; Popp, B. N.; Hoham, C. H. Compound-specific isotopic analyses: A novel tool for reconstruction of ancient biogeochemical processes. *Org. Geochem.* **1990**, *16*, 1115-1128.
- (10) Coplen, T. B. New IUPAC guidelines for the reporting of stable hydrogen, carbon, and oxygen isotope-ratio data. *J. Res. Natl. Inst. Stand. Technol.* **1995**, *100*, 285.
- (11) Mariotti, A.; Germon, J. C.; Hubert, P.; Kaiser, P.; Letolle, R.; Tardieux, A.; Tardieux, P. Experimental determination of nitrogen kinetic isotope fractionation: some principles; illustration for the denitrification and nitrification processes. *Plant Soil* **1981**, *62*, 413-430.
- (12) Sturchio, N. C.; Clausen, J. L.; Heraty, L. J.; Huang, L.; Holt, B. D.; Abrajano, T. A. Chlorine isotope investigation of natural attenuation of trichloroethene in an aerobic aquifer. *Environ. Sci. Technol.* **1998**, *32*, 3037-3042.
- (13) Heraty, L. J.; Fuller, M. E.; Huang, L.; Abrajano, T.; Sturchio, N. C. Isotopic fractionation of carbon and chlorine by microbial degradation of dichloromethane. *Org. Geochem.* **1999**, *30*, 793-799.
- (14) Hunkeler, D.; Aravena, R.; Butler, B. J. Monitoring microbial dechlorination of tetrachloroethene (PCE) in groundwater using compound-specific stable carbon isotope ratios: Microcosm and field studies. *Environ. Sci. Technol.* **1999**, *33*, 2733-2738.

- (15) Meckenstock, R. U.; Morasch, B.; Warthmann, R.; Schink, B.; Annweiler, E.; Michaelis, W.; Richnow, H. H. C-13/C-12 isotope fractionation of aromatic hydrocarbons during microbial degradation. *Environ. Microbiol.* **1999**, *1*, 409-414.
- (16) Sherwood Lollar, B.; Slater, G. F.; Ahad, J.; Sleep, B.; Spivack, J.; Brennan, M.; MacKenzie, P. Contrasting carbon isotope fractionation during biodegradation of trichloroethylene and toluene: Implications for intrinsic bioremediation. *Org. Geochem.* **1999**, *30*, 813-820.
- (17) Hoefs, J. *Stable isotope geochemistry*; 4th. completely rev., upd, and enl. edition ed.; Springer Verlag: Berlin, Heidelberg, 1997.
- (18) Ahad, J. M. E.; Sherwood Lollar, B.; Edwards, E. A.; Slater, G. F.; Sleep, B. E. Carbon isotope fractionation during anaerobic biodegradation of toluene: Implications for intrinsic bioremediation. *Environ. Sci. Technol.* **2000**, *34*, 892-896.
- (19) Wilkes, H.; Boreham, C.; Harms, G.; Zengler, K.; Rabus, R. Anaerobic degradation and carbon isotopic fractionation of alkylbenzenes in crude oil by sulphate-reducing bacteria. *Org. Geochem.* **2000**, *31*, 101-115.
- (20) Hunkeler, D.; Andersen, N.; Aravena, R.; Bernasconi, S. M.; Butler, B. J. Hydrogen and carbon isotope fractionation during aerobic biodegradation of benzene. *Environ. Sci. Technol.* **2001**, *35*, 3462-3467.
- (21) Morasch, B.; Richnow, H. H.; Schink, B.; Meckenstock, R. U. Stable hydrogen and carbon isotope fractionation during microbial toluene degradation: Mechanistic and environmental aspects. *Appl. Environ. Microbiol.* **2001**, *67*, 4842-4849.
- (22) Morasch, B.; Richnow, H. H.; Schink, B.; Vieth, A.; Meckenstock, R. U. Carbon and hydrogen stable isotope fractionation during aerobic bacterial degradation of aromatic hydrocarbons. *Appl. Environ. Microbiol.* **2002**, *68*, 5191-5194.
- (23) Mancini, S. A.; Ulrich, A. C.; Lacrampe-Couloume, G.; Sleep, B.; Edwards, E. A.; Sherwood Lollar, B. Carbon and hydrogen isotopic fractionation during anaerobic biodegradation of benzene. *Appl. Environ. Microbiol.* **2003**, *69*, 191-198.
- (24) Morasch, B.; Richnow, H. H.; Vieth, A.; Schink, B.; Meckenstock, R. U. Stable isotope fractionation caused by glycol radical enzymes during bacterial degradation of aromatic compounds. *Appl. Environ. Microbiol.* **2004**, *70*, 2935-2940.
- (25) Hunkeler, D.; Butler, B. J.; Aravena, R.; Barker, J. F. Monitoring biodegradation of methyl tert-butyl ether (MTBE) using compound-specific carbon isotope analysis. *Environ. Sci. Technol.* **2001**, *35*, 676-681.
- (26) Gray, J. R.; Lacrampe-Couloume, G.; Gandhi, D.; Scow, K. M.; Wilson, R. D.; Mackay, D. M.; Sherwood Lollar, B. Carbon and hydrogen isotopic fractionation during biodegradation of methyl tert-butyl ether. *Environ. Sci. Technol.* **2002**, *36*, 1931-1938.
- (27) Kolhatkar, R.; Kuder, T.; Philp, P.; Allen, J.; Wilson, J. T. Use of compound-specific stable carbon isotope analyses to demonstrate anaerobic biodegradation of MTBE in groundwater at a gasoline release site. *Environ. Sci. Technol.* **2002**, *36*, 5139-5146.
- (28) Bloom, Y.; Aravena, R.; Hunkeler, D.; Edwards, E.; Frape, S. K. Carbon isotope fractionation during microbial dechlorination of trichloroethene, cis-1,2-dichloroethene, and vinyl chloride: Implications for assessment of natural attenuation. *Environ. Sci. Technol.* **2000**, *34*, 2768-2772.
- (29) Slater, G. F.; Sherwood Lollar, B.; Sleep, B. E.; Edwards, E. A. Variability in carbon isotopic fractionation during biodegradation of chlorinated ethenes: Implications for field applications. *Environ. Sci. Technol.* **2001**, *35*, 901-907.
- (30) Barth, J. A. C.; Slater, G.; Schüth, C.; Bill, M.; Downey, A.; Larkin, M.; Kalin, R. M. Carbon isotope fractionation during aerobic biodegradation of trichloroethene by *Burkholderia cepacia* G4: a tool to map degradation mechanisms. *Appl. Environ. Microbiol.* **2002**, *68*, 1728-1734.
- (31) Chu, K. H.; Mahendra, S.; Song, D. L.; Conrad, M. E.; Alvarez-Cohen, L. Stable carbon isotope fractionation during aerobic biodegradation of chlorinated ethenes. *Environ. Sci. Technol.* **2004**, *38*, 3126-3130.
- (32) Hirschorn, S. K.; Dinglasan, M. J.; Elsner, M.; Mancini, S. A.; Lacrampe-Couloume, G.; Edwards, E. A.; Sherwood Lollar, B. Pathway dependent isotopic fractionation during aerobic biodegradation of 1,2-dichloroethane. *Environ. Sci. Technol.* **2004**, *38*, 4775-4781.
- (33) Shouakar-Stash, O.; Frape, S. K.; Drimmie, R. J. Stable hydrogen, carbon and chlorine isotope measurements of selected chlorinated organic solvents. *J. Contam. Hydrol.* **2003**, *60*, 211-228.
- (34) VanStone, N. A.; Focht, R. M.; Mabury, S. A.; Sherwood Lollar, B. Effect of iron type on kinetics and carbon isotopic enrichment of chlorinated ethylenes during abiotic reduction on Fe(0). *Ground Water* **2004**, *42*, 268-276.
- (35) Dayan, H.; Abrajano, T.; Sturchio, N. C.; Winsor, L. Carbon isotopic fractionation during reductive dehalogenation of chlorinated ethenes by metallic iron. *Org. Geochem.* **1999**, *30*, 755-763.
- (36) Bill, M.; Schüth, C.; Barth, J. A. C.; Kalin, R. M. Carbon isotope fractionation during abiotic reductive dehalogenation of trichloroethene (TCE). *Chemosphere* **2001**, *44*, 1281-1286.

- 
- (37) O'Malley, V. P.; Abrajano, T. A.; Hellou, J. Determination of the  $^{13}\text{C}/^{12}\text{C}$  ratios of individual PAH from environmental samples: can PAH sources be apportioned? *Org. Geochem.* **1994**, *21*, 809-822.
- (38) Mansuy, L.; Philp, R. P.; Allen, J. Source identification of oil spills based on the isotopic composition of individual components in weathered oil samples. *Environ. Sci. Technol.* **1997**, *31*, 3417-3425.
- (39) Hammer, B. T.; Kelley, C. A.; Coffin, R. B.; Cifuentes, L. A.; Mueller, J. G. Delta C-13 values of polycyclic aromatic hydrocarbons collected from two creosote-contaminated sites. *Chem. Geol.* **1998**, *152*, 43-58.
- (40) Mazeas, L.; Budzinski, H. Quantification of petrogenic PAH in marine sediment using molecular stable carbon isotopic ratio measurement. *Analisis* **1999**, *27*, 200-203.
- (41) Okuda, T.; Kumata, H.; Naraoka, H.; Takada, H. Origin of atmospheric polycyclic aromatic hydrocarbons (PAHs) in Chinese cities solved by compound-specific stable carbon isotopic analyses. *Org. Geochem.* **2002**, *33*, 1737-1745.
- (42) Stark, A.; Abrajano, T.; Hellou, J.; Metcalf-Smith, J. L. Molecular and isotopic characterization of polycyclic aromatic hydrocarbon distribution and sources at the international segment of the St. Lawrence River. *Org. Geochem.* **2003**, *34*, 225-237.
- (43) Dempster, H. S.; Sherwood Lollar, B.; Feenstra, S. Tracing organic contaminants in groundwater: A new methodology using compound-specific isotopic analysis. *Environ. Sci. Technol.* **1997**, *31*, 3193-3197.
- (44) Jarman, W. M.; Hilkert, A.; Bacon, C. E.; Collister, J. W.; Ballschmiter, K.; Risebrough, R. W. Compound-specific carbon isotopic analysis of Aroclors, Clophens, Kaneclors, and Phenoclor. *Environ. Sci. Technol.* **1998**, *32*, 833-836.
- (45) Drenzek, N. J.; Tarr, C. H.; Eglinton, T. I.; Heraty, L. J.; Sturchio, N. C.; Shiner, V. J.; Reddy, C. M. Stable chlorine and carbon isotopic compositions of selected semi-volatile organochlorine compounds. *Org. Geochem.* **2002**, *33*, 437-444.
- (46) Smallwood, B. J.; Philp, R. P.; Burgoyne, T. W.; Allen, J. D. The use of stable isotopes to differentiate specific source markers for MTBE. *Environ. Forensics* **2001**, *2*, 215-221.
- (47) van Warmerdam, E. M.; Frape, S. K.; Aravena, R.; Drimmie, R. J.; Flatt, H.; Cherry, J. A. Stable chlorine and carbon isotope measurements of selected chlorinated organic solvents. *Appl. Geochem.* **1995**, *10*, 547-552.
- (48) Beneteau, K. M.; Aravena, R.; Frape, S. K. Isotopic characterization of chlorinated solvents-laboratory and field results. *Org. Geochem.* **1999**, *30*, 739-753.
- (49) Jendrzewski, N.; Eggenkamp, H. G. M.; Coleman, M. L. Characterisation of chlorinated hydrocarbons from chlorine and carbon isotopic compositions: scope of application to environmental problems. *Appl. Geochem.* **2001**, *16*, 1021-1031.
- (50) Hunkeler, D.; Chollet, N.; Pittet, X.; Aravena, R.; Cherry, J. A.; Parker, B. L. Effect of source variability and transport processes on carbon isotope ratios of TCE and PCE in two sandy aquifers. *J. Contam. Hydrol.* **2004**, *74*, 265-282.
- (51) Slater, G. F.; Dempster, H. S.; Sherwood Lollar, B.; Ahad, J. Headspace analysis: A new application for isotopic characterization of dissolved organic contaminants. *Environ. Sci. Technol.* **1999**, *33*, 190-194.
- (52) Harrington, R. R.; Poulson, S. R.; Drever, J. I.; Colberg, P. J. S.; Kelly, E. F. Carbon isotope systematics of monoaromatic hydrocarbons: vaporization and adsorption experiments. *Org. Geochem.* **1999**, *30*, 765-775.
- (53) Huang, L.; Sturchio, N. C.; Abrajano, T.; Heraty, L. J.; Holt, B. D. Carbon and chlorine isotope fractionation of chlorinated aliphatic hydrocarbons by evaporation. *Org. Geochem.* **1999**, *30*, 777-785.
- (54) Poulson, S. R.; Drever, J. I. Stable isotope (C, Cl, and H) fractionation during vaporization of trichloroethylene. *Environ. Sci. Technol.* **1999**, *33*, 3689-3694.
- (55) Wang, Y.; Huang, Y. Hydrogen isotopic fractionation of petroleum hydrocarbons during vaporization: implications for assessing artificial and natural remediation of petroleum contamination. *Appl. Geochem.* **2003**, *18*, 1641-1651.
- (56) Slater, G. F.; Ahad, J. M. E.; Sherwood Lollar, B.; Allen-King, R.; Sleep, B. Carbon isotope effects resulting from equilibrium sorption of dissolved VOCs. *Anal. Chem.* **2000**, *72*, 5669-5672.
- (57) Schüth, C.; Taubald, H.; Bolaño, N.; Maciejczyk, K. Carbon and hydrogen isotope effects during sorption of organic contaminants on carbonaceous materials. *J. Contam. Hydrol.* **2003**, *64*, 269-281.
- (58) Kopinke, F. D.; Georgi, A.; Voskamp, M.; Richnow, H. H. Carbon isotope fractionation of organic contaminants due to retardation on humic substances: Implications for natural attenuation studies in aquifers. *Environ. Sci. Technol.* **2005**, *39*, 6052-6062.
- (59) Botalova, O. Sorption-based isotope fractionation. Master thesis, Center for Applied Geoscience, Eberhard-Karls-University. Tübingen, **2006**: 49 pp.
- (60) Fischer, A.; Bauer, J.; Meckenstock, R. U.; Stichler, W.; Griebler, C.; Maloszewski, P.; Kästner, M.; Richnow, H. H. A multitracer test proving the reliability of Rayleigh equation-based approach for assessing biodegradation in a BTEX contaminated aquifer. *Environ. Sci. Technol.* **2006**, *40*, 4245-4252.

## **2. Compound-Specific Isotope Analysis of Volatile Organic Compounds (VOCs) at Trace Levels**

### ***2.1. Introduction***

Due to their widespread use, chlorinated hydrocarbons (CHCs) and soluble fuel compounds such as tetra- and trichloroethene, benzene, toluene, ethylbenzene, and xylene-isomers (BTEX) are among the most prevalent volatile organic groundwater contaminants. In environmental sciences, compound-specific isotope analysis (CSIA) is an emerging technique for the allocation of contaminant sources, and for the identification and quantification of (bio)transformation reactions on scales ranging from batch experiments to field sites (1-3). A limitation of CSIA, especially in field applications, is the fact that an accurate carbon isotope ratio measurement requires at least 1 nmol carbon of a given compound on column (optimal chromatographic resolution and peak sharpness presumed). Turner et al. emphasized the need for developing reliable techniques for isotope measurements on compounds at field concentrations in the low  $\mu\text{g/L}$ -range to assess microbial degradation processes and reactive transport at catchment scales and to address pertinent research and application areas such as fate studies of pesticides, and differentiation between diffuse and point sources of contaminants based on their isotope signature (3). These limitations and requirements motivate the development of efficient enrichment techniques to lower method detection limits in GC/IRMS applications.

To overcome this limitation, preconcentration techniques for on-line CSIA have been developed to meet the instrumental sensitivity of the GC/IRMS. For volatile organic compounds solid-phase microextraction (SPME) and purge-and-trap (P&T) have been shown to be the most effective techniques to preconcentrate the analytes prior to CSIA without compromising accurate and precise isotope ratio determinations (4,5). For compound-specific isotope analysis SPME has been applied directly in the water phase (direct immersion) as well as in the headspace of the sample (4,6,7). SPME is a solvent-free, highly sensitive and rapid extraction method for the determination of analytes (8). The SPME device consists of a re-usable, polymer-coated fiber in a syringe-like holder. The fiber is exposed to the sample matrix, where analytes partition between coating and the sample (8,9). According to their sorption affinity, compounds are extracted into the stationary phase of the fiber and then thermally desorbed in the gas chromatographic injector. P&T is commonly referred to as a dynamic headspace technique where the compounds are

purged/stripped from the sample (e.g. water) with a stream of inert gas, subsequently trapped directly on a sorbent or cold trap and thermally desorbed prior to analysis. P&T is implemented in several US Environmental Protection Agency protocols for the quantification of volatiles in drinking, waste and hazardous waste water (e.g. US EPA method 524.4 (10)) and has also been used successfully for determining isotope ratios of a wide range of VOCs in aqueous samples at low concentrations (5,11,12). SPME and P&T method validation included comparisons of  $\delta^{13}\text{C}$  values determined by GC/IRMS with EA/IRMS measurements as well as comparisons of values obtained with different injection modes (4,5,11,12). Isotopic fractionation effects of the various processes involved in SPME and/or P&T (i.e., evaporation, sorption, desorption, and condensation of the analytes) were within the range of analytical uncertainty ( $< 0.5\text{‰}$ ) for most of the compounds studied (4,11,12); greater deviations were found to be compound-specific (5,11,12). Zwank et al. (5) reported that SPME lowered the method detection limits by 3-4 orders of magnitude compared with liquid injection, while P&T extraction was the most efficient preconcentration technique reaching method detection limits (MDLs) below  $5\ \mu\text{g/L}$ . In combination with cryofocusing of analytes, P&T gave the best resolution of adjacent peaks (5). Slight but highly reproducible deviations of the  $\delta^{13}\text{C}$  signatures compared to EA/IRMS measurements of pure phase compounds occurred in all of the evaluated injection and preconcentration techniques (5). Hence, the choice of the optimal technique used within the following work depended mainly on the concentrations observed at the individual field sites and the required method detection limits.

As P&T is the most sensitive preconcentration technique for on-line CSIA of volatile organic compounds, a commercially available P&T system was modified to further enhance the sensitivity to allow for GC/IRMS measurements of volatile compounds at trace concentrations. An improvement of the sample concentration for P&T was achieved by increasing the amount of water purged (12). The improved P&T method showed good reproducibility and high linearity with significant deviations ( $> 0.5\text{‰}$ ) from pure phase values only observable for chloroform. MDLs for monoaromatic compounds between  $0.07$  and  $0.35\ \mu\text{g/L}$  are the lowest values reported so far for continuous-flow isotope ratio measurements using an automated system. MDLs for halogenated hydrocarbons were between  $0.76$  and  $27\ \mu\text{g/L}$  (12). More recently, the development of a custom made continuous-flow purge and trap system was described which allowed for an adaptation of the sample size and by using an ultrasonic nebuliser extremely low MDLs were achieved (11). Although highly efficient, the instrumentation is not automated and not commercially available.

Previous work showed that synthetic polymers in devices used for sampling groundwater, such as flexible tubings made of polytetrafluoroethylene (PTFE), polyvinyl chloride (PVC), or polypropylene (PP) significantly absorb organic compounds from aqueous solution (13,14). As the commercially available P&T-GC/IRMS device was equipped with a PTFE sample transfer loop, the present study aimed to evaluate an alternative material for sample transfer and thus, to further increase the detection limits of a commercially available P&T system. The present work aims to demonstrate the performance of SPME and P&T extraction techniques for determining  $\delta^{13}\text{C}$  values of VOCs in environmental samples. To this end, site investigations are performed at different sampling locations to cover the broad variety of contaminants, concentrations and hydrologic and geochemical conditions that are typically found at NA field investigation sites. Innovative sampling techniques were applied in order to extend the information attained by CSIA measurements at contaminated sites, especially when the number of sampling wells is limited. Major goals were to evaluate if NA processes are active and to quantify the rate of *in-situ* degradation in the contaminant plumes.

## **2.2. Materials and Methods**

**Chemicals and Reagents.** As a solvent for the preparation of standard solutions for CSIA, Millipore water from a Milli-Q Plus water purification system (Millipore, Bedford, MA, USA) was used. Aromatic hydrocarbon standards contained benzene (99.5%, Fluka, Buchs, Switzerland), toluene (99.9%, Merck, Darmstadt, Germany), ethylbenzene (99.8%, Acros Organics, Geel, Belgium), *para*-xylene (99%, Aldrich, Steinheim, Germany), *n*-propylbenzene (98%, Aldrich), isopropylbenzene (99%, Aldrich), 1,3,5-trimethylbenzene (99%, Fluka), 1,2,4-trimethylbenzene (98%, Aldrich) and 1,2,3-trimethylbenzene (90-95%, Fluka). Chlorinated hydrocarbon standards included *trans*-1,2-dichloroethene (*trans*-DCE, 98%, Aldrich), *cis*-1,2-dichloroethene (*cis*-DCE, 97%, Aldrich), trichloroethene (TCE, 99.5%, Merck) and tetrachloroethene (PCE, 99.9%, Aldrich). Tests for vinyl chloride measurements were performed with vinyl chloride solution in methanol purchased from Sigma-Aldrich. Concentration analyses of field samples were carried out in external laboratories.

**GC/IRMS Instrumentation.** The compound-specific isotope ratios in the present work were determined using a Trace gas chromatograph (Thermo Finnigan, Milan, Italy) coupled to an isotope ratio mass spectrometer (DeltaPLUS XP; Thermo Finnigan MAT, Bremen, Germany) via a combustion interface (GC Combustion III; Thermo Finnigan MAT) maintained at 940 °C. The



gas chromatograph was equipped with a programmable temperature vaporizer (PTV) injector (Optic 3; ATAS GL International B.V., Veldhoven, The Netherlands). Sample introduction was performed with a CombiPAL autosampler system. According to the recommendation given by Zwank et al. (5) reoxidation of the CuO/NiO/Pt combustion reactor was carried out regularly after approximately 40 measurements.

**Solid-Phase Microextraction (SPME).** Two different fibers, a polydimethylsiloxane (PDMS, film thickness 100  $\mu\text{m}$ ) and a 75  $\mu\text{m}$  Carboxen/PDMS for autosampler use, were obtained from Supelco (Supelco, Bellefonte, PA, USA). Before use, the fibers were conditioned in the needle heater of the CombiPAL system for 0.5-2 h and at 250-300  $^{\circ}\text{C}$ , according to the instructions provided by the manufacturer. Aqueous samples containing only PCE and in concentration higher than 300  $\mu\text{g/L}$  were extracted using the PDMS fiber. The Carboxen/PDMS fiber was most appropriate for samples that contained chlorinated hydrocarbons in concentrations between 15 to 40  $\mu\text{g/L}$ . 18 mL of sample were placed in 20-mL headspace vials with magnetic screw caps sealed with PTFE-coated septa. Extraction of the analytes was carried out by immersing the fiber in the aqueous phase (direct immersion, with an agitational speed of 500 rpm) at 35  $^{\circ}\text{C}$  for 20 min. Since the samples did not contain unresolved cosolvents, direct immersion SPME could be applied to increase extraction efficiencies (4). After extraction, the analytes were thermally desorbed from the fiber in the splitless liner of the GC injector port for 1 min at 250  $^{\circ}\text{C}$  (100  $\mu\text{m}$  PDMS fiber) or 270  $^{\circ}\text{C}$  (75  $\mu\text{m}$  Carboxen/PDMS fiber). Following each injection the fiber was conditioned in the needle heater (maintained at 250  $^{\circ}\text{C}$  and 300  $^{\circ}\text{C}$ , respectively) for 2-3 min. Blanks were run periodically to check for carryover.

**Purge-and-Trap Sample Extraction.** A purge and trap sample concentrator (Velocity XPT<sup>TM</sup>) equipped with a liquid autosampler AquaTek 70<sup>TM</sup> (both Tekmar-Dohrmann, Mason, OH, USA) was coupled online to the PTV injector unit of the GC/IRMS. To increase sample volumes, the autosampler tray holder was modified to carry twenty 100-mL glass bottles. Aqueous samples were either filled into 40-mL VOC vials or into 100-mL amber glass bottles sealed with PTFE-coated silicone septa screw caps (free of headspace). For 40-mL vials, a 25-mL aliquot of the sample was transferred by the autosampler into a fritted sparging glassware and purged for 11 min with He (40 mL/min). For 100-mL bottles 76 mL of sample were transferred to the sparger, purged for 16 min at a He flow of 50 mL/min; technical constraints of the autosampler did not allow to transfer an aliquot greater than 76 mL of the sample from the bottle to the system. To allow for purging higher sample volumes, the 25-mL fritted sparger was modified to keep 100 mL of an aqueous sample and the original sample loop was replaced by a 50 m long 1/8"-

polytetrafluoroethylene (PTFE) tubing (1.6 mm i.d.). The replacement parts (tray holder, frit sparger and sample loop) were provided by PAS Analytik (Magdala, Germany). To further improve the sensitivity by reducing sorptive losses, the PTFE sample loop was replaced by a 27 m long 1/8"-polyetheretherketone (PEEK) tubing (2.0 mm i.d.) purchased from MedChrom GmbH (Eppelheim, Germany).

The purged analytes were trapped on a VOCARB 3000 (Supelco) trap at room temperature. By heating the trap to 250 °C for 1 min, the analytes were thermodesorbed and transferred to the GC injection port. The GC temperature program was started with the end of desorption. The injector and transfer line temperatures of the P&T instrument were held at 250 °C. The GC was equipped with a deactivated precolumn (0.4 m x 0.53 mm) leading through a cryofocusing unit, where the analytes were trapped at -100 °C during transfer from the P&T instrument. The cryofocusing unit is cooled by gas flowing through a heat exchanger immersed in a Dewar with liquid nitrogen (LN<sub>2</sub>). The use of nitrogen gas instead of compressed air is recommended as water vapour present in the air freezes and might block the gas flow through the heat exchanger. For the thermal desorption process, the cryotrap was heated with a rate of 30 °C/s to 240 °C. Cooling and heating of the trap are controlled by the OPTIC 3 control unit.

Method parameters optimized by Zwank et al. (5) were applied to the non-modified P&T-system in order to obtain sufficient extraction efficiencies. The P&T parameters for the modified 100-mL system were thoroughly evaluated in our recent study Jochmann et al. (12). The optimized parameters have also been applied to the PEEK system. All P&T parameters for the three different methods applied within the present work are summarized in the Appendix of this chapter. The performance of the P&T-system equipped with the PEEK sample transfer loop was tested for the most commonly detected chlorinated solvents *trans*-1,2-dichloroethene, *cis*-1,2-dichloroethene, trichloroethene and tetrachlorethene (*trans*-DCE, *cis*-DCE, TCE and PCE). Method parameters used for measurement of samples from the different contaminated sites, the techniques involved and GC parameters for separation of the analytes are listed in the Appendix of this chapter.

### **2.3. Description of Field Sites**

**KORA-Site Rosengarten-Ehestorf.** VOC containing aqueous samples for analyte extraction by SPME were obtained from a former dry-cleaning site located near Hamburg (15). A substantial chlorinated hydrocarbon spillage into a deep unsaturated zone led to the development of a PCE

plume in the saturated zone. The location is a demonstration site for field-scale quantification of the potential of NA in a deep large-scale aquifer as the groundwater contamination plume lies at a depth of >40 m. A special concern is the proximity of the local drinking water supply downgradient of the site. Major goals were to evaluate if NA processes are active and to what extent the contamination might effect the downstream groundwater quality by CSIA measurements. Due to the difficulties associated with investigations in deep aquifers the number of groundwater wells is limited. Therefore, innovative techniques were combined with CSIA to extend the validity of only few measuring points available at the site. A dense monitoring network would be required for point-scale isotope values as they need to be representative for the entire aquifer system (16). Therefore, a combined approach of immission pumping tests together with CSIA was applied to provide isotope information comprising differences owing to heterogeneities of the aquifer system. A multilevel sampling technique was applied to provide depth-discrete groundwater samples and a more vertically resolved profile of microbial activity within the contaminant plume.

**KORA-Site OLES-Epple.** VOC containing aqueous samples for the conventional P&T technique (40-mL vials) were obtained from a former mineral oil facility located in Stuttgart (17). The site provides an illustrative example of an urban industrial area with multiple potential releases of chlorinated hydrocarbons that is underlain by a complex bedrock aquifer with preferential flow and various layers partly connected through vertical faults. East of the site, important urban mineral springs are located, which explains the major interest in contaminant fate by local authorities. Aim of this work was to use isotope data in combination with existing geochemical data and hydrogeological modeling to distinguish various sources of the contaminants within the plume and to estimate the potential of natural attenuation in the aquifers investigated. Further details and results are given in chapters 5 and 6 of this thesis.

**KORA-Sites Brand and Niedergörsdorf TL1.** BTEX containing groundwater samples for the validation of the enhanced volume P&T-GC/IRMS method were obtained at disused military airfields located south of Berlin (18), in the state of Brandenburg. During the use of the areas, especially beneath the fuel handling and storage facilities, massive subsurface contamination with kerosene jet fuel occurred. Low-flow sampling of groundwater at wells that have direct contact to the surrounding sediment allow for a relatively undisturbed point-sampling to resolve vertical concentration gradients e.g. of contaminants and geochemical parameters. Wells are placed using direct-push techniques; the wells are screened over the desired depth of the aquifer at which concentration gradients were supposed to occur. Due to time-intensive, depth-discrete

groundwater sampling strategies using inflatable double packer systems and pneumatic driven mini pumps, only 120 mL of a sample could be provided for isotopic analyses. During the whole sampling procedure, the groundwater stayed within a closed system to minimize losses of volatile compounds.  $^{13}\text{C}/^{12}\text{C}$ -isotope ratio measurements have been performed for important volatile groundwater contaminants such as the monoaromatics benzene, toluene, ethylbenzene and xylene isomers (BTEX) and various isomers of trimethylbenzene.

**Stuttgart – Bad Cannstatt.** For VOC containing aqueous samples contaminated at trace concentrations water was sampled at some of the mineral springs located in Stuttgart-Bad Cannstatt. Stuttgart is ranked right after Budapest as having the second largest source of mineral water in Europe; the total discharge rate of the system is around 500 L/s (19,20). Chlorinated solvents, which were detected at low concentrations since 1984 in the overlying Keuper aquifer, pose a significant risk to the resource (21). The complex hydrogeological setting of the area with confined aquifers and artesian outflow, highly mineralised water rich in carbon dioxide, as well as vertical interaction with under- and overlying groundwater bodies, demand special procedures and methods to gain better information on sources and fate of the contaminants. To prevent or minimize losses of volatile compounds during sampling, the sampling campaigns at the  $\text{CO}_2$ -rich mineral-water fountains were performed during two days in March 2008, when ambient temperatures were below 7 °C, sampling bottles contained some drops of NaOH (to adjust the pH to ~8), and the sampling was performed as free of disturbance as possible. Samples were transported on ice, measured at the day of sampling and the bottles used for sampling were the same as used for P&T-analyses to avoid losses due to storage or sample preparation.

## **2.4. Results**

### **2.4.1. P&T-analysis with enhanced purge volume and PEEK sample loop**

**Extraction Efficiency.** The extraction efficiency of the improved sample transfer was tested with an aqueous standard solution containing *trans*- and *cis*-DCE, TCE and PCE at a concentration of 2.5, 2.6, 3.0 and 3.3  $\mu\text{g/L}$ , respectively. Figure 2-1 shows a comparison of the extraction efficiencies for the two different types of sample transfer tubing used. Extraction efficiencies for *cis*-DCE ( $\log K_{ow}$  1.86) (22), showed comparable peak heights for the PTFE- and PEEK- type loop. For *trans*-DCE ( $\log K_{ow}$  of 2.08) (22), the extraction efficiency was slightly better (~10%) for the PEEK-system. The extraction efficiencies for TCE and especially for PCE were

significantly higher using the PEEK tubing for sample transfer. In line with their higher octanol-water partition coefficients ( $\log K_{ow}$  2.42 and 2.88, respectively) (22), the sorptive loss to PTFE was 20% for TCE and more than 40% for PCE, respectively.

A good linear correlation of the amount of substance lost to PTFE and PTFE-water partitioning constants (23) was observed for the studied compounds (Figure 2-2). The results demonstrate that the sorptive loss of compounds to sample transfer tubings made of PTFE can be quite substantial, especially for those compounds with higher  $K_{ow}$ -values. However, Legett et al. (23) showed that the sorptive loss to PTFE correlates well with  $K_{ow}$  only within specific classes of compounds. The aromatic hydrocarbon *p*-xylene, for example, has a much higher  $K_{ow}$  ( $\log K_{ow}$  3.27) (22) compared to the chlorinated hydrocarbon PCE ( $\log K_{ow}$  2.88) (22), but shows a  $P_{PTFE}$  smaller compared to PCE (see Figure 2-2). Within the group of aromatic compounds again, sorptive loss to PTFE is highest for *p*-xylene compared to ethylbenzene, toluene, chlorobenzene and benzene ( $\log P_{PTFE}$  1.63, 1.47, 1.21, 1.05 and 0.90, respectively) (23) and correlates well with  $K_{ow}$  values for these compounds ( $\log K_{ow}$  3.27, 3.20, 2.69, 2.78 and 2.17, respectively) (22).

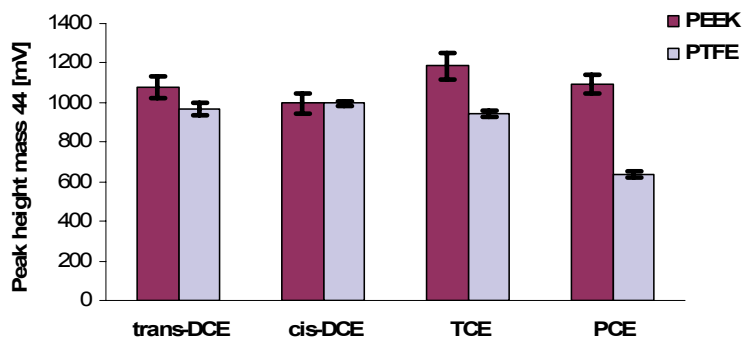


**Figure 2-1.** Effect of two different polymer tubings on extraction efficiency. Extraction efficiencies are represented by amplitude height of the mass 44 peak achieved during enhanced-volume P&T-analyses using PTFE- and PEEK- tubings for sample transfer. Error bars represent the standard deviation based on a triplicate measurement.

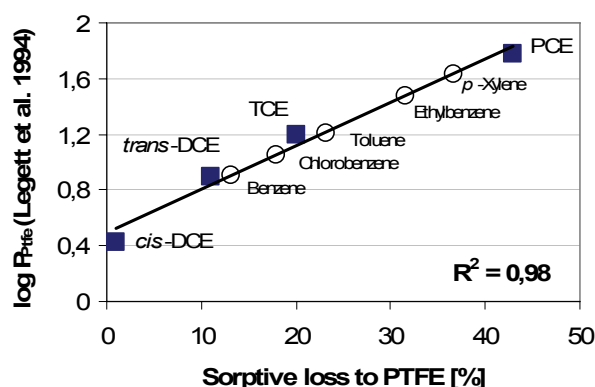


**Figure 2-2.** Sorptive loss to PTFE (filled squares, given in %-difference of amplitude heights of  $m/z$  44 peaks relative to PEEK) versus experimental equilibrium PTFE-water partitioning constants ( $\log P_{\text{PTFE}}$ , (23)). Open circles represent the theoretical loss for aromatic hydrocarbons according to  $\log P_{\text{PTFE}}$  values given by (23).

**Determination of Method Detection Limits.** Variations in  $\delta^{13}\text{C}$  values are commonly observed in continuous-flow isotope ratio determination at low signal sizes (23-27). To evaluate these amount-dependent fractionation effects, the influence of different concentrations on  $\delta^{13}\text{C}$  values was studied with the improved P&T-system (Figure 2-3). Over the whole concentration range ( $\leq 0.4 \mu\text{g/L}$  to  $\geq 5.5 \mu\text{g/L}$ ), a linear correlation of extraction yield (peak height of mass 44 signal) versus concentration was observed for all the investigated chlorinated ethenes ( $R^2 \geq 0.996$ , see Figure 2-3) demonstrating that the extraction yield is independent of the absolute amount of an analyte present. In contrast,  $\delta^{13}\text{C}$  values depend on the amount of compound present (open symbols in Figure 2-3). The most pronounced amount-dependent isotope fractionation effect could be observed for *trans*-DCE, while the other compounds showed only slight deviations. The  $\delta^{13}\text{C}$  values for *trans*-DCE were strongly depleted in  $^{13}\text{C}$  (-2‰) for a concentration below  $1 \mu\text{g/L}$  compared to the values measured for a higher concentration. This non-linearity effect was less pronounced for the other compounds, but still observable in both, enriched and depleted  $\delta^{13}\text{C}$  values at concentrations below  $0.5 \mu\text{g/L}$  (Figure 2-3). The MDLs were determined according to the methodology described in Jochmann et al. (12). For the four compounds, investigated for P&T equipped with a PEEK tubing as sample transfer loop, the detection limits are  $1 \mu\text{g/L}$  for *trans*-DCE, and  $\leq 0.5 \mu\text{g/L}$  for *cis*-DCE, TCE and PCE, which are the lowest MDLs for an automated P&T system reported so far (5,12,28). As already indicated in earlier studies, P&T is a technique that, due to the absence of a solvent and the use of cryofocusing, allows to determine reliable isotope data even at signals below 500 mV (5,12).

Overall, the results show, that replacing the PTFE tubing by a sample transfer loop made of PEEK further enhances the sensitivity of the P&T-method, especially for compounds with a high affinity to organic polymers, such as the chlorinated solvent tetrachloroethene (PCE). The analytical technique tested here can be easily adapted for the measurement of other volatile organics such as BTEX, naphthalene or MTBE.

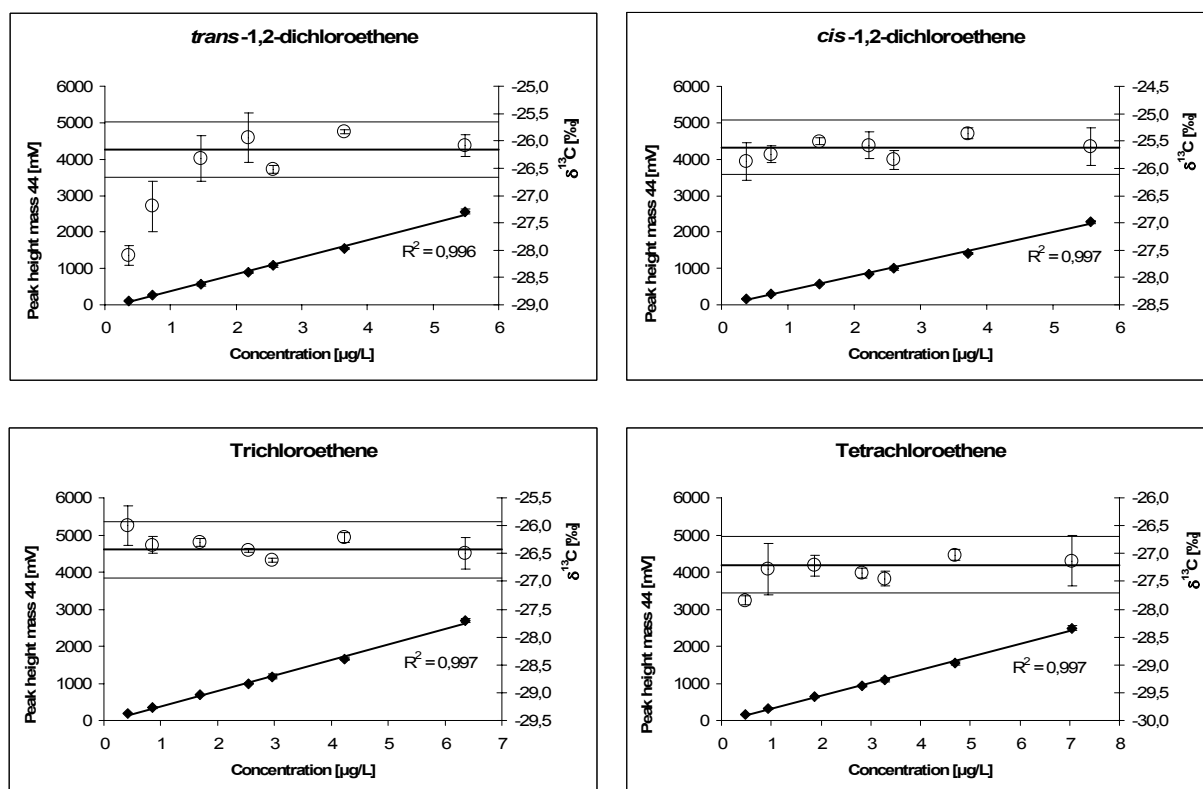


**Figure 2-3.** Evaluation of method detection limits (MDLs) for the investigated compounds. Open circles are representing  $\delta^{13}\text{C}$  values; diamonds show the signal size of mass 44 peak. The linear behavior of signal size versus concentration is indicated by correlation coefficients ( $R^2$ ) always better than 0.996. Error bars represent the standard deviation based on triplicate measurements. The horizontal lines represent the mean isotopic value for each compound ( $\pm 0.5\%$ ).

#### 2.4.2. Comparison of accuracy and reproducibility

The accuracy of GC/IRMS measurements can be expressed as the relative difference between the known EA/IRMS and the measured isotope values presented in Table 2-1. The isotope values measured with GC/IRMS are highly accurate for TCE and PCE for all sample extraction techniques applied. The accuracy for *cis*-DCE is high for the P&T-analyses, while for SPME measurements the  $\delta^{13}\text{C}$  value slightly deviates to a more depleted value. The measured values for *trans*-DCE show also slight deviations to more depleted values compared to the EA/IRMS value

of the pure phase compound. Although most phase transfer processes are involved in purge-and-trap extraction, the technique resulted in isotope values that are in good agreement compared to pure phase standards. As shown in Table 1 all methods allowed highly reproducible carbon isotope ratio determinations with standard deviations that were in general  $\leq 0.3\%$ . Higher standard deviations could be observed only for *trans*-DCE extracted with P&T, when cryofocussing of the analyte failed due to problems with the cryotrap cooling. These results are in contrast to previous studies where poor reproducibilities were observed when SPME was used for highly chlorinated compounds (4,5).

As the oxidation capacity of the combustion unit can strongly affect  $\delta^{13}\text{C}$  determinations of the compounds (5), the CuO/NiO/Pt combustion reactor was regularly reoxidized after a set of approximately 40 measurements. Overall, the results demonstrate that all methods applied in this study allow for an accurate and highly reproducible carbon isotope ratio determination.

**Table 2-1.** Accuracy and reproducibility of VOC extraction methods applied within this study;  $\delta^{13}\text{C}$  values given in per mill (‰); signal heights  $\geq 1000\text{mV}$ .

		<i>trans</i> -DCE	<i>cis</i> -DCE	TCE	PCE
<b>EA/IRMS</b>	<b>Pure phase compound</b> <sup>1</sup>	-25.5 ( $\pm 0.1$ )	-25.8 ( $\pm 0.1$ )	-26.7 ( $\pm 0.1$ )	-27.3 ( $\pm 0.2$ )
<b>GC/IRMS</b>	<b>SPME (Carboxen/PDMS)</b> <sup>2</sup>	-25.9 ( $\pm 0.1$ )	-26.4 ( $\pm 0.1$ )	-26.7 ( $\pm 0.2$ )	-27.2 ( $\pm 0.1$ )
	<b>P&amp;T (40 mL)</b> <sup>3</sup>	-26.4 ( $\pm 0.5$ )	-26.0 ( $\pm 0.3$ )	-26.8 ( $\pm 0.2$ )	-27.2 ( $\pm 0.2$ )
	<b>P&amp;T (100 mL, PTFE)</b> <sup>4</sup>	-26.2 ( $\pm 0.4$ )	-25.8 ( $\pm 0.3$ )	-26.6 ( $\pm 0.3$ )	-27.2 ( $\pm 0.3$ )
	<b>P&amp;T (100 mL, PEEK)</b> <sup>5</sup>	-26.1 ( $\pm 0.3$ )	-25.8 ( $\pm 0.3$ )	-26.5 ( $\pm 0.3$ )	-27.1 ( $\pm 0.2$ )

<sup>1</sup> n=3; <sup>2</sup> this study, n=58; <sup>3</sup> this study, n=54 (except *trans*-DCE n=40), values available for vinyl chloride (-30.2‰;  $\pm 0.2$ ; n=5); <sup>4</sup> Jochmann et al. (12), n=12-33; <sup>5</sup> this study, n=30

### 2.4.3. Application to environmental field studies

**Solid-Phase Microextraction (SPME).** The SPME extraction technique to carbon isotope analysis of chlorinated ethenes was applied at a former dry cleaning site (*KORA-site: Rosengarten-Ehestorf*)(15). Results for a multilevel well are exemplarily shown in Figure 2-4. The steep concentration gradient of PCE towards the unsaturated zone hardly shows a change in isotopic composition, which suggests that no transformation is involved. In contrast, the concentration decrease towards the aquitard is accompanied by enrichment in  $^{13}\text{C}$ . Preferential microbial degradation of the light isotopologues results in an isotopic fractionation leading to a



progressive enrichment of heavy isotopologues in the residual reactant and the formation of a product depleted in heavy isotopes. Plotting the aquitard-near values via the Rayleigh equation results in a field isotope enrichment factor of  $\epsilon_{\text{field}} = -2.5\text{‰}$ . Under the anoxic conditions prevailing in this aquifer, the observed enrichment factor is quite consistent with reported data on anaerobic PCE degradation in batch experiments of  $\epsilon = -2\text{‰}$  (29) and  $\epsilon = -2.7$  to  $-5.5\text{‰}$  (30), respectively. The vertically resolved isotope profile observed in well B2 could not be confirmed in later sampling campaigns, indicating a dynamic groundwater system with non-consistent flow paths and changing zones of microbial activity. The most recent sampling campaign included the further downgradient well B5 (Figure 2-5). While the flow path B1 to B2 provides no evidence for degradation, the data observed along the flow path B2 to B5 clearly indicate *in-situ* biodegradation. The PCE concentration decreases are associated with an enrichment in  $^{13}\text{C}$  by almost 5‰. Calculation of isotope enrichment factors resulted in  $\epsilon_{\text{field}}$  values between  $-1.2\text{‰}$  and  $-2.4\text{‰}$  (dependent on the flow path), indicating that besides biodegradation, other, non-degradative attenuation processes are involved in concentration reduction at the site.

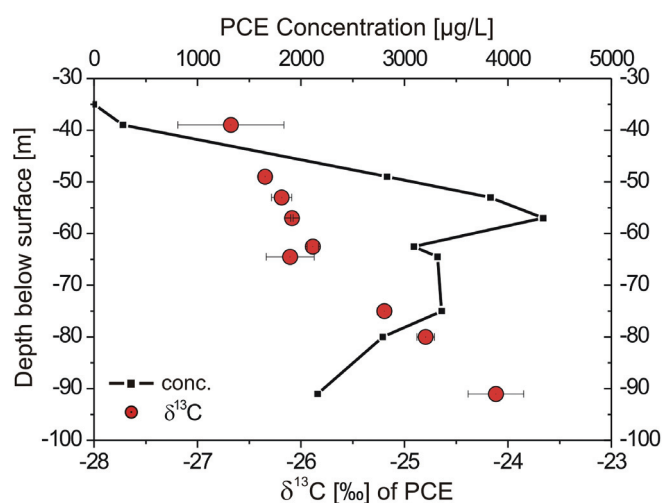


**Figure 2-4.** Concentration and carbon isotope data for PCE changing with depth of the aquifer. Internal reproducibility based on triplicate injections of samples and standards is generally  $< 0.5\text{‰}$ .

As isotopic compositions in natural groundwater systems are not significantly affected by sorption and dilution (see Chapter 1), the extent of *in-situ* biodegradation can be described independent of other attenuation processes that reduce the concentration of contaminants. Based on laboratory-derived isotope fractionation factors ( $\alpha$ ), the extent of biodegradation (B) can be

described as the relative amount of contaminant removal caused by *in-situ* biodegradation which is needed to alter the isotopic composition (see Chapter 1). The published range of fractionation factors (0.9945 to 0.998) (29,30) was applied to assess the extent of *in-situ* biodegradation based on the observed shifts in isotope ratios between the source area and the downgradient parts of the plume. The most depleted  $\delta^{13}\text{C}$  value at the site measured in source well B1 was assumed to represent the isotopic composition of the source ( $R_0 = -27.1\text{‰}$ ). The estimates of the percentage of biodegradation (B) along the profile B1 to B2 and B3, ranged from 5-14% and 15-37%, respectively. Along the flow path to the most downgradient well B5 estimates for the percentage of PCE biodegraded in the contaminated aquifer increased to 59% - 91%. Concerning complete reductive dehalogenation, some evidence such as  $\delta^{13}\text{C}$  enrichment of *cis*-DCE, isotopic mass balance considerations (Appendix of Chapter 2) and the presence of vinyl chloride (detected at G1 in May 2005 (15), no isotope data available), suggest that microbial degradation exceeds *cis*-DCE at the site.

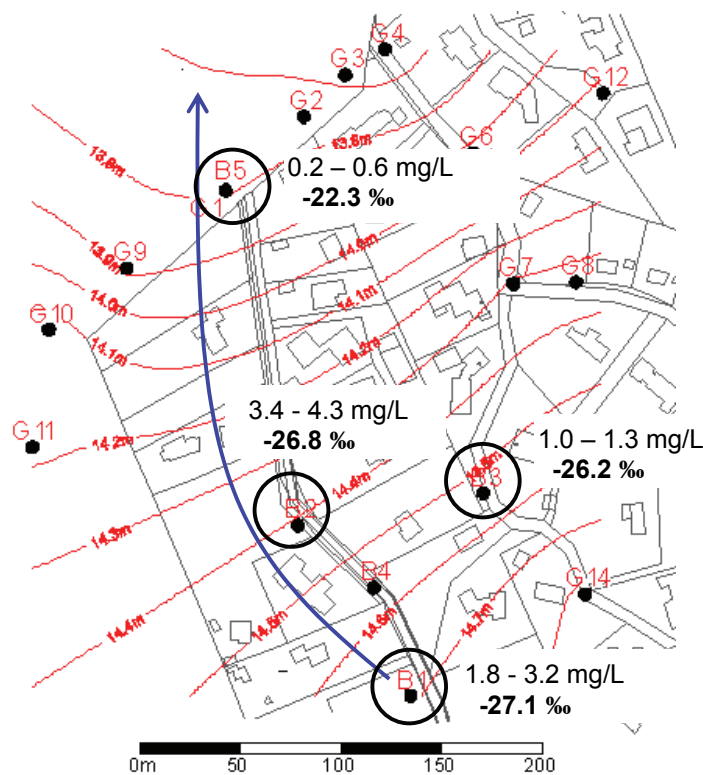
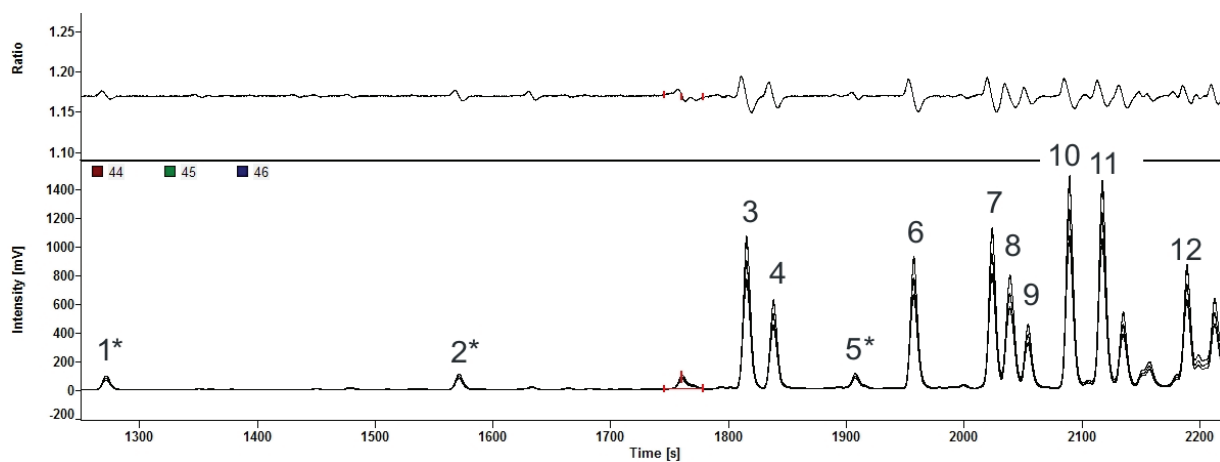


**Figure 2-5.** Concentration and  $\delta^{13}\text{C}$  values for PCE as qualitative evidence for microbial reductive dehalogenation along the water flow path B2 to B5. The most downgradient well of the site shows the lowest concentration associated with significantly enriched  $\delta^{13}\text{C}$  values. The estimates of biodegradation (B) along this flow path range from 59% to 91%.

**Purge-and-Trap Analysis with Enhanced Volume.** The improved P&T-system (equipped with PTFE-tubing) has been applied to low contaminated groundwater samples of the *KORA-sites Brand and Niedergörsdorf, Tanklager 1 (18)*. A representative GC/IRMS chromatogram (Figure 2-6) illustrates the good performance of the system. Although the compound concentration within this sample was below 1.5 µg/L, the improved P&T-system allowed to reliably determine  $\delta^{13}\text{C}$  values; except for compounds with a concentration of <0.1 µg/L (resulting in signal intensities below the method detection limit).

Exemplarily shown for benzene and 1,3,5-trimethylbenzene in Figure 2-7, the isotopic values determined by P&T-GC/IRMS give a clear indication for intrinsic biodegradation at the Niedergörsdorf-site. Decreases in concentration are associated with enrichment in  $^{13}\text{C}$  along the groundwater flow path. *In-situ* biodegradation can be demonstrated by the Rayleigh equation where the isotope fractionation factor ( $\alpha$ ) describes the relation between concentration and isotopic composition over the course of the reaction. A good correlation between the decreasing concentration and the enrichment of  $^{13}\text{C}$  in the contaminant indicates a biological transformation reaction along the observed groundwater flow path, as demonstrated by the plots in Figure 2-7 (with correlation coefficients always better than 0.9). The slope of the linear regression curve shows the extent of isotope fractionation (expressed as  $\epsilon_{\text{field}}$ ). Previous studies suggest that sulphate-reducing conditions are predominant at the site. The field-derived isotope enrichment factors (e.g.  $\epsilon_{\text{field}}$  for benzene -1.4‰) are significantly lower than enrichment factors obtained during laboratory (batch) biodegradation experiments at sulphate-reducing conditions (-3.6‰ (31)). Overall, the results obtained at Niedergörsdorf suggest that besides biodegradation, other, non-isotope fractionating, concentration-reducing processes (mainly dilution, dispersion) play an important role at this site.



\* Below MDL, <sup>1</sup> Benzene, <sup>2</sup> Toluene, <sup>3</sup> Ethylbenzene, <sup>4</sup> m-/p-Xylene, <sup>5</sup> o-Xylene, <sup>6</sup> Isopropylbenzene, <sup>7</sup> Propylbenzene, <sup>8</sup> 3,4-Ethyltoluene, <sup>9</sup> 1,3,5-Trimethylbenzene, <sup>10</sup> 2-Ethyltoluene, <sup>11</sup> 1,2,4-Trimethylbenzene, <sup>12</sup> 1,2,3-Trimethylbenzene

**Figure 2-6.** Representative GC/IRMS-chromatogram for groundwaters contaminated with kerosene, sampled at Niedergörsdorf TL1, extraction performed with enlarged-volume-P&T (PTFE tubing), concentration of compounds  $\leq 1.5 \mu\text{g/L}$ . The upper trace, representing the ratio of mass 45/44, serves as indicator for good chromatographic performance of the system.

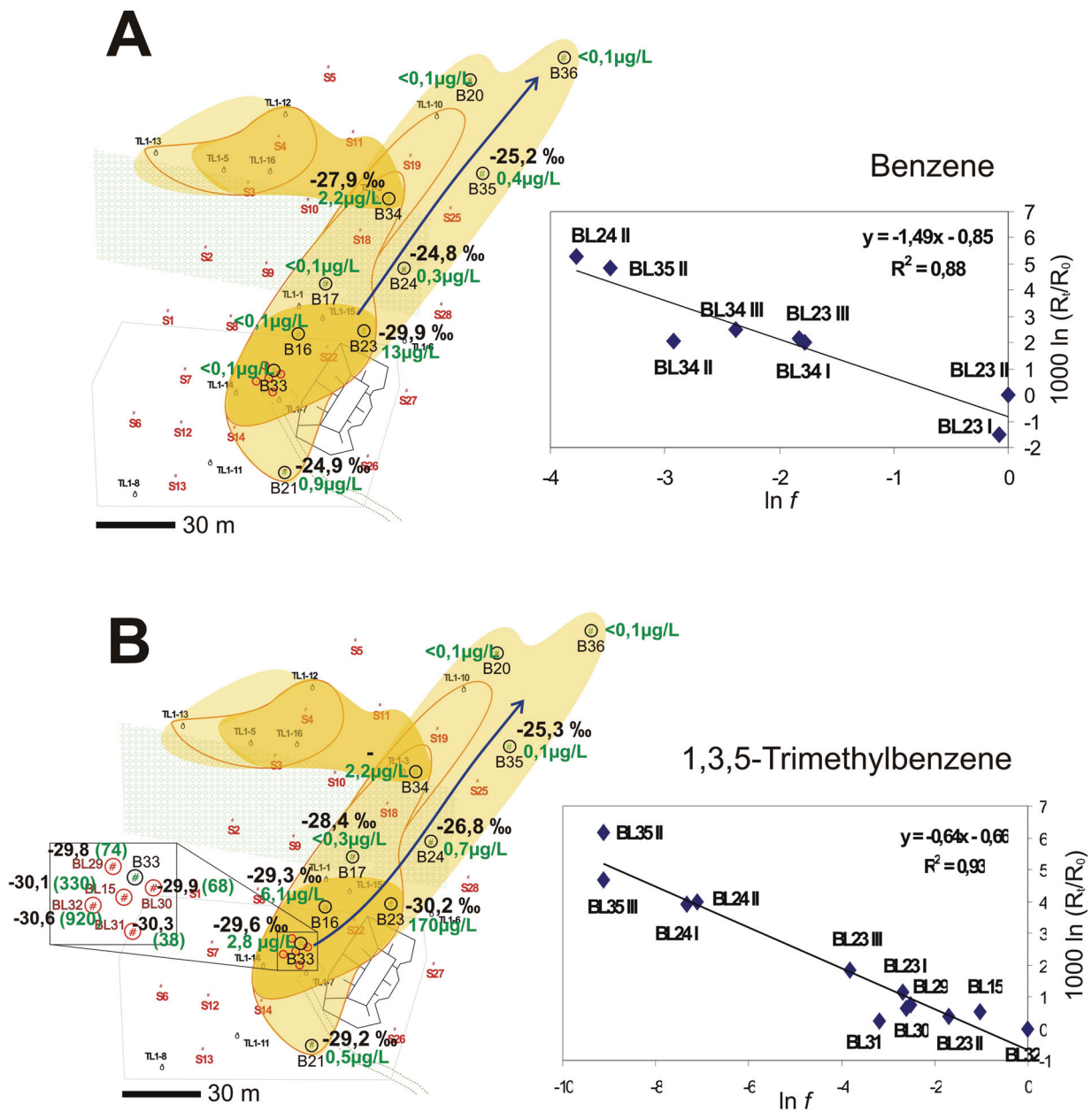
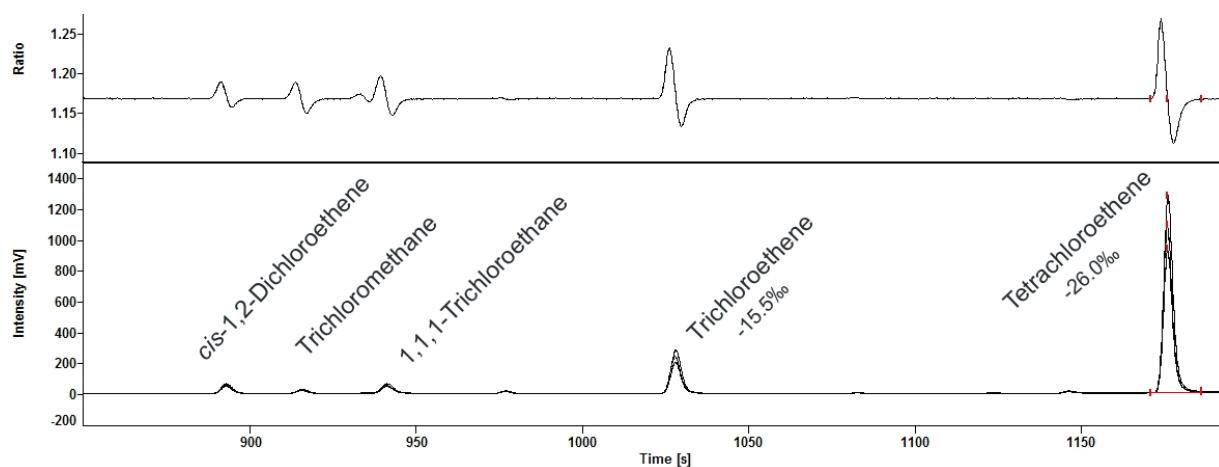


Figure 2-7. Left: Map of Niedergörsdorf illustrating concentration distribution and isotopic composition for A) benzene and B) 1,3,5-trimethylbenzene at the site. Right: Linear correlation of isotope composition versus concentration indicate *in-situ* biodegradation according to the Rayleigh equation (plotted wells are located along the flow path illustrated as blue arrows in the maps).

The further developed system using a PEEK-tubing for sample transfer has been applied to low level contaminated mineral waters of *mineral springs in Stuttgart-Bad Cannstatt*. The waters of the mineral springs contain the chlorinated solvents tetrachloroethene (up to 2.28  $\mu\text{g/L}$ ), trichloroethene (max. 0.83  $\mu\text{g/L}$ ) and traces of cis-1,2-dichloroethene that were below the MDLs of the GC/MS ( $<0.1$   $\mu\text{g/L}$ ), while vinyl chloride was absent. A chromatogram (Figure 2-8) illustrates the performance of the newly developed P&T-system for a mineral water contaminated with chlorinated hydrocarbons. The  $\delta^{13}\text{C}$  values measured for TCE within these mineral waters are all heavier than  $-17.9\text{‰}$ , indicating substantial TCE degradation. Overall, the results obtained for real groundwater samples demonstrate that the sample pre-concentration and extraction techniques applied are well suited for the compound-specific carbon isotope analysis of volatile compounds at trace concentrations. In addition, the techniques presented here provide the opportunity for GC/IRMS measurements of other stable isotope systems such as  $^{15}\text{N}/^{14}\text{N}$ ,  $^{18}\text{O}/^{16}\text{O}$  or D/H ratios, which require up to 10 times (32) higher analyte concentrations than  $^{13}\text{C}/^{12}\text{C}$  analyses.



**Figure 2-8.** GC/IRMS-chromatogram obtained for the analysis of a low-contaminated mineral water (Mombachquelle, Stuttgart) using the enhanced-volume P&T-system equipped with a PEEK-tubing as sample transfer loop. Signal intensities for cis-DCE, trichloromethane and 1,1,1-trichloroethane (0.1, 0.13 and 0.17  $\mu\text{g/L}$ , resp.) were below the MDL;  $\delta^{13}\text{C}$  values for TCE (0.36  $\mu\text{g/L}$ ) and PCE (2.28  $\mu\text{g/L}$ ) could be reliably determined.

## 2.5. References

- (1) Slater, G. F. Stable isotope forensics - When isotopes work. *Environ. Forensics* **2003**, *4*, 13-23.
- (2) Meckenstock, R. U.; Morasch, B.; Griebler, C.; Richnow, H. H. Stable isotope fractionation analysis as a tool to monitor biodegradation in contaminated aquifers. *J. Contam. Hydrol.* **2004**, *75*, 215-255.
- (3) Turner, J.; Albrechtsen, H. J.; Bonell, M.; Duguet, J. P.; Harris, B.; Meckenstock, R.; McGuire, K.; Moussa, R.; Peters, N.; Richnow, H. H.; Sherwood Lollar, B.; Uhlenbrook, S.; van Lanen, H. Future trends in transport and fate of diffuse contaminants in catchments, with special emphasis on stable isotope applications. *Hydrol. Process.* **2006**, *20*, 205-213.
- (4) Hunkeler, D.; Aravena, R. Determination of compound-specific carbon isotope ratios of chlorinated methanes, ethanes, and ethenes in aqueous samples. *Environ. Sci. Technol.* **2000**, *34*, 2839-2844.
- (5) Zwank, L.; Berg, M.; Schmidt, T. C.; Haderlein, S. B. Compound-specific carbon isotope analysis of volatile organic compounds in the low-microgram per liter range. *Anal. Chem.* **2003**, *75*, 5575-5583.
- (6) Dayan, H.; Abrajano, T.; Sturchio, N. C.; Winsor, L. Carbon isotopic fractionation during reductive dehalogenation of chlorinated ethenes by metallic iron. *Org. Geochem.* **1999**, *30*, 755-763.
- (7) Dias, R. F.; Freeman, K. H. Carbon isotope analyses of semivolatile organic compounds in aqueous media using solid-phase microextraction and isotope ratio monitoring GC/MS. *Anal. Chem.* **1997**, *69*, 944-950.
- (8) Arthur, C. L.; Pawliszyn, J. Solid phase microextraction with thermal desorption using fused silica optical fibers. *Anal. Chem.* **1990**, *62*, 2145-2148.
- (9) Koziel, J.; Jia, M.; Khaled, A.; Noah, J.; Pawliszyn, J. Field air analysis with SPME device. *Anal. Chim. Acta* **1999**, *400*, 153-162.
- (10) Measurement of Purgeable Organic Compounds in Water by Capillary Column Gas Chromatography/Mass Spectrometry; Method 524.4, Revision 4.1, US Environmental Protection Agency. Cincinnati, OH, **1995**: 48 pp.
- (11) Auer, N. R.; Manzke, B. U.; Schulz-Bull, D. E. Development of a purge and trap continuous flow system for the stable carbon isotope analysis of volatile halogenated organic compounds in water. *J. Chromatogr. A* **2006**, *1131*, 24-36.
- (12) Jochmann, M. A.; Blessing, M.; Haderlein, S. B.; Schmidt, T. C. A new approach to determine method detection limits for compound-specific isotope analysis of volatile organic compounds. *Rapid Commun. Mass Spectrom.* **2006**, *20*, 3639-3648.
- (13) Barcelona, M. J.; Helfrich, J. A.; Garske, E. E. Sampling Tubing Effects on Groundwater Samples. *Anal. Chem.* **1985**, *57*, 460-464.
- (14) Reynolds, G. W.; Hoff, J. T.; Gillham, R. W. Sampling Bias Caused by Materials Used To Monitor Halocarbons in Groundwater. *Environ. Sci. Technol.* **1990**, *24*, 135-142.
- (15) Martac, E.; Zamfirescu, D.; Teutsch, G.; *KORA – TV3.5: Gemeinsamer Schlussbericht, Förderkennzeichen 02WN0437*; Feldmaßstäbliche Quantifizierung des NA-Potentials in mächtigen Grundwasserleitern mit hohem Flurabstand; Beispiel: CKW-Schaden, Chemische Reinigung in Rosengarten-Ehestorf; Tübingen, **2006**.
- (16) Peter, A.; Steinbach, A.; Liedl, R.; Ptak, T.; Michaelis, W.; Teutsch, G. Assessing microbial degradation of o-xylene at field-scale from the reduction in mass flow rate combined with compound-specific isotope analyses. *J. Contam. Hydrol.* **2004**, *71*, 127-154.
- (17) Amt für Umweltschutz Stuttgart, *KORA - TV1: Forschungsbericht, Förderkennzeichen 02WN0353*; Projekt 1.3: Natürlicher Abbau und Rückhalt eines komplexen Schadstoffcocktails in einem Grundwasserleiter am Beispiel des ehemaligen Mineralölwerks Epple; Stuttgart, **2007**.
- (18) Peter, A.; Miles, B.; Teutsch, G.; *KORA – TV1: Abschlussbericht zum Forschungsvorhaben, Förderkennzeichen 02WN0352*; Natural Attenuation (NA) and Enhanced Natural Attenuation (ENA) an typischen Mineralölstandorten am Beispiel Brand und Niedergörsdorf; Tübingen, **2007**.
- (19) Armbruster, H.; Dornstädter, J.; Kappelmeyer, O.; Ufrecht, W. Thermische Untersuchungen im Neckar zwischen Bad-Cannstatt und Münster zum Nachweis von Mineralwasseraustritten. *Deutsche Gewässerkundliche Mitteilungen* **1998**, *42*, 9-14.
- (20) Ufrecht, W. Vulnerabilität und Schutzmaßnahmen im Quellgebiet der Stuttgarter Mineral- und Heilwässer. *Zeitschrift für Angewandte Geologie* **2001**, *47*, 47-54.
- (21) Goldscheider, N.; Hötzl, H.; Käss, W.; Ufrecht, W. Combined tracer tests in the karst aquifer of the artesian mineral springs of Stuttgart, Germany. *Environmental Geology* **2003**, *43*, 922-929.
- (22) Schwarzenbach, R. P.; Gschwend, P. M.; Imboden, D. M. *Environmental Organic Chemistry*; 2nd edition ed.; John Wiley & Sons: New York, 2003.
- (23) Leggett, D. C.; Parker, L. V. Modeling the Equilibrium Partitioning of Organic Contaminants between PTFE, PVC, and Groundwater. *Environ. Sci. Technol.* **1994**, *28*, 1229-1233.

- (24) Glaser, B.; Amelung, W. Determination of C-13 natural abundance of amino acid enantiomers in soil: methodological considerations and first results. *Rapid Commun. Mass Spectrom.* **2002**, *16*, 891-898.
- (25) Schmitt, J.; Glaser, B.; Zech, W. Amount-dependent isotopic fractionation during compound-specific isotope analysis. *Rapid Commun. Mass Spectrom.* **2003**, *17*, 970-977.
- (26) Sherwood Lollar, B.; Hirschorn, S. K.; Chartrand, M. M. G.; Lacrampe-Couloume, G. An approach for assessing total instrumental uncertainty in compound-specific carbon isotope analysis: Implications for environmental remediation studies. *Anal. Chem.* **2007**, *79*, 3469-3475.
- (27) Wilcke, W.; Krauss, M.; Amelung, W. Carbon isotope signature of polycyclic aromatic hydrocarbons (PAHs): Evidence for different sources in tropical and temperate environments? *Environ. Sci. Technol.* **2002**, *36*, 3530-3535.
- (28) Song, D. L.; Conrad, M. E.; Sorenson, K. S.; Alvarez-Cohen, L. Stable carbon isotope fractionation during enhanced in situ bioremediation of trichloroethene. *Environ. Sci. Technol.* **2002**, *36*, 2262-2268.
- (29) Hunkeler, D.; Aravena, R.; Butler, B. J. Monitoring microbial dechlorination of tetrachloroethene (PCE) in groundwater using compound-specific stable carbon isotope ratios: Microcosm and field studies. *Environ. Sci. Technol.* **1999**, *33*, 2733-2738.
- (30) Slater, G. F.; Sherwood Lollar, B.; Sleep, B. E.; Edwards, E. A. Variability in carbon isotopic fractionation during biodegradation of chlorinated ethenes: Implications for field applications. *Environ. Sci. Technol.* **2001**, *35*, 901-907.
- (31) Mancini, S. A.; Ulrich, A. C.; Lacrampe-Couloume, G.; Sleep, B.; Edwards, E. A.; Sherwood Lollar, B. Carbon and hydrogen isotopic fractionation during anaerobic biodegradation of benzene. *Appl. Environ. Microbiol.* **2003**, *69*, 191-198.
- (32) Schmidt, T. C.; Zwank, L.; Elsner, M.; Berg, M.; Meckenstock, R. U.; Haderlein, S. B. Compound-specific stable isotope analysis of organic contaminants in natural environments: a critical review of the state of the art, prospects, and future challenges. *Anal. Bioanal. Chem.* **2004**, *378*, 283-300.



## 2.6. Appendix

**Extraction Parameters and Analytical Conditions.** GC column used for analyte separation. The analytical separation of VOCs was carried out with an Rtx-VMS capillary column (60 m x 0.32 mm, 1.8  $\mu$ m film thickness; Restek Corp., Bellefonte, PA, USA). The temperature programs used to obtain baseline separation of the target analytes are presented in Table A2-1.

Table A2-1. Purge-and-trap parameters and gas chromatographic conditions.

Extraction/Purge Mode		Desorption / Injection		GC-Conditions	
<b>Conventional P&amp;T-System (40 mL-vials):</b>				<b>CHC Epple samples:</b>	
<b>Purge volume</b>	25 mL	<b>Temp</b>	240 °C	<b>Temp ini</b>	40 °C
<b>Pressurize time</b>	0.70 min	<b>Time</b>	2 min	<b>Hold time</b>	11 min
<b>Transfer time</b>	0.80 min	<b>Flow</b>	200 mL/min	<b>Ramp 1</b>	7 °C/min
<b>Purge time</b>	11 min	<b>Transfer temp</b>	250 °C	<b>Temp (hold)</b>	100 °C (2 min)
<b>Purge flow</b>	40 mL/min	<b>Cryotrap</b>	-100°C (VC -130°C)	<b>Ramp 2</b>	20 °C/min
<b>Dry purge</b>	3 min	<b>Cryo heat</b>	240 °C (30 °C/sec)	<b>Temp fin</b>	220 °C
		<b>Split flow 1</b>	splitless (0 mL/min)	<b>Hold time</b>	4 min
		<b>Transfer flow</b>	2 mL/min	<b>Column flow</b>	1.0 mL/min
		<b>Split flow 2</b>	10 mL/min		
<b>Enhanced Volume P&amp;T, PTFE loop (100 mL-bottles):</b>				<b>BTEX samples:</b>	
<b>Purge volume</b>	76 mL	<b>Temp</b>	250 °C	<b>Temp ini</b>	40 °C
<b>Pressurize time</b>	2.80 min	<b>Time</b>	2 min	<b>Hold time</b>	10 min
<b>Transfer time</b>	3.20 min	<b>Flow</b>	200 mL/min	<b>Ramp 1</b>	4 °C/min
<b>Purge time</b>	15 min	<b>Transfer temp</b>	250 °C	<b>Temp 1 (hold)</b>	100 °C (2 min)
<b>Purge flow</b>	50 mL/min	<b>Cryotrap</b>	-100 °C	<b>Ramp 2</b>	10 °C/min
<b>Dry purge</b>	4 min	<b>Cryo heat</b>	240 °C (30 °C/sec)	<b>Temp 2 (hold)</b>	170 °C (2 min)
		<b>Split flow 1</b>	splitless (0 mL/min)	<b>Ramp 3</b>	10 °C/min
		<b>Transfer flow</b>	2 mL/min	<b>Temp fin (hold)</b>	200 °C (2 min)
		<b>Split flow 2</b>	10 mL/min	<b>Column flow</b>	1.0 mL/min
<b>Enhanced Volume P&amp;T, PEEK loop (100 mL-bottles):</b>				<b>CHC samples:</b>	
<b>Purge volume</b>	76 mL	<b>Temp</b>	250 °C	<b>Temp ini</b>	40 °C
<b>Pressurize time</b>	1.5 min	<b>Time</b>	2 min	<b>Hold time</b>	7 min
<b>Transfer time</b>	1.6 min	<b>Flow</b>	200 mL/min	<b>Ramp 1</b>	7 °C/min
<b>Purge time</b>	15 min	<b>Transfer temp</b>	250 °C	<b>Temp (hold)</b>	100 °C (1 min)
<b>Purge flow</b>	50 mL/min	<b>Cryotrap</b>	-100 °C	<b>Ramp 2</b>	20 °C/min
<b>Dry purge</b>	4 min	<b>Cryo heat</b>	240 °C (30 °C/sec)	<b>Temp fin</b>	200 °C
		<b>Split flow 1</b>	splitless (0 mL/min)	<b>Hold time</b>	2 min
		<b>Transfer flow</b>	2 mL/min	<b>Column flow</b>	1.5 mL/min
		<b>Split flow 2</b>	10 mL/min		

**Isotope Mass Balance at Rosengarten-Ehestorf.** The  $\delta^{13}\text{C}$  of the total of all chlorinated ethenes was calculated by multiplying the molar concentration of each compound with its  $\delta^{13}\text{C}$  value, adding all contributions and dividing the sum by the total molar concentration. If all chlorinated ethenes are present and sampled at the site,  $\delta^{13}\text{C}$  value of the sum ( $\delta^{13}\text{C}$  total, Table A2-2) should reflect the initial isotopic composition of the initial contaminant. The  $\delta^{13}\text{C}$  measurements performed in 2004 during immission pumping tests revealed most depleted values of -27.4‰ for source-near PCE. Due to imbalance of the isotopic mass balance it can be assumed that the degradation exceeds cis-DCE to vinyl chloride or complete mineralisation (although not detected). An additional indication is the presence of vinyl chloride measured in a geoprobe well (G1, later multi-level well B5). Further isotope data of several sampling campaigns and immission pumping tests performed at the site are available in our joint project report:

Martac, E.; Zamfirescu, D.; Teutsch, G.; *KORA – TV3.5: Gemeinsamer Schlussbericht, Förderkennzeichen 02WN0437*; Feldmaßstäbliche Quantifizierung des NA-Potentials in mächtigen Grundwasserleitern mit hohem Flurabstand; Beispiel: CKW-Schaden, Chemische Reinigung in Rosengarten-Ehestorf; Tübingen, **2006**.

**Table A2-2.** Isotopic mass balance considerations at the site.

	Concentration [ $\mu\text{g/L}$ ]				Concentration [ $\mu\text{mol/L}$ ]				$\delta^{13}\text{C}$ [‰]			
	PCE	TCE	cDCE	total	PCE	TCE	cDCE	total	PCE	TCE	cDCE	total
<b>B1</b>	1590.00	16.40	48.40	1655	9.59	0.12	0.50	10.21	-27.0	-28.0	-19.5	-26.6
<b>B2</b>	1490.00	45.50	146.00	1682	8.99	0.35	1.51	10.84	-26.3	-27.7	-23.2	-25.9
<b>B3</b>	608.67	29.23	28.42	666	3.67	0.22	0.29	4.19	-25.6	-23.0	-25.5	-25.5
<b>B5</b>	38.60	6.48	24.60	70	0.23	0.05	0.25	0.54	-22.3	-24.2	-24.2	-23.4

**Estimates on Biodegradation (%) at Niedergörsdorf.** The published range of enrichment factors ( $\epsilon_{\text{min}}$  to  $\epsilon_{\text{max}}$ , given in Table 2-A3) was applied to assess the extent of *in-situ* biodegradation based on the observed shifts in isotope ratios between the source area and the downgradient parts of the plume. The most depleted  $\delta^{13}\text{C}$  value at the site measured in the source area was assumed to represent the initial isotopic composition. The estimates of the percentage of biodegradation (B) along the downgradient flowpath (depicted in Figure 2-7, Chapter 2) at Niedergörsdorf are shown in Figure A2-1.

Additional isotope data and discussions for the two former military airfield sites at Brand and Niedergörsdorf are available in our joint KORA project report:

Peter, A.; Miles, B.; Teutsch, G.; *KORA – TV1: Abschlussbericht zum Forschungsvorhaben, Förderkennzeichen 02WN0352*; Natural Attenuation (NA) und Enhanced Natural Attenuation (ENA) an typischen Mineralölstandorten am Beispiel Brand und Niedergörsdorf; Tübingen, **2007**.

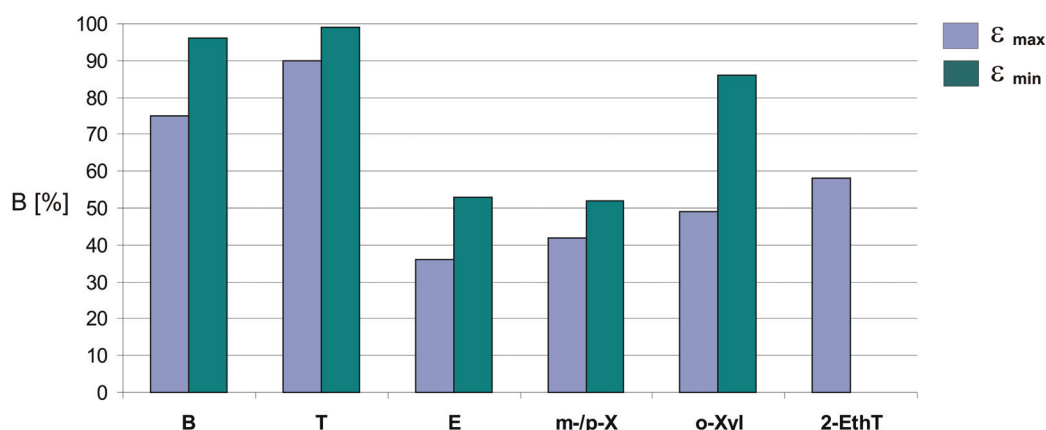


Figure A2-1. Biodegradation estimates for kerosene-contamination at KORA-site Niedergörsdorf (in percent).

Table A2-3. Applied enrichment factors (batch experiments) for biodegradation estimates.

	Enrichment factors (‰)	
	$\epsilon_{\max}$	$\epsilon_{\min}$
Benzene	-3.6 (1)	-1.5 (2)
Toluene	-2.2 (3)	-0.8 (4)
Ethylbenzene	-3.7 (5)	-2.2 (6)
m-/p-Xylene	-2.3 (7)	-1.8 (8)
o-Xylene	-3.2 (5)	-1.1 (9)
2-Ethyltoluene	-3.7 (5)	-

- (1) Mancini, S. A.; Ulrich, A. C.; Lacrampe-Couloume, G.; Sleep, B.; Edwards, E. A.; Sherwood Lollar, B. Carbon and hydrogen isotopic fractionation during anaerobic biodegradation of benzene. *Appl. Environ. Microbiol.* **2003**, *69*, 191-198.
- (2) Hunkeler, D.; Anderson, N.; Aravena, R.; Bernasconi, S. M.; Butler, B. J. Hydrogen and carbon isotope fractionation during aerobic biodegradation of benzene. *Environ. Sci. Technol.* **2001**, *35*, 3462-3467.
- (3) Morasch, B.; Richnow, H. H.; Schink, B.; Meckenstock, R. U. Stable hydrogen and carbon isotope fractionation during microbial toluene degradation: Mechanistic and environmental aspects. *Appl. Environ. Microbiol.* **2001**, *67*, 4842-4849.
- (4) Ahad, J. M. E.; Sherwood Lollar, B.; Edwards, E. A.; Slater, G. F.; Sleep, B. E. Carbon isotope fractionation during anaerobic biodegradation of toluene: Implications for intrinsic bioremediation. *Environ. Sci. Technol.* **2000**, *34*, 892-896.
- (5) Wilkes, H.; Boreham, C.; Harms, G.; Zengler, K.; Rabus, R. Anaerobic degradation and carbon isotopic fractionation of alkylbenzenes in crude oil by sulphate-reducing bacteria. *Org. Geochem.* **2000**, *31*, 101-115.
- (6) Meckenstock, R. U.; Morasch, B.; Griebler, C.; Richnow, H. H. Stable isotope fractionation analysis as a tool to monitor biodegradation in contaminated aquifers. *J. Contam. Hydrol.* **2004**, *75*, 215-255.
- (7) Morasch, B.; Richnow, H. H.; Schink, B.; Vieth, A.; Meckenstock, R. U. Carbon and hydrogen stable isotope fractionation during aerobic bacterial degradation of aromatic hydrocarbons. *Appl. Environ. Microbiol.* **2002**, *68*, 5191-5194.
- (8) Morasch, B.; Richnow, H. H.; Vieth, A.; Schink, B.; Meckenstock, R. U. Stable isotope fractionation caused by glycol radical enzymes during bacterial degradation of aromatic compounds. *Appl. Environ. Microbiol.* **2004**, *70*, 2935-2940.
- (9) Richnow, H. H.; Annweiler, E.; Michaelis, W.; Meckenstock, R. U. Microbial in situ degradation of aromatic hydrocarbons in a contaminated aquifer monitored by carbon isotope fractionation. *J. Contam. Hydrol.* **2003**, *65*, 101-120.

### **3. Semi-Volatile Contaminants at Trace Concentrations: Evaluation of a Large Volume Injection – GC/IRMS-Method**

#### ***3.1. Introduction***

Compound-specific isotope analysis (CSIA) allows to determine the isotopic composition of individual contaminants by hyphenated gas chromatography and isotope ratio mass spectrometry (GC/IRMS) with applications ranging from pharmacology, doping analysis, food adulteration to the broad field of forensic and environmental studies (1). Especially in the past decade, CSIA has emerged as a mature technique to investigate both the fate and the source of organic contaminants in environmental forensics (2). Polycyclic aromatic hydrocarbons (PAHs) are ubiquitous environmental contaminants, naturally occurring in coal, crude oil and gasoline and their byproducts, e.g. coal tar or creosote. PAHs are primarily derived through combustion processes of organic materials, such as wood or fossil fuels (3). For example, PAHs are often found at coal gasification sites, persistently impairing the quality of soil, water and air. Several studies have demonstrated the usefulness of compound-specific isotope analysis as a tool for the apportionment of multiple sources of PAH contaminants in the environment (4-8).

IRMS detectors are designed for measuring isotope ratios with a very high precision at or near their natural abundance; four orders of magnitude greater than with a conventional mass spectrometer (9). Typically, 1 nmol carbon of each analyte is necessary for an adequate and reliable determination of  $\delta^{13}\text{C}$  with GC/IRMS instruments (9,10). That means, in case of a 1  $\mu\text{L}$ -splitless injection a concentration of 83 mg/L for tetrachloroethene, and 13 mg/L for naphthalene is demanded in the solvent extract. A requirement that would premise aqueous concentrations that are often much higher than actually found at a contaminated field site, especially at the fringes of a plume. With increasing demand of lowering detection limits in GC/IRMS applications, efficient methods for preconcentration of the analytes and improved injection techniques have been developed. Methods that were evaluated for this purpose include, in order of increasing sensitivity, split/splitless injection (11,12), on-column injection (12), headspace methods (13-15), solid-phase microextraction (SPME) (12,16-19), and the purge and trap (P&T) extraction technique (12,20,21) as method with the lowest detection limits. In quantitative analysis of semi-volatile compounds such as PAHs, large volume injection (LVI) techniques for gas chromatography have been developed that can easily improve sensitivity by injecting larger

volumes instead of injecting the conventional 1 to 2  $\mu\text{L}$  of a solvent extract into the capillary GC system. While SPME and P&T are well established methods for the compound-specific isotope analysis of individual organic compounds at trace concentrations, the application of large volume injection techniques has been restricted to quantitative analysis. LVI techniques have been applied to environmental measurements since the early 1990s (22); most of the methods are based on programmed temperature vaporizer (PTV) injectors where the sample is injected at a temperature below the boiling point of the solvent. The solvent is subsequently evaporated from the liner while simultaneously the less volatile compounds are trapped in the cold liner (23). During the last decade a number of papers applying large volume injection techniques to the quantitative analysis of semi-volatile compounds such as polychlorinated biphenyls, pesticides and polycyclic aromatic hydrocarbons have been published (22-25).

It has been shown that isotope fractionation during sample injection may lead to systematic errors due to mass discrimination effects (26-28). Large volume sample introduction using a PTV-split/splitless-injector might be sensitive to isotope fractionation, e.g. due to the process of solvent evaporation or adsorption of analytes to the liner packing. Therefore, particular attention should be paid to the possibility of isotope fractionation associated with the application of this new method in GC/IRMS. This work presents a method validation for a PTV-based large volume injection technique linked with a GC/IRMS device. A PTV-based solvent-split injection technique where the sample is injected at temperatures below the boiling point of the solvent was applied. The solvent is subsequently vented via the split outlet, while the analytes of interest are retained on the liner packing. The PTV is then heated with a defined speed to a temperature, necessary for the complete evaporation of the sample and the analytes are transferred to the analytical column in splitless mode. The analytical methodology was thoroughly evaluated in terms of its accuracy, precision, linearity, reproducibility and limits of detection. A sensitive and precise sample introduction strategy for measuring isotope compositions of individual compounds (LVI-GC/IRMS) was developed, especially important for the environmental analysis of semi-volatile organic contaminants at trace levels. Finally, the method was validated in a case study to distinguish the origin of polycyclic aromatic hydrocarbons in soil samples taken from a former mineral oil facility with long and in parts unknown operational history.

### 3.2. Experimental Section

**Reagents and Solvents.** Naphthalene (N, 99%), acenaphthylene (Ay, 97%), acenaphthene (Ace, 99%), dibenzofuran (Dbf, 99%), fluorene (Fl, 98%), phenanthrene (Phe, 98-99%), fluoranthene (Fla, 98-99%), pyrene (Pyr, 99%), benzo(a)anthracene (BaA, 99%) were all obtained from Aldrich. Perylene (Per, 99.9%) and 1-methylnaphthalene (MeN, 99.8%) were purchased from Dr. Ehrenstorfer and RiedelDeHaen, respectively. Cyclohexane (CH, SupraSolv® from Merck) was used to prepare the stock solution. CH (SupraSolv®) and *n*-pentane (UniSolv®) both from Merck were used to dilute for standard solutions. Acetone (SupraSolv® from Merck) was used for soil sample extractions; silica gel 60 (0.063-0.2 mm, from Carl Roth), CH and Trichloromethane (HPLC grade from Aldrich) were used for cleanup of the extracts.

**Compound-Specific Isotope Analysis (CSIA).** Carbon isotope compositions ( $\delta^{13}\text{C}$ ) of individual PAHs were determined using a gas chromatograph (Trace GC ultra, Thermo Finnigan, Milan, Italy) that was connected to a Delta<sup>PLUS</sup> XP (Thermo Finnigan, Bremen, Germany) isotope ratio mass spectrometer. The device was coupled on-line via a combustion interface (GC Combustion III) operated at 940 °C (with CuO, NiO and Pt wires as the oxidant and catalyst, respectively). The gas chromatograph was equipped with a DB-5ms capillary column, 30m length, 0.25 mm i.d., and 0.25  $\mu\text{m}$  film thickness from J&W Scientific (Agilent Technologies). For separation of PAH compounds, the GC oven temperature program started from 45 °C (4 min isothermal), was heated at a rate of 10 °C/min to 310 °C and held isothermally at this temperature for 5 min until the end of the GC run. Helium<sup>5.0</sup> was used as carrier gas at a column flow rate of 2 mL/min. Isotope signatures of the compounds are reported in the  $\delta$ -notation relative to Vienna Pee Dee Belemnite (VPDB) and were obtained using CO<sub>2</sub> that was calibrated against referenced CO<sub>2</sub>. Before each measurement three pulses of CO<sub>2</sub> reference gas were injected via the interface unit to the IRMS. The combustion reactor was reoxidized before each set of samples (approximately every 30-35 measurements). Each data point was recorded in triplicate.

**PTV Solvent Vent Mode Injections.** The injection system consisted of a programmable temperature vaporizer (PTV) injector (Optic 3, ATAS GL, Veldhoven, The Netherlands). Large-volume injections were performed using the CombiPAL autosampler with a 250  $\mu\text{L}$  syringe set to an injection speed of 25  $\mu\text{L/s}$ . Injection volumes were 50, 100, and 150  $\mu\text{L}$ , respectively. The PTV injector was equipped with an ATAS GL 8270 LVI packed liner (3.4 mm liner i.d.) developed to meet all US EPA Method 8270 performance requirements for the analysis of semi-volatiles by GC and GC-MS. (The material of the liner packing is unknown.) The volume of the

inserted liner allows sample amounts to be injected of up to 150  $\mu\text{L}$  (23). During large-volume injection the inlet temperature was held at 20  $^{\circ}\text{C}$  for pentane, and 60 $^{\circ}\text{C}$  for cyclohexane, while the flow rate through the split vent was set to 100 mL/min. Adequate solvent elimination was performed automatically, as the end time of venting was controlled by a solvent level sensor (set to 1, 5 and 10% of solvent remaining, resp.). After the split valve was closed, subsequent heating with a rate of 15  $^{\circ}\text{C}/\text{sec}$  until 300  $^{\circ}\text{C}$  transferred the analytes to the analytical column with a flow of 3 mL for 1 min. For comparison of the results 1 $\mu\text{L}$  injections were performed in splitless mode. The injector was then equipped with a splitless liner and operated at 300  $^{\circ}\text{C}$ . Concentrations and volumes injected were chosen to deliver a sample amount of approximately between 2 to 2.5 and 200 to 300 ng C per compound on the column (between 10-15 and 150-220 ng for 1  $\mu\text{L}$  injections).

**Preparation of Soil Samples.** Soil samples taken from a former mineral oil facility were extracted with pressurized solvent extraction working with acetone at 100  $^{\circ}\text{C}$  and 100 bar using an accelerated solvent extractor (ASE 200 from Dionex, Sunnyvale, CA, USA). The collected solvent extracts were exchanged to 15 mL cyclohexane by liquid-liquid extraction (with addition of millipore water). After concentrating the cyclohexane extracts to 5 mL (rotary evaporator at 40  $^{\circ}\text{C}$  and 230 mbar), the extracts were purified on a 18 cm silica gel column with flash chromatography using non-polar solvents. Details on the clean-up procedure are provided in the Appendix at the end of this chapter.

**Validation of the Method.** Different injection parameters have been tested for a representative set of individual PAH compounds ranging from 2- to 5-ring molecular structures (naphthalene to perylene). In addition, a medium sized heterocyclic aromatic compound was included (dibenzofuran). Volumes of 50, 100 and 150  $\mu\text{L}$  of the same standard solution were injected, different solvents and injection temperatures and various solvent levels (set to 1, 5 and 10% of solvent remaining, resp.) were compared. Comparisons included also the results of a conventional 1  $\mu\text{L}$  injection versus large volume injection (LVI). The concentrations used to test for amount-dependent non-linearity effects in this work range from 0.05 to 1.9-2.9 mg/L (according to compound) for PTV-large volume injections and from 10-15 to 150-220 mg/L (according to compound) for the conventional 1 $\mu\text{L}$ -splitless injections. Signal intensities are reported using the area or peak height of the  $^{12}\text{CO}_2$  peak ( $m/z$  44),  $\delta^{13}\text{C}$  values are given in ‰ relative to VPDB, standard deviations (Stdev, S) are based on triplicate measurements. Method detection limits are determined according to a previously described approach that assesses the total instrumental uncertainty in GC/IRMS analysis (29).

### 3.3. Results and Discussion

**Discrimination Effects and Signal Intensity.** To study the effect of different solvents on the instrumental response, PAH standards were diluted in cyclohexane and *n*-pentane and injected with varying initial PTV inlet temperatures. Injection of cyclohexane extracts was performed at 60 °C and 20 °C, respectively, and *n*-pentane extracts were injected at 20 °C and 10 °C, respectively. Working with these solvents at the different PTV initial temperatures resulted in significant differences in sensitivities, especially for low-molecular weight PAH compounds (illustrated in Figure 3-1). Substantial loss of volatile compounds of the PAH mixture diluted in cyclohexane occurred at 60 °C and at 20 °C, due to co-evaporation with the solvent. Similar observations were reported for quantitative analysis where PTV initial inlet temperatures were a critical factor in determining the sensitivity of PAHs with 2 to 3 rings (22,23). However, the discrimination effects observed show that the limiting factor is not merely the PTV initial temperature, but also the fact that the difference in boiling points between the solvent and the compound of interest needs to be high enough (>200 °C). Responses for compounds with molecular structures larger than fluorene increased with higher PTV initial inlet temperatures (60 °C for cyclohexane and 20 °C for *n*-pentane, respectively.) The slight increase in recoveries with increasing initial temperatures for high-molecular weight PAHs was also reported by Norlock et al. (22). Appropriate analysis of the 2- to 3-ring PAH compounds requires the use of *n*-pentane (at 10 or 20 °C) as a solvent. Both, 20 °C for cyclohexane and 10 °C for *n*-pentane required impractically long evaporation times and hence, are not considered in the following. The general enhancement in sensitivities with LVI-GC/IRMS is illustrated in exemplary chromatograms of PAH standards comparing a 100 µL PTV large volume injection with a conventional 1 µL splitless injection (see Figure 3-5 in the chromatographical resolution section). A linear correlation of instrumental response (peak area) and amount of compound injected was observed. Coefficients of determination ( $R^2$ ) were better than 0.99 for all compounds under the various parameters that were tested, with the exception of low-molecular weight PAHs diluted in cyclohexane. Correlation coefficients for cyclohexane are increasing with dibenzofuran ( $R^2$  0.58) and fluorene ( $R^2 >0.95$ ) and are better than 0.99 for all compounds with a molecular weight of phenanthrene and higher. Figure 3-2 shows the linear behavior exemplarily for a 2-ring and a 5-ring PAH molecule. The effect of different rates of solvent elimination on peak area was tested with the PTV solvent level sensor set to 1, 5 and 10%, respectively, during injection of 100 µL of PAH standards diluted in *n*-pentane. A linear relationship of injection volume versus peak area



could be confirmed for all compounds diluted in *n*-pentane. As the LVI liners used in this study (3.4 mm i.d.), can retain 150  $\mu\text{L}$  of solvent (23), volumes of samples injected were 50, 100 and 150  $\mu\text{L}$ . The proportional improvement of peak areas with increasing injection volume is exemplarily shown for naphthalene and perylene in Figure 3-3. As the response for various solvent levels was observed to be slightly better for 1% (see Figure 3-2) and to prevent the system from high levels of solvent being introduced with the injection of large sample volumes, the end of venting was adjusted to the lowest solvent level of 1% for all measurements.

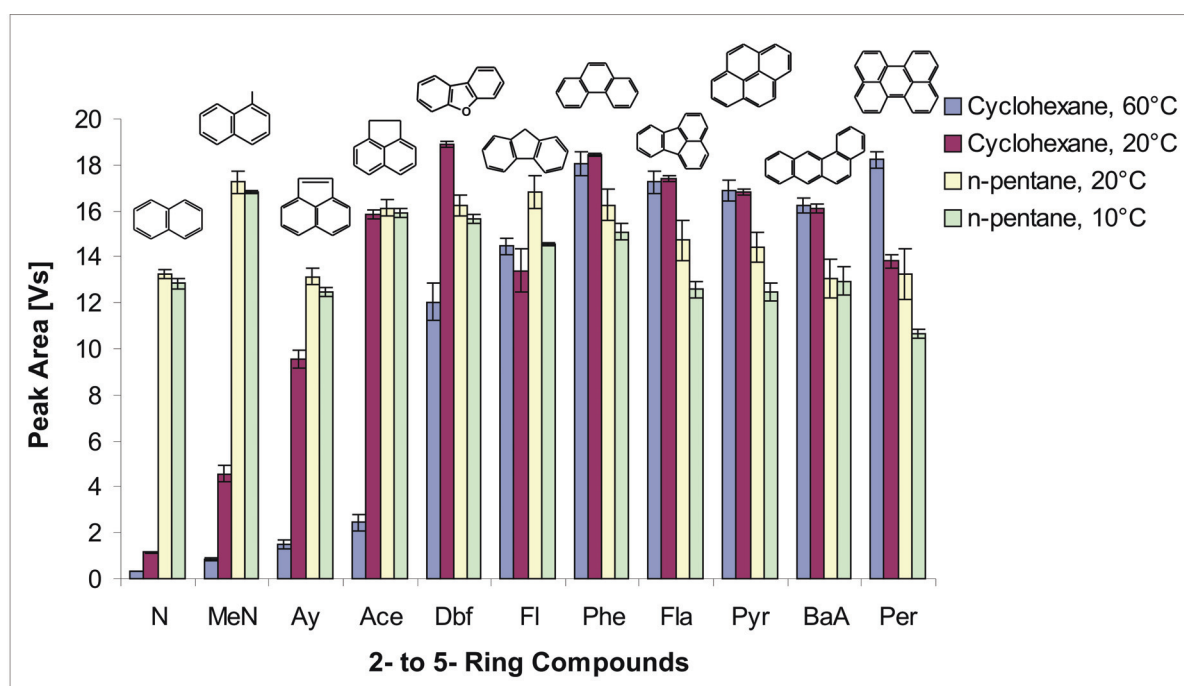


**Figure 3-1.** Effect of solvent and PTV initial temperatures on the instrument response for selected 2- to 5-ring compounds. Injections were made at 100  $\mu\text{L}$  each with same analyte concentration, error bars are indicating the standard deviation of a triplicate measurement.

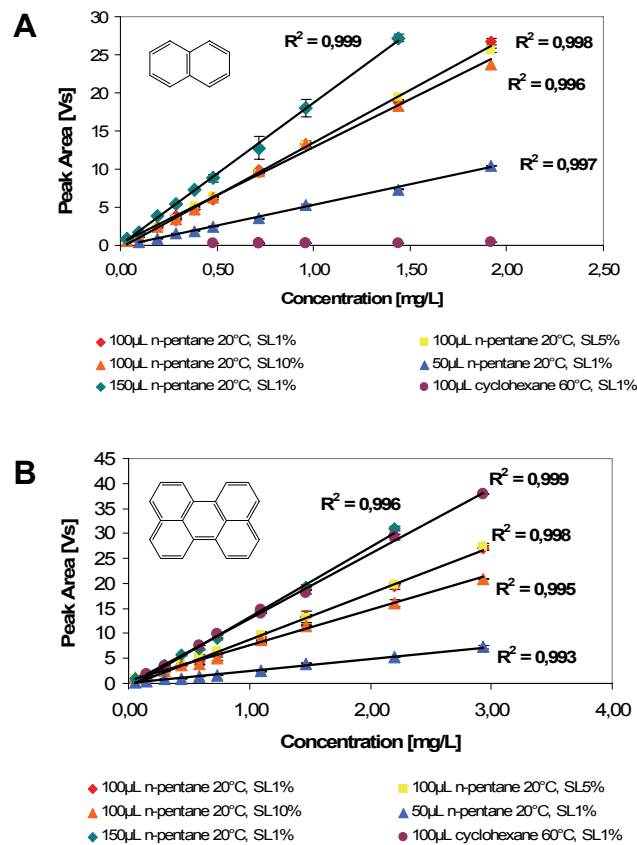


**Figure 3-2.** Linear correlation of peak area and amount of compound injected illustrated for **A)** naphthalene and **B)** perylene. Results are given for various solvents, initial PTV inlet temperatures and solvent levels (SL); error bars represent standard deviations based on three injections (in most cases smaller than the symbol size).

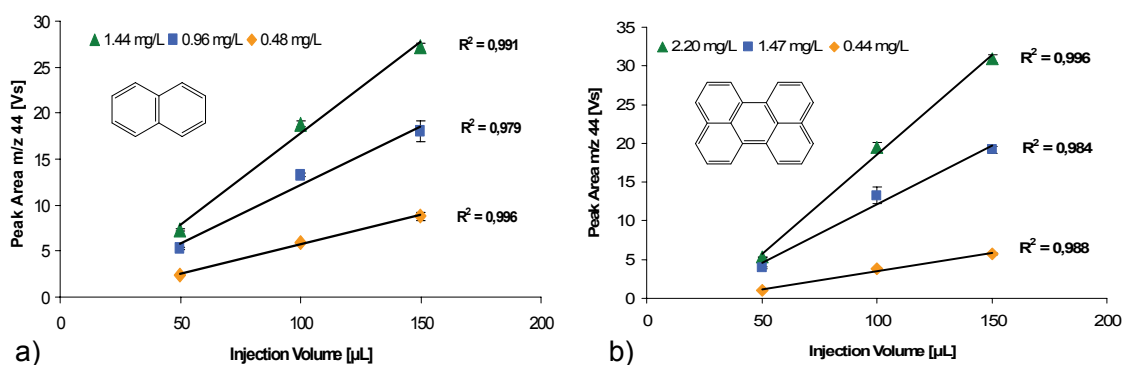


**Figure 3-3.** Peak areas as a function of sample volume injected exemplarily shown for **a)** naphthalene and **b)** perylene. Volumes of samples injected were 50, 100 and 150 μL.

**$\delta^{13}\text{C}$  Values of the Analytes.** Co-evaporation effects during large volume injections with cyclohexane as a solvent involve substantial losses for volatile PAHs, resulting in a shift to more depleted mean  $\delta^{13}\text{C}$  values for the remaining fraction of the analytes including naphthalene to dibenzofuran. With increasing molecular weight and boiling points (starting from fluorene), the effect is much less pronounced and reliable results were achieved for analytes from fluorene to perylene dissolved in cyclohexane (see below). Injections performed with *n*-pentane gave good results for low-molecular weight PAH compounds. However, with increasing molecular size and or boiling point (starting with fluorene),  $\delta^{13}\text{C}$  values show substantial errors with no systematic trend when *n*-pentane is used. Results are exemplarily illustrated for naphthalene and perylene in Figure 3-4. The uncertainties of the  $\delta^{13}\text{C}$  values for high-molecular weight compounds diluted in *n*-pentane might be explained by isotope fractionation through incomplete transfer of the analytes from the liner packing (as shown by decreased signal intensities in Figure 3-1). The same effect of stronger isotopic deviations could be observed for perylene diluted in cyclohexane when PTV initial temperatures were reduced from 60 °C to 20 °C (data not shown). So far, there is no reasonable explanation for the uncommon behavior of high-molecular weight PAHs for large volume injections performed with *n*-pentane.

Comparisons with  $\delta^{13}\text{C}$  values of a conventional 1  $\mu\text{L}$  splitless injection (with signal sizes >2000mV) were considered as a means to ascertain the optimal LVI conditions for each compound (Table 3-1). PTV-LVI results agreed very well for low-molecular weight PAHs if diluted in *n*-pentane and for high-molecular weight compounds if diluted in cyclohexane. Table 3-1 shows results of the evaluation for a 100  $\mu\text{L}$  injection of PAH standards diluted in cyclohexane and *n*-pentane at PTV initial temperatures of 60 °C and 20 °C, respectively. Measured  $\delta^{13}\text{C}$  values are a function of signal size, and in all cases  $\delta^{13}\text{C}$  values of the analytes show stronger deviations at signal sizes below 500 mV. The deviations observed at low signal size were in both directions, to more depleted and to more enriched  $\delta^{13}\text{C}$  values, as well. Variations in  $\delta^{13}\text{C}$  at low signal sizes are a common observation in continuous-flow isotope ratio determination (7,28-30). Wilcke et al. (7), e.g., used an injection volume of 1  $\mu\text{L}$  and different concentrations of naphthalene and perylene. A linear correlation of  $\delta^{13}\text{C}$  values and  $\ln$  (peak areas) was observed and used to account for the amount-dependence of the  $\delta^{13}\text{C}$  signals (7). As the deviations below 500 mV were highly variable within our experiments, an approach for correction was not considered in our study. Sherwood Lollar et al. (29) recently emphasized that

offsets from the actual value may not only vary from one compound to another but also with time, suggesting that corrections should only be performed with great care.

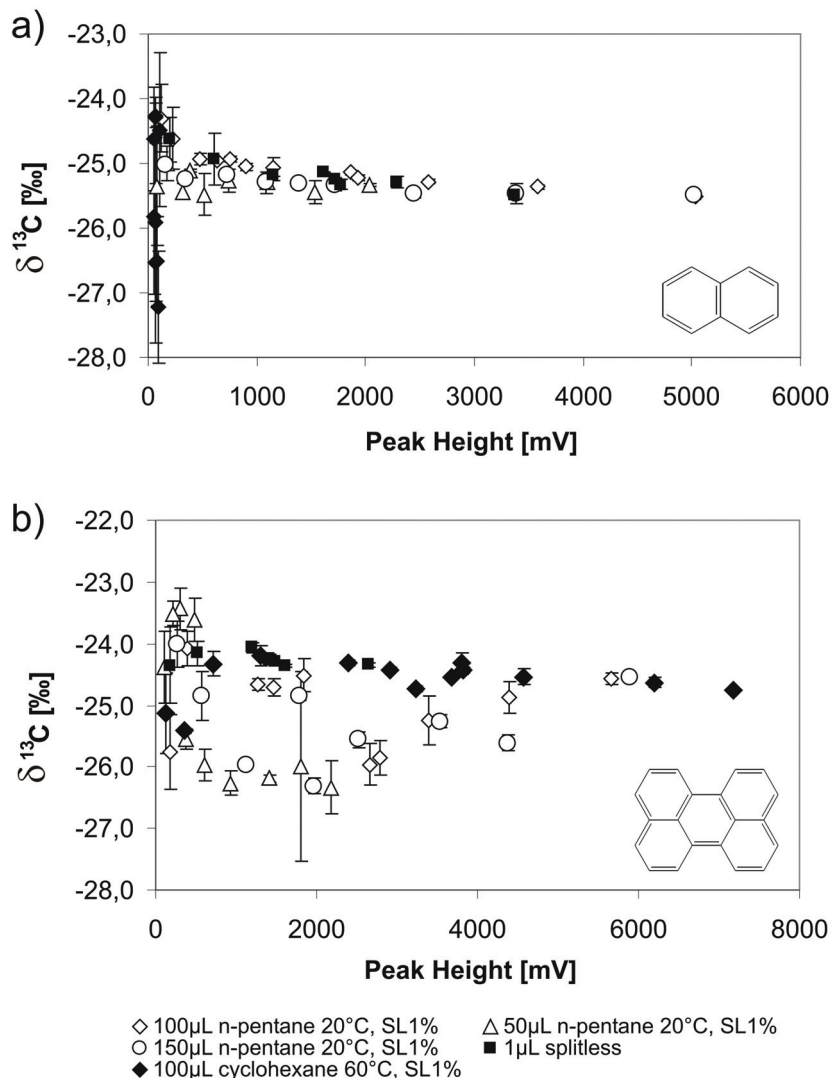


**Figure 3-4.** Results for PTV-LVI injections measuring  $\delta^{13}\text{C}$  as a function of different concentrations (represented by different signal sizes) illustrated for a) naphthalene and b) perylene. Varying parameters are volume of injection and solvents injected at optimized PTV initial temperatures, with a solvent level (SL) set to 1%. For comparison, results for a conventional 1  $\mu\text{L}$  splitless injection are included. Error bars are indicating the standard deviation of a triplicate injection.

**Table 3-1.** Results for a 100  $\mu\text{L}$  injection of PAH working standards diluted in cyclohexane and *n*-pentane at PTV initial temperatures of 60°C and 20 °C, respectively; based on  $n=30-40$  for each compound and method applied.

		$\delta^{13}\text{C}$ ( $\pm s$ ) in ‰ according to signal size of $m/z$ 44 peak				1 $\mu\text{L}$ splitless >2000 mV
		<500 mV	500-1000 mV	1000-2000 mV	>2000 mV	
Naphthalene	Cyclohexane	-25.8 ( $\pm 1.3$ )				
	<i>n</i> -pentane	-24.6 ( $\pm 0.4$ )	-25.0 ( $\pm 0.1$ )	-25.1 ( $\pm 0.1$ )	-25.4 ( $\pm 0.1$ )	-25.3 ( $\pm 0.1$ )
1-Methylnaphthalene	Cyclohexane	-31.0 ( $\pm 1.0$ )				
	<i>n</i> -pentane	-30.1 ( $\pm 0.5$ )	-30.7 ( $\pm 0.1$ )	-30.7 ( $\pm 0.1$ )	-30.9 ( $\pm 0.2$ )	-31.0 ( $\pm 0.1$ )
Acenaphthylene	Cyclohexane	-22.5 ( $\pm 0.3$ )	-22.8 ( $\pm 0.2$ )			
	<i>n</i> -pentane	-21.6 ( $\pm 0.5$ )	-21.8 ( $\pm 0.2$ )	-21.8 ( $\pm 0.1$ )	-22.2 ( $\pm 0.1$ ) *1	-22.3 ( $\pm 0.1$ )
Acenaphthene	Cyclohexane	-23.3 ( $\pm 0.3$ )	-23.7 ( $\pm 0.2$ )	-23.8 ( $\pm 0.2$ )		
	<i>n</i> -pentane	-23.1 ( $\pm 0.2$ )	-23.5 ( $\pm 0.6$ )	-23.1 ( $\pm 0.1$ )	-23.3 ( $\pm 0.3$ ) *2	-23.3 ( $\pm 0.1$ )
Dibenzofuran	Cyclohexane	-25.5 ( $\pm 0.2$ )	-23.4 ( $\pm 0.8$ )	-23.1 ( $\pm 0.2$ )	-23.8 ( $\pm 0.2$ )	
	<i>n</i> -pentane	-23.4 ( $\pm 0.3$ )	-23.6 ( $\pm 0.4$ )	-23.2 ( $\pm 0.2$ )	-23.1 ( $\pm 0.1$ )	-23.0 ( $\pm 0.1$ )
Fluorene	Cyclohexane	-23.4 ( $\pm 0.5$ )	-23.7 ( $\pm 0.1$ )	-23.7 ( $\pm 0.1$ )	-24.2 ( $\pm 0.3$ )	-24.0 ( $\pm 0.2$ )
	<i>n</i> -pentane	-27.2 ( $\pm 0.4$ )	-28.9 ( $\pm 1.6$ )	-26.2 ( $\pm 1.9$ )	-25.6 ( $\pm 0.8$ )	
Phenanthrene	Cyclohexane	-22.9 ( $\pm 0.4$ )	-23.3 ( $\pm 0.2$ )	-23.4 ( $\pm 0.1$ )	-23.7 ( $\pm 0.1$ )	-23.6 ( $\pm 0.1$ )
	<i>n</i> -pentane	-23.2 ( $\pm 0.2$ )	-24.8 ( $\pm 0.6$ )	-24.0 ( $\pm 0.6$ )	-24.0 ( $\pm 0.1$ )	
Fluoranthene	Cyclohexane	-23.9 ( $\pm 0.5$ )	-24.5 ( $\pm 0.3$ )	-24.5 ( $\pm 0.1$ )	-24.5 ( $\pm 0.1$ )	-24.3 ( $\pm 0.1$ )
	<i>n</i> -pentane	-24.1 ( $\pm 0.3$ )	-26.3 ( $\pm 0.3$ )	-25.3 ( $\pm 0.7$ )	-25.2 ( $\pm 0.4$ )	
Pyrene	Cyclohexane	-25.1 ( $\pm 0.3$ )	-25.0 ( $\pm 0.3$ )	-25.2 ( $\pm 0.1$ )	-25.5 ( $\pm 0.1$ )	-25.4 ( $\pm 0.1$ )
	<i>n</i> -pentane	-24.9 ( $\pm 0.1$ )	-26.8 ( $\pm 0.4$ )	-25.9 ( $\pm 0.3$ )	-25.9 ( $\pm 0.2$ )	
Benzo(a)anthracene	Cyclohexane	-26.4 ( $\pm 0.1$ )	-26.9 ( $\pm 0.1$ )	-27.0 ( $\pm 0.1$ )	-27.2 ( $\pm 0.1$ )	-26.9 ( $\pm 0.2$ )
	<i>n</i> -pentane	-27.3 ( $\pm 0.6$ )	-29.1 ( $\pm 0.3$ )	-27.5 ( $\pm 0.3$ )	-28.3 ( $\pm 0.6$ )	
Perylene	Cyclohexane	-25.2 ( $\pm 0.5$ )	-24.3 ( $\pm 0.2$ )	-24.2 ( $\pm 0.2$ )	-24.5 ( $\pm 0.2$ )	-24.3 ( $\pm 0.1$ )
	<i>n</i> -pentane	-25.1 ( $\pm 1.0$ )	-26.9 ( $\pm 0.5$ )	-24.6 ( $\pm 0.2$ )	-25.3 ( $\pm 0.6$ )	

\*1 Values >6500mV were excluded, due to stronger deviations (mean  $\delta^{13}\text{C}$  -23.5‰,  $\pm 0.4$ ), \*2 Values >3500mV were excluded due to deviations (mean  $\delta^{13}\text{C}$  -23.6‰,  $\pm 0.4$ ), most reliable method for the respective compound is highlighted.

**Reproducibility (Precision) and Accuracy.** To study the general accuracy of the method, pure PAH working standards were independently characterized with EA/IRMS. Results for the 1 $\mu\text{L}$  splitless injection, EA/IRMS values and the results for PTV-LVI measurements (compared in Table 3-2) are in good agreement. As shown above,  $\delta^{13}\text{C}$  values depend on the amount of compound injected, represented by signal size intervals in Table 3-1. Remarkably, high precision of a triplicate analysis is maintained even for those measurements that exhibit inaccurate  $\delta^{13}\text{C}$  values (below 500 mV). Precision in terms of reproducibility of the method was therefore evaluated based on PAH working standards analyzed at different days of measurement within one week. Longterm reproducibility is demonstrated with  $\delta^{13}\text{C}$  values for a 3- to 4-ring PAH working standard diluted in cyclohexane that was determined several months apart (independent from the

other measurements). For optimized injection parameters values were in general highly reproducible (with standard deviations  $\leq 0.3\%$ , based on  $n=12$ ) as shown in Table 3-2. For comparison values of a conventional 1  $\mu\text{L}$  splitless injection are also included. For most compounds  $\delta^{13}\text{C}$  values remained reproducible and accurate also for high signal sizes (5 to 8 Volt). The variations in  $\delta^{13}\text{C}$  observed during *n*-pentane injections at signal sizes of  $>6500$  mV for acenaphthylene and  $>3500$  mV for acenaphthene (see Table 3-1), might be due to incomplete oxidation of these compounds in the combustion unit (30,31).

**Table 3-2.** Reproducibility and accuracy of the PTV-LVI method. Values are highly reproducible for optimized injection parameters and accurate compared to values of the same working standards measured by off-line EA/IRMS. (Values in light grey represent the results for compounds injected with the 'wrong' solvent.)

	100 $\mu\text{L}$ LVI <i>n</i> -pentane <sup>*.1</sup>	100 $\mu\text{L}$ LVI <i>c</i> -hexane <sup>*.1</sup>	100 $\mu\text{L}$ LVI <i>c</i> -hexane <sup>*.2</sup>	1 $\mu\text{L}$ splitless <sup>*</sup>	EA/IRMS <sup>3</sup>
1) Naphthalene	-25.2 ( $\pm 0.1$ )	-25.4 ( $\pm 1.3$ )	#	-25.3 ( $\pm 0.1$ )	-25.27 ( $\pm 0.01$ )
2) 1-Methylnaphthalene	-30.8 ( $\pm 0.1$ )	-30.9 ( $\pm 1.5$ )	#	-31.0 ( $\pm 0.1$ )	-30.69 ( $\pm 0.18$ )
3) Acenaphthylene	-22.1 ( $\pm 0.1$ )	-22.6 ( $\pm 0.3$ )	#	-22.3 ( $\pm 0.1$ )	-22.35 ( $\pm 0.21$ )
4) Acenaphthene	-23.4 ( $\pm 0.3$ )	-23.7 ( $\pm 0.2$ )	-23.7 ( $\pm 0.1$ )	-23.3 ( $\pm 0.1$ )	-23.05 ( $\pm 0.04$ )
5) Dibenzofuran	-23.1 ( $\pm 0.1$ )	-23.6 ( $\pm 0.2$ )	#	-23.0 ( $\pm 0.1$ )	-22.90 ( $\pm 0.05$ )
6) Fluorene	-25.3 ( $\pm 1.0$ )	-24.2 ( $\pm 0.3$ )	-23.7 ( $\pm 0.1$ )	-24.0 ( $\pm 0.2$ )	-23.55 ( $\pm 0.06$ )
7) Phenanthrene	-23.9 ( $\pm 0.2$ )	-23.7 ( $\pm 0.1$ )	-23.5 ( $\pm 0.1$ )	-23.6 ( $\pm 0.1$ )	-23.52 ( $\pm 0.01$ )
8) Fluoranthene	-25.0 ( $\pm 0.6$ )	-24.5 ( $\pm 0.1$ )	-24.3 ( $\pm 0.1$ )	-24.3 ( $\pm 0.1$ )	-24.04 ( $\pm 0.04$ )
9) Pyrene	-25.8 ( $\pm 0.2$ )	-25.5 ( $\pm 0.1$ )	-25.5 ( $\pm 0.1$ )	-25.4 ( $\pm 0.1$ )	-25.39 ( $\pm 0.04$ )
10) Benzo(a)anthracene	-28.5 ( $\pm 0.7$ )	-27.2 ( $\pm 0.1$ )	#	-26.9 ( $\pm 0.2$ )	-27.24 ( $\pm 0.04$ )
11) Perylene	-25.5 ( $\pm 0.7$ )	-24.5 ( $\pm 0.2$ )	#	-24.3 ( $\pm 0.1$ )	-24.33 ( $\pm 0.20$ )

<sup>\*</sup> Signal size of *m/z* 44 peaks between 2 and 5 Volt, results based on  $n=12$ ; <sup>1</sup> working standards within one week; <sup>2</sup> working standard measured at different campaign; <sup>3</sup> externally measured isotopic composition of pure standard compounds, results based on  $n=3$ ; # PAH compound not included in laboratory working standard

**Method Detection Limits (MDLs).** Method detection limits were determined according to Sherwood Lollar et al. (29). The methodology incorporates both, accuracy and reproducibility of the measurements and are based on all measurements that were performed using a solvent level of 1% (see Table 3-3). Injections with *n*-pentane are based on three runs each with a set of different concentrations and injection volumes, each measurement again was performed in triplicate resulting in a total number of analyses of  $n=90$ . Cyclohexane injections are based on available 100  $\mu\text{L}$  injections with 60 and 20  $^{\circ}\text{C}$ , respectively; each value is reported in triplicate resulting in a total number of analyses of  $n=60$  (except for perylene, see above). Table 3-3 shows

variability in  $\delta^{13}\text{C}$  measurements for signal size intervals ranging from below 500 mV to 6-8 Volt. Measurements with signal sizes  $>500$  mV show already a good statistical variance in  $\delta^{13}\text{C}$  values and are in good agreement with the desired value for all compounds tested. Hence, for a 150  $\mu\text{L}$  injection, the minimum requirement for an accurate and precise  $\delta^{13}\text{C}$  determination is a concentration of 0.1 mg/L per PAH in the solvent extract. Injecting 150  $\mu\text{L}$  of a sample (after solvent extraction with a water to solvent ratio of 100:1) allows then to reliably determine carbon isotope ratios of individual PAH compounds at aqueous concentrations as low as 1  $\mu\text{g/L}$ . The PAH concentration required for soil samples would correspond to 10-20  $\mu\text{g/kg}$  (assumed that 30 to 50 g of soil are extracted and the solvent extract is concentrated to 4 to 5 mL).

**Table 3-3.** Variance in  $\delta^{13}\text{C}$  values for different signal size intervals.

			Signal size of m/z 44 peak (mVolt)			
			<500	500-1000	1000-2000	>2000
Naphthalene	<i>n</i> -pentane	$\delta^{13}\text{C}$ ( $\pm\text{s}$ )	-25.0 ( $\pm 0.5$ )	-25.2 ( $\pm 0.2$ )	-25.3 ( $\pm 0.1$ )	-25.4 ( $\pm 0.1$ )
		Variance ( $\text{s}^2$ )	0.23	0.058	0.016	0.009
1-Methylnaphthalene	<i>n</i> -pentane	$\delta^{13}\text{C}$ ( $\pm\text{s}$ )	-30.8 ( $\pm 1.0$ )	-30.7 ( $\pm 0.1$ )	-30.7 ( $\pm 0.1$ )	-30.9 ( $\pm 0.2$ )
		Variance ( $\text{s}^2$ )	0.92	0.017	0.008	0.023
Acenaphthylene	<i>n</i> -pentane	$\delta^{13}\text{C}$ ( $\pm\text{s}$ )	-21.8 ( $\pm 0.4$ )	-21.7 ( $\pm 0.2$ )	-21.9 ( $\pm 0.1$ )	-22.1 ( $\pm 0.2$ )
		Variance ( $\text{s}^2$ )	0.19	0.027	0.021	0.034 <sup>*1</sup>
Acenaphthene	<i>n</i> -pentane	$\delta^{13}\text{C}$ ( $\pm\text{s}$ )	-23.2 ( $\pm 0.6$ )	-23.0 ( $\pm 0.3$ )	-23.1 ( $\pm 0.2$ )	-23.3 ( $\pm 0.2$ )
		Variance ( $\text{s}^2$ )	0.39	0.083	0.042	0.054 <sup>*2</sup>
Dibenzofuran	<i>n</i> -pentane	$\delta^{13}\text{C}$ ( $\pm\text{s}$ )	-22.8 ( $\pm 2.3$ )	-23.0 ( $\pm 0.3$ )	-23.1 ( $\pm 0.2$ )	-23.2 ( $\pm 0.2$ )
		Variance ( $\text{s}^2$ )	5.5	0.11	0.036	0.025
Fluorene	Cyclohexane	$\delta^{13}\text{C}$ ( $\pm\text{s}$ )	-23.2 ( $\pm 0.5$ )	-23.8 ( $\pm 0.2$ )	-23.7 ( $\pm 0.1$ )	-24.2 ( $\pm 0.2$ )
		Variance ( $\text{s}^2$ )	0.22	0.030	0.014	0.065
Phenanthrene	Cyclohexane	$\delta^{13}\text{C}$ ( $\pm\text{s}$ )	-23.0 ( $\pm 0.3$ )	-23.3 ( $\pm 0.1$ )	-23.4 ( $\pm 0.1$ )	-23.7 ( $\pm 0.1$ )
		Variance ( $\text{s}^2$ )	0.11	0.021	0.007	0.009
Fluoranthene	Cyclohexane	$\delta^{13}\text{C}$ ( $\pm\text{s}$ )	-23.6 ( $\pm 0.4$ )	-24.3 ( $\pm 0.3$ )	-24.2 ( $\pm 0.2$ )	-24.5 ( $\pm 0.1$ )
		Variance ( $\text{s}^2$ )	0.15	0.13	0.052	0.022
Pyrene	Cyclohexane	$\delta^{13}\text{C}$ ( $\pm\text{s}$ )	-24.7 ( $\pm 0.6$ )	-25.0 ( $\pm 0.3$ )	-25.3 ( $\pm 0.1$ )	-25.5 ( $\pm 0.1$ )
		Variance ( $\text{s}^2$ )	0.40	0.11	0.007	0.017
Benzo(a)anthracene	Cyclohexane	$\delta^{13}\text{C}$ ( $\pm\text{s}$ )	-26.4 ( $\pm 0.2$ )	-26.9 ( $\pm 0.1$ )	-27.0 ( $\pm 0.3$ )	-27.1 ( $\pm 0.1$ )
		Variance ( $\text{s}^2$ )	0.035	0.014	0.069	0.020
Perylene	Cyclohexane	$\delta^{13}\text{C}$ ( $\pm\text{s}$ )	-25.5 ( $\pm 0.7$ )	-24.3 ( $\pm 0.2$ )	-24.2 ( $\pm 0.2$ )	-24.5 ( $\pm 0.2$ )
		Variance ( $\text{s}^2$ )	0.52	0.027	0.028	0.027

<sup>\*1</sup> Values  $>6500\text{mV}$  were excluded, due to stronger deviations (mean  $\delta^{13}\text{C}$  -23.6‰,  $\pm 0.3$ ,  $\text{s}^2$  0.12  $n=5$ ); <sup>\*2</sup> Values  $>3500\text{mV}$  were excluded due to deviations (mean  $\delta^{13}\text{C}$  -23.8‰,  $\pm 0.3$ ,  $\text{s}^2$  0.092,  $n=22$ )

**Chromatographic Resolution.** To fully exploit the advantages of a large volume injection, a good separation of target compounds from matrix interferences is essential (32). This is especially true in CSIA where all negative effects of the introduction of large sample volumes impair the peak resolution. While quantitative analyses are often performed using the single ion monitoring function of GC/MS, GC/IRMS systems require high-purity solvents to avoid problems with interfering compounds. A comparison of GC/IRMS chromatographic traces in Figure 3-5 illustrates that peak shapes and good chromatographic resolution are maintained even after large sample volumes are introduced into the GC system. Cooling of the PTV injector prevents losses of low-molecular weight compounds and assures excellent peak shapes, no other peaks due to impurities of the solvent are observed. Not only large volumes of solvent impurities may be introduced into the GC system, interferences from GC vial septa and from dirty matrix samples need also to be considered when LVI is applied (22), examples and chromatograms are provided in Chapter 4.4.

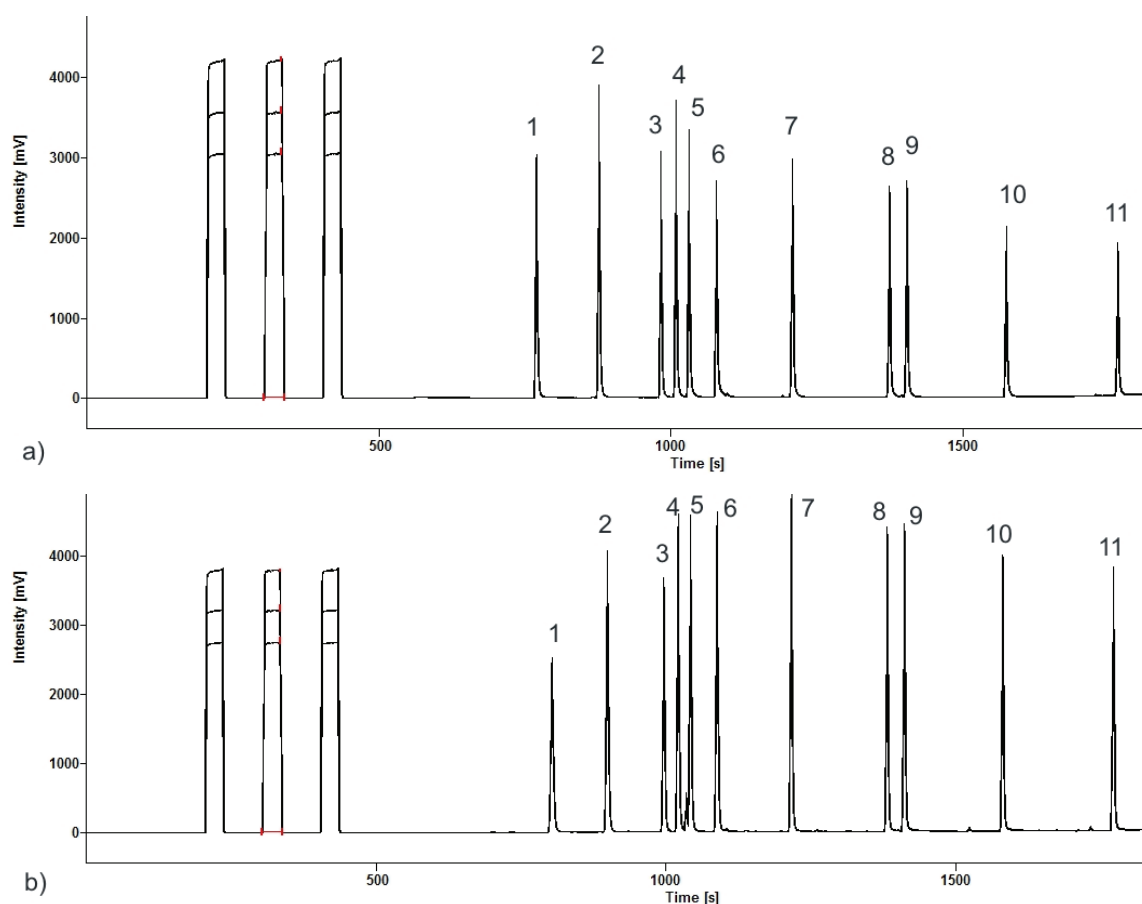


**Figure 3-5.** Comparison of GC/IRMS chromatograms of **a)** a conventional 1  $\mu\text{L}$  injection of a 75 mg/L and **b)** a 100  $\mu\text{L}$  large volume injection of a 750  $\mu\text{g/L}$  PAH working standard diluted in *n*-pentane shows good chromatographical peak resolution, PTV inlet temperatures during the injection were a) 300 °C and b) 20 °C, numbers of compounds correspond to the numbers given Table 3-2.



**Application to Environmental Samples.** The applicability of the method is demonstrated for a source apportionment case study. Solvent extracts of soil samples from a former mineral oil facility with long operational history were studied by CSIA to determine the isotopic composition of individual semi-volatile PAHs. Possible sources for contamination at the site are heavy fuel oils, waste oil, creosotes, and petroleum fuel oils. Purification of the PAH containing fraction was performed prior to compound-specific isotope analysis to ensure baseline separation of individual peaks. To provide accurate GC/IRMS measurements, cleanup of the extracts should not involve the danger of isotope fractionation. The effect of soil sample extraction and purification on initial isotopic composition of the compounds was thoroughly studied and reported to be within analytical error; shifts of the  $\delta^{13}\text{C}$  values were less than 0.5‰ (7,33-35). Analytical precision of individual  $\delta^{13}\text{C}$  values was reported to be 0.2-0.3 ‰ for *n*-alkanes with no background and more variable standard deviations of 0.1-1.5 ‰ for complex mixtures due to coelution effects (36). After soil sample cleanup with cyclohexane, PTV-based large volume injections of the PAH containing fractions have been performed to ensure reliable  $\delta^{13}\text{C}$  measurements of individual compounds by GC/IRMS (see Figure 3-6). As stable isotope values of individual semi-volatile compounds can be used to infer contaminant sources, we compared our results with other PAH source values reported in the literature (Figure 3-7). Our results show  $\delta^{13}\text{C}$  values indicative for creosote (5) as the most likely contamination source for the soil samples from the former mineral oil facility. Recently, we also applied the method to forest soil samples containing perylene of unknown origin (37).

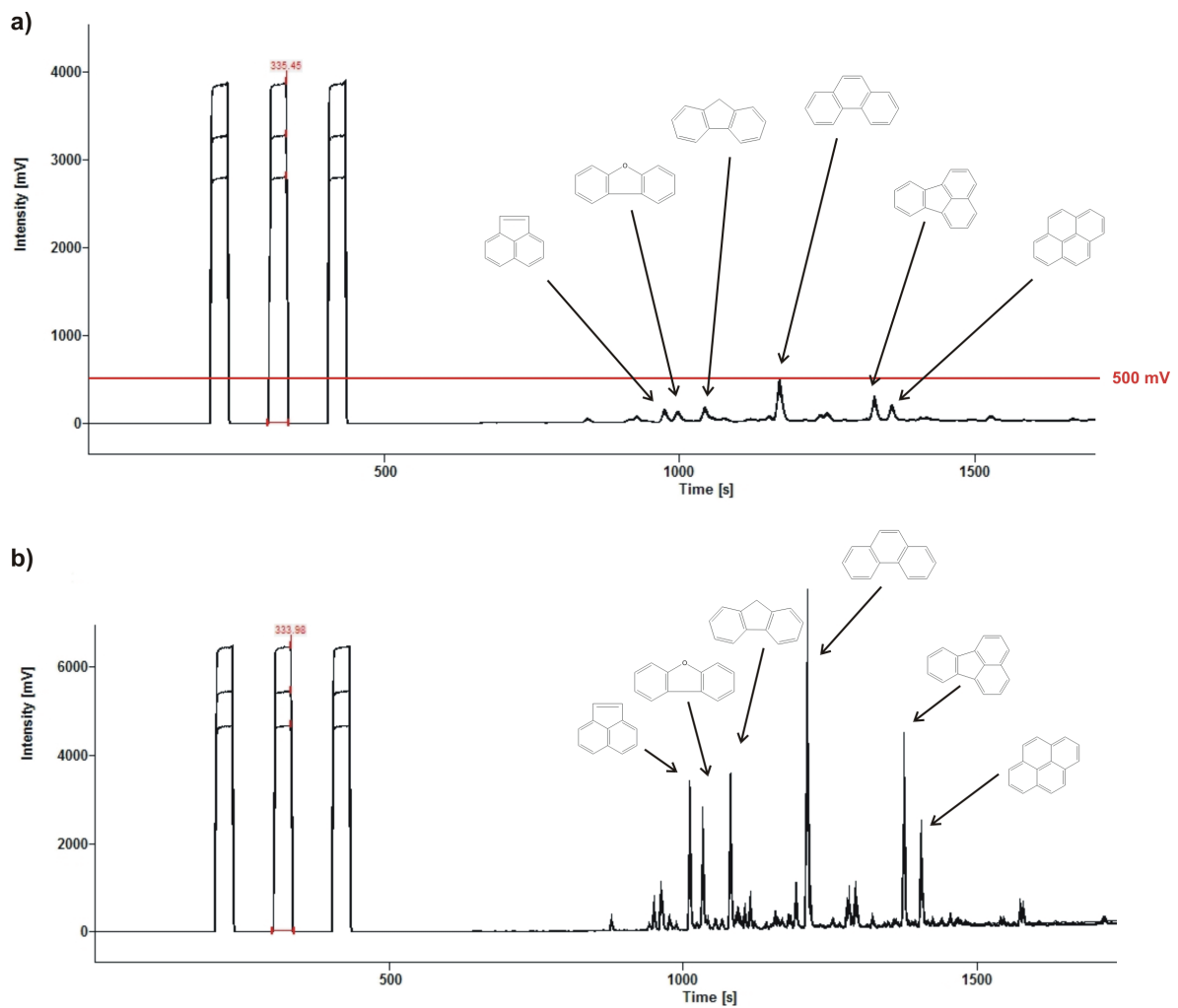


**Figure 3-6.** Chromatograms of a soil sample extract after conventional  $1\ \mu\text{L}$  injection and after a LVI-GC/IRMS to ensure peak heights above the method detection limit of 500 mV.

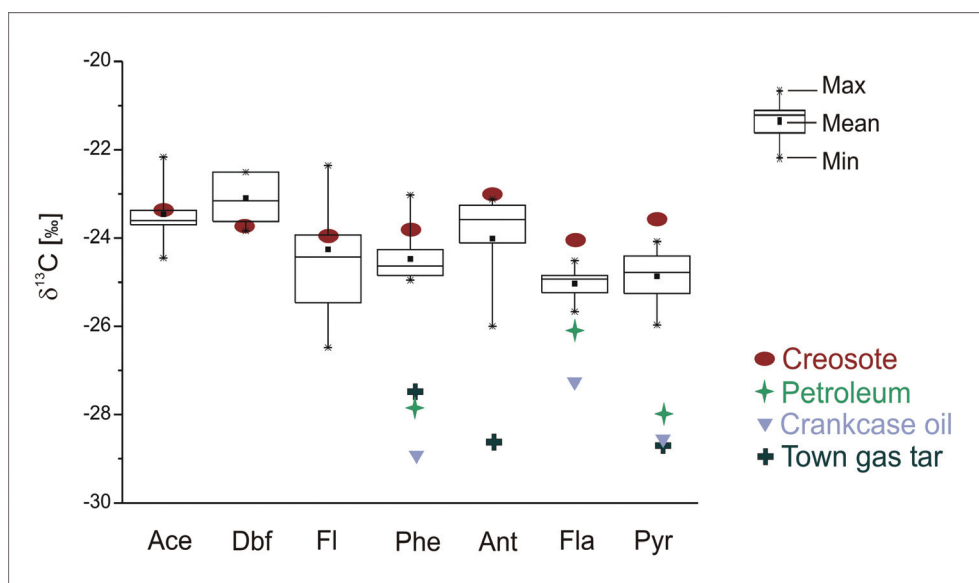


**Figure 3-7.** Box-whisker-diagram for individual PAH compounds of the soil samples taken at the site compared to reported mean isotopic compositions of creosote (5), petroleum (38), crankcase oil (39) and town gas process tar (40).

### 3.4. Conclusions

This work presents a new analytical approach to determine  $\delta^{13}\text{C}$  values of individual semi-volatile organic compounds at trace concentrations. For the first time, a PTV-based large volume injection technique was validated for the application in GC/IRMS. The methodology (LVI-GC/IRMS) was thoroughly evaluated in terms of its accuracy, precision, linearity, reproducibility and limits of detection. While peak areas exhibited a linear correlation of response and amount injected (except for compounds that are co-evaporated with cyclohexane),  $\delta^{13}\text{C}$  values behave significantly different for the various parameters that were evaluated in this work. It was demonstrated that if not an appropriate solvent is applied,  $\delta^{13}\text{C}$  values can vary significantly from the accurate value. If optimized PTV injection parameters are applied to the specific compounds of interest, the technique proved to be very accurate and highly precise. Practical consequences are to use an appropriate solvent for a certain application, the values gained with different solvents might be not comparable or only with great care, and thus, a thorough method validation in terms of isotope fractionation is necessary for each specific application. Every sample introduction technique has its own advantages and disadvantages. The most obvious advantage

by LVI-GC/IRMS is that the instrumental limit of detection can be easily and significantly improved just by introducing larger volumes of a sample. It is a user-friendly, automated technique that can be applied in a broad range of applications. Off-line sample pretreatment can be avoided or simplified, e.g. in combination with preparative HPLC it offers an effective, fast, time and labour efficient method for the determination of isotopic compositions of semi-volatiles even in difficult matrices. Dirty extracts, and thus, matrix interferences place special demands on large volume injection and often require improved clean-up strategies. However, matrix components, which might be present even after sample clean-up, can be retained in the liner packing material. Problems with volatile compounds that are co-evaporated with the solvent can be avoided if the volatility of the solvent used is significantly lower than that of the compounds that are trapped in the cooled packed liner. The choice of the LVI injection technique depends largely on the composition of the sample and the type of analytes to be determined.

### 3.5. References

- (1) Benson, S.; Lennard, C.; Maynard, P.; Roux, C. Forensic applications of isotope ratio mass spectrometry - A review. *Forensic Sci.Int.* **2006**, *157*, 1-22.
- (2) Philp, R. P. The emergence of stable isotopes in environmental and forensic geochemistry studies: a review. *Environ. Chem. Lett.* **2007**, *5*, 57-66.
- (3) Poster, D. L.; Schantz, M. M.; Sander, L. C.; Wise, S. A. Analysis of polycyclic aromatic hydrocarbons (PAHs) in environmental samples: A critical review of gas chromatographic (GC) methods. *Anal. Bioanal. Chem.* **2006**, *386*, 859-881.
- (4) O'Malley, V. P.; Abrajano, T. A.; Hellou, J. Determination of the  $^{13}\text{C}/^{12}\text{C}$  ratios of individual PAH from environmental samples: can PAH sources be apportioned? *Org. Geochem.* **1994**, *21*, 809-822.
- (5) Hammer, B. T.; Kelley, C. A.; Coffin, R. B.; Cifuentes, L. A.; Mueller, J. G. Delta C-13 values of polycyclic aromatic hydrocarbons collected from two creosote-contaminated sites. *Chem. Geol.* **1998**, *152*, 43-58.
- (6) McRae, C.; Sun, C. G.; McMillan, C. F.; Snape, C. E.; Fallick, A. E. Sourcing of fossil fuel-derived PAH in the environment. *Polycycl. Aromat. Compd.* **2000**, *20*, 97-109.
- (7) Wilcke, W.; Krauss, M.; Amelung, W. Carbon isotope signature of polycyclic aromatic hydrocarbons (PAHs): Evidence for different sources in tropical and temperate environments? *Environ. Sci. Technol.* **2002**, *36*, 3530-3535.
- (8) Sun, C. G.; Cooper, M.; Snape, C. E. Use of compound-specific delta C-13 and delta D stable isotope measurements as an aid in the source apportionment of polyaromatic hydrocarbons. *Rapid Commun. Mass Spectrom.* **2003**, *17*, 2611-2613.
- (9) Sessions, A. L. Isotope-ratio detection for gas chromatography. *J. Sep. Sci.* **2006**, *29*, 1946-1961.
- (10) Meier-Augenstein, W. On-line Recording of  $^{13}\text{C}/^{12}\text{C}$  Ratios and Mass Spectra in one Gas Chromatographic Analysis. *J. High Resol. Chromatogr.* **1995**, *18*, 28-32.
- (11) Dempster, H. S.; Sherwood Lollar, B.; Feenstra, S. Tracing organic contaminants in groundwater: A new methodology using compound-specific isotopic analysis. *Environ. Sci. Technol.* **1997**, *31*, 3193-3197.
- (12) Zwank, L.; Berg, M.; Schmidt, T. C.; Haderlein, S. B. Compound-specific carbon isotope analysis of volatile organic compounds in the low-microgram per liter range. *Anal. Chem.* **2003**, *75*, 5575-5583.
- (13) Slater, G. F.; Dempster, H. S.; Sherwood Lollar, B.; Ahad, J. Headspace analysis: A new application for isotopic characterization of dissolved organic contaminants. *Environ. Sci. Technol.* **1999**, *33*, 190-194.

- (14) Kalin, R. M.; Hamilton, J. T. G.; Harper, D. B.; Miller, L. G.; Lamb, C.; Kennedy, J. T.; Downey, A.; McCauley, S.; Goldstein, A. H. Continuous flow stable isotope methods for study of  $\delta^{13}\text{C}$  fractionation during halomethane production and degradation. *Rapid Commun. Mass Spectrom.* **2001**, *15*, 357-363.
- (15) Morrill, P. L.; Lacrampe-Couloume, G.; Sherwood Lollar, B. Dynamic headspace: a single-step extraction for isotopic analysis of  $\mu\text{g/L}$  concentrations of dissolved chlorinated ethenes. *Rapid Commun. Mass Spectrom.* **2004**, *18*, 595-600.
- (16) Dias, R. F.; Freeman, K. H. Carbon isotope analyses of semivolatile organic compounds in aqueous media using solid-phase microextraction and isotope ratio monitoring GC/MS. *Anal. Chem.* **1997**, *69*, 944-950.
- (17) Hunkeler, D.; Aravena, R. Determination of compound-specific carbon isotope ratios of chlorinated methanes, ethanes, and ethenes in aqueous samples. *Environ. Sci. Technol.* **2000**, *34*, 2839-2844.
- (18) Ferchaud-Roucher, V.; Albert, C.; Champ, M.; Krempf, M. Solid-phase microextraction method for carbon isotopic analysis of volatile carboxylic acids in human plasma by gas chromatography/combustion/isotope ratio mass spectrometry. *Rapid Commun. Mass Spectrom.* **2006**, *20*, 3573-3578.
- (19) Yamada, K.; Yoshida, N.; Calderone, G.; Guillou, C. Determination of hydrogen, carbon and oxygen isotope ratios of ethanol in aqueous solution at millimole levels. *Rapid Commun. Mass Spectrom.* **2007**, *21*, 1431-1437.
- (20) Auer, N. R.; Manzke, B. U.; Schulz-Bull, D. E. Development of a purge and trap continuous flow system for the stable carbon isotope analysis of volatile halogenated organic compounds in water. *J. Chromatogr. A* **2006**, *1131*, 24-36.
- (21) Jochmann, M. A.; Blessing, M.; Haderlein, S. B.; Schmidt, T. C. A new approach to determine method detection limits for compound-specific isotope analysis of volatile organic compounds. *Rapid Commun. Mass Spectrom.* **2006**, *20*, 3639-3648.
- (22) Norlock, F. M.; Jang, J. K.; Zou, Q.; Schoonover, T. M.; Li, A. Large-volume injection PTV-GC-MS analysis of polycyclic aromatic hydrocarbons in air and sediment samples. *J. Air & Waste Manage. Assoc.* **2002**, *52*, 19-26.
- (23) Mol, H. G. J.; Althuisen, M.; Janssen, H. G.; Cramers, C. A.; Brinkman, U. A. T. Environmental applications of large volume injection in capillary GC using PTV injectors. *J. High Resol. Chromatogr.* **1996**, *19*, 69-79.
- (24) Vecera, Z.; Bartosikova, A.; Sklenska, J.; Mikuska, P. A large volume injection procedure for GC-MS determination of PAHs and PCBs. *Chromatographia* **2005**, *61*, 197-200.
- (25) Yusà, V.; Pardo, O.; Pastor, A.; de la Guardia, M. Optimization of a microwave-assisted extraction large-volume injection and gas chromatography-ion trap mass spectrometry procedure for the determination of polybrominated diphenyl ethers, polybrominated biphenyls and polychlorinated naphthalenes in sediments. *Anal. Chim. Acta* **2006**, *557*, 304-313.
- (26) Baylis, S. A.; Hall, K.; Jumeau, E. J. The analysis of the C1-C5 components of natural gas samples using gas chromatography-combustion-isotope ratio mass spectrometry. *Org. Geochem.* **1994**, *21*, 777-785.
- (27) Meier-Augenstein, W. Applied gas chromatography coupled to isotope ratio mass spectrometry. *J. Chromatogr. A* **1999**, *842*, 351-371.
- (28) Schmitt, J.; Glaser, B.; Zech, W. Amount-dependent isotopic fractionation during compound-specific isotope analysis. *Rapid Commun. Mass Spectrom.* **2003**, *17*, 970-977.
- (29) Sherwood Lollar, B.; Hirschorn, S. K.; Chartrand, M. M. G.; Lacrampe-Couloume, G. An approach for assessing total instrumental uncertainty in compound-specific carbon isotope analysis: Implications for environmental remediation studies. *Anal. Chem.* **2007**, *79*, 3469-3475.
- (30) Glaser, B.; Amelung, W. Determination of C-13 natural abundance of amino acid enantiomers in soil: methodological considerations and first results. *Rapid Commun. Mass Spectrom.* **2002**, *16*, 891-898.
- (31) Merritt, D. A.; Freeman, K. H.; Ricci, M. P.; Studley, S. A.; Hayes, J. M. Performance and Optimization of a Combustion Interface for Isotope Ratio Monitoring Gas Chromatography/Mass Spectrometry. *Anal. Chem.* **1995**, *67*, 2461-2473.
- (32) Cavagnino, D.; Magni, P.; Zilioli, G.; Trestianu, S. Comprehensive two-dimensional gas chromatography using large sample volume injection for the determination of polynuclear aromatic hydrocarbons in complex matrices. *J. Chromatogr. A* **2003**, *1019*, 211-220.
- (33) Bakel, A. J.; Ostrom, P. H.; Ostrom, N. E. Carbon isotopic analysis of individual n-alkanes: evaluation of accuracy and application to marine particulate organic material. *Org. Geochem.* **1994**, *21*, 595-602.
- (34) Kim, M. K.; Kennicutt, M. C.; Qian, Y. R. Polycyclic aromatic hydrocarbon purification procedures for compound specific isotope analysis. *Environ. Sci. Technol.* **2005**, *39*, 6770-6776.
- (35) Mazeas, L.; Budzinski, H. Molecular and stable carbon isotopic source identification of oil residues and oiled bird feathers sampled along the Atlantic coast of France after the Erika oil spill. *Environ. Sci. Technol.* **2002**, *36*, 130-137.

- (36) Schoell, M.; McCaffrey, M. A.; Fago, F. J.; Moldowan, J. M. Carbon isotopic compositions of 28,30-bisnorhopanes and other biological markers in a Monterey crude oil. *Geochim. Cosmochim. Acta* **1992**, *56*, 1391-1399.
- (37) Gocht, T.; Barth, J. A. C.; Epp, M.; Jochmann, M.; Blessing, M.; Schmidt, T. C.; Grathwohl, P. Indications for pedogenic formation of perylene in a terrestrial soil profile: Depth distribution and first results from stable carbon isotope ratios. *Appl. Geochem.* **2007**, *22*, 2652-2663.
- (38) Mazeas, L.; Budzinski, H. Polycyclic aromatic hydrocarbon C-13/C-12 ratio measurement in petroleum and marine sediments - Application to standard reference materials and a sediment suspected of contamination from the Erika oil spill. *J. Chromatogr. A* **2001**, *923*, 165-176.
- (39) O'Malley, V. P.; Burke, R. A.; Schlotzhauer, W. S. Using GC-MS/Combustion/IRMS to determine the C-13/C-12 ratios of individual hydrocarbons produced from the combustion of biomass materials - application to biomass burning. *Org. Geochem.* **1997**, *27*, 567-581.
- (40) McRae, C.; Sun, C. G.; Snape, C. E.; Fallick, A. E.; Taylor, D. Delta C-13 values of coal-derived PAHs from different processes and their application to source apportionment. *Org. Geochem.* **1999**, *30*, 881-889.

### 3.6. Appendix

**Clean-up of Soil Sample Extracts.** The extracts were purified on silica gel with flash chromatography using non-polar solvents. The column was filled with a 2 cm sand layer followed by the loading of an 18 cm layer of silica gel 60 in cyclohexane (wet packing). Settlement and packing was supported by pressure from a rubber ball (hand pump). 3 mL of sample extract was loaded on the column. A solvent gradient of cyclohexane (CH) and trichloromethane (TCM) was applied for sequential elution of the PAHs from the column, starting with 20 mL CH, then 50 mL CH/TCM 95/5 (v/v), followed by 44 mL CH/TCM 90/10 (v/v). The first 39 mL of eluent were discarded, then the PAH containing fraction was collected (78 mL) and concentrated to 5 mL with a rotary evaporator at 40 °C and 230 mbar. As discussed in the main section of this thesis, sample purification does not involve significant isotope fractionation (see Chapters 3.3 and 4.4). To exclude any bias due to concentrating the extracts by solvent evaporation, a cyclohexane solution containing PAH standards with known isotopic composition was reduced from 30 to 5 mL (rotary evaporator conditions: 40 °C, 235 mbar, 70 r/min).  $\delta^{13}\text{C}$  values of the standards before and after evaporation are compared in Figure A3-1. Similar  $\delta^{13}\text{C}$  values indicate that solvent evaporation does not significantly affect the isotopic composition of the analytes tested.

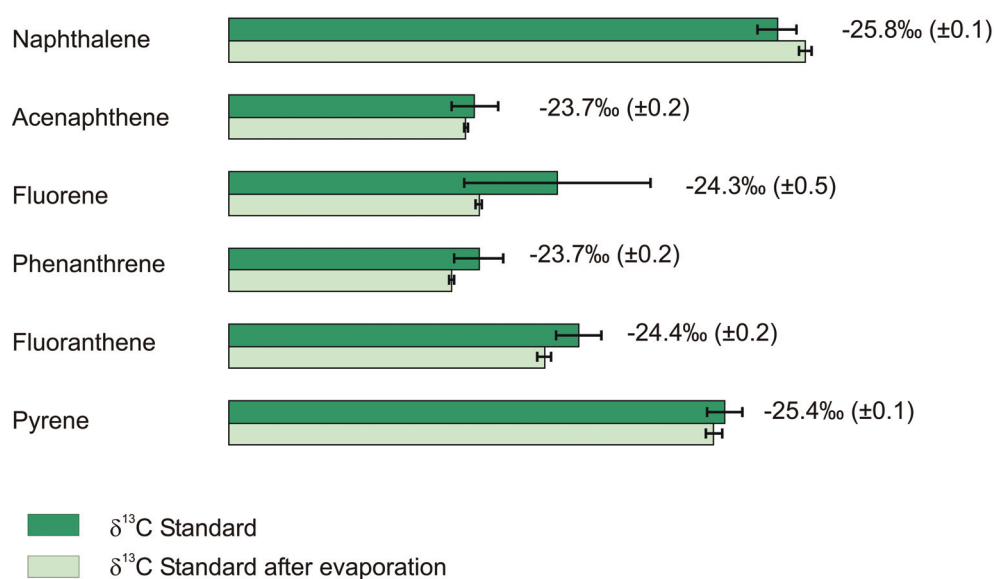


Figure A3-1. Effect of solvent evaporation on  $\delta^{13}\text{C}$  values of individual PAH compounds (not significant).

## **4. Analytical Problems and Limitations in Compound-Specific Isotope Analysis of Environmental Samples**

### **4.1. Introduction**

Since 1976, when it was introduced, the technique of measuring stable isotope ratios of individual GC peaks was further developed (1-4). Since the early 90ies, when GC/IRMS systems became commercially available, the technique has become known as compound-specific isotope analysis (CSIA) (5-7). Especially over the past decade, CSIA has evolved as a indispensable tool in many areas where an allocation of sources is required, such as in food authenticity studies, pharmaceutical research, doping analysis, and environmental chemistry (8-11).

Numerous studies have demonstrated CSIA as a useful tool in contaminated site assessment. Instrumental effects and other technical issues in the determination of compound-specific isotope ratios have been thoroughly discussed in the early stages of GC/IRMS (12-14). Accuracy, precision and quality assurance were always carefully considered in isotope data processing. Sherwood Lollar et al. (15) defined explicit criteria which have to be met for applications of CSIA to biodegradation field studies. Recent reviews of Slater (16), Schmidt et al. (10), Meckenstock et al. (17) and Elsner et al. (18) have focussed on the potentials of CSIA techniques and cover important aspects for assessing biodegradation and source identification with CSIA. They all, and most recently, a consensus guide (19) focus on possible areas of applications of CSIA and interpretation of data rather than isotope measurements in CSIA. The more fundamental technical aspects have been addressed in previous reviews (9,20) without focussing on environmental sample analysis and the more practical aspects regarding field applications. Since CSIA is gaining more and more popularity and an increasing numbers of environmental authorities and environmental consultancies are interested in the application of the method in contaminated site remediation, it is important to demonstrate the problems and limitations associated with environmental samples. Recent GC and separation papers that were not as extensively focused on in past reviews, will be discussed, aspects that have to be considered when applying GC/IRMS in contaminated site management will be highlighted and additional material with respect to environmental samples will be provided.



## 4.2. Groundwater Sampling

**Well Locations.** Most field applications have relied on sampling plans collecting data from different parts of the contaminant plumes, but at only one point in time (21). Chartrand et al. (21) emphasized the need to study fluctuating hydraulic systems time-resolved to more reliably assess the temporal variability and the effectiveness of biodegradation. Due to heterogeneities of the aquifer system and thus preferential flowpaths, point-scale measurements of the groundwater might lead to unacceptable levels of uncertainty with respect to the flow and contamination situation. As discussed by Peter et al. (22), point-scale isotope values need to be representative for the entire aquifer system, and hence would require a dense monitoring network covering both the fringes and the center of a contaminant plume, which is hardly possible at sites with complex hydrogeology. Their study, therefore, used a combined approach of CSIA and integral pumping tests that allows for a more reliable determination of the degree of biodegradation in heterogeneous aquifer systems (22). An important point that should be considered in terms of well locations is that some modeling approaches require sampling wells to be positioned on the center line of the contaminant plume to reliably estimate first order degradation rate constants, especially if combined with compound-specific stable isotope data (23).

Depth-discrete sampling, where an aquifer system can be vertically resolved should be favoured over whole screen sampling. Otherwise, due to heterogeneities within aquifer systems, one might miss important information on active degradation processes in parts of the plume. If mixing of different flow paths with different extents of degradation occurs during sampling, the measured isotopic composition of this mixed sample will reflect the isotope ratio of the fraction with the highest contaminant concentration (commonly the less degraded fraction). Hence, the true extent of biodegradation will be underestimated (24,25), a problem common to all hydrogeological sampling and analytical approaches. This is especially true for wells located near the contaminant source as isotope fractionation due to degradation can be masked due to continual dissolution of fresh, undegraded material (26). The major advantage of depth-discrete groundwater sampling is illustrated in Figure 4-1. A multi-level well system allows to investigate the vertical profile of a structured contaminant plume and to elucidate the different zones of microbial activity within the aquifer system (*KORA site Rosengarten-Ehestorf*, discussed in Chapter 2.4.3). In this well, conventional sampling would have resulted in a mean concentration of 2900  $\mu\text{g/L}$  for PCE and a mixed overall  $\delta^{13}\text{C}$  value of -25.7 ‰ (weighted average) and would have missed important *in-situ* information on effective degradation processes.

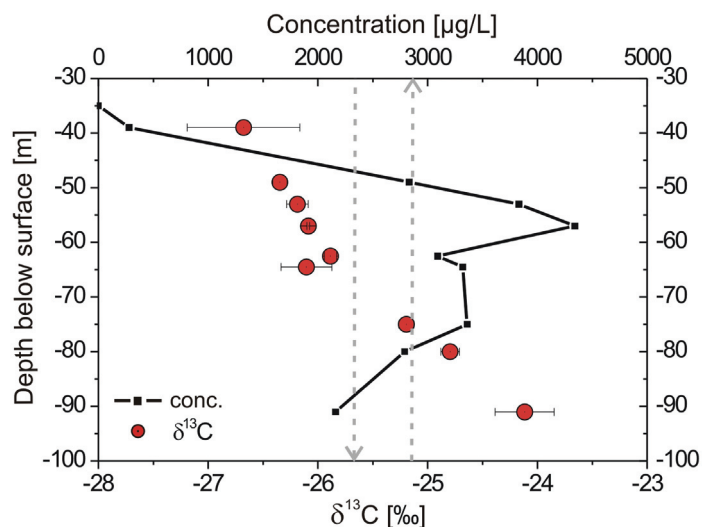


**Figure 4-1.** Tetrachloroethene (PCE) concentrations in  $\mu\text{g/L}$  (squares) and  $\delta^{13}\text{C}$  ratios in ‰ (circles) in groundwater samples taken from different sampling depths by a multilevel sampling well. Dotted vertical lines represent a mean concentration of  $2900 \mu\text{g/L}$  and a concentration-weighted average  $\delta^{13}\text{C}$  value of  $-25.7\text{‰}$  that would have been obtained by conventional groundwater sampling of a fully screened well.

**Sampling Procedure.** All forms of sample treatment are subject to possible analyte loss, contamination, or isotope fractionation and thus, sources of uncertainty when interpreting stable isotope data. Hence sampling procedure, sample preservation and a rapid transport to the laboratory are as important as laboratory sample handling and the analytical method applied. Appropriate measurements of field parameters, groundwater chemistry, and control/validation of external laboratory analyses should be mandatory for a comprehensive data interpretation. Sampling protocols are manifold. To summarize common advices, sampling should be performed as disturbance-free as possible, the groundwater should stay within a closed system to minimize loss of volatile compounds and inert tubing should be selected in order to avoid detrimental effects due to diffusion or sorption into the material. Of course, sampling equipment should eliminate any possibility of an isotope fractionation effect. Recently, we presented a study on a modified purge-and-trap system (P&T) using  $50 \text{ m} \times 1.6 \text{ mm id}$  ( $3.2 \text{ mm od}$ ) Teflon tubing for sample transfer (27). A comparison of  $\delta^{13}\text{C}$  values obtained by P&T with external elemental analyzer measurements of the pure liquid phase showed no significant deviations ( $\leq 0.5\text{‰}$ ) for almost all analyzed BTEX and chlorinated hydrocarbons. Since no significant isotope shifts could be detected we conclude that using stainless steel or Teflon tubing should minimize bias during sampling with regard to isotope fractionation.

**Sample Preservation and Storage.** It is recommended to collect groundwater samples according to EPA standard guidelines for VOC samples in brown glass bottles, free of headspace, sealed with Teflon lined screw caps, cooled and kept refrigerated at 4 °C until isotope analysis. A duplicate water sample should be obtained to avoid headspace if re-analysis should become necessary. The application of traditional preservation agents such as hydrochloric acid to  $\text{pH} \leq 2$  is routine, but might cause problems due to reactions with the analytical equipment, such as sorbent traps (SPME fibers, analytical trap of the P&T-system) or the CuO/NiO/Pt catalyst within the combustion furnace. Antimicrobial treatment with trisodium phosphate (to  $\text{pH} 10.5$ ) is another option, especially in case of fuel oxygenate analysis (28). Kovacs and Kampbell (29) tested the performance of trisodium phosphate, sulfuric acid and mercuric chloride. Although being very effective, the use of sodium azide or mercury salts should be carefully considered regarding their higher toxicity and waste management problematic. As is routine in analytical chemistry, all samples should be analyzed as soon as possible after collection. BTEX containing groundwater samples stored without headspace in volatile organic analyte (VOA) vials and preserved with hydrochloric acid did not show substantial loss and isotope fractionation within 4 weeks after sampling (30). Similar results have been obtained in our laboratory for storage of aqueous samples contaminated with chlorinated hydrocarbons. Table 4-1 exemplifies data for groundwater samples containing 1 to 3 mg/L PCE. The constant  $\delta^{13}\text{C}$  values indicate no substantial degradation even after a very long storage period of four months. The samples were not chemically treated, kept at 4°C in the dark, and stored without headspace (for additional results refer to Appendix of Chapter 5). However, since geochemical conditions in environmental samples and susceptibility of target analytes towards degradation vary to a large extent, in general preservation agents should be added if storage times exceed a few days. An effective way of preservation was recently proposed by Elsner and coworkers (31). Stable carbon isotope ratios confirmed that trichloroethene (TCE) was preserved in frozen suspensions of zerovalent iron, whereas storage at 7 °C was ineffective, and in the latter case, complete degradation of TCE occurred within four weeks. Hence, freezing may stop even abiotic chemical reactions that would not be prevented by cooling or traditional preservation agents (31).

**Table 4-1:** Effect of  $\delta^{13}\text{C}$  on storage time for groundwater samples containing perchloroethene (PCE) with concentrations between 1 and 3 mg/L, stored at 4 °C in the dark, without headspace. Each sample was measured in triplicates ( $n = 3$ ). Sampling was performed at KORA-site Rosengarten-Ehestorf (described in Chapter 2).

Sample	$\delta^{13}\text{C}$ in ‰ after 2 weeks	Standard deviation ( $n = 3$ )	$\delta^{13}\text{C}$ in ‰ after 4 months	Standard deviation ( $n = 3$ )
sample no.1	-27,2	$\pm 0.3$	-27,2	$\pm 0.1$
sample no.2	-27,1	$\pm 0.3$	-27,0	$\pm 0.1$
sample no.3	-27,1	$\pm 0.1$	-26,9	$\pm 0.1$
sample no.4	-27,1	$\pm 0.2$	-26,7	$\pm 0.1$

### 4.3. Sensitivity and Linearity of CSIA

IRMS systems provide specialised and highly sensitive detectors achieving a precision four orders of magnitude better than conventional (mass-scanning) mass spectrometers. However, to achieve this level of precision in continuous-flow techniques coupled with gas-chromatography, ca. 1 nmol of carbon or 8 nmol of hydrogen need to be injected on-column. Sensitivity and precision of continuous-flow IRMS measurements have been discussed in detail recently by Sessions (20). Deciphering the source and fate of contaminants with the help of CSIA is nowadays possible even at low contaminant concentrations that are frequently found in the fringe zones of contaminant plumes. Effective extraction and pre-concentration techniques for the analysis of isotope ratios for analytes in the low  $\mu\text{g/L}$  range are available. Another benefit of these techniques is that there is no, or at least a reduced consumption of organic solvents. Although pre-concentration techniques such as LVI (large volume injection), SPME (solid-phase microextraction) or purge-and-trap (P&T) have been well established in several analytical working laboratories, the use of these techniques in combination with GC/IRMS is much less routine. Hence, some potential pitfalls of these techniques are discussed in the following.

Higher sensitivities for apolar and non-volatile contaminants in soil samples can be attained by liquid extraction techniques such as accelerated solvent extraction (ASE) or Soxhlet extraction. As already mentioned, methods for sample preparation might introduce an isotope fractionation and, thus, need a careful evaluation by means of internal standards of known isotopic composition. Soxhlet extraction, for example, did not significantly change the isotopic composition of PAH compounds (32). Graham et al. (33) reported that ASE followed by cleanup, resulted in more consistent and reproducible stable carbon isotope data compared with other extraction techniques applied.

It has been reported that split/splitless injectors are sensitive to isotope fractionation effects (34,35). The flow conditions in the injector can cause an amount-dependent isotope fractionation during split injections. Thus, early work strongly favored on-column injection or splitless injection with long enough splitless times. An optimization of injection parameters is highly recommended to prevent or at least minimize fractionation effects. Smallwood et al. (36) studied four different injection techniques for analysing MTBE samples with GC/IRMS in comparison with a conventional dual-inlet isotope measurement. They concluded that both direct and headspace injection of neat MTBE into a split/splitless-injector (with a split ratio 100:1) provided a precise method for determining  $\delta^{13}\text{C}$  values. Headspace analysis of water samples containing MTBE was neither precise nor accurate, whereas a purge-and-trap sample concentrator interfaced to the GC/IRMS provided the most accurate and precise method for determination of  $\delta^{13}\text{C}$  values of MTBE in groundwater samples (36). While Smallwood and coworkers questioned the use of headspace analysis for MTBE, other authors demonstrated the headspace or headspace-SPME technique could indeed be used precisely (37-39). For CSIA of volatile groundwater constituents, analyte pre-concentration techniques such as SPME and P&T can be employed to improve sensitivity (27,40). An isotope fractionation effect of SPME- and P&T-techniques has been evaluated thoroughly (27,40,41), see also results obtained in this study (Chapter 2). To maximize partitioning into the headspace, NaCl is often added to the sample. The procedure, which increases the ionic strength of the solution, does not induce isotope fractionation (40,42).

Since low contaminant concentrations in groundwater samples may require the extraction of large water volumes with very small amounts of solvent, microseparator systems can be used to guarantee complete recovery of the solvent phase (43). As discussed in Chapter 3, PTV (programmable temperature vaporizer) injectors allow for the injection of large volumes of extracts (LVI) enhancing the detection limit of the IRMS 100 to 200 times compared to a standard 1 to 2  $\mu\text{L}$  injection (for a comparison in signal size, see Figures 4-2b and 4-2c). When working with LVI systems, there is a need to assure that the extractant is of sufficiently high purity to permit its use without compromising the accuracy of the determination. Dempster et al. (44) used liquid liquid extraction (LLE) with *n*-pentane as solvent for the extraction of dissolved BTEX in water. Their study confirmed that LLE is isotopically non-fractionating regardless of extraction efficiency. The same observation was made for  $\delta^{13}\text{C}$  and  $\delta^2\text{H}$  of selected monoaromatic and polyaromatic hydrocarbons after pentane extraction (43).

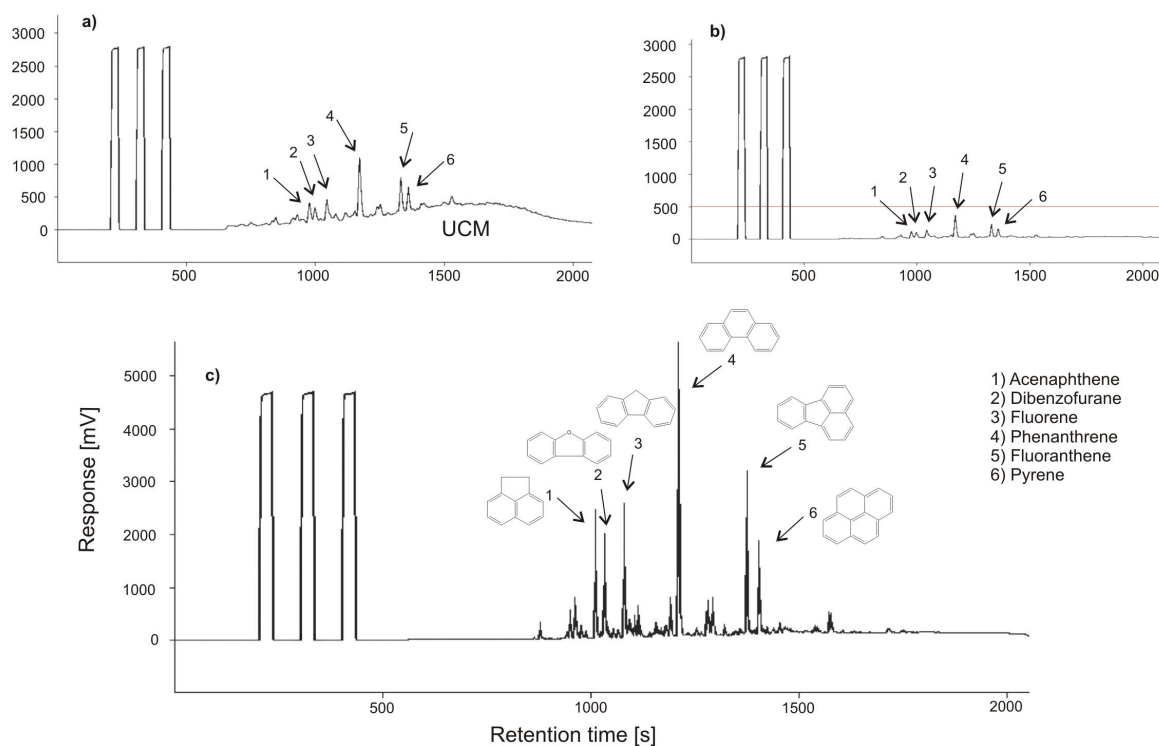


**Figure 4-2.** **A**, GC/IRMS chromatogram of a soil sample after accelerated solvent extraction (ASE) shows a raised baseline due to unresolved complex mixture (UCM) present in the sample. **B**, GC/IRMS chromatogram of the same soil sample after accelerated solvent extraction (ASE) and cleanup on silica gel. Complete removal of UCM hump but the response (amplitude) of the target compounds is below the linear range of the IRMS at ca. 500 mV (horizontal line). **C**, GC/IRMS chromatogram of the same soil sample after ASE, silica gel cleanup and large volume injection (LVI). Baseline separation of all peaks of interest is achieved, and peak amplitudes are within the linear range of the IRMS and allow for an accurate and precise determination of  $\delta^{13}\text{C}$  values.

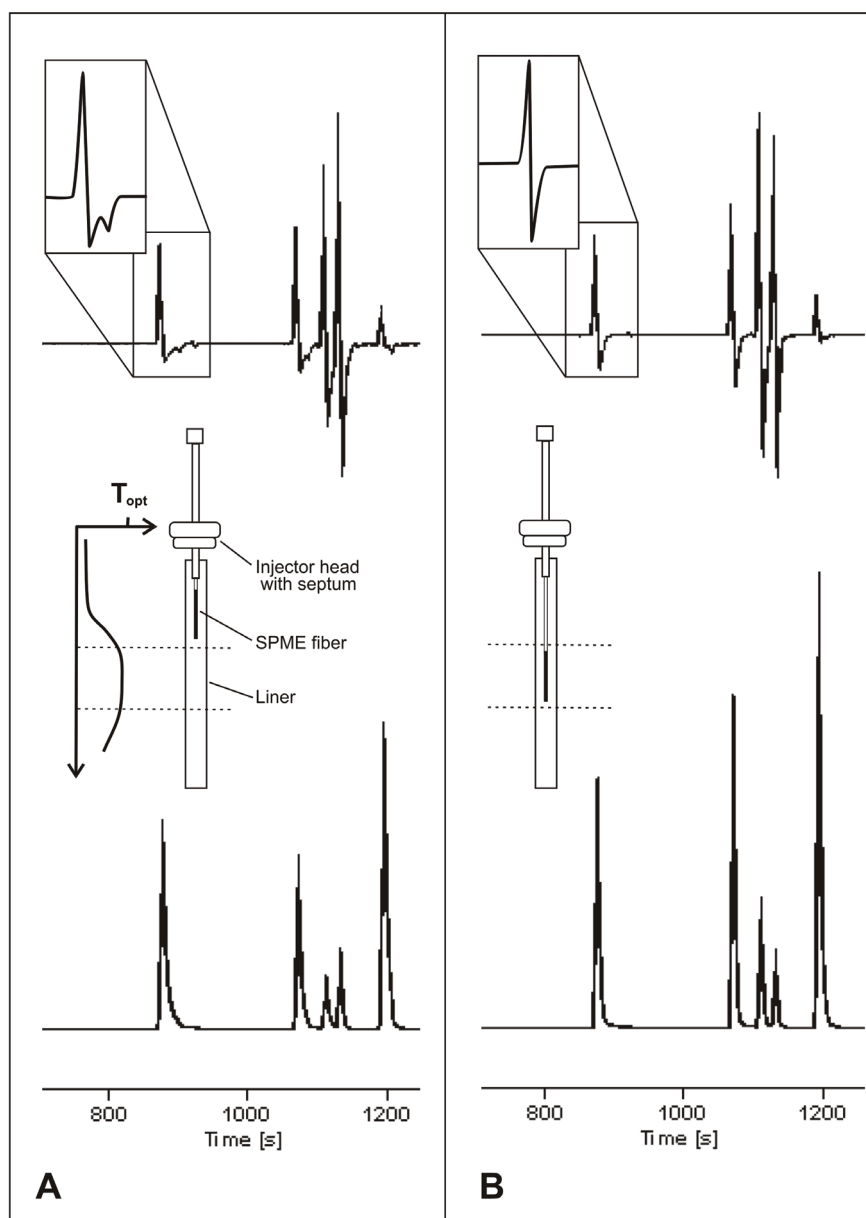


**Figure 4-3.** A) illustrates the detrimental effect on chromatographical resolution due to wrong SPME fiber exposure in a GC-injector. Non-ideal thermal desorption results in peak broadening (mass 44 chromatogram in the lower part of the figure) and poor isotope swings with secondary fluctuations recognized in the instantaneous ratio signal (upper trace). B) shows the same GC/IRMS analysis but with a correctly placed SPME fiber for comparison. As indicated in the upper trace, isotope swings (S-shaped ratio of mass 45/44) can serve as indicator for good chromatographic performance.

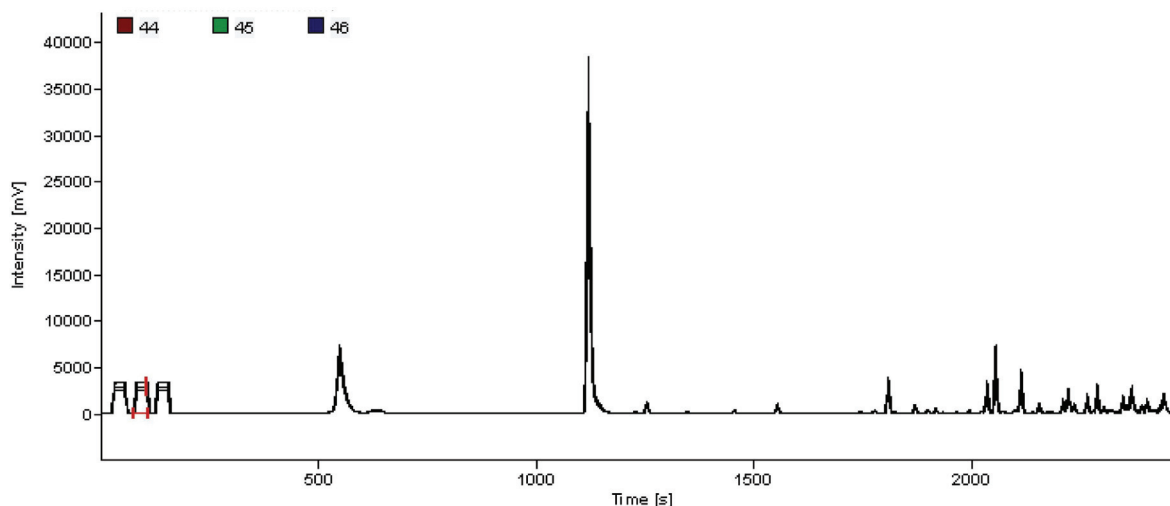


**Figure 4-4.** GC/IRMS chromatogram of a BTEX containing groundwater sample (obtained at KORA-site former military airfield Brand) that was not completely screened by GC/MS before analysis. An unexpected high MTBE concentration (signal size 40 Volt) caused severe contamination of the analytical equipment.

All system parameters involved in the analytical process need to be evaluated and well-adjusted in order to achieve a maximum in instrumental performance (exemplified by Figure 4-3 for the desorption process during SPME analyses). As with any pre-concentration method, a non-target screening analysis of samples prior to CSIA measurements should be obligatory to avoid contamination of the analytical system or oversaturation of the ion source. Figure 4-4 illustrates a worst case scenario in environmental compound-specific isotope analysis, where only BTEX concentrations had been reported by the contract laboratory. High MTBE concentrations had not been included in quantitative analysis and caused severe contamination problems within both the P&T and the GC/IRMS system. Any source of chromatographic interference caused by sample extraction and pre-concentration techniques, such as impurities in the purge gas, contact of the solvent extract to rubber septa (Figure 4-5), SPME fiber adulteration, carryover, etc., must be avoided. Blanks should always serve as a check on such contamination. Calibration by reference gas alone is not sufficient to exclude problems caused by incomplete combustion or poor performance of sample introduction or chromatography. Dependent on the question asked, the precision required and the matrix of the measured samples, the performance of the GC/IRMS-systems needs to be regularly tested by analyzing a set of standard compounds with known isotopic composition. Our recommendation for laboratories working on a routine level would be every 6 to 9 measurements. Although time- and cost-efficiency is a major concern in contaminated site remediation, ideally all measurements are carried out in triplicate or at least duplicate to avoid misinterpretation of data due to outliers.



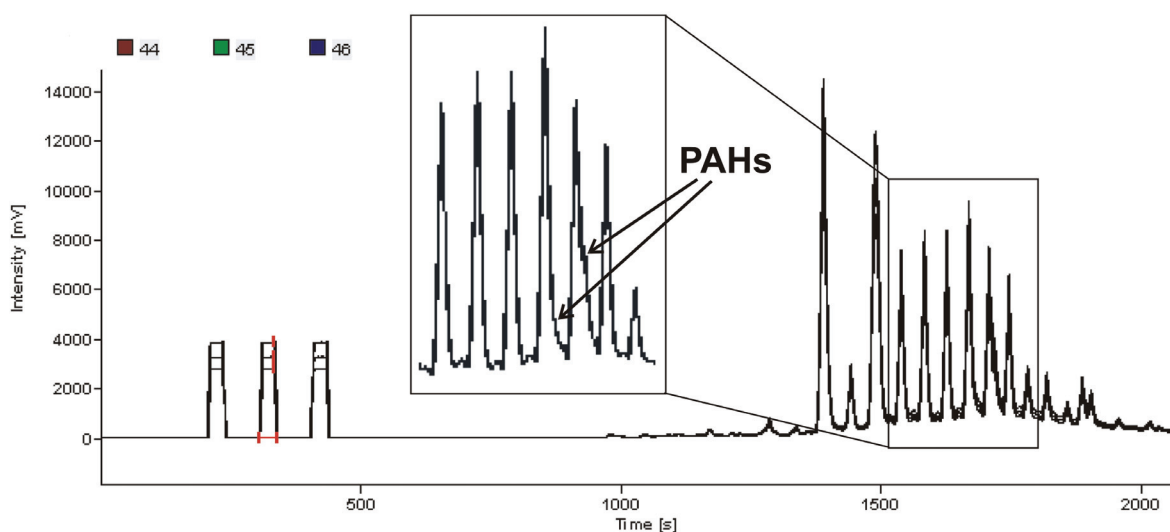


**Figure 4-5.** GC/IRMS chromatogram of a pentane extract containing phthalates (main peaks) leached out of septum material. Coeluting PAH target peaks (as illustrated in the left) could not be resolved and inhibited an isotope analysis.

Reproducibility and accuracy have always been critical points in GC/IRMS data assessment. In some previous studies a relationship between isotope signal ( $\delta$ -value) and response (signal size) has been observed (25,35,45) that the authors attributed to the non-linearity of the system. Hall et al. (46), therefore, proposed recalculation of  $\delta$ -values at low concentrations. Schmitt et al. (35) also suggested to correct for the amount-dependent isotope fractionation or non-linearity effects. But as demonstrated by Richnow et al. (25) and Sherwood Lollar et al. (47), there is no general trend to be followed, which excludes or limits the possibility of correcting  $\delta$ -values for non-linearity effects. Hence, if the amounts of carbon introduced are below the dynamic linearity range of the instrument correction procedures remain problematic and the difficulties or even errors associated with recalculations are still under discussion. Reported  $\delta$ -values should always yield a response above the value where systematic errors due to non-linearity effects become significant (25). Thus, linearity of the specific instrument must be ensured for each compound of interest, as most of the scientific working laboratories do. Jochmann et al. (27) suggested an approach to define method detection limits by a thorough investigation of  $\delta^{13}\text{C}$  values of various compounds in relation to their corresponding signal size. The concentration range where  $\delta^{13}\text{C}$  values are within an  $\pm 0.5$  ‰ interval around the running mean represents the linear range of the instrument (refer to Figure 4-6 for illustration). A method for assessing the total instrumental uncertainty, incorporating both accuracy and reproducibility of CSIA measurements was described recently by Sherwood Lollar et al. (47).

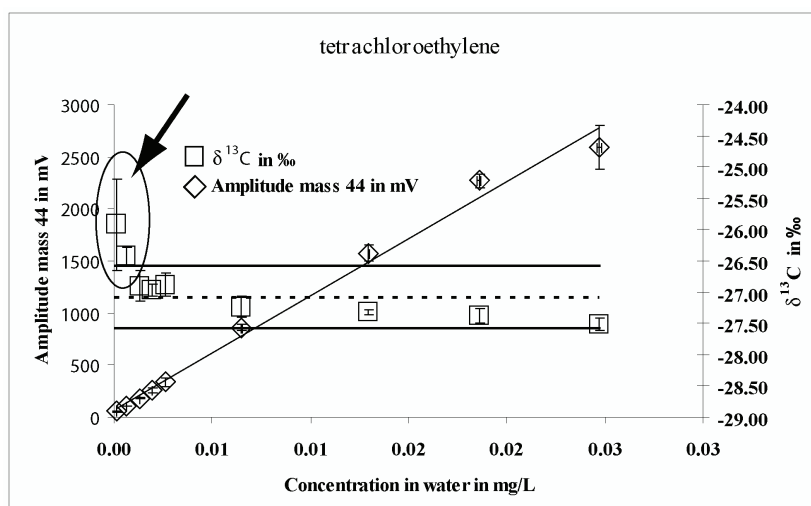


**Figure 4-6.** Amount dependency on  $\delta^{13}\text{C}$  measurements for PCE. Square symbols represent the carbon isotope value in ‰, diamonds indicate signal size of the mass 44 peak in mV. The horizontal broken line represents the iteratively calculated mean  $\delta^{13}\text{C}$  value, solid lines indicate the  $\pm 0.5$  ‰ interval. Values outside the linear range of the IRMS are circled. Measurements were performed in triplicates, the standard deviation of each point is indicated by error bars. The major principles illustrated in this figure are described in Jochmann et al. (27).

#### 4.4. Problems Related to Chromatographic Resolution

**Gaschromatographic Separation.** Recently, Sessions (20) highlighted various aspects of gas chromatography adapted to isotope ratio measurements. A prerequisite of accurate compound-specific isotope ratio determination is that compounds of interest need to be separated well. Gaschromatographic separation must provide complete resolution of individual compounds because the heavier isotopologues are eluted slightly earlier from the GC-column than the lighter isotopologues (48). Adjacent component peaks might overlap which then alters the  $\delta$ -values of both (5). The inverse isotope effect during chromatographic separation results in an isotope swing (S-shaped 45/44-ratio) (8,9). Please refer to Figure 4-3 for an illustration of the isotope swing. Hence, a high data quality in GC/IRMS measurements requires peak integration from baseline to baseline, without loss of peak data due to partial peak integration and without any peak overlap due to interferences with coeluting compounds (9). If neighbouring peaks are not baseline resolved, wrong baseline measurements and hence, a wrong data correction will be performed. Brenna et al. (49) studied the detrimental effects of overlapping peaks on data precision and accuracy. They reported that even a small extent of peak overlap may have a dramatic effect on isotope ratios although precision measured with repeated injections were excellent. The effect was even more pronounced for the smaller peak of a mismatched pair (49). This also indicates that high precision alone can not be used as a demonstration of quality assurance for measured

data. Figure 4-7 illustrates the aforementioned effect of poor chromatographic resolution with an example for *trans*-1,2-DCE and MTBE. The poor resolution results in inaccurate isotope values, although precision was  $\leq 0.2\%$ . Isotope swings serve as a good indicator for good chromatographic performance (50). As is illustrated in Figure 4-3a, inappropriate SPME fiber exposure depth during desorption in the injector causes poor peak shapes and poor isotope swings, and thus might influence peak separation. This again emphasizes the need for optimal parameter adjustment in order to achieve accurate CSIA measurements. The accuracy of measured isotope ratios has to be confirmed for different pre-concentration and separation conditions by means of working standards consisting of all compounds of interest with known isotopic composition. To assure reliable and precise isotope data within a reasonable standard deviation it is recommended to perform several test runs with working standards within a range of concentrations of individual compounds which are representative for the 'real' sample.

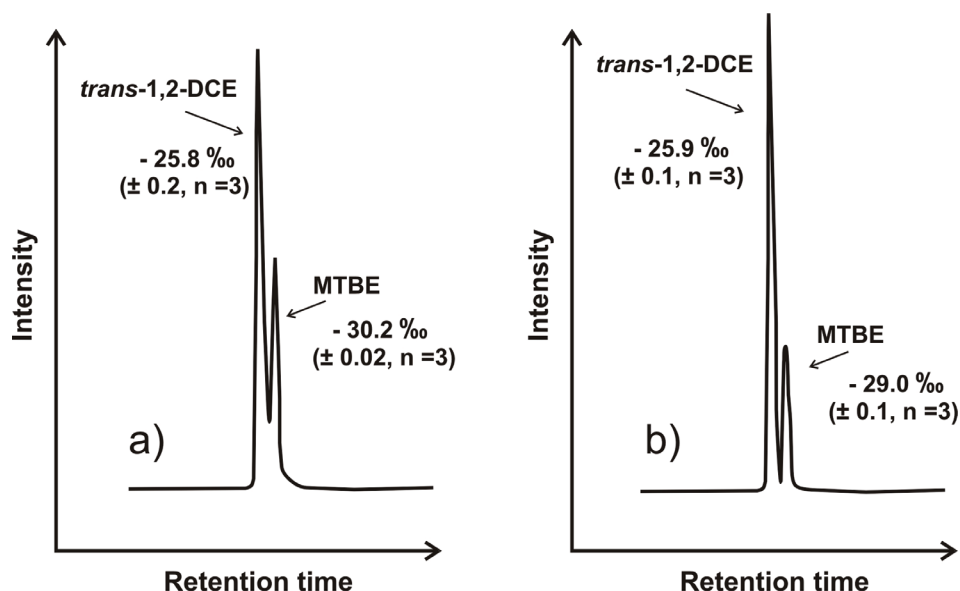


**Figure 4-7.** Effect of poor chromatographic resolution on  $\delta^{13}\text{C}$  values of adjacent peaks. Isotope values for single compound injections were:  $-26.0\text{‰}$  ( $\pm 0.1$ ,  $n=3$ ) for *trans*-1,2-DCE and  $-28.8\text{‰}$  ( $\pm 0.1$ ,  $n=3$ ) for MTBE. The measured isotope ratio for the smaller peak shown in **a**) deviates significantly from its actual value. Good peak resolution as indicated in **b**) results in almost accurate isotope values for both compounds.

Although baseline-separated peaks and complete resolution of the individual components are required for precise GC/IRMS measurements (9), there are environmental samples in which peak overlapping simply cannot be avoided. Gas chromatograms of fuel-contaminated water or soil, i.e., contain many coeluting peaks and also a wide range of concentrations of different compounds (see Figure 4-2). Due to high background signals in samples from close to a petroleum fuel source, Spence et al. (37) admitted that analyses were not reliable and thus not

reported. Optimal peak separation was only achieved for samples containing relatively few analytes (37). Note that the compounds or constituents of environmental samples often show large differences in their individual concentrations within one sample, which often prevents an adjustment for optimal precision of the isotope measurement in a single analysis and thus results in larger standard deviations at small analyte concentrations (25). Yanik et al. (51) concluded in their study that variations in the isotope ratio might not represent different sources but may in fact represent contributions of minor compounds influencing the isotopic composition of even well-resolved compounds. The GC/IRMS-system allows not only for backflushing of solvent peaks at the beginning of a chromatogram, but also at different times within a single run. Hence, one way to circumvent the problem would be to adjust for peaks with low concentrations and backflush components with higher concentrations to avoid oversaturation of the ion source. Backflushing of single compounds is often restricted by the time necessary for transferring the compound from the GC to the IRMS system. If given time windows are too short, one might miss either the  $^{13}\text{C}$ -enriched part at the beginning of a peak or the  $^{13}\text{C}$ -depleted part at the end of a peak of interest. Thus, backflushing of single compounds needs a thorough, system-specific pre-investigation with standards of known isotopic composition. Furthermore, in case that isotope analysis of major components is also required, samples need to be split and analyzed twice, once with appropriate dilution, once without dilution and the described backflushing.

**Strategies to Avoid Matrix Interference.** A limiting factor in CSIA of environmental samples is the fact that an organic contamination often contains hundreds of different compounds resulting in interferences in the chromatography. In particular, the unresolved complex mixture (UCM) of hydrocarbons in petroleum-contaminated soils and sediments often hamper reliable isotope ratio measurements. The term UCM is referring to the hump-shaped baseline raise that is often found in gas chromatograms of petroleum products (see Figure 4-2a). Due to the complex chemical composition of predominantly high-molecular weight, complex hydrocarbons, such as branched alkanes, cycloalkanes and PAHs (52), also peaks of interest remain unresolved in the UCM hump. Corrections required for coeluting and unresolved baseline components might be achieved using background subtraction software (53), if only low levels of background matrix or UCM are present. As compounds of interest need to be well resolved from neighbouring peaks in CSIA, and due to the detrimental influence of co-extracted compounds on almost every GC analysis step (54), there is a strong demand of improved cleanup strategies. Figure 4-2 exemplarily shows a GC/IRMS chromatogram of PAHs before and after cleanup with silica column chromatography that allowed to completely remove the UCM hump.

As mentioned before, all sample treatment procedures hold the potential of isotope fractionation. Hence, every step of the sample preparation protocol must be thoroughly evaluated by means of standards with known isotopic composition that are treated identical to the samples. ASE extraction of soil samples and purification using alumina/silica column chromatography resulted in a maximum  $\delta^{13}\text{C}$  shift of -0.5 ‰ for individual PAHs (45), which is within standard precision of GC/IRMS instruments. Cleanup using a alumina column eluted with hexane/toluene and cleanup on a silica column using dichloromethane as the eluting solvent resulted in almost the same hydrocarbon  $\delta^{13}\text{C}$  values (33). Kim et al. (55) reported that, although extensive cleanup incorporating alumina/silica gel column, gel permeation, and thin layer chromatography was performed, the original carbon isotopic composition of individual PAHs could be preserved. Mazeas and Budzinski (56) tested three different purification procedures and concluded that it did not introduce any significant isotope fractionation to the initial standard solution. O'Malley et al. (32) did not achieve complete elimination of the UCM. Paying close attention to background corrections in samples with prominent UCM, they introduced internal standards with known isotopic composition to aid a careful selection of background points and thus, a reliable determination of  $\delta^{13}\text{C}$  values of individual PAHs even if significant UCM was present.

Another way to achieve an increased sensitivity due to reduction in background and elimination of coeluting compounds is to use two-dimensional gas chromatography prior to combustion although this combination so far has hardly been reported in literature (57). In 2D-GC/IRMS, the GC-system needs to be equipped with a column switching device such as moving capillary stream switching (MCSS). By column switching parts of the effluent from the first column are cut and transferred to a second column, where separation of compounds of interest can be enhanced. Horii et al. (57) demonstrated  $\delta^{13}\text{C}$  measurements of individual congeners of polychlorinated biphenyls and chloronaphthalenes by application of the MCSS technique. As reported by Sessions (20) comprehensive GCxGC methods and fast GC, respectively, require very fast detector response times and thus, seem not to be appropriate analyte separation techniques for continuous-flow IRMS.

#### **4.5. CSIA of Non-Volatile Compounds**

GC-based applications are limited to volatile and thermally stable analytes. To improve chromatographic separation of non-volatile compounds and organic functional groups,

derivatization is commonly performed. Some requirements need to be fulfilled to guarantee accurate isotope analysis. Derivatizing reagents have to react quantitatively with the analytes, isotope dilution effects by addition of the element being analyzed should be excluded or limited, the reagents should not cause any adverse chromatographic effects and should have no detrimental effects on the reaction interface or result in an incomplete combustion (9,20). Due to the several potential problems of derivatization in CSIA there have been many attempts to hyphenate liquid chromatography with IRMS. Earlier approaches include a thermospray/particle beam interface (58) and a moving-wire interface (59,60). Although the latter has seen recent advances for the very sensitive carbon isotope analysis of discrete liquid samples (61), these interfaces have never been commercialized and thus their use remains restricted to the developing laboratories. In 2004, though, another interface design based on an on-line TOC equipment has been commercialized that is much more promising for future work (62). So far, on-line LC/IRMS based on this interface has been applied successfully for the isotope analysis of various analyte classes including proteins (63), carbohydrates (64), underivatized amino acids (65), and volatile fatty acids (66). However, there are still major challenges in this area. First, the commercial interface only allows for carbon isotope analysis. Second, separation is limited to pure aqueous eluents which requires the development of fully new separation approaches. Besides pH and ionic strength of the eluent that can be optimized for the separation of ionic compounds, temperature is one of the parameters that might be used to influence retention. Thus, LC/IRMS will certainly benefit from further developments in the area of high-temperature HPLC. Third, with regard to trace contaminants in environmental chemistry, the sensitivity of LC/IRMS may not be sufficient, thus requiring validated preconcentration steps. For example, Penning and Elsner estimated sensitivity to be 8 times lower for the carbon isotope analysis of isoproturon using LC/IRMS instead of GC/IRMS (67). The lower sensitivity currently achieved in LC/IRMS is partly due to the non-negligible background of carbon stemming in particular from column bleed.

#### **4.6. Uncertainties of Data Interpretation**

As both isotope analysis and further data processing can include sources of uncertainty (47), a strong collaboration of the isotope analyst and the customers is necessary to assure a high quality in data interpretation. Furthermore, it has to be emphasized that a prerequisite of environmental field work is a thorough characterization of field sites, for example, detailed knowledge on groundwater flow regimes and site-specific geochemical parameters. Slater (16) discussed

important points to be considered when interpreting data from field applications in a realistic and defensible way. He pointed out the challenge of determining the isotopic composition of the source zone, the problems connected with temporal variability of  $\delta$ -values in field applications, as well as the importance to obtain transects of samples at a high density. The study also mentioned quantification problems related to the application of the Rayleigh model at field sites. Overestimation of degradation rates is a major concern in assessing the natural attenuation potential at a contaminated site. Laboratory studies have shown that different bacterial strains may cause different magnitudes of isotope fractionation (from large to non-detectable) dependent on the substrate and the different mechanisms in the rate-limiting step of the enzymatic reaction (17). Studies by Meckenstock et al. (17) and Abé and Hunkeler (68) demonstrated the difficulties when calculating the extent of *in-situ* biodegradation at field sites, an in-depth discussion of this issue is provided by Morrill et al. (69). Fischer et al. (70) reported on the relevance of non-fractionating processes in estimating *in-situ* degradation rates from field data. Those difficulties are especially important as systems become more and more complex. One should always keep in mind that most of the field studies reported in literature have focussed on homogeneous and unconsolidated aquifer systems. Until now, only a few were considering hydrogeological complex and heterogeneous systems, e.g., fractured bedrock (37,21).

#### 4.7. References

- (1) Sano, M.; Yotsui, Y.; Abe, H.; Sasaki, S. A new technique for the detection of metabolites labelled by the isotope  $^{13}\text{C}$  using mass fragmentography. *Biomed. Mass Spectrom.* **1976**, *3*, 1-3.
- (2) Matthews, D. E.; Hayes, J. M. Isotope-ratio-monitoring gas chromatography-mass spectrometry. *Anal. Chem.* **1978**, *50*, 1465-1473.
- (3) Barrie, A.; Bricout, J.; Koziat, J. Gas chromatography - stable isotope ratio analysis at natural abundance levels. *Biomed. Mass Spectrom.* **1984**, *11*, 583-588.
- (4) Freedman, P. A.; Gillyon, E. C. P.; Jumeau, E. J. Design and application of a new instrument for GC-isotope ratio MS. *Am. Lab.* **1988**, *20*, 114-119.
- (5) Hayes, J. M.; Freeman, K. H.; Popp, B. N.; Hoham, C. H. Compound-specific isotopic analyses: A novel tool for reconstruction of ancient biogeochemical processes. *Org. Geochem.* **1990**, *16*, 1115-1128.
- (6) Schoell, M.; McCaffrey, M. A.; Fago, F. J.; Moldowan, J. M. Carbon isotopic compositions of 28,30-bisnorhopanes and other biological markers in a Monterey crude oil. *Geochim. Cosmochim. Acta* **1992**, *56*, 1391-1399.
- (7) Ruble, T. E.; Bakel, A. J.; Philp, R. P. Compound specific isotopic variability in Uinta Basin native bitumens: paleoenvironmental implications. *Org. Geochem.* **1994**, *21*, 661-671.
- (8) Brand, W. A. High precision isotope ratio monitoring techniques in mass spectrometry. *J. Mass Spectrom.* **1996**, *31*, 225-235.
- (9) Meier-Augenstein, W. Applied gas chromatography coupled to isotope ratio mass spectrometry. *J. Chromatogr. A* **1999**, *842*, 351-371.
- (10) Schmidt, T. C.; Zwank, L.; Elsner, M.; Berg, M.; Meckenstock, R. U.; Haderlein, S. B. Compound-specific stable isotope analysis of organic contaminants in natural environments: a critical review of the state of the art, prospects, and future challenges. *Anal. Bioanal. Chem.* **2004**, *378*, 283-300.

- (11) Benson, S.; Lennard, C.; Maynard, P.; Roux, C. Forensic applications of isotope ratio mass spectrometry - A review. *Forensic Sci. Int.* **2006**, *157*, 1-22.
- (12) Eakin, P. A.; Fallick, A. E.; Gerk, J. Some instrumental effects in the determination of stable carbon isotope ratios by gas chromatography-isotope ratio mass spectrometry. *Chem. Geol.* **1992**, *101*, 71-79.
- (13) Ricci, M. P.; Merritt, D. A.; Freeman, K. H.; Hayes, J. M. Acquisition and processing of data for isotope-ratio-monitoring mass spectrometry. *Org. Geochem.* **1994**, *21*, 561-571.
- (14) Merritt, D. A.; Freeman, K. H.; Ricci, M. P.; Studley, S. A.; Hayes, J. M. Performance and Optimization of a Combustion Interface for Isotope Ratio Monitoring Gas Chromatography/Mass Spectrometry. *Anal. Chem.* **1995**, *67*, 2461-2473.
- (15) Sherwood Lollar, B.; Slater, G. F.; Ahad, J.; Sleep, B.; Spivack, J.; Brennan, M.; MacKenzie, P. Contrasting carbon isotope fractionation during biodegradation of trichloroethylene and toluene: Implications for intrinsic bioremediation. *Org. Geochem.* **1999**, *30*, 813-820.
- (16) Slater, G. F. Stable isotope forensics - When isotopes work. *Environ. Forensics* **2003**, *4*, 13-23.
- (17) Meckenstock, R. U.; Morasch, B.; Griebler, C.; Richnow, H. H. Stable isotope fractionation analysis as a tool to monitor biodegradation in contaminated aquifers. *J. Contam. Hydrol.* **2004**, *75*, 215-255.
- (18) Elsner, M.; Zwank, L.; Hunkeler, D.; Schwarzenbach, R. P. A new concept linking observable stable isotope fractionation to transformation pathways of organic pollutants. *Environ. Sci. Technol.* **2005**, *39*, 6896-6916.
- (19) Hunkeler, D.; Meckenstock, R. U.; Sherwood Lollar, B.; Schmidt, T. C.; Wilson, J. T. A. A consensus guide for assessing biodegradation and source identification with compound-specific isotope analysis (CSIA). **2007**, submitted.
- (20) Sessions, A. L. Isotope-ratio detection for gas chromatography Review. *J. Sep. Sci.* **2006**, *29*, 1946-1961.
- (21) Chartrand, M. M. G.; Morrill, P. L.; Lacrampe-Couloume, G.; Sherwood Lollar, B. Stable isotope evidence for biodegradation of chlorinated ethenes at a fractured bedrock site. *Environ. Sci. Technol.* **2005**, *39*, 4848-4856.
- (22) Peter, A.; Steinbach, A.; Liedl, R.; Ptak, T.; Michaelis, W.; Teutsch, G. Assessing microbial degradation of o-xylene at field-scale from the reduction in mass flow rate combined with compound-specific isotope analyses. *J. Contam. Hydrol.* **2004**, *71*, 127-154.
- (23) Blum, P.; Kamkar, P.; Melzer, R. Sensitivitätsanalyse von Natural Attenuation anhand analytischer Transportmodelle. *Altlasten Spektrum* **2007**, *2*, 74-81.
- (24) Kopinke, F. D.; Georgi, A.; Voskamp, M.; Richnow, H. H. Carbon isotope fractionation of organic contaminants due to retardation on humic substances: Implications for natural attenuation studies in aquifers. *Environ. Sci. Technol.* **2005**, *39*, 6052-6062.
- (25) Richnow, H. H.; Annweiler, E.; Michaelis, W.; Meckenstock, R. U. Microbial in situ degradation of aromatic hydrocarbons in a contaminated aquifer monitored by carbon isotope fractionation. *J. Contam. Hydrol.* **2003**, *65*, 101-120.
- (26) Song, D. L.; Conrad, M. E.; Sorenson, K. S.; Alvarez-Cohen, L. Stable carbon isotope fractionation during enhanced in situ bioremediation of trichloroethene. *Environ. Sci. Technol.* **2002**, *36*, 2262-2268.
- (27) Jochmann, M. A.; Blessing, M.; Haderlein, S. B.; Schmidt, T. C. A new approach to determine method detection limits for compound-specific isotope analysis of volatile organic compounds. *Rapid Commun. Mass Spectrom.* **2006**, *20*, 3639-3648.
- (28) McLoughlin, P. W.; Pirkle, R. J.; Fine, D.; Wilson, J. T. TBA production by acid hydrolysis of MTBE during heated headspace analysis and evaluation of a base as a preservative. *Ground Water Monit. Remediat.* **2004**, *24*, 57-66.
- (29) Kovacs, D. A.; Kampbell, D. H. Improved method for the storage of groundwater samples containing volatile organic analytes. *Arch. Environ. Contamin. Toxicol.* **1999**, *36*, 242-247.
- (30) Kelley, C. A.; Hammer, B. T.; Coffin, R. B. Concentrations and stable isotope values of BTEX in gasoline-contaminated groundwater. *Environ. Sci. Technol.* **1997**, *31*, 2469-2472.
- (31) Elsner, M.; Lacrampe-Couloume, G.; Sherwood Lollar, B. Freezing to preserve groundwater samples and improve headspace quantification limits of water-soluble organic contaminants for carbon isotope analysis. *Anal. Chem.* **2006**, *78*, 7528-7534.
- (32) O'Malley, V. P.; Abrajano, T. A.; Hellou, J. Determination of the <sup>13</sup>C/<sup>12</sup>C ratios of individual PAH from environmental samples: can PAH sources be apportioned? *Org. Geochem.* **1994**, *21*, 809-822.
- (33) Graham, M. C.; Allan, R.; Fallick, A. E.; Farmer, J. G. Investigation of extraction and clean-up procedures used in the quantification and stable isotopic characterisation of PAHs in contaminated urban soils. *Sci. Total Environ.* **2006**, *360*, 81-89.
- (34) Baylis, S. A.; Hall, K.; Jumeau, E. J. The analysis of the C1-C5 components of natural gas samples using gas chromatography-combustion-isotope ratio mass spectrometry. *Org. Geochem.* **1994**, *21*, 777-785.
- (35) Schmitt, J.; Glaser, B.; Zech, W. Amount-dependent isotopic fractionation during compound-specific isotope analysis. *Rapid Commun. Mass Spectrom.* **2003**, *17*, 970-977.



- (36) Smallwood, B. J.; Philp, R. P.; Burgoyne, T. W.; Allen, J. D. The use of stable isotopes to differentiate specific source markers for MTBE. *Environ. l Forensics* **2001**, *2*, 215-221.
- (37) Spence, M. J.; Bottrell, S. H.; Thornton, S. F.; Richnow, H. H.; Spence, K. H. Hydrochemical and isotopic effects associated with petroleum fuel biodegradation pathways in a chalk aquifer. *J. Contam. Hydrol.* **2005**, *79*, 67-88.
- (38) Hunkeler, D.; Butler, B. J.; Aravena, R.; Barker, J. F. Monitoring biodegradation of methyl tert-butyl ether (MTBE) using compound-specific carbon isotope analysis. *Environ. Sci. Technol.* **2001**, *35*, 676-681.
- (39) Gray, J. R.; Lacrampe-Couloume, G.; Gandhi, D.; Scow, K. M.; Wilson, R. D.; Mackay, D. M.; Sherwood Lollar, B. Carbon and hydrogen isotopic fractionation during biodegradation of methyl tert-butyl ether. *Environ. Sci. Technol.* **2002**, *36*, 1931-1938.
- (40) Zwank, L.; Berg, M.; Schmidt, T. C.; Haderlein, S. B. Compound-specific carbon isotope analysis of volatile organic compounds in the low-microgram per liter range. *Anal. Chem.* **2003**, *75*, 5575-5583.
- (41) Hunkeler, D.; Aravena, R. Determination of compound-specific carbon isotope ratios of chlorinated methanes, ethanes, and ethenes in aqueous samples. *Environ. Sci. Technol.* **2000**, *34*, 2839-2844.
- (42) Slater, G. F.; Dempster, H. S.; Sherwood Lollar, B.; Ahad, J. Headspace analysis: A new application for isotopic characterization of dissolved organic contaminants. *Environ. Sci. Technol.* **1999**, *33*, 190-194.
- (43) Steinbach, A.; Seifert, R.; Annweiler, E.; Michaelis, W. Hydrogen and carbon isotope fractionation during anaerobic biodegradation of aromatic hydrocarbons - A field study. *Environ. Sci. Technol.* **2004**, *38*, 609-616.
- (44) Dempster, H. S.; Sherwood Lollar, B.; Feenstra, S. Tracing organic contaminants in groundwater: A new methodology using compound-specific isotopic analysis. *Environ. Sci. Technol.* **1997**, *31*, 3193-3197.
- (45) Wilcke, W.; Krauss, M.; Amelung, W. Carbon isotope signature of polycyclic aromatic hydrocarbons (PAHs): Evidence for different sources in tropical and temperate environments? *Environ. Sci. Technol.* **2002**, *36*, 3530-3535.
- (46) Hall, J. A.; Barth, J. A. C.; Kalin, R. M. Routine analysis by high precision gas chromatography mass selective detector isotope ratio mass spectrometry to 0.1 parts per mil. *Rapid Commun. Mass Spectrom.* **1999**, *13*, 1231-1236.
- (47) Sherwood Lollar, B.; Hirschorn, S. K.; Chartrand, M. M. G.; Lacrampe-Couloume, G. An approach for assessing total instrumental uncertainty in compound-specific carbon isotope analysis: Implications for environmental remediation studies. *Anal. Chem.* **2007**, *79*, 3469-3475.
- (48) van Hook, W. A.; Emmet, P. H. The Gas Chromatographic Determination of Hydrogen, Deuterium and HD. *J. Physical Chem.* **1960**, 673-675.
- (49) Brenna, J. T.; Corso, T. N.; Tobias, H. J.; Caimi, R. J. High-precision continuous-flow isotope ratio mass spectrometry. *Mass Spectrom. Reviews* **1997**, *16*, 227-258.
- (50) Hilker, A. W.; Douthitt, C. B.; Schlüter, H. J.; Brand, W. A. Isotope ratio monitoring gas chromatography mass spectrometry of D H by high temperature conversion isotope ratio mass spectrometry. *Rapid Commun. Mass Spectrom.* **1999**, *13*, 1226-1230.
- (51) Yanik, P. J.; O'Donnell, T. H.; Macko, S. A.; Qian, Y.; Kennicutt, M. C. Source apportionment of polychlorinated biphenyls using compound specific isotope analysis. *Org. Geochem.* **2003**, *34*, 239-251.
- (52) Frysinger, G. S.; Gaines, R. B.; Xu, L.; Reddy, C. M. Resolving the unresolved complex mixture in petroleum-contaminated sediments. *Environ. Sci. Technol.* **2003**, *37*, 1653-1662.
- (53) Sun, Y. G.; Sheng, G. Y.; Peng, P.; Fu, J. M. Compound-specific stable carbon isotope analysis as a tool for correlating coal-sourced oils and interbedded shale-sourced oils in coal measures: an example from Turpan basin, north-western China. *Org. Geochem.* **2000**, *31*, 1349-1362.
- (54) Dabrowski, L.; Giergielewicz-Mozajska, H.; Gorski, L.; Biziuk, M.; Namiesnik, J.; Janicki, B. Determination of environmental pollutants in soil and sediments - Some aspects of sample clean-up and GC analysis. *J. Sep. Sci.* **2002**, *25*, 290-296.
- (55) Kim, M.; Kennicutt II, M. C.; Qian, Y. Polycyclic aromatic hydrocarbon purification procedures for compound specific isotope analysis. *Environ. Sci. Technol.* **2005**, *39*, 6770-6776.
- (56) Mazeas, L.; Budzinski, H. Polycyclic aromatic hydrocarbon C-13/C-12 ratio measurement in petroleum and marine sediments - Application to standard reference materials and a sediment suspected of contamination from the Erika oil spill. *J. Chromatogr. A* **2001**, *923*, 165-176.
- (57) Horii, Y.; Kannan, K.; Petrick, G.; Gamo, T.; Falandysz, J.; Yamashita, N. Congener-specific carbon isotopic analysis of technical PCB and PCN mixtures using two-dimensional gas chromatography - Isotope ratio mass spectrometry. *Environ. Sci. Technol.* **2005**, *39*, 4206-4212.
- (58) Teffera, Y.; Kusmierz, J. J.; Abramson, F. P. Continuous-Flow Isotope Ratio Mass Spectrometry Using the Chemical Reaction Interface with Either Gas or Liquid Chromatographic Introduction. *Anal. Chem.* **1996**, *68*, 1888-1894.
- (59) Caimi, R. J.; Brenna, J. T. High-precision liquid chromatography-combustion isotope ratio mass spectrometry. *Anal. Chem.* **1993**, *65*, 3497-3500.

- (60) Brand, W. A.; Dobberstein, P. Isotope-ratio-monitoring liquid chromatography mass spectrometry (IRM-LCMS): First results from a moving wire interface system. *Isot. Environ. Health Stud.* **1996**, *32*, 275-283.
- (61) Sessions, A. L.; Sylva, S. P.; Hayes, J. M. Moving-Wire Device for Carbon Isotopic Analyses of Nanogram Quantities of Nonvolatile Organic Carbon. *Anal. Chem.* **2005**, *77*, 6519-6527.
- (62) Krummen, M.; Hilker, A. W.; Juchelka, D.; Duhr, A.; Schlüter, H. J.; Pesch, R. A new concept for isotope ratio monitoring liquid chromatography/mass spectrometry. *Rapid Commun. Mass Spectrom.* **2004**, *18*, 2260-2266.
- (63) Godin, J. P.; Hau, J.; Fay, L. B.; Hopfgartner, G. Isotope ratio monitoring of small molecules and macromolecules by liquid chromatography coupled to isotope ratio mass spectrometry. *Rapid Commun. Mass Spectrom.* **2005**, *19*, 2689-2698.
- (64) Cabanero, A. I.; Recio, J. L.; Ruperez, M. Liquid chromatography coupled to isotope ratio mass spectrometry: A new perspective on honey adulteration detection. *J. Agricul. Food Chem.* **2006**, *54*, 9719-9727.
- (65) McCullagh, J. S. O.; Juchelka, D.; Hedges, R. E. M. Analysis of amino acid C-13 abundance from human and faunal bone collagen using liquid chromatography/isotope ratio mass spectrometry. *Rapid Commun. Mass Spectrom.* **2006**, *20*, 2761-2768.
- (66) Heuer, V.; Elvert, M.; Tille, S.; Krummen, M.; Mollar, X. P.; Hmelo, L. R.; Hinrichs, K. U. Online delta C-13 analysis of volatile fatty acids in sediment/porewater systems by liquid chromatography-isotope ratio mass spectrometry. *Limnol. Oceanogr. Meth.* **2006**, *4*, 346-357.
- (67) Penning, H.; Elsner, M. **2007**. GSF Neuherberg, Germany, personal communication.
- (68) Abe, Y.; Hunkeler, D. Does the Rayleigh Equation Apply to Evaluate Field Isotope Data in Contaminant Hydrogeology? *Environ. Sci. Technol.* **2006**, *40*, 1588-1596.
- (69) Morrill, P. L.; Lacrampe-Couloume, G.; Slater, G. F.; Sleep, B. E.; Edwards, E. A.; McMaster, M. L.; Major, D. W.; Sherwood Lollar, B. Quantifying chlorinated ethene degradation during reductive dechlorination at Kelly AFB using stable carbon isotopes. *J. Contam. Hydrol.* **2005**, *76*, 279-293.
- (70) Fischer, A.; Theuerkorn, K.; Stelzer, N.; Gehre, M.; Thullner, M.; Richnow, H. H. Applicability of Stable Isotope Fractionation Analysis for the Characterization of Benzene Biodegradation in a BTEX-contaminated Aquifer. *Environ. Sci. Technol.* **2007**, *41*, 3689-3696.

## 5. Delineation of Multiple Chlorinated Ethene Sources in an Industrialized Area

### 5.1. Introduction

Extensive groundwater contamination has been caused by the almost ubiquitous use of the chlorinated solvents tetrachloroethene (PCE), trichloroethene (TCE), carbon tetrachloride (CT), and 1,1,1-trichloroethane (1,1,1-TCA), as cleaning and degreasing solvents (1,2). These compounds are toxic and/or carcinogenic and are regulated in drinking water at low levels (3). Especially in fractured bedrock aquifers these dense non-aqueous phase liquids (DNAPL) lead to a very complex contamination pattern and due to their slow dissolution rates provide a persistent source of contamination for decades (4).

Liabilities for expensive field investigations and remediation effort may be assessed by different means of environmental forensic litigation, including historical records, mathematical methods, chemical fingerprinting, and isotope analyses. However, all of these methods have severe drawbacks and thus rarely provide the required information on their own. Historical records documenting the usage of chemicals, although often not available or incomplete, typically serve as starting point. Evaluation of concentration data with mathematical methods such as probabilistic and geostatistical simulation, inverse modeling and regression approaches usually require homogeneous aquifer parameters with simple geometries and flow conditions (5-7). Environmental fingerprinting can be powerful for complex mixtures of contaminants such as oil, fuel or gasoline (8) but may be ambiguous if heavy weathering has occurred (9). Because of these limitations, stable isotope analysis has emerged as an important additional tool in forensic investigations (10,11). Studies where compound-specific isotope analysis (CSIA) have been successfully applied, include source allocation of polycyclic aromatic compounds (9,12,13). Several priority groundwater contaminants such as benzene, toluene, ethylbenzene, xylenes (BTEX), methyl *tert*-butyl ether, and chlorinated solvents exhibit different stable isotope signatures in products of different manufacturers (14). Hunkeler et al. (15) delineated different zones, each representing a different episode and location of DNAPL release using CSIA data at a site contaminated with PCE. Studies, so far, suggested that if no biodegradation occurs and sufficient field data are available, source differentiation can be successful when isotope signatures of PCE from various sources differ by more than 1‰ in  $\delta^{13}\text{C}$  (14,15). Surprisingly,

CSIA has not yet been applied in a forensic study to allocate different sources of chlorinated solvents at a contaminated site although these compounds may differ in carbon or chlorine isotope signatures depending on their manufacturing process (1,16-18).

Most of the reported CSIA field studies on chlorinated hydrocarbons focus on identification and quantification of *in-situ* biodegradation in unconsolidated porous aquifers (19-24). Stable carbon isotope analysis was applied to confirm degradation pathways at a field site contaminated with a complex mixture of chlorinated compounds (24). Measurements of isotope ratios not only allowed for estimating enrichment factors and quantifying transformation processes; they also provided insight into the origin of degradation products (24). Thus, CSIA data help to demonstrate if a substance was already present as a primary contaminant or if it is a degradation byproduct and to specify the precursor it originates from. CSIA has also been used to assess biodegradation of chlorinated ethenes at a hydrogeologically complex site (25). When CSIA is used as a sole technique, source apportionment may be problematic when more than two possible sources are involved in the contamination (26). A multiple-line-of-evidence approach including evaluation of historical, hydrological, geochemical and isotopic data as well as statistical analysis was applied to unravel the contamination scenario at the site. A major purpose of this study was to determine under which conditions stable isotope ratios can be used for environmental forensic purposes in the presence of adverse conditions such as biodegradation and complex hydrogeological conditions. A key factor turned out to be the determination of highly precise  $\delta^{13}\text{C}$  values of chlorinated ethenes in groundwater even at concentrations in the low  $\mu\text{g/L}$ -range which allowed to cover a wide range of the contaminant plumes. The results presented here provide the first successful example of a forensic isotope field study on chlorinated ethenes in a fractured bedrock aquifer.

## **5.2. Material and Methods**

**Field Site.** The site is located in an early industrialized urban area in southwestern Germany with a long operational history. At the end of the 19th century parts of the region were used extensively by industry and trade. Heavy industry in the region included metal working industries and reprocessing of used mineral oil. A substantial contamination with chemicals used by these industries occurred in the soil and the groundwater in the region, particularly through damage during World War II. During the reconstruction period, industry in the valley expanded further uphill. Most notably the widespread use of chlorinated solvents by various industrial production

facilities induced severe contamination of the soil and the associated bedrock groundwater system. Consequently, multiple suspected contaminant sources were created over the past decades resulting in several overlapping plumes. Main organic contaminants are chlorinated ethenes; mineral oil hydrocarbons, BTEX and polycyclic aromatic hydrocarbons (PAHs) have also been detected in some of the wells. Site-specific historical information is available within the city's register of contaminated sites.

**Geology and Hydrogeology.** The site is located in fractured Keuper rocks which are overlain by a few meters of artificial fill and Quaternary deposits. The subsurface at the site is part of the 'Gipskeuper', a geological unit that is characterized by its high gypsum content consisting of alternating sequences of marl, a lime-rich mudstone, claystone and dolomites. The geology leads to several hydrostratigraphical units including the two aquifers (Dunkelroter Mergel, DRM and Bochinger Horizont, BH) where the contamination was detected. A hydraulic connection between the DRM and the BH aquifer attributed to fissures and fractures within the formation has been observed (27). The majority of the contaminant mass remained in the upper aquifer (DRM), a reddish-brown claystone containing thin layers of lime-rich mudstone with a dense network of fine, connected fissures. The general groundwater flow conditions and the distribution of contaminants at the site are given in Figure 5-1a. Likewise, additional data are accessible from earlier groundwater sampling campaigns. An east-west fault zone with low hydraulic conductivity may constrain the contaminant mass transport from north to south (27). The distance between the contamination under investigation and the region's main groundwater wells is between 500 m and 1700 m. Due to their length and extension the chlorinated solvent plumes are therefore of major concern to local authorities.

**Groundwater Sampling.** Within the framework of a groundwater sampling campaign throughout the industrial zone in April 2005 samples were collected from 68 monitoring wells for hydrogeochemical characterization and contaminant concentration analyses. Concentration data were provided for the upper (DRM) and the subjacent aquifer (BH). A total of 27 of these groundwater wells have been sampled for isotope analysis of the specific chlorinated ethene compounds PCE, TCE, *cis*-1,2-dichloroethene (*cis*-DCE) and vinyl chloride (VC). Samples for isotope analysis were filled in 1-L amber glass bottles without headspace, sealed with Teflon-lined caps and kept at 4 °C until analysis; a preservation agent was not added. Carbon isotope measurements were performed within 1 to 10 weeks after sampling; an effect of holding times on isotope values can be excluded (data shown in the Appendix of this chapter). Figure 5-1b shows the location of all observation wells that were sampled for isotope measurements. As the main

mass load of chlorinated solvents and their daughter products was detected in the upper aquifer, water sampling for isotope analysis focused on wells that are located in the upper section of the groundwater system. Sampling locations where the monitoring wells are screened in the lower, 2<sup>nd</sup> aquifer (BH) are labeled with ‘\*’ in the following.

**Chemical and Isotope Analysis.** Field measurements included specific conductance, temperature, pH, dissolved oxygen, and  $E_h$ . Analysis of geochemical parameters have been performed for ammonium (detection limit 0.01 mg/L), nitrite, nitrate, sulphate, dissolved manganese, total and dissolved ferrous iron. Sulphate is not suitable here as a redox indicator because of its ubiquitous presence at the site due to a gypsum-containing underlying geological formation. Chlorinated ethene concentrations were analyzed using headspace gas chromatography-mass spectrometry (GC-MS) with an analytical error of  $\pm 5\%$ . Compound-specific stable carbon isotope analyses were performed using a gas chromatograph-combustion-isotope ratio mass spectrometry system (GC/IRMS). The GC/IRMS system consists of a Trace GC Ultra (Thermo Finnigan, Milan, Italy) coupled to a Delta<sup>PLUS</sup> XP (Thermo Finnigan MAT, Bremen, Germany) via a combustion interface (GC Combustion III; Thermo Finnigan MAT) operated at 940°C. Low concentrations of chlorinated ethenes in some of the groundwater samples required preconcentration prior to isotope analysis using a purge-and-trap (P&T) concentrator (VelocityXPT, Tekmar-Dohrmann, Mason, USA). Method detection limit of P&T-GC/IRMS for the compounds relevant in our study is  $\leq 2.2 \mu\text{g/L}$  (28). A more detailed description for isotope analyses is provided in the Appendix.

**Quality Assurance for Isotope Analyses.** If concentration differences within one sample prevented the measurement of isotopic compositions of all compounds within one run, several runs were performed with concentrations adjusted to signal sizes within the linear range of the CO<sub>2</sub> reference gas peaks (chromatograms provided in the Appendix, Figure A5-2). To ensure optimal performance of the GC/IRMS, especially for PCE, great care was taken that the GC-IRMS signals had amplitudes above 0.5 V (m/z 44). Measurements were performed at least in duplicates. If the error was greater than the typical accuracy and reproducibility of continuous flow isotope analysis techniques ( $>0.5\%$ ) (29), the values are given in brackets (Table A5-3). Reoxidation of the CuO/NiO/Pt combustion reactor was carried out at regular intervals ( $\pm$  every 40 measurements). To test for accuracy and reproducibility of CSIA measurements chlorinated ethene standards with known isotopic compositions were regularly measured using the same analytical procedure as for the samples. In addition, linearity effects were investigated by injecting the PCE working standard at a range of signal sizes (data provided in the Appendix).

### **5.3. Results and Discussion**

**Historical Approach.** Environmental forensic testimony to distinguish polluters and allocate contaminants to their sources requires several (independent) lines of evidence. Historical surveys are usually consulted first in the investigation of contaminated areas. In the present study, site-specific historical information obtained by the city's register of contaminated sites, indicated at least 5 different potential polluters. Companies operating with chlorinated solvents, and buildings on properties where chemicals were stored, filled and used could thereby be localized (depicted as shaded areas in Figure 5-1b). While such historical records may serve as a first line of evidence, the mere existence of a company working with chlorinated ethenes can, of course, not provide conclusive evidence in environmental litigation.

**Groundwater Hydrology.** Groundwater potentials (Figure 5-1) indicate that the groundwater flow direction is generally to the south-east towards a river flood plain (27). The general flow pattern is characterized by local heterogeneities and a system of faults crossing from west to east (Figure 5-1b) which may account for *in-situ* differences in hydraulic conductivity and locally variable flow directions. For instance, it cannot be ruled out that upgradient chlorinated solvent contamination detected at area E could have affected the contamination detected at area D. Hydraulic studies allow estimates on contaminant transport, but do not provide evidence if groundwater flow conditions remain insufficiently resolved or if contaminant sources are allocated on joint streamlines.





**Figure 5-1 (preceding page).** **a)** Map with groundwater potential lines and pie chart diagrams illustrating contaminant distribution found at the site. **b)** Map showing locations of groundwater monitoring wells sampled for concentration and isotope analysis, locations of potential polluters, and suggested location of fault system. Areas A to G depict the various parts of the contaminant plume(s) as discussed in the text. Response for  $\delta^{13}\text{C}$  values of PCE was  $>0.5$  Volt, with the exception of B23 ( $\delta^{13}\text{C}$  given in brackets). Top right: Site-specific geochemistry depicted by manganese concentration isolines (as concentration of dissolved manganese at all individual wells correlates very well with the distribution of anaerobic and aerobic environments within the aquifer system, isolines of manganese distribution have been chosen to depict the site-specific geochemistry). For further details refer to Table 5-1.

**Contaminant Concentration Analyses.** The concentrations of chlorinated compounds give an overview of the contaminant distribution found at the site (Figure 5-1a, for data refer to Table A5-3 in the Appendix). A hot spot with high chlorinated ethene concentrations, could be detected in well B8F suggesting this area as one contamination source zone (depicted as chlorinated hydrocarbon source zone F in Figure 5-1b). Trichlorotrifluoroethane (F113), a generally rare trace contaminant, was detected in two neighboring wells (B1Eck and B30). However, the proximity of those wells to the source zone F suggests that contaminants might originate from there; the lack of F113 in well B8F may be due to anaerobic degradation (below). Another rare trace contaminant, *trans*-DCE, was present in small amounts only in wells that exhibit strong reductive dechlorination, suggesting that it was produced as minor byproduct during reductive TCE degradation. Thus, being a secondary product rather than an initial pollutant (unlike F113), *trans*-DCE could not serve as indicator for source allocation. In summary, concentration analyses show that the general contamination pattern throughout the site is not conclusive enough to differentiate unequivocally between the contaminant inputs from the various potential source zones.

**Isotope Ratio Monitoring.** The environmental fate and transport of chlorinated ethenes may be affected by biodegradation processes at a site. Under anaerobic conditions chlorinated ethenes are subject to sequential reductive dechlorination and anaerobic cometabolism. Biodegradation of PCE is strictly limited to reducing groundwater environments whereas aerobic conditions allow for cometabolic transformation of TCE, DCE and VC (30). Reliable interpretation of stable isotope data in terms of source allocation and differentiation require knowledge of site-specific degradation reactions:

**Areas E and A.** Area E represents the location of a manufacturing site with long operational history and known chlorinated solvent and PAH contamination of the subsoil (Figure 5-1). Steady-state contaminant transport is assumed based on available geochemical data of redox conditions, chlorinated hydrocarbon concentrations and piezometric measurements at the site during an earlier sampling campaign between April and September 2004, and during the April

2005 campaign (27). Measured groundwater potentials suggest a possible influence of site E on groundwater contamination appearing in the southern part of the industrial area. Reported initial pure phase  $\delta^{13}\text{C}$  values of PCE produced by different manufacturers cover a range from -37.2‰ to -23.2‰ (18). On-site monitoring well B10, and downgradient well B3 show  $\delta^{13}\text{C}$  values of PCE that range in the higher end of these values (-24.6 and -23.5‰, respectively). Geochemical parameters measured indicate that aquifer conditions in this part of the plume are slightly aerobic (Table 5-1). In the area north of source zone E only minor amounts of PCE were detected. The geochemistry in this area (area A, Table 5-1) indicates strongly reducing conditions. Measured degradation products showed values indicative for reductive dehalogenation. As degradation processes are associated with a kinetic isotope fractionation and a shift in the substrates ratio of heavy to light isotopes (31,32), it can be expected that the  $\delta^{13}\text{C}$  of the residual PCE in area A would be more enriched in  $^{13}\text{C}$  compared to the isotopic composition of its source. Non-degrading, physical processes that act on the compound as a whole (such as dissolution, advective-dispersive transport, diffusion, volatilization, and equilibrium sorption/desorption) show either only small or no significant isotope fractionation ((33,34), and references therein) and thus, do not change the initial isotopic composition to a significant extent in the field. Due to the absence of PCE degradation under aerobic conditions in area A, the  $\delta^{13}\text{C}$  of PCE should reflect initial source values. Since the opposite is observed (isotope ratios of PCE in area A are more depleted than in area E) there is an indication that the source for area A is different from source zone E. As concentrations of PCE in wells B34, B45, B23 and B28 were already too low for an appropriate determination of  $\delta^{13}\text{C}$  values and the  $\delta^{13}\text{C}$  value of PCE measured in B23 is not well supported, an uncertainty remains (see area B).

**Table 5-1.** Site-specific geochemical parameters and resultant redox conditions; areas depicted in Figure 5-1b; the wells of each area are included in the statistical diagram Figure 5-3; data available in Table A5-3 in the Appendix.

Location (map)	Wells	$\text{NH}_4^+$	$\text{Fe}_{\text{tot}}$	Mn, Fe (dissolved)	$\text{NO}_3^-$	$\text{NO}_2^-$	$\text{E}_h, \text{O}_2$	Resultant conditions
A	B34, B45, B23, B28	++	++	++	-	-/+	-	anaerobic
B	B25, B37, B54	-	++	--	++	--	+	aerobic
C	B11, B44, B50, B101, B103	+	+/-	+/-	-/+	+	-	weakly anaerobic
D	Br1W, B102, B32, B42, B51	--	-/-	--	+	--	+	aerobic
E	B3, B10	-	+/-	-	-/+	+	+	weakly aerobic
F	B8F, B3F, P1F*	++	+/++	++	-	+	-	anaerobic
G	B30, B31*, B1Eck, B39*, B1M, P836*	--	-/-	--	+	--	+	aerobic

-, --: low or not present, respectively; +, ++: elevated or high, respectively

**Area B.** Field measurements of redox potential and dissolved oxygen content indicate aerobic conditions in wells B25, B37 and B54. Accordingly, groundwater chemistry of these samples is characterized by elevated nitrate concentrations, low concentrations of dissolved iron and manganese, and no detectable concentrations of ammonium (Table 5-1). Constant isotope signatures of PCE (-24.5 to -24.3‰) in the presence of oxic conditions suggest that they have derived from the same contaminant pool, possibly indicating the presence of a new source. However, as historical files contain no suspected contamination source, PCE might be deriving from solvent barrels bunkered in the 1940s. Groundwater flow conditions may provide a hydraulic connection in this northern part of the aquifer system, therefore it can also not be excluded that the manufacturing site responsible for areas A and E may be also responsible in that case. As the values measured in area A are not well supported and the  $\delta^{13}\text{C}$  values of PCE measured in wells B3 and B10 (area E) and those measured in area B are within error of each other, the assumption is reasonable (compare with the statistical evaluation of the complete data set given in Figure 5-3).

**Area C.** Southern wells B11, B44, B101, B103 and B50 exhibit  $\delta^{13}\text{C}$  values of PCE between -27.5 and -26.7‰ and are within error of each other (for statistical significance refer to Figure 5-3). Geochemistry of these waters reveal weakly anaerobic aquifer conditions (Table 5-1), which is also supported by field measurements of dissolved oxygen and redox potential ( $E_h$ ). High amounts of the degradation product *cis*-DCE and the presence of VC in some of these wells are indicating reductive dechlorination processes active in this part of the aquifer. To summarize: we observe *aerobic* conditions and PCE *enriched* in  $^{13}\text{C}$  in source zone E (-24.6 to -23.5‰) whereas in the wells located in area C we observe reductive dechlorination processes occurring under *anaerobic* conditions but PCE much more *depleted* in  $^{13}\text{C}$  (ranging from -27.5 to -26.7‰). Consequently, those samples represent a contamination derived from an other, isotopically distinct chlorinated solvent source. These findings are corroborated by hydrological pumping tests where an influence of source zone E on downgradient wells B50, B102 and B32 located in the southern part of the aquifer was excluded (27) and do support the assumption of two separated flow streams attributed to the east-western fault disturbance within this area.

**Area D.** Well Br1W and its downgradient wells until B42 in the southern part of the contaminated aquifer show  $\delta^{13}\text{C}$  values of PCE between -27.5 and -26.9‰ (within error of each other, Figure 5-3). Under aerobic conditions (Table 5-1) the isotope signatures of PCE remain constant in this aquifer section (area D). Thus, the source location for this contamination is apparently located in the western, upgradient part of the aquifer. Indicated by almost identical

isotope ratios, the contaminations in this area derive most likely from the same source that is responsible for the contamination detected in area C. Under strongly aerobic aquifer conditions biodegradation of PCE is absent (supported by constant isotope signatures of PCE). In contrast, pronounced isotope shifts for TCE (from -12.8‰ subsequently enriched to +14.6‰) and *cis*-DCE (enrichment from -22 to -3.9‰) suggest aerobic biodegradation processes successively occurring with flow direction.

**Area F.** Massive contaminant concentrations alone provide already evidence from yet another source in this area. At the same time, parent to daughter relationships (high *cis*-DCE/TCE concentration ratios, presence of VC), product isotope ratios and redox conditions indicate significant anaerobic reductive dehalogenation. The geochemistry within this area indicates strongly reducing conditions: Samples are characterized by low nitrate concentrations, a high  $Fe_{diss}/Fe_{tot}$  ratio and elevated concentrations of dissolved iron and manganese. Additionally, ammonium was present in this zone. Furthermore, although less reliable, field measurements of dissolved oxygen and redox potential ( $E_h$ ) indicate reducing conditions. Anaerobic degradation of chlorinated compounds requires hydrogen as an electron donor, which has to be provided by other sources of carbon (30). Indeed, a significant co-contamination with petroleum-derived hydrocarbons (mineral oil hydrocarbons and PAHs downgradient of source zone E) detected in well B3F provides a source of organic carbon in this part of the plume that in course of degradation reactions consumes oxygen and other electron acceptors available. Carbon isotope composition of PCE observed in source area F (B8F/P1F) are consistent with anaerobic reductive dechlorination and shows an enrichment in  $^{13}C$  with  $\delta^{13}C$  values of -23.4 and -22.9‰, respectively. Unfortunately, no free-phase DNAPL was available to determine the initial  $\delta^{13}C$  values. Taken isotope fractionation associated with reductive dehalogenation into account, the initial  $\delta^{13}C$  of the original PCE source in area F must have been more depleted than -23‰. All information together, confirm the assumption of the presence of a new source in area F compared to areas A,C and E.

**Area G.** In contrast to anaerobic conditions in area F, groundwater samples further downgradient are characterized by geochemical parameters that indicate aerobic conditions (Table 5-1), with B30/B31\* being located in the anaerobic/aerobic transition zone. An anaerobic source area that is followed further downgradient by a plume that exhibits aerobic behavior is a quite common observation at contaminated sites (30,35). Since PCE degradation does not take place under aerobic conditions, prevalent attenuation mechanisms of PCE will be dilution and dispersion in this part of the plume and hence, downgradient carbon isotope compositions of PCE should

remain constant. However,  $\delta^{13}\text{C}$  values of PCE measured in wells B30, B31\*, B39\* and B1Eck show carbon isotope compositions depleted in  $^{13}\text{C}$  (-25.5‰) in comparison with source zone F. A first supposition would be that another source might be involved, as it was discussed in areas E and C, for example. Considering the geological situation and historical files, an alternative explanation seems to be more realistic: Figure 5-2 shows a conceptual model to illustrate our view of the contaminant distribution in this part of the fractured bedrock aquifer system. DNAPLs in bedrock penetrate the subsurface and spread along fractures and fissures. Vertical PCE isotope profiles from well pairs B8F/P1F\* (-23.4/-22.9‰), B30/B31\* (-25.4/-25.0‰) and B1Eck/B39\* (-25.7/-26.1‰), respectively, with similar  $\delta^{13}\text{C}$  of PCE ( $\pm 0.5\%$  variance within each well pair) support that the two aquifers are connected via vertical fractures. In the aerobic zone G, dissolution of PCE from DNAPL trapped in fractures might create an input of undegraded, isotopically depleted, original material deriving from source area F. Considering the concentration distribution of PCE, TCE and *cis*-DCE in well B8F compared to downgradient well B30 and their corresponding  $\delta^{13}\text{C}$  values entail only a minor influence of already degraded material and hence a higher amount of “fresh”, isotopically light source material. A strong influence of undegraded source material is also well reflected by the depleted isotope signature of -27.6‰ for *cis*-DCE measured in well B30. Assuming a linear mixing model ( $\delta^{13}\text{C}_{\text{mixture}} = f_{\text{degraded}} \delta^{13}\text{C}_{\text{degraded}} + f_{\text{initial}} \delta^{13}\text{C}_{\text{initial}}$ ) the isotope signature of PCE observed in well B30 (-25.4‰) would represent a mixture of already degraded (-23‰ measured in upgradient wells) and freshly dissolved (undegraded) material. Based on a linear mixing model of > 60% undegraded and < 40% degraded contaminants would then reflect an initial isotope value for PCE of approximately -27‰.

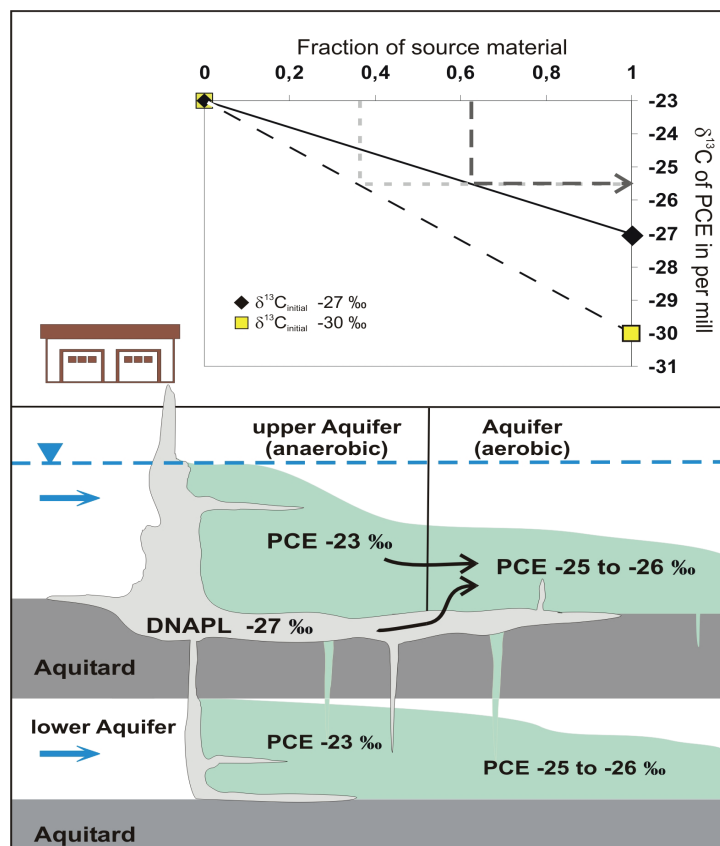


**Figure 5-2.** Conceptual model of the contamination scenario observed in source zone F and zone G. DNAPL is spreading along fractures in the contaminated bedrock aquifer system. Anaerobic conditions drive reductive dechlorination and isotopic enrichment of chlorinated compounds in parts of the aquifer. Dissolution of PCE from DNAPL in the aerobic zone creates an input of undegraded material, i.e. not enriched in  $^{13}\text{C}$ . Linear mixing models explain the isotope signature of PCE observed in well B30 (-25.4‰) representing a mixture of already degraded material with an isotope value of -23‰ (measured in upgradient wells) and of freshly dissolved (undegraded) material with assumed values of -30‰ (not likely) and -27‰ (more likely).

Further downgradient wells P836 and B1M show PCE that is even more depleted in  $^{13}\text{C}$ , (-30.6‰ and -28.8‰, respectively) than observed in the upgradient wells and hence, indicating a different contamination source. The assumption of a more depleted initial value of around -30‰ at source zone F (which would then serve as a common source for all contaminations within this area) would involve less original source material to cause the observed shift PCE isotope ratios and would contradict the mass balance considerations as discussed in the former paragraph (also depicted in Figure 5-2 as a dashed line). The assumption of the presence of a new source (or even two distinct sources, see box-whisker-diagram illustrated in Figure 5-3) is further supported by the much higher concentration of PCE in these wells compared to upgradient wells B39, B1Eck and B42, and historical facts: two other companies in this area worked with chlorinated solvents. As aerobic conditions prevail in this part of the aquifer  $\delta^{13}\text{C}$  values of PCE are conserved and

offer representative means, if necessary, for potential source allocation in further downgradient wells.

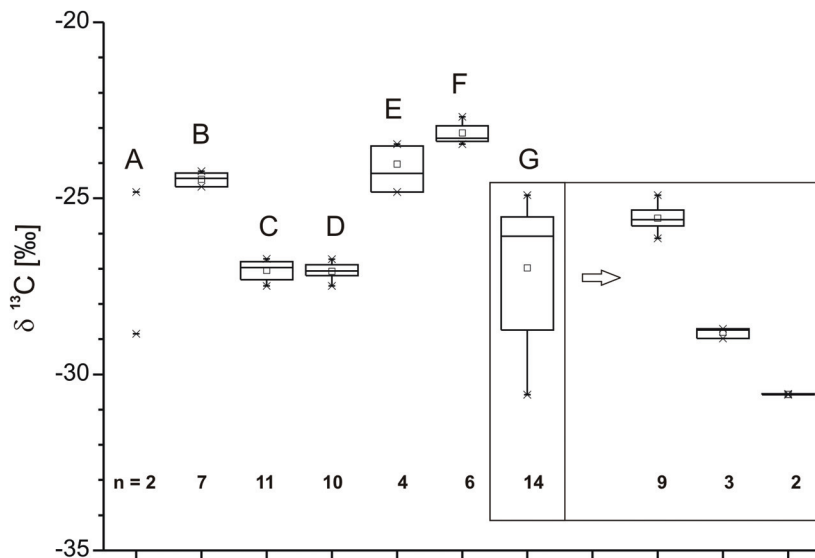


**Figure 5-3.** Box-whisker-diagram illustrating the statistical significance of all  $\delta^{13}\text{C}$  measurements for PCE ( $n$  = number of values); the groups represent areas of same geochemical conditions as depicted in Figure 5-1b, the groundwater wells of each group or area are listed in Table 5-S4. The likeliness for the contamination in area C and D being derived from the same source is strongly supported; Area G can be further separated into 3 different zones: the area of mixing processes (wells B30, B31, B1Eck, B39\*) and two additional CHC source zones (wells B1M and P836\*, respectively).

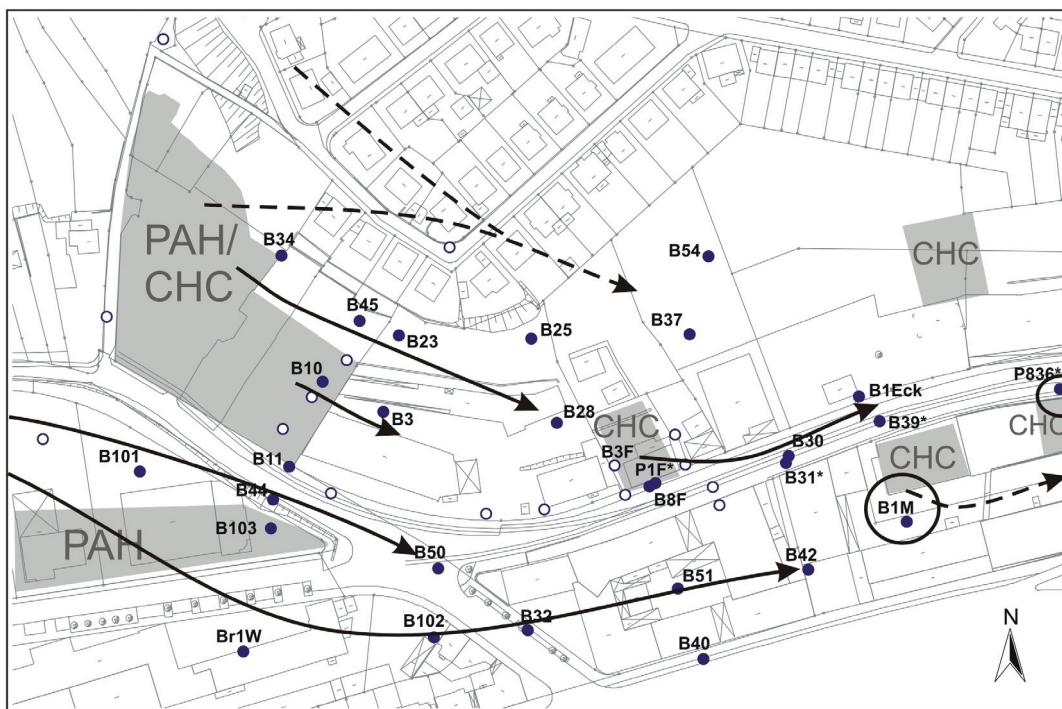


**Figure 5-4.** Origin and transport paths of contaminants evidenced by compound-specific carbon isotope signatures combined with geochemical data, concentration analyses, historical and hydrological information.

**CSIA-Forensic Field Study, Statistical Significance and General Implications.** The field study exemplified how isotope ratios can be used together with conventional data and analyses in a complex contamination scenario, i.e. in the presence of biodegradation and without presumption of constant initial isotope ratios. Data assessment with reasonable care (see methods part and information and data given in the Appendix) allowed to distinguish the different chlorinated ethene sources based on the isotopic composition of PCE with high statistical support (Figure 5-3). We constructed the contamination scenario for a complex site (Figure 5-4) based on historical site information, hydrological data and concentration analyses in combination with compound-specific carbon isotope signatures to decipher the different contamination sources explained in the previous sections. On-line coupling of a purge-and-trap concentrator to GC/IRMS allowed to determine  $\delta^{13}\text{C}$  values of PCE, and the further degradation products trichloroethene (TCE) and *cis*-1,2-dichloroethene (*cis*-DCE) in groundwater even at concentrations in the low  $\mu\text{g/L}$ -range providing essential information on *in-situ* degradation processes active at the site. CSIA serves as a strong line of evidence for contaminant transformation and elimination in part A of the plume where complete anaerobic dehalogenation eliminated PCE and prevented its transport to downgradient wells. CSIA data from area C and E of the plume showed that two additional sources exist. Overall, these cases exemplify how compound-specific isotope signatures can be used to differentiate between sources of nearby located contamination areas, if additional information and considerations on contaminant concentration, redox parameters and groundwater flow are available to further constrain the situation. Eastwards, with flow direction the situation becomes even more complex as the downgradient contamination might either be due to contaminant transport or caused by additional suspected pollutants. Elevated concentrations and/or isotope ratios can indicate the presence of new contaminant sources (as was the case in area F), while invariant isotope signatures and corresponding redox conditions may serve as a strong indication for a contamination source that is located farther upgradient (as in areas B and D, respectively). At the site studied reductive dechlorination reactions changed the initial isotope ratios in parts of the plume and did not allow a direct comparison of  $\delta^{13}\text{C}$  values. However, as suggested by Hunkeler et al. a comparison of  $\delta^{13}\text{C}$  values of PCE in high concentration zones aided discrimination of multiple contamination sources in the studied aquifer (15). Predominantly, isotope signatures of PCE were sufficient, but isotope ratios of degradation products delivered important additional information, helpful for conclusive interpretation. A linear mixing model explained the observed contaminant distribution and measured isotope ratios by mixing of already degraded PCE and input of undegraded PCE



due to DNAPL dissolution in area G. Our study showed that careful interpretation of isotope ratios, geochemical data and site-specific additional information are essential for a comprehensive site assessment. It could be demonstrated that a comprehensive CSIA approach can provide the extra information for a conclusive source allocation despite hydrologically complex transport of chlorinated ethenes in fractured bedrock aquifer systems if detection limits are sufficiently low to cover a wide range of the plume and additional constraining geochemical and historical data is available. Small differences in isotope signatures between sources may, however, hamper a reliable discrimination, especially if additional lines of evidence are missing or controversial data have to be discussed. In such cases two dimensional CSIA (multiple isotope analysis, e.g.  $\delta^{37}\text{Cl}$  or  $\delta^2\text{H}$ ) may further improve the conclusive power for constraining contaminant sources.

#### 5.4. References

- (1) Beneteau, K. M.; Aravena, R.; Frapce, S. K. Isotopic characterization of chlorinated solvents-laboratory and field results. *Org. Geochem.* **1999**, *30*, 739-753.
- (2) Doherty, R. E. A History of the Production and Use of Carbon Tetrachloride, Tetrachloroethylene, Trichloroethylene and 1,1,1-Trichloroethane in the United States: Part 1--Historical Background; Carbon Tetrachloride and Tetrachloroethylene. *Environ. Forensics* **2000**, *1*, 69 - 81.
- (3) U.S. Environmental Protection Agency. National primary drinking water regulations, list of drinking water contaminants & their MCLs, EPA 816-F-03-016. <http://www.epa.gov/safewater/consumer/pdf/mcl.pdf>. **2003**.
- (4) Johnson, R. L.; Pankow, J. F. Dissolution of dense chlorinated solvents into groundwater. 2. Source functions for pools of solvent. *Environ. Sci. Technol.* **1992**, *26*, 896-901.
- (5) Woodbury, A.; Sudicky, E.; Ulrych, T. J.; Ludwig, R. Three-dimensional plume source reconstruction using minimum relative entropy inversion. *J. Contam. Hydrol.* **1998**, *32*, 131-158.
- (6) Alapati, S.; Kabala, Z. J. Recovering the release history of a groundwater contaminant using a non-linear least-squares method. *Hydrological Processes* **2000**, *14*, 1003-1016.
- (7) Atmadja, J.; Bagtzoglou, A. C. State of the art report on mathematical methods for groundwater pollution source identification. *Environ. Forensics* **2001**, *2*, 205-214.
- (8) Alimi, H.; Ertel, T.; Schug, B. Fingerprinting of hydrocarbon fuel contaminants: Literature review. *Environ. Forensics* **2003**, *4*, 25-38.
- (9) Mansuy, L.; Philp, R. P.; Allen, J. Source identification of oil spills based on the isotopic composition of individual components in weathered oil samples. *Environ. Sci. Technol.* **1997**, *31*, 3417-3425.
- (10) Smallwood, B. J.; Philp, R. P.; Allen, J. D. Stable carbon isotopic composition of gasolines determined by isotope ratio monitoring gas chromatography mass spectrometry. *Org. Geochem.* **2002**, *33*, 149-159.
- (11) Benson, S.; Lennard, C.; Maynard, P.; Roux, C. Forensic applications of isotope ratio mass spectrometry - A review. *Forensic Sci.Int.* **2006**, *157*, 1-22.
- (12) Walker, S. E.; Dickhut, R. M.; Chisholm-Brause, C.; Sylva, S.; Reddy, C. M. Molecular and isotopic identification of PAH sources in a highly industrialized urban estuary. *Org. Geochem.* **2005**, *36*, 619-632.
- (13) Okuda, T.; Kumata, H.; Naraoka, H.; Takada, H. Origin of atmospheric polycyclic aromatic hydrocarbons (PAHs) in Chinese cities solved by compound-specific stable carbon isotopic analyses. *Org. Geochem.* **2002**, *33*, 1737-1745.
- (14) Slater, G. F. Stable isotope forensics - When isotopes work. *Environ. Forensics* **2003**, *4*, 13-23.
- (15) Hunkeler, D.; Chollet, N.; Pittet, X.; Aravena, R.; Cherry, J. A.; Parker, B. L. Effect of source variability and transport processes on carbon isotope ratios of TCE and PCE in two sandy aquifers. *J. Contam. Hydrol.* **2004**, *74*, 265-282.

- (16) Holt, B. D.; Sturchio, N. C.; Abrajano, T. A.; Heraty, L. J. Conversion of Chlorinated Volatile Organic Compounds to Carbon Dioxide and Methyl Chloride for Isotopic Analysis of Carbon and Chlorine. *Anal. Chem.* **1997**, *69*, 2727-2733.
- (17) Jendrzewski, N.; Eggenkamp, H. G. M.; Coleman, M. L. Characterisation of chlorinated hydrocarbons from chlorine and carbon isotopic compositions: scope of application to environmental problems. *Appl. Geochem.* **2001**, *16*, 1021-1031.
- (18) vanWarmerdam, E. M.; Frape, S. K.; Aravena, R.; Drimmie, R. J.; Flatt, H.; Cherry, J. A. Stable chlorine and carbon isotope measurements of selected chlorinated organic solvents. *Appl. Geochem.* **1995**, *10*, 547-552.
- (19) Chartrand, M. M. G.; Hirschorn, S. K.; Lacrampe-Couloume, G.; Sherwood Lollar, B. Compound specific hydrogen isotope analysis of 1,2-dichloroethane: potential for delineating source and fate of chlorinated hydrocarbon contaminants in groundwater. *Rapid Commun. Mass Spectrom.* **2007**, *21*, 1841-1847.
- (20) Hunkeler, D.; Aravena, R.; Butler, B. J. Monitoring microbial dechlorination of tetrachloroethene (PCE) in groundwater using compound-specific stable carbon isotope ratios: Microcosm and field studies. *Environ. Sci. Technol.* **1999**, *33*, 2733-2738.
- (21) Morrill, P. L.; Lacrampe-Couloume, G.; Slater, G. F.; Sleep, B. E.; Edwards, E. A.; McMaster, M. L.; Major, D. W.; Sherwood Lollar, B. Quantifying chlorinated ethene degradation during reductive dechlorination at Kelly AFB using stable carbon isotopes. *J. Contam. Hydrol.* **2005**, *76*, 279-293.
- (22) Sherwood Lollar, B.; Slater, G. F.; Sleep, B.; Witt, M.; Klecka, G. M.; Harkness, M.; Spivack, J. Stable carbon isotope evidence for intrinsic bioremediation of tetrachloroethene and trichloroethene at area 6, Dover Air Force Base. *Environ. Sci. Technol.* **2001**, *35*, 261-269.
- (23) Song, D. L.; Conrad, M. E.; Sorenson, K. S.; Alvarez-Cohen, L. Stable carbon isotope fractionation during enhanced in situ bioremediation of trichloroethene. *Environ. Sci. Technol.* **2002**, *36*, 2262-2268.
- (24) Hunkeler, D.; Aravena, R.; Berry-Spark, K.; Cox, E. Assessment of degradation pathways in an aquifer with mixed chlorinated hydrocarbon contamination using stable isotope analysis. *Environ. Sci. Technol.* **2005**, *39*, 5975-5981.
- (25) Chartrand, M. M. G.; Morrill, P. L.; Lacrampe-Couloume, G.; Sherwood Lollar, B. Stable isotope evidence for biodegradation of chlorinated ethenes at a fractured bedrock site. *Environ. Sci. Technol.* **2005**, *39*, 4848-4856.
- (26) Glaser, B.; Dreyer, A.; Bock, M.; Fiedler, S.; Mehring, M.; Heitmann, T. Source apportionment of organic pollutants of a highway-traffic-influenced urban area in Bayreuth (Germany) using biomarker and stable carbon isotope signatures. *Environ. Sci. Technol.* **2005**, *39*, 3911-3917.
- (27) Amt für Umweltschutz Stuttgart, KORA - TV1: Forschungsbericht, Förderkennzeichen 02WN0353; Projekt 1.3: Natürlicher Abbau und Rückhalt eines komplexen Schadstoffcocktails in einem Grundwasserleiter am Beispiel des ehemaligen Mineralölwerks Epple; Stuttgart, **2007**.
- (28) Zwank, L.; Berg, M.; Schmidt, T. C.; Haderlein, S. B. Compound-specific carbon isotope analysis of volatile organic compounds in the low-microgram per liter range. *Anal. Chem.* **2003**, *75*, 5575-5583.
- (29) Slater, G. F.; Dempster, H. S.; Lollar, B. S.; Ahad, J. Headspace analysis: A new application for isotopic characterization of dissolved organic contaminants. *Environ. Sci. Technol.* **1999**, *33*, 190-194.
- (30) Wiedemeier, T. H.; Rifai, H. S.; Newell, C. J.; Wilson, J. T. *Natural attenuation of fuels and chlorinated solvents in the subsurface*; John Wiley & Sons Inc.: New York, **1999**.
- (31) Schmidt, T. C.; Zwank, L.; Elsner, M.; Berg, M.; Meckenstock, R. U.; Haderlein, S. B. Compound-specific stable isotope analysis of organic contaminants in natural environments: a critical review of the state of the art, prospects, and future challenges. *Anal. Bioanal. Chem.* **2004**, *378*, 283-300.
- (32) Meckenstock, R. U.; Morasch, B.; Griebler, C.; Richnow, H. H. Stable isotope fractionation analysis as a tool to monitor biodegradation in contaminated aquifers. *J. Contam. Hydrol.* **2004**, *75*, 215-255.
- (33) Elsner, M.; McKelvie, J.; Lacrampe-Couloume, G.; Sherwood Lollar, B. Insight into methyl tert-butyl ether (MTBE) stable isotope fractionation from abiotic reference experiments. *Environ. Sci. Technol.* **2007**, *41*, 5693-5700.
- (34) Elsner, M.; Zwank, L.; Hunkeler, D.; Schwarzenbach, R. P. A new concept linking observable stable isotope fractionation to transformation pathways of organic pollutants. *Environ. Sci. Technol.* **2005**, *39*, 6896-6916.
- (35) Lee, M. D.; Odom, J. M.; Buchanan Jr., R. J. New perspectives on microbial dehalogenation of chlorinated solvents: Insights from the field. *Annu. Rev. Microbiol.* **1998**, *52*, 423-452.
- (36) Jochmann, M. A.; Blessing, M.; Haderlein, S. B.; Schmidt, T. C. A new approach to determine method detection limits for compound-specific isotope analysis of volatile organic compounds. *Rapid Commun. Mass Spectrom.* **2006**, *20*, 3639-3648.

## 5.5. Appendix

**Detailed Information on GC/IRMS Measurements.** Compound-specific stable carbon isotope analyses were performed using the gas chromatograph-combustion-isotope ratio mass spectrometry system (GC/IRMS) described in Chapter 2.2. Low concentrations of chlorinated ethenes in some of the groundwater samples required preconcentration prior to isotope analysis. To this end a purge-and-trap (P&T) concentrator (VelocityXPT, Tekmar-Dohrmann, Mason, USA) equipped with an AQUATek 70 autosampler (Tekmar-Dohrmann) was coupled online to the PTV injector of the GC/IRMS system. Volatile compounds were extracted from the samples by purging 25 mL of the groundwater in a fritted sparger with helium at 40 mL/min for 11 min and trapped on a VOCARB 3000 (Supelco, Bellefonte, USA) at room temperature. After heating the trap to 240 °C for 2 min to desorb the compounds, they were then transferred to the GC/IRMS. The transfer line between the P&T instrument and the PTV injector was held at 250 °C. Analytes were preconcentrated in a deactivated precolumn with cooled nitrogen gas in an on-column cryofocusing unit (ATAS GL International), which was held at -100 °C during analyte transfer from the P&T instrument. Samples containing vinyl chloride (VC) were preconcentrated at -130 °C. For the thermal desorption process, the cryofocusing unit was heated with a rate of 30°C/s to 240°C. A 60 m x 0.32 mm Rtx-VMS capillary column with a film thickness of 1.8 µm (Restek, Bellefonte, USA) was used for the analytical separation of the chlorinated compounds. The GC temperature program used to obtain separation of compounds of interest started at 40 °C held for 11 min, increased at a rate of 7 °C/min to 100 °C held for 2 min, then to 220 °C at 20 °C/min for additional 4 min (Helium<sup>5.0</sup> was used as carrier gas; column flow: 1 mL/min).

**Accuracy and Reproducibility of CSIA Measurements.** Chlorinated ethene standards with known isotopic compositions were regularly measured using the same analytical procedure as for the samples. Precision and reproducibility of  $\delta^{13}\text{C}$  values determined by purge-and-trap GC/IRMS are given in Table A5-1. Measurements of those standards was performed regularly every 5th to 6th measurement, at least in duplicates. The  $\delta^{13}\text{C}$  values obtained were compared to externally measured isotope values (EA/IRMS, n=3, see Table A5-1). The results demonstrate that the P&T-GC/IRMS provides both accurate and reproducible  $\delta^{13}\text{C}$  values. Only trans-DCE shows higher deviations, which is a common observation in P&T-GC/IRMS for this compound (1,2). Figure A5-1 shows the results of investigating the effect of signal size on  $\delta^{13}\text{C}$

measurements of PCE (linearity effects). According to the procedure described in Sherwood Lollar et al. (3), the linearity of the system was tested by injecting the isotopically characterized PCE working standard material over a range of signal sizes.

- (1) Zwank, L.; Berg, M.; Schmidt, T. C.; Haderlein, S. B. Compound-specific carbon isotope analysis of volatile organic compounds in the low-microgram per liter range. *Anal. Chem.* **2003**, *75*, 5575-5583.
- (2) Jochmann, M. A.; Blessing, M.; Haderlein, S. B.; Schmidt, T. C. A new approach to determine method detection limits for compound-specific isotope analysis of volatile organic compounds. *Rapid Commun. Mass Spectrom.* **2006**, *20*, 3639-3648.
- (3) Sherwood Lollar, B.; Hirschorn, S. K.; Chartrand, M. M. G.; Lacrampe-Couloume, G. An approach for assessing total instrumental uncertainty in compound-specific carbon isotope analysis: Implications for environmental remediation studies. *Anal. Chem.* **2007**, *79*, 3469-3475.

**Table A5-1.** Precision and reproducibility of  $\delta^{13}\text{C}$  values determined by purge-and-trap GC/IRMS (number of replicates  $n = 55$ ).

	<i>trans</i> -DCE	<i>cis</i> -DCE	TCE	PCE
GC/IRMS $\delta^{13}\text{C}$ values, ‰	-26.4	-25.9	-26.7	-27.2
Standard deviation (SD), ‰	0.7	0.4	0.3	0.3
Amplitude height of mass 44 peak, mV	2500	3300	2700	2800
EA/IRMS $\delta^{13}\text{C}$ values and SD, ‰	-25.54 ( $\pm 0.03$ )	-25.81 ( $\pm 0.08$ )	-26.69 ( $\pm 0.11$ )	-27.35 ( $\pm 0.25$ )

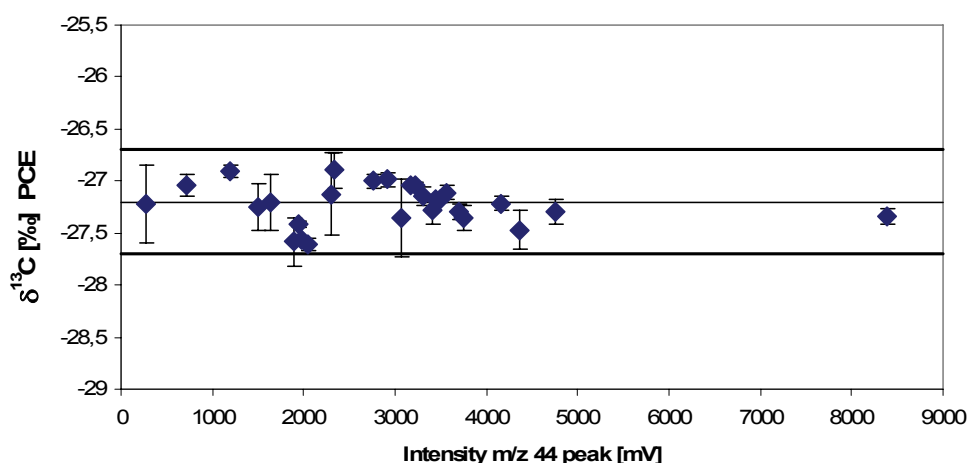


**Figure A5-1.** Linearity of  $\delta^{13}\text{C}$  values for PCE standard (mean value -27.2‰) measured by purge-and-trap-GC/IRMS, intensities represent various standard concentrations yielding signal intensities (m/z 44 signals) from 270 to 8400 mV, horizontal lines indicate the mean  $\delta^{13}\text{C}$  value  $\pm 0.5$ ‰ accuracy range, error bars represent the standard deviation of duplicate or triplicate measurements, respectively.

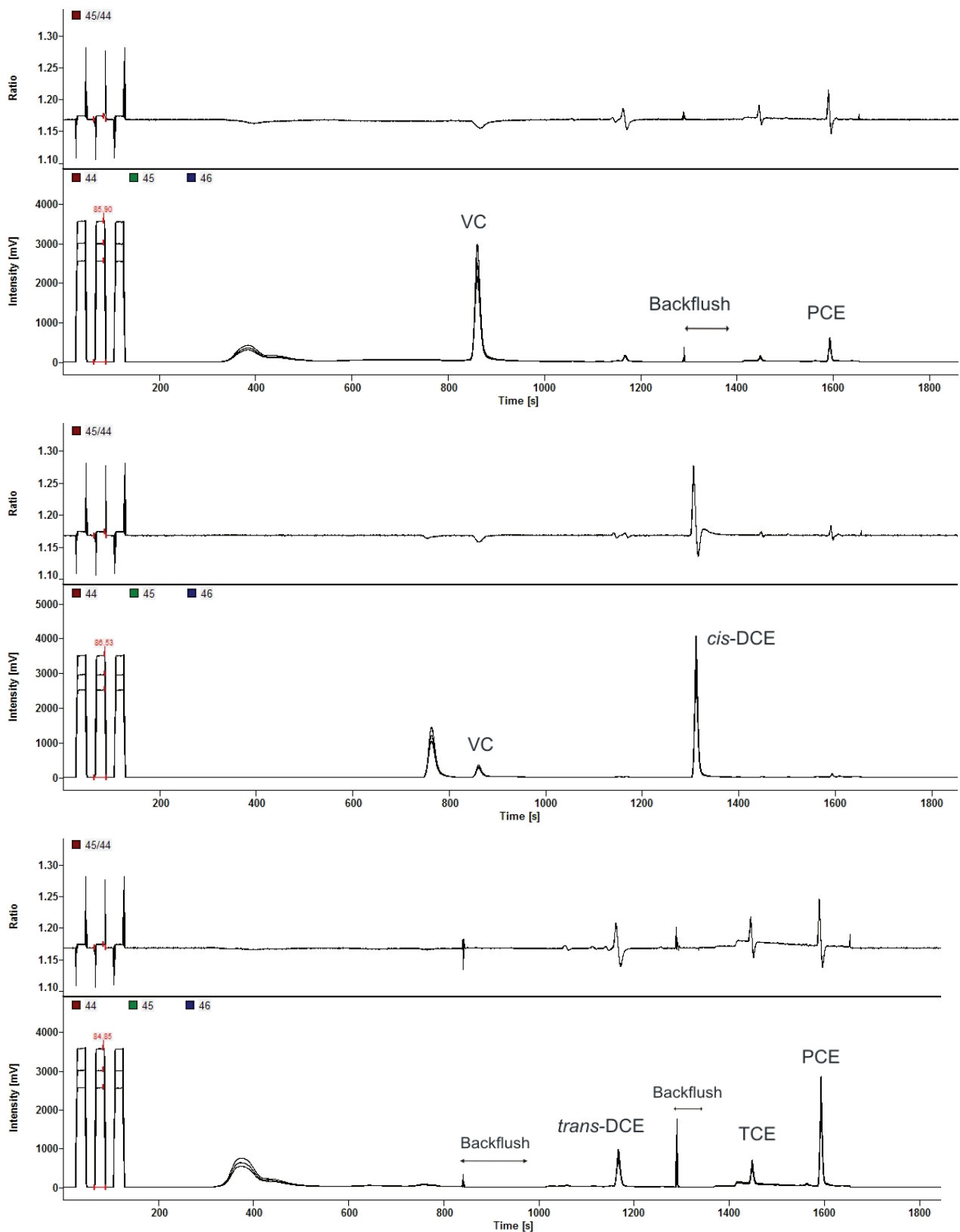


Figure A5-2. Representative GC/IRMS chromatograms of sample B8F. Due to high differences in concentrations of each analyte, several runs have been performed with concentrations adjusted to the linear range of the  $\text{CO}_2$  reference gas peaks to ensure reproducible  $\delta^{13}\text{C}$  values.

**Effect of Storage Time on  $\delta^{13}\text{C}$  Values.** Stable isotope measurements in our study were performed within 1 to 10 weeks after sampling. Samples were stored in amber glass bottles without headspace, sealed with Teflon-lined caps and kept at 4°C until analysis. For quality assurance reasons the influence of different holding times on the isotopic composition will be discussed here. Storage of groundwater samples from an anaerobic aquifer contaminated with tetrachloroethene (PCE) was discussed in Chapter 4. The samples were not chemically treated, but stored without headspace at 4 °C in the dark. The constant  $\delta^{13}\text{C}$  values of PCE indicated no substantial degradation even after a very long storage period of 4 months (see Chapter 4).  $\delta^{13}\text{C}$  values were measured after different holding times of an aerobic groundwater sample containing 220  $\mu\text{g/L}$  PCE, storage without headspace at 4 °C. One week after groundwater sampling the measured  $\delta^{13}\text{C}$  value was -24.2‰ ( $\pm 0.05\%$ , n=3), after two months holding time measured  $\delta^{13}\text{C}$  was -24.6‰ ( $\pm 0.1\%$ , n=3), although the sample did not contain any preservation agents. To ensure data quality within our case study, the influence of different holding times on the isotopic composition of the samples was checked; the results are shown in Table A5-2.

**Table A5-2.**  $\delta^{13}\text{C}$  values (‰) of samples that have been remeasured after different storage times.

	<b>Sample P1F</b>	<b>Storage 6 weeks</b>	<b>Sample B44</b>	<b>Storage 6 weeks</b>	<b>Sample B54</b>	<b>Storage 8 months</b>
VC	-32.2 (-)	31.8 ( $\pm 0.1$ )	-	-		
<i>trans</i> -DCE	-31.3 (-)	-30.5 (-)	-	-		
<i>cis</i> -DCE	-12.9 ( $\pm 1.8$ )	-11.7 (-)	-20.9 ( $\pm 0.1$ )	-21.2 (-)		
TCE	-11.9 (-)	-12.5 (-)	-18.1 ( $\pm 0.1$ )	-18.2 (-)		
<b>PCE</b>	<b>-23.1 (-)</b>	<b>-22.7 (-)</b>	<b>-26.8 (<math>\pm 0.1</math>)</b>	<b>-26.7 (-)</b>	<b>-24.5 (<math>\pm 0.1</math>)</b>	<b>-24.9 (<math>\pm 0.2</math>)</b>

Table A5-3. Data of field measurements, concentration and compound-specific isotope analyses of samples discussed within Chapter 5.

Monitoring well		B 3	B 10	B 11	B 23	B 25	B 25	B 28	B 28	B 30	B 31 * B 32	B 34	B 34	B 37	B 39 *	B 42	B 44	B 45	B 45	
Aquifer	DRM	DRM	DRM	DRM	DRM	DRM	DRM	DRM	DRM	DRM	BH	DRM	DRM	DRM	BH	DRM	DRM	DRM	DRM	
Field parameters:	Apr 05	Apr 05	Apr 05	Apr 05	Apr 05	Apr 05	Dec 05	Apr 05	Dec 05	Apr 05	Apr 05	Apr 05	Apr 05	Apr 05	Apr 05	Apr 05	Apr 05	Apr 05	Dec 05	
Conductivity	2180	2160	2250	5310	1269	1282	1150	1198	1309	1427	1642	1315	1336	1240	1691	1588	2180	1282	1344	
Temperature	13.1	10	14.1	13	14	13	15	14.5	16.6	16.6	16.6	14.4	13.9	14.6	15.7	15.2	13.6	14.3	14.8	
pH	6.9	7.1	6.8	12.7	6.9	6.7	6.6	6.7	6.9	6.9	7.0	6.6	6.7	7	6.8	7.0	6.9	6.8	6.7	
Oxygen, dissolved	3.45	2.24	0.40	2	9.1	1	0.9	0.69	1.96	1.59	5.12	1.11	7.4	5.46	0.71	4.88	0.23	1.69	8.45	
Redox potential	229	97	-26	-120	157	159	-127	-133	206	209	216	-251	-263	128	210	166	81	-159	-157	
<b>Geochemical analyses:</b>																				
Ammonium	0.01	<0.01	0.04	0.36	<0.01	0.07	0.05	0.08	<0.01	<0.01	<0.01	0.05	0.12	<0.01	<0.01	<0.01	0.03	0.01	0.07	
Nitrite	0.13	0.15	<0.01	3.1	0.08	<0.01	0.1	<0.01	<0.01	<0.01	<0.01	<0.01	<0.01	<0.01	<0.01	<0.01	0.12	<0.01	<0.01	
Nitrate	15	24	35	16	79	73	<0.5	<0.5	59	60	38	<0.5	<0.5	83	38	39	16	<0.5	<0.5	
Sulphate	1010	1020	1120	818	203	154	268	22	199	307	430	306	49	148	493	478	900	237	78	
Manganese, dissolved	0.04	0.068	0.64	<0.005	0.089	0.14	0.53	0.67	0.007	0.017	<0.005	1.2	<0.005	<0.005	<0.005	<0.005	1	0.81	1	
Iron, dissolved	<0.01	0.015	0.8	<0.01	<0.01	0.037	1.4	1.3	<0.01	0.01	0.013	1.2	0.96	<0.01	<0.01	0.013	0.053	2	1.9	
Iron	0.98	0.066	0.88	1.5	0.32	2.7	2.3	2	0.19	0.089	0.059	2	1.9	3	0.022	0.026	0.073	2.3	2.2	
<b>Concentration analysis chlorinated hydrocarbons (CHC):</b>																				
Vinyl chloride (VC)	<5	<5	<5	930	<5	<5	<5	<5	<5	<5	<5	95	60	<5	<5	<5	8	510	250	
trans-1,2-dichloroethene	<5	<5	<5	12	<5	<5	<5	<5	130	34	20	74	28	<5	<5	<5	99	28	26	
cis-1,2-dichloroethene	27	71	33	310	<5	<5	9	<5	<5	0.2	0.5	0.3	<0.1	0.6	0.3	0.2	0.2	<0.1	<0.1	
Trichloroethane	0.2	0.2	0.3	<0.1	<0.1	<0.1	<0.1	<0.1	<0.1	<0.1	<0.1	<0.1	<0.1	<0.1	<0.1	0.6	1.2	0.5	<0.1	
1,1,1-trichloroethane	1.1	1	0.2	<0.1	<0.1	<0.1	<0.1	<0.1	<0.1	61	4.7	2.1	0.4	3	6.2	2.4	8.5	2.5	<0.1	
Trichloroethene (TCE)	25	33	4	7.3	1.6	1.4	0.3	0.3	53	61	4.7	2.1	0.4	3	6.2	2.4	8.5	2.5	<0.1	
Tetrachloroethene (PCE)	23	6.6	27	5	24	28	1.9	0.6	260	35	230	3.2	0.8	120	130	210	28	3.1	0.9	
Trichlorofluoroethane	<1	<1	<1	<1	<1	<1	<1	<1	54	6	<1	<1	<1	<1	9	<1	<1	<1	<1	
CHC (BBodSchV) sum	76.3	111.8	64.5	1264.3	25.6	29.4	11.2	0.9	497.2	136.5	256.3	185.3	97.2	123.6	157.1	221.8	144.2	543.6	277.1	
<b>Concentration analysis of co-contaminants:</b>																				
BTEX (BBodSchV) sum	n.d.	n.d.	n.d.	137	n.d.	n.d.	n.d.	n.d.	n.d.	n.d.	n.d.	305	400	n.d.	n.d.	n.d.	n.d.	189	170	
PAH (16) sum	n.d.	n.d.	n.d.	3174	n.d.	n.d.	36	63	n.d.	n.d.	n.d.	4410	2862	n.d.	n.d.	n.d.	n.d.	234	321	
Mineral oil hydrocarbons	280	n.d.	n.d.	460	230	110	1800	6900	n.d.	n.d.	n.d.	9300	4700	n.d.	n.d.	n.d.	n.d.	370	660	
<b>Compound-specific stable isotope analysis (CSIA):</b>																				
Vinyl chloride (VC)	‰			-21.6																
δ <sup>13</sup> C-values	‰			-37.4																
trans-1,2-Dichloroethene	‰																			
δ <sup>13</sup> C-values	‰																			
cis-1,2-Dichloroethene	‰			-14.1	-21.3	-25.5	-8.7		-27.6	(-17.5)	(-11.0)		1.7	-28.9	(10.8)	(-3.9)	-21.0		-6.4	
δ <sup>13</sup> C-values	‰																			
Trichloroethene (TCE)	‰			-9.5	(-17.4)	-14.0	-23.5		-23.4	d.i.	d.i.	-22.7	-23.6	(4.6)		-22.1	-2.0	14.6	-18.2	d.i.
δ <sup>13</sup> C-values	‰																			
Tetrachloroethene (PCE)	‰			-23.5	-24.6	-26.9	(-26.8)		-24.5	d.i.	d.i.	-25.4	-25.0	-26.9		-24.3	-26.1	-27.0	-26.7	d.i.
δ <sup>13</sup> C-values	‰																			

n.d. not detectable or <10 µg/L; d.i. below detection limit; isotope analysis performed in duplicate or triplicate, uncertainty associated with isotope measurements in general < 0.5‰ (otherwise values are given in brackets)

Table A5-3 (continued).

Monitoring well	B 50	B 51	B 54	B 54	BriW	B101	B102	B103	PIF*	B3F	B8F	B1Eck	B1Eck	B 1 M	P 836 *
Aquifer	DRM	DRM	DRM	DRM	DRM	DRM	DRM	DRM	BH	DRM	DRM	DRM	DRM	DRM	BH
Campaign	Apr 05	Apr 05	Dec 05	Apr 05	Apr 05	Apr 05	Apr 05	Apr 05	Apr 05	Apr 05	Apr 05	Apr 05	Dec 05	Dec 05	Dec 05
<b>Field parameters:</b>															
Conductivity	µS/cm	2360	1339	1317	1578	2300	1629	2210	1729	1180	1338	1446	1431	1507	1376
Temperature	°C	14.4	13.1	12.7	13.6	13.3	14.7	14	14.6	13.5	13.5	15.7	12.5	16.2	12.5
pH	-	6.8	7.0	7.0	7.4	7.0	6.9	6.9	6.8	6.9	6.8	6.9	6.9	6.9	7.0
Oxygen, dissolved	mg/L	0.16	4.96	7.19	10.58	0.38	3.56	0.23	0.86	0.6	2.96	0.56	0.41	2.31	9.26
Redox potential	mV	138	181	118	246	96	207	100	111	-251	-62	263	229	178	273
<b>Geochemical analyses:</b>															
Ammonium	mg/L	0.04	<0.01	0.04	0.06	0.01	<0.01	<0.01	0.07	0.66	0.59	<0.01	<0.01	<0.01	<0.01
Nitrite	mg/L	0.06	<0.01	<0.01	<0.01	0.05	<0.01	0.51	0.04	0.03	0.05	<0.01	<0.01	0.01	<0.01
Nitrate	mg/L	28	39	111	97	33	33	18	38	<0.5	<0.5	37	43	34	70
Sulphate	mg/L	984	423	210	152	1030	408	861	551	248	127	299	231	372	149
Manganese, dissolved	mg/L	1.1	<0.005	<0.005	<0.005	0.021	<0.005	0.88	0.35	0.52	1.2	<0.005	0.14	0.055	<0.005
Iron, dissolved	mg/L	<0.01	0.01	0.013	0.072	0.017	0.012	0.022	<0.01	0.94	0.034	<0.01	0.045	0.026	0.011
Iron	mg/L	0.044	0.026	4	1.8	0.047	0.25	0.065	0.13	1.3	0.22	0.13	0.13	0.1	0.046
<b>Concentration analysis chlorinated hydrocarbons (CHC):</b>															
Vinyl chloride (VC)	µg/L	<5	<5	<5	<5	<5	<5	15	1400	14	14000	<5	<5	<5	<5
trans-1,2-Dichloroethene	µg/L	<5	<5	<5	<5	<5	<5	<5	21	<5	170	<5	<5	<5	<5
cis-1,2-Dichloroethene	µg/L	50	12	<5	58	50	27	69	2800	35	31000	120	66	57	<5
Trichloroethane	µg/L	0.2	0.1	<0.1	0.2	0.3	0.3	0.3	0.1	0.1	0.2	0.3	0.2	0.1	0.2
1,1,1-Trichloroethane	µg/L	0.3	1.3	<0.1	1.1	0.7	2.2	0.3	<0.1	<0.1	<0.1	0.3	0.1	0.5	0.3
Trichloroethene (TCE)	µg/L	5.4	3	0.4	8.3	6.5	5.4	4.2	12	0.6	76	75	56	22	1.9
Tetrachloroethene (PCE)	µg/L	26	200	57	100	44	270	21	32	4	430	130	79	2300	930
Trichlorofluoroethane	µg/L	<1	<1	<1	<1	<1	<1	<1	<1	<1	<1	21	13	<1	<1
<b>CHC (BBodSchV) sum</b>	µg/L	<b>81.9</b>	<b>216.6</b>	<b>57.5</b>	<b>100.9</b>	<b>177.6</b>	<b>304.9</b>	<b>109.8</b>	<b>4265.1</b>	<b>53.7</b>	<b>45676.2</b>	<b>346.6</b>	<b>214.3</b>	<b>2379.6</b>	<b>932.4</b>
<b>Concentration analysis of co-contaminants:</b>															
BTEX (BBodSchV) sum	µg/L	n.d.	n.d.	n.d.	n.d.	n.d.	n.d.	n.d.	14	n.d.	n.d.	n.d.	n.d.	n.d.	n.d.
PAH (16) sum	µg/L	n.d.	n.d.	n.d.	n.d.	n.d.	n.d.	30.3	n.d.	65	11	n.d.	n.d.	n.d.	n.d.
Mineral oil hydrocarbons	µg/L	n.d.	n.d.	n.d.	n.d.	n.d.	n.d.	n.d.	n.d.	83000	460	n.d.	n.d.	n.d.	n.d.
<b>Compound-specific stable isotope analysis (CSIA):</b>															
<b>Vinyl chloride (VC)</b>															
δ <sup>13</sup> C-values	‰														
trans-1,2-Dichloroethene	‰								-31.9						
δ <sup>13</sup> C-values	‰														
cis-1,2-Dichloroethene	‰														
δ <sup>13</sup> C-values	‰														
Trichloroethene (TCE)	‰														
δ <sup>13</sup> C-values	‰														
Tetrachloroethene (PCE)	‰														
δ <sup>13</sup> C-values	‰														

n.d. not detectable or <10 µg/L; d.l. below detection limit; isotope analysis performed in duplicate or triplicate, uncertainty associated with isotope measurements in general < 0.5‰ (otherwise values are given in brackets)



## 6. Quantitative Assessment of Aerobic Biodegradation of Chlorinated Ethenes in a Fractured Bedrock Aquifer (\*)

### 6.1. Introduction

Releases of dense chlorinated hydrocarbons (CHC) often cause substantial and persistent sources of groundwater contamination, potentially hazardous to the aquatic environment and human health. *In-situ* processes such as biodegradation, chemical transformation, dispersion, sorption, or volatilization, determine the fate of chlorinated ethenes in groundwater (1,2) and need to be quantified when monitored natural attenuation is considered as a remedial approach.

CHCs, especially the highly chlorinated solvents perchloroethene (PCE) and trichloroethene (TCE), are biodegradable under highly anaerobic conditions via sequential reductive dehalogenation (1,2). The less chlorinated CHCs, dichloroethene (DCE) and vinyl chloride (VC), can be oxidized in the presence of molecular oxygen by various aerobic bacteria (3,4). A wide range of chlorinated solvents (including TCE) can also be biodegraded under aerobic conditions by cometabolic transformations (5,6). While reductive dehalogenation has frequently been detected under field conditions (7-9), aerobic degradation of TCE is sparsely documented (10,11). PCE, however, is generally not expected to degrade aerobically (1,2).

Methods to assess natural attenuation at field scales may include monitoring of contaminant mass and/or contaminant and electron acceptor/donor concentrations over time, appearance of specific co-metabolites and metabolic by-products and/or enzymes, degradation intermediates and products, or specific analyses to identify the microbial populations present. However, evidence of reduction of contaminant mass often is not precise enough, and clearly demonstrating CHC degradation in aquifers remains difficult. Therefore compound-specific isotope analysis (CSIA) has gained significant attention as a technique to assess both the occurrence and extent of *in-situ* transformation of organic pollutants in contaminated aquifers (12-18). The method relies on the kinetic isotope fractionation effect during transformation reactions which produces an enrichment of heavy isotopes in the parent compound and a concomitant formation of isotopically lighter products. In contrast, nondegradative attenuation processes that act on the compound as a whole

---

\* performed in collaboration with K.E. Pooley, K.T.B. MacQuarrie and H. Prommer

such as advective-dispersive transport, volatilization or sorption/desorption are assumed not to significantly alter isotopic compositions (e.g. (18) and references therein). Carbon isotope fractionation during biological and chemical transformations of CHCs is a well-documented process, observed in laboratory experiments as well as in the field (16-18).

The extent of carbon isotope fractionation between substrate and product and the amount of contaminant degraded can be quantitatively described using the Rayleigh equation (7,12-15)

$$R_s = R_{s,0} f^{(\alpha-1)}$$

where  $R_s$  is the carbon isotope ratio ( $^{13}\text{C}/^{12}\text{C}$ ) at a fraction of substrate or contaminant remaining ( $f$  or concentration of the residual contaminant =  $c_t/c_0$ ) at time  $t$ ,  $R_{s,0}$  is the initial isotopic composition of the contaminant and  $\alpha$  is the fractionation factor. The fractionation factor  $\alpha$  is often expressed as the enrichment factor  $\varepsilon$ , where  $\varepsilon = 1000(\alpha-1)$ .

The isotope enrichment factor for each compound being degraded may vary with, and thus can be indicative of, degradation pathways (18-20). A compilation of isotope enrichment factors for various specific biochemical conditions is provided in Meckenstock et al. (16). Significant differences in isotope fractionation of chlorinated ethenes was also observed for abiotic processes with zerovalent iron from different iron sources (21). Dissimilar enrichment factors for different bacterial strain isolates, compared to an enrichment culture, reveals the inherent difficulties in predicting isotope fractionation for undefined bacterial communities (22). While a qualitative assessment of degradation based on fractionation is always possible, the actual extent of *in-situ* transformation may only be quantified from isotope ratios measured in the field, if an appropriate laboratory-derived  $\varepsilon$ , valid for the specific-site conditions, is known.

The Rayleigh model of fractionation, however, becomes invalid when the degradation process involves competing parallel degradation pathways and where fractionation factors are pathway dependent (18). Furthermore, it is applicable only to well mixed systems and thus unsuited for those field site where differential flow/transport is significant (18,23). To overcome these limitations numerical modeling approaches have been developed. They can account for heterogeneous flow and transport, aid in the identification of relevant degradation pathways (18,24,25), and provide information on the relative rates of intermediate degradation steps (26-28). For example, one-dimensional (1D) simulations of PCE degradation were used to demonstrate how the incorporation of isotope data may improve the efficiency and accuracy of determining reaction rates and concentration profiles (24). Using a two-dimensional (2D) Lagrangian approach, Abé and Hunkeler (23) demonstrated systematic errors of the Rayleigh model for the quantification of biodegradation and estimation of first-order rate constants for

varying reactive transport parameters including plume width, reaction rate and transverse dispersion. To date, however, no reported full-scale application of reactive transport modeling exists which demonstrates organic contaminant isotope enrichment in the field.

The present study uses a reactive transport modeling approach to simulate the isotopic enrichment of CHCs observed at a hydrogeologically complex field site (see Chapter 5). The field scale model was used to simulate the transport and degradation of both the organic contaminants as well as their transformation products. The transformations considered involved multiple, redox-dependent degradation pathways of which each potentially exhibits distinct fractionation behavior. The objective of this work was to assess the usefulness of a reactive transport based modeling approach for the integrated interpretation of the geochemical and isotope field data. Specifically, our goal was to quantitatively elucidate degradation of chlorinated ethenes at a field site where aerobic biodegradation of TCE was observed.

## **6.2. Material and Methods**

**Field Site.** The site is located in an early industrialized urban area in southwestern Germany. The general groundwater flow conditions and the contamination situation at the site are given in Figure 6-1. The area of focus is located in the most southern part, containing wells in a downgradient sequence (Br1W to B42) which were identified by carbon isotope signatures of PCE as being associated with a distinct contaminant source (Chapter 5). A chlorinated ethene plume, containing PCE, TCE, *cis*-DCE, and VC, was detected upstream of this area and a former chlorinated solvent above-ground storage tank located near well GWM1 was identified as being the most plausible source for the contamination observed in the Br1W to B42 series wells. The tank was historically stored alongside others containing petroleum and waste oil, which can or could have potentially served as a primary energy source during both reductive dechlorination and aerobic, cometabolic degradation of chlorinated ethenes. In the Br1W to B42 series wells TCE and *cis*-DCE exhibited a strong isotope fractionation while  $\delta^{13}\text{C}$  signatures of PCE remained constant.

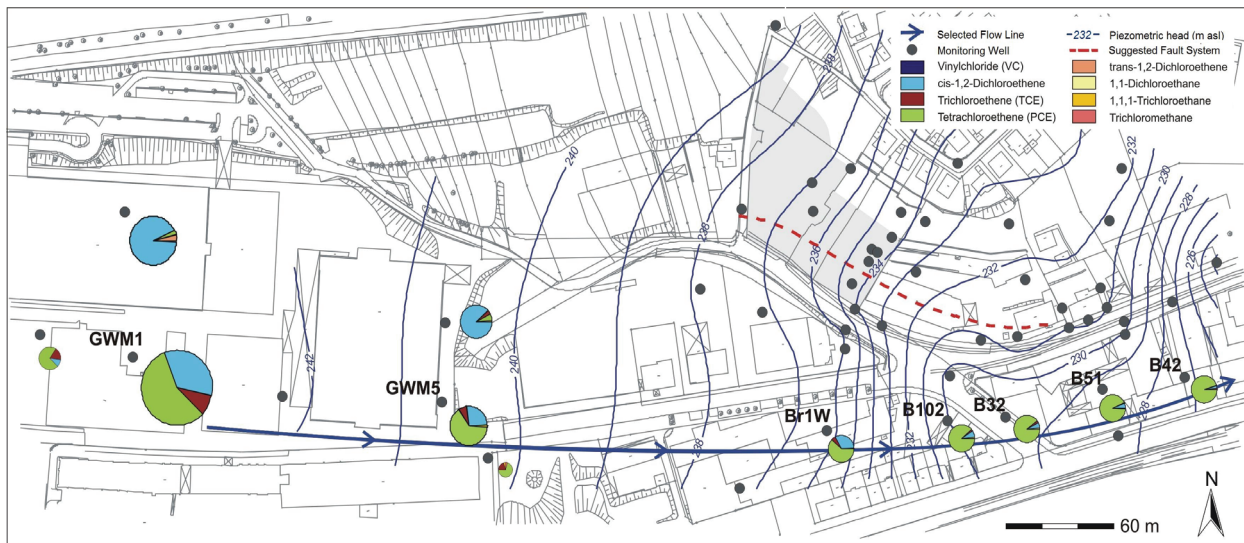


**Figure 6-1.** Map illustrating groundwater flow conditions and VOC contamination in the area of focus. The dashed line indicates suggested location of fault system.

The site is located in fractured Keuper rocks which are overlain by a few meters of artificial fill and Quaternary deposits. The geological units at the site (“Gipskeuper”) are characterized by a high gypsum content and alternating sequences of marl, a lime-rich mudstone, claystone and dolomites. The local hydrogeology comprises several hydrostratigraphic units including the two aquifers (Dunkelroter Mergel, DRM and Bochinger Horizont, BH) where the contamination was detected. However, the majority of the contaminant mass remained in the upper aquifer (DRM), a claystone containing thin layers of lime-rich mudstone with a dense network of fine, connected fissures. A hydraulic connection between the DRM and the BH aquifer has been attributed to faults and fractures within the formation (29). For the 2D flow and reactive transport modeling the hydrogeological properties of the DRM aquifer were extracted from a calibrated 3D flow model, which honored the observed flow fields and hydraulic influences of the deeper BH aquifer.

**Chemical and Isotope Analysis.** The redox conditions at individual wells were characterized based on chemical analyses of dissolved redox sensitive inorganic species (see Chapter 5). Concentrations of CHCs were analyzed by headspace-GC-MS. Compound-specific stable carbon isotope analyses were performed using GC/IRMS coupled on-line to a purge-and-trap sample extractor to enable accurate and highly sensitive (as low as 2 µg/L) determinations of  $\delta^{13}\text{C}$  values of CHCs (30,31). CHC concentrations from wells of the focus area are provided in Table 6-1. In the following, DCE refers to *cis*-DCE, the dominant form of the two DCE isomers found at the field site and is assumed to originate exclusively from reductive dechlorination processes.

Occasionally *trans*-DCE was found but always at concentrations an order of magnitude lower than *cis*-DCE. Based on concentration data obtained during two sampling periods between April and September 2004, and between April and June 2005, steady state groundwater flow and contaminant transport were assumed. The April 2005 observations were chosen for model calibration in this study.

**Model-Based Data Analysis.** Differences in the reaction rates for  $^{12}\text{C}$ - and  $^{13}\text{C}$ -isotopologues, and hence kinetic isotope fractionation, can be simulated using numerical model approaches (23-25,28,32). Assuming first-order kinetics the reactions of heavy and light isotope-containing compounds can be defined independently as

$$^{12}\text{C}_s = ^{12}\text{C}_{s,0} \exp(-\lambda_{12}t)$$

$$^{13}\text{C}_s = ^{13}\text{C}_{s,0} \exp(-\lambda_{13}t)$$

where  $\lambda$  is the reaction rate constant of the corresponding heavy or light isotope. In this scenario, the fractionation factor,  $\alpha$ , is equal to the ratio of the rate constants of the heavy to light isotope as demonstrated in Mariotti et al. (33)

$$\alpha = \lambda_{13}/\lambda_{12}$$

In this study, the multicomponent reactive transport model PHT3D (34) was used for one- and two-dimensional integrated simulations of degradation reactions and the corresponding isotopic changes (25,28,35).

**1D Simulations.** One-dimensional (1D) simulations were initially undertaken to explore and identify potential biodegradation pathways; model setup and properties are given in the Appendix of this chapter. In this initial phase well GWM5 (Figure 6-1) was used as the location for the upstream model boundary of the reactive transport simulations. In this well, a relatively high concentration of *cis*-DCE was found, an intermediate of reductive dechlorination of PCE or TCE. The locations of the downgradient wells were set such that the travel time to these wells correlated with those computed by particle tracking in the 3D flow model. Based on the review of potential degradation pathways of chlorinated solvents (1,2,5,36) and the geochemical and redox conditions at the site, a mineralizing aerobic and a sequential anaerobic pathway were identified as the two most likely degradation pathways. Although generally aerobic conditions were observed in the Southern region, some doubt existed whether the documented contaminant concentration decreases could be attributed to aerobic degradation: Firstly, the sampling wells were fully screened and therefore represent a mixture of water compositions (including redox states) from a geochemically stratified aquifer, and, secondly, the aquifer may not be considered a homogeneous system but rather a system with interactions between fractures, fissures, and rock

matrix, with potential for dual-domain behavior and therefore two distinct redox conditions within the same control volume. Due to this uncertainty, modeling scenarios initially included both potential pathways. Based on the review of existing reaction models for chlorinated ethenes (4,8,28,37,38), a first-order degradation rate was assumed to be suitable for both the aerobic and anaerobic pathways.

The principal assumption for the 1D model was that simulated data were reasonably representative of the 3D contaminant plume, as would be the case with an infinitely wide source and/or negligible transverse dispersivity,  $\alpha_T$ , and a contaminant concentration that is distributed evenly with depth. Underpinned by measured time series of piezometric heads from the site and regionally (29), both the flow field and reactive transport processes were assumed to be at steady state. To quantify biodegradation reactions via isotope fractionation we considered published  $\epsilon$ -values from microcosm experiments.

**2D Simulations.** To examine the effect of hydrodynamic dispersion on contaminant concentrations and isotope signatures, and to assess the influence of a range of potential source widths, 2D simulations were conducted. Using the same hydraulic parameters as those used in the 1D model, the upgradient extent of the model domain was shifted to well GWM1 and the length of the model was extended to a total length of 650 m.

### **6.3. Results and Discussion**

**1D Simulation of Field Isotopic Enrichment.** For the reductive dechlorination scenario measured concentrations of PCE, TCE and DCE from well GWM5 (Table 6-1) were used to define the composition of the contamination source. Two different scenarios regarding PCE degradation rate constants,  $0.0008 \text{ d}^{-1}$  and  $0.008 \text{ d}^{-1}$ , were investigated at an enrichment factor  $\epsilon$  of  $-5.2\%$  (14,28). TCE degradation rate constants were varied between  $0.02$  and  $0.4 \text{ d}^{-1}$  to investigate how  $\delta^{13}\text{C}$  evolves under these two scenarios. Assuming a PCE degradation rate constant of  $0.008 \text{ d}^{-1}$ , the corresponding TCE degradation rates had to be high relative to PCE degradation rates in order to produce the relative concentrations of PCE and TCE observed in the downgradient series wells. This is because the observed PCE concentration is an order of magnitude higher than TCE. Under these conditions, the evolution of  $\delta^{13}\text{C}_{\text{TCE}}$  was governed solely by the evolution of  $\delta^{13}\text{C}_{\text{PCE}}$  independent of the reaction rate of TCE. Even for a very low degradation rate constant of  $0.0008 \text{ d}^{-1}$ , the  $\delta^{13}\text{C}_{\text{TCE}}$  was only slightly more sensitive to the TCE degradation rate. The simulated  $\delta^{13}\text{C}_{\text{TCE}}$  in the most downgradient well, B42, was approximately

-18‰, which is significantly less enriched than that measured in the field (Table 6-1). Since molar concentrations of PCE are an order of magnitude higher than TCE, the  $\delta^{13}\text{C}$  of the product, TCE, at any snapshot in time, is governed by the equation that describes an infinite reservoir of substrate relative to product generation (35)

$$\delta^{13}\text{C}_p = \delta^{13}\text{C}_s + \varepsilon$$

At the lower PCE degradation rate, the simulated DCE concentrations and isotope data matched the field data better than those of TCE. However, the required DCE degradation rate constant was 30 times higher than that of PCE. For reductive dechlorination this is very unlikely, because PCE is the more oxidized species (1,2). From these simulation results it was concluded that the reductive dechlorination pathway is not consistent with the measured TCE fractionation in the downgradient wells.

**Table 6-1.** Concentration and isotope data for chlorinated ethenes in the downgradient series wells

Well		Mean $\delta^{13}\text{C}$ in ‰	Concentration in $\mu\text{g/L}$	Concentration in $\mu\text{mol/L}$
GWM1	PCE		5400	33
	TCE		1200	9.1
	cis-DCE		3600	37
GWM5	PCE	-27.5	480	2.9
	TCE	-10.3	23	0.18
	cis-DCE	-21.2	180	1.9
Br1W	PCE	-27.5	110	0.66
	TCE	-12.8	8.3	0.063
	cis-DCE	-22	58	0.60
B102	PCE	-27.2	270	1.6
	TCE	3.5	5.4	0.041
	cis-DCE	-12	27	0.28
B32	PCE	-26.9	230	1.4
	TCE	4.6	4.7	0.036
	cis-DCE	-11	20	0.21
B51	PCE	-26.9	200	1.2
	TCE	9.8	3	0.023
	cis-DCE	-6.2	12	0.12
B42	PCE	-27	210	1.3
	TCE	14.6	2.4	0.018
	cis-DCE	-3.9	8	0.083

To simulate aerobic degradation processes, biodegradation rates and isotope enrichment factors were optimized to match observed concentrations and carbon isotope signatures, respectively (Figure 6-2). TCE and DCE were initially assumed to be present in groundwater near GWM5. PCE was assumed recalcitrant under oxic conditions (2). An optimized fit was easily achieved under this aerobic scenario because both TCE and DCE are mineralized and the degradation

processes of both compounds proceed independent of each other. For degradation rate constants of  $0.02 \text{ d}^{-1}$  for TCE and  $0.025 \text{ d}^{-1}$  for DCE, the estimated enrichment factors were  $-12$  and  $-6.7\%$  respectively (Figure 6-2). It can also be seen from Figure 6-2 that a longitudinal dispersivity of  $10 \text{ m}$  versus  $0.5 \text{ m}$  had a relatively minor effect on the 1D simulation results. Stoichiometric calculations indicated that the aerobic degradation of TCE would only have a minor impact on the ambient oxygen concentrations.

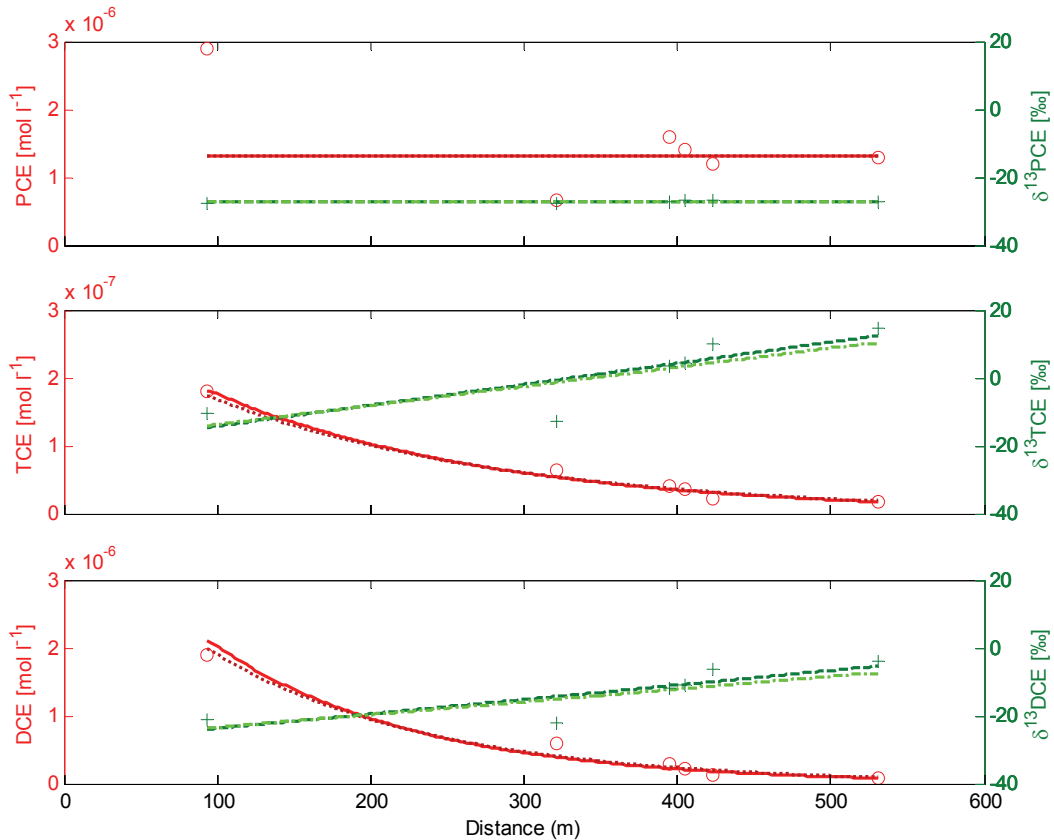


**Figure 6-2.** One-dimensional aerobic degradation scenario. Degradation rates for TCE and *cis*-DCE were  $0.02$  and  $0.025 \text{ d}^{-1}$ , respectively. The corresponding isotope fractionation factors were  $-12.0$  and  $-6.7\%$ , respectively. PCE was assumed not to degrade. Longitudinal dispersivities of  $0.5 \text{ m}$  and  $10 \text{ m}$  are represented by dark and light green lines, respectively.

**Application of the Rayleigh Equation.** As an alternative to reactive transport modeling of the concentration and isotope data site-specific *in-situ* enrichment factors can be computed from normalized concentrations in cases where a conservative tracer is available. The Rayleigh equation then makes use of a tracer-corrected remaining fraction,  $f_{\text{corr}}$ :

$$f_{\text{corr}} = C_{\text{corr}} / C_0$$



where  $C_0$  is the initial (source) concentration, and  $C_{\text{corr}}$  is the tracer-corrected concentration based on the measured concentration  $C$  at any location downstream (39)

$$C_{\text{corr}} = C (C_{0,\text{tracer}} / C_{\text{tracer}})$$

where  $C_{0,\text{tracer}}$  is the initial tracer concentration and  $C_{\text{tracer}}$  is the measured tracer concentration at any downgradient location.

As expected under aerobic conditions (2), no significant isotope fractionation was observed for PCE in the downgradient series wells, making it a suitable conservative tracer relative to other chlorinated ethenes. Since for aerobic biodegradation both TCE and *cis*-DCE react and fractionate as independent parent compounds the Rayleigh equation can be directly applied to the PCE-tracer corrected TCE and DCE concentrations. Substituting  $f_{\text{corr}}$  into the Rayleigh equation, one obtains a linear relationship with a slope equal to the enrichment factor,  $\epsilon$ :

$$\delta^{13}\text{C}_s - \delta^{13}\text{C}_{s,0} = (\epsilon) \ln f_{\text{corr}}$$

where  $\delta^{13}\text{C}_{s,0}$  is the initial (source) isotope signature.

The resulting relationship is plotted in Figure 6-3 for the aerobic degradation of TCE and *cis*-DCE in the studied wells. Using this approach the *in-situ* (field-derived)  $\epsilon$  values for TCE and *cis*-DCE at this site are estimated as -15.0 and -7.2‰, respectively.

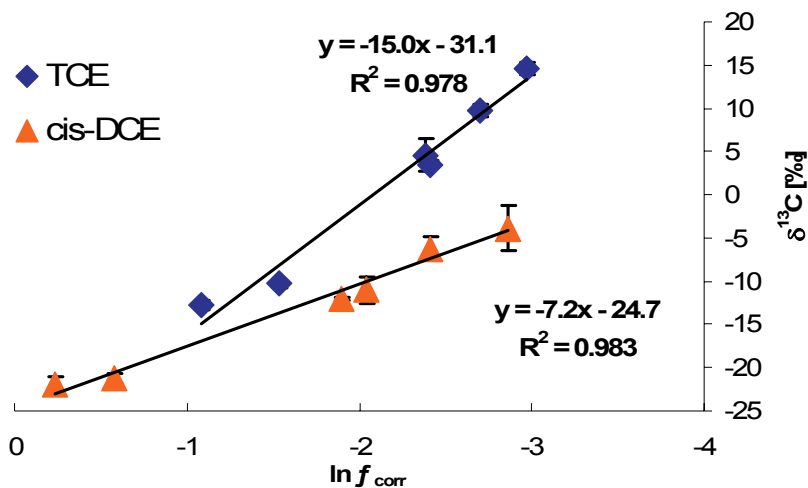


**Figure 6-3.** Quantification of enrichment factors for TCE and *cis*-DCE undergoing aerobic degradation based on field data.  $f_{\text{corr}}$  represents a “corrected” fraction remaining where the concentration at any downgradient location is corrected for dilution using PCE as a conservative tracer. The equations shown are linear regression models where, according to the Rayleigh equation, the slope represents the isotope enrichment factor. The  $R^2$  value represents the coefficient of determination.

**2D Simulations.** To study the influence of dispersive processes on the interpretation of field data, the 1D model was modified and extended to 2D. In the absence of detailed information on the geometry of the source zone located near GWM1, scenarios with a range of source widths were investigated in combination with varying horizontal transverse dispersivities ( $\alpha_T$ ), using the observed PCE concentrations as constraints. The sampled wells were assumed to be located at or near the plume centerline. Results of plume simulations, demonstrated that the range of possible plume widths extends to around 6 m at the most, for a reasonable range of transverse dispersivity values. A source width of 4m most closely matched the measured PCE concentrations for  $\alpha_T$  of 1 m, which was adopted for the 2D simulations (see Appendix of this chapter).

The simulated 2D concentration and isotope values for TCE obtained by fitting degradation rates relative to isotope data are presented in Figure 6-4. The degradation rates required to obtain the best linear fit of the isotope data in the 2D model differed slightly from those estimated by the PCE-tracer corrected Rayleigh equation, because of the effect of longitudinal dispersion demonstrated in Figure 6-2. For the scenario presented,  $\lambda_{TCE}$  was  $0.015 \text{ d}^{-1}$  and  $\lambda_{DCE}$  was  $0.023 \text{ d}^{-1}$ . This can be seen by plotting the plume centerline data for this scenario, shown in Figure 6-5a. In this figure, the concentration and isotope data along the centerline of the plume were plotted together with the 0D batch (zero dispersion) simulation having the same degradation rates. The simulated 2D plume exhibits the same isotopic changes as the corresponding 1D case with the same longitudinal dispersion, suggesting that for first-order degradation the transverse dispersion has no effect on isotope data at the centerline of the plume. Off the center line, the modeled isotope signature of the degrading parent compounds TCE and *cis*-DCE are slightly affected by transverse dispersion in that  $\delta^{13}\text{C}$  gradually increases the more offset a measurement point is from the centerline of the plume (Figure 6-4).

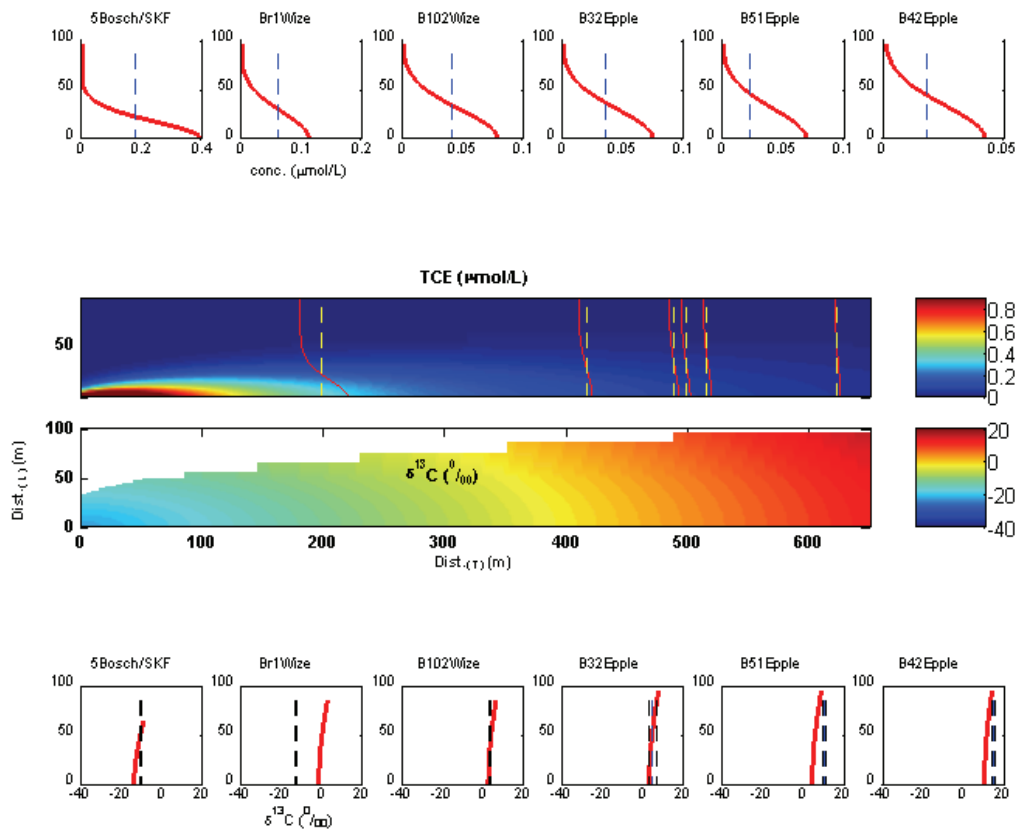
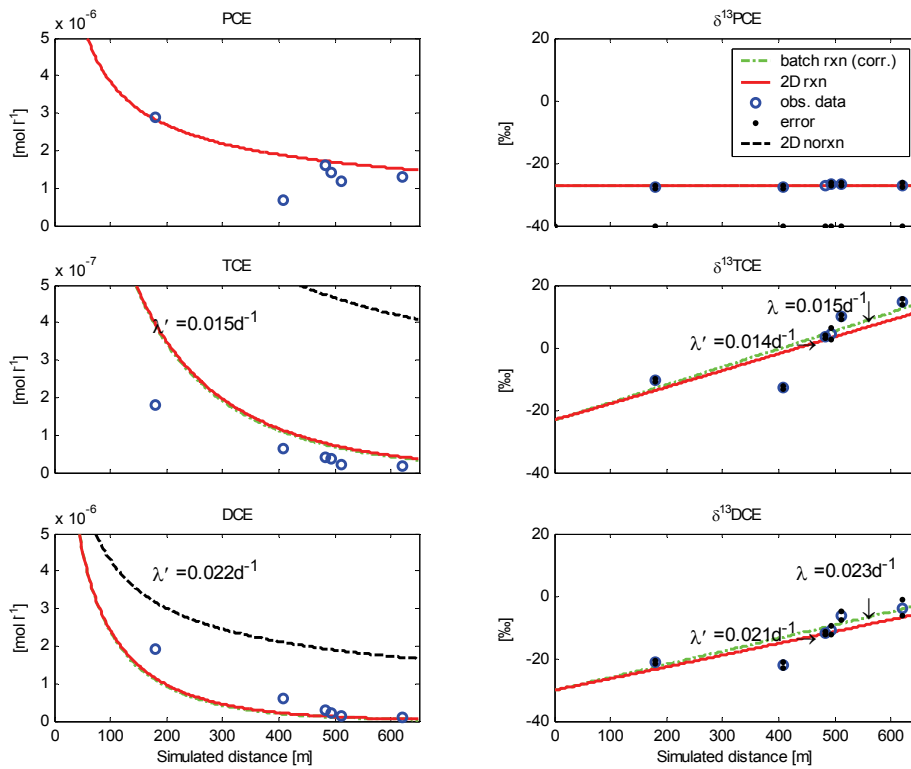


**Figure 6-4.** Concentration and isotope data of TCE simulated for a 4m source width using reaction rates to suite regression-optimized TCE isotope signatures. Plume is located in the lower left hand corner and half of a symmetric plume is shown. The observed data (dashed lines) for each well is compared with the simulated values (red line) relative to the distance from the plume centerline.

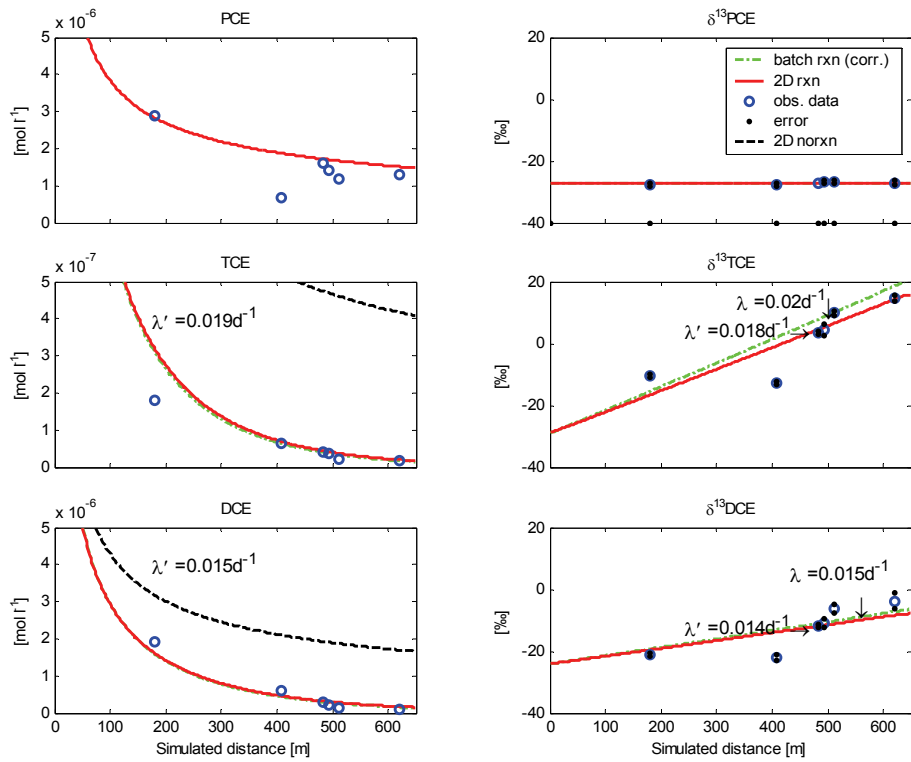
By ignoring longitudinal dispersion and assuming samples are taken from at or near the center line of a plume, an approximate degradation rate  $\lambda'$  can be calculated:

$$\lambda' = -\text{slope } v / \varepsilon$$

By adjusting the degradation rate constants for this effect, an improved fit to the isotope data can be made although the influence of longitudinal dispersion on rate estimates is minor. A similar adjustment can be performed for determining degradation rates based on conservative tracer corrections and the results of these corrections are shown in Figure 6-5b.



a)



b)

**Figure 6-5.** Centerline of two-dimensional model based on calculated enrichment factors, adjusting TCE and cis-DCE degradation rates to suit regression-optimized **a)** isotope signatures, and **b)** concentrations, where  $\lambda'_{left} = v \ln(C_{corr}/C_0)$ ;  $\lambda'_{right} = -slope \cdot v/\epsilon$ .

Plotting the Rayleigh function for the 2D plume demonstrates the difference between isotope reactive transport modeling and analytical modeling using a simple Rayleigh equation (36). The plot compares different representations of remaining fractions: the first based on measured concentrations, where  $f = C/C_0$ ; the second based on concentration corrections by advective-dispersive nonreactive transport modeling, where  $f = C/C_{\text{disp}}$ ; and the third based on corrections using a conservative tracer, where  $f = C_{\text{corr}}/C_0$ . It was shown that correction by advective-dispersive nonreactive transport modeling and correction using a conservative tracer produce the same results (see Appendix of this chapter). The interpreted enrichment factors based on these correction methods do not equate precisely to the “true” (i.e., model) enrichment factors, a result of longitudinal dispersion effects.

**Systematic Effects on Enrichment Factors.** The calculated enrichment factor for TCE (Figure 6-3) is within the range of those reported for aerobic degradation (-1.1 to -20.7‰). This large range, however, is based on only two studies, each using an isolated bacterial strain under controlled laboratory conditions. A strong enrichment of TCE during aerobic degradation was reported by Barth et al. for aerobic cometabolism of TCE by the toluene-degrading strain, *Burkholderia cepacia* G4 (40). In contrast, *Methylosinus trichosporium* OB3b growing on methane as primary substrate caused insignificant fractionation for aerobic co-metabolic biodegradation of both *cis*-DCE and TCE (41).

Possible errors related to the estimated enrichment factors, besides sampling and analytical errors in the concentration and isotope measurements, may result from longitudinal dispersion (minor but not accounted for in the conservative tracer method; Figure 6-2), vertically heterogeneous flow, and the assumption of first-order reaction rates. Effects of longitudinal dispersion and heterogeneous flow will underestimate enrichment factors by dilution-corrected methods which may result in slight overestimation of degradation rates. This effect is demonstrated by comparing the variations in  $\epsilon$  with increasing  $\alpha_L$  for each compound in the Rayleigh plots, where a maximum deviation of 0.9‰ in the true  $\epsilon_{\text{TCE}}$  was calculated for the highest longitudinal dispersion of 20 m (see Appendix of this chapter), which is a considerably larger dispersivity than reported for most aquifers (42). The degree of underestimation, however, is much lower than when estimating an enrichment factor from field data using a direct application of the Rayleigh equation.

**Implications for Field Sites.** This study demonstrates the potential for aerobic degradation of chlorinated ethenes, TCE and *cis*-DCE, under natural field conditions. Aerobic TCE degradation has been described earlier in lab experiments as a cometabolic process (37). At a site with an

extensive history of industrial activity such as this one, sufficient organic primary substrate should be present. Prior to this study, fractionation due to aerobic TCE degradation has only been studied for two particular strains of bacteria and never for a mixed culture. Fractionation due to aerobic DCE degradation is even less well documented. This study may present the first field based mixed aerobic microbial enrichment factor for these compounds, as well as being the first reactive transport-based *in-situ* enrichment factor reported.

Using reactive transport modeling with carbon isotope fractionation, the relationship between a source and an observed plume can be better understood. A comparison of isotope analysis only at the field scale to isotope analysis with reactive transport modeling has demonstrated the need, when quantifying natural attenuation processes, for an integrated approach, particularly when similar degradation processes can result in a range of enrichment factors. In addition, modeling changing isotope ratios of contaminants degrading through different reactive pathways and the production/consumption of sequential daughter products may allow for the verification of the relevant processes occurring in the contaminant plume. Because (intrinsic) reaction kinetics rather than supply of oxygen was rate limiting in this field study, simulation of dissolved oxygen dispersion/diffusion was not necessary. In cases where oxygen supply is limited by physical mixing processes (diffusion/dispersion), the isotopic changes will vary greatly depending on the location of an observation well relative to the plume fringe (35). This aspect will need to be considered in the quantification of biodegradation rates and overall mass removal at a field site.

As seen from the Rayleigh plots of the 2D simulation results, the direct application of isotope data to quantify enrichment factors will result in underestimated enrichment factors and therefore overestimated biodegradation. This is due to the fact that when plotting a Rayleigh equation of  $f = C/C_0$ , the assumption is that all decreases in concentration are due to biodegradation and all calculated mass removals using this enrichment value will maintain this assumption. Microcosm quantification of a mixed microbial community sampled from a field site of interest should be representative of fractionation processes *in-situ* and has been, until now, the only direct method of quantifying biodegradation of contaminants *in-situ*, in the absence of a conservative tracer (16). In this study, corrections for dispersive processes were made with the conservative tracer method prior to the calculation of enrichment factors. There is potential to achieve similarly robust estimates of degradation rates by multi-parameter optimization of transport and degradation processes integrating both concentration and isotope field data into reactive transport modeling.

## 6.4. References

- (1) Lee, M. D.; Odom, J. M.; Buchanan Jr., R. J. New perspectives on microbial dehalogenation of chlorinated solvents: Insights from the field. *Annu. Rev. Microbiol.* **1998**, *52*, 423-452.
- (2) Wiedemeier, T. H.; Swanson, M. A.; Moutoux, D. E.; Gordon, E. K.; Wilson, J. T.; Wilson, B. H.; Kampbell, D. H.; Haas, P. E.; Miller, R. N.; Hansen, J. E.; Chapelle, F. H. Technical Protocol for Evaluating Natural Attenuation of Chlorinated Solvents in Ground Water. *EPA/600/R-98/128 National Risk Management Research Laboratory, Office of Research and Development, U. S. Environmental Protection Agency; Cincinnati, Ohio* **1998**.
- (3) Davis, J. W.; Carpenter, C. L. Aerobic biodegradation of vinyl chloride in groundwater samples. *Appl. Environ. Microbiol.* **1990**, *56*, 3878-3880.
- (4) Bradley, P. M.; Chapelle, F. H. Effect of contaminant concentration on aerobic microbial mineralization of DCE and VC in stream-bed sediments. *Environ. Sci. Technol.* **1998**, *32*, 553-557.
- (5) Ensley, B. D. Biochemical diversity of trichloroethylene metabolism. *Annu. Rev. Microbiol.* **1991**, *45*, 283-299.
- (6) Fliermans, C. B.; Phelps, T. J.; Ringelberg, D.; Mikell, A. T.; White, D. C. Mineralization of trichloroethylene by heterotrophic enrichment cultures. *Appl. Environ. Microbiol.* **1998**, *54*, 1709-1714.
- (7) Sherwood Lollar, B.; Slater, G. F.; Sleep, B.; Witt, M.; Klecka, G. M.; Harkness, M.; Spivack, J. Stable carbon isotope evidence for intrinsic bioremediation of tetrachloroethene and trichloroethene at area 6, Dover Air Force Base. *Environ. Sci. Technol.* **2001**, *35*, 261-269.
- (8) Clement, T. P.; Johnson, C. D.; Sun, Y. G.; Klecka, G. M.; Bartlett, C. Natural attenuation of chlorinated ethene compounds: model development and field-scale application at the Dover site. *J. Contam. Hydrol.* **2000**, *42*, 113-140.
- (9) Song, D. L.; Conrad, M. E.; Sorenson, K. S.; Alvarez-Cohen, L. Stable carbon isotope fractionation during enhanced in situ bioremediation of trichloroethene. *Environ. Sci. Technol.* **2002**, *36*, 2262-2268.
- (10) Sturchio, N. C.; Clausen, J. L.; Heraty, L. J.; Huang, L.; Holt, B. D.; Abrajano, T. A. Chlorine isotope investigation of natural attenuation of trichloroethene in an aerobic aquifer. *Environ. Sci. Technol.* **1998**, *32*, 3037-3042.
- (11) Sorenson, K. S. J.; Peterson, L. N.; Hinchee, R. E.; Ely, R. L. An evaluation of aerobic trichloroethene attenuation using first-order rate estimation. *Bioremediation* **2000**, *4*, 337-357.
- (12) Hunkeler, D.; Aravena, R.; Butler, B. J. Monitoring microbial dechlorination of tetrachloroethene (PCE) in groundwater using compound-specific stable carbon isotope ratios: Microcosm and field studies. *Environ. Sci. Technol.* **1999**, *33*, 2733-2738.
- (13) Sherwood Lollar, B.; Slater, G. F.; Ahad, J.; Sleep, B.; Spivack, J.; Brennan, M.; MacKenzie, P. Contrasting carbon isotope fractionation during biodegradation of trichloroethylene and toluene: Implications for intrinsic bioremediation. *Org. Geochem.* **1999**, *30*, 813-820.
- (14) Slater, G. F.; Sherwood Lollar, B.; Sleep, B. E.; Edwards, E. A. Variability in carbon isotopic fractionation during biodegradation of chlorinated ethenes: Implications for field applications. *Environ. Sci. Technol.* **2001**, *35*, 901-907.
- (15) Mancini, S. A.; Lacrampe-Couloume, G.; Jonker, H.; Breukelen, B. M. V.; Groen, J.; Folkering, F.; Sherwood Lollar, B. Hydrogen isotope enrichment: An indicator of biodegradation at a petroleum hydrocarbon field site. *Environ. Sci. Technol.* **2002**, *36*, 2464-2470.
- (16) Meckenstock, R. U.; Morasch, B.; Griebler, C.; Richnow, H. H. Stable isotope fractionation analysis as a tool to monitor biodegradation in contaminated aquifers. *J. Contam. Hydrol.* **2004**, *75*, 215-255.
- (17) Schmidt, T. C.; Zwank, L.; Elsner, M.; Berg, M.; Meckenstock, R. U.; Haderlein, S. B. Compound-specific stable isotope analysis of organic contaminants in natural environments: a critical review of the state of the art, prospects, and future challenges. *Anal. Bioanal. Chem.* **2004**, *378*, 283-300.
- (18) Elsner, M.; Zwank, L.; Hunkeler, D.; Schwarzenbach, R. P. A new concept linking observable stable isotope fractionation to transformation pathways of organic pollutants. *Environ. Sci. Technol.* **2005**, *39*, 6896-6916.
- (19) Morasch, B.; Richnow, H. H.; Schink, B.; Meckenstock, R. U. Stable hydrogen and carbon isotope fractionation during microbial toluene degradation: Mechanistic and environmental aspects. *Appl. Environ. Microbiol.* **2001**, *67*, 4842-4849.
- (20) Nijenhuis, I.; Andert, J.; Beck, K.; Kästner, M.; Diekert, G.; Richnow, H. H. Stable isotope fractionation of tetrachloroethene during reductive dechlorination by *Sulfurospirillum multivorans* and *Desulfitobacterium* sp strain PCE-S and abiotic reactions with cyanocobalamin. *Appl. Environ. Microbiol.* **2005**, *71*, 3413-3419.
- (21) VanStone, N. A.; Focht, R. M.; Mabury, S. A.; Sherwood Lollar, B. Effect of iron type on kinetics and carbon isotopic enrichment of chlorinated ethylenes during abiotic reduction on Fe(0). *Ground Water* **2004**, *42*, 268-276.

- (22) Lee, P. K. H.; Conrad, M. E.; Alvarez-Cohen, L. Stable carbon isotope fractionation of chloroethenes by dehalorespiring isolates. *Environ. Sci. Technol.* **2007**, *41*, 4277-4285.
- (23) Abé, Y.; Hunkeler, D. Does the Rayleigh equation apply to evaluate field isotope data in contaminant hydrogeology? *Environ. Sci. Technol.* **2006**, 1588-1596.
- (24) Béranger, S. C.; Sleep, B. E.; Sherwood Lollar, B.; Monteagudo, F. P. Transport, biodegradation and isotopic fractionation of chlorinated ethenes: Modeling and parameter estimation methods. *Advances in Water Resources* **2005**, *28*, 87-98.
- (25) Prommer, H.; Aziz, L. H.; Bolaño, N.; Taubald, H.; Schüth, C. Modelling of geochemical and isotopic changes in a column experiment for degradation of TCE by zero-valent iron. *J. Contam. Hydrol.* **2008**, *97*, 13-26.
- (26) Hunkeler, D.; Aravena, R.; Cox, E. Carbon isotopes as a tool to evaluate the origin and fate of vinyl chloride: Laboratory experiments and modeling of isotope evolution. *Environ. Sci. Technol.* **2002**, *36*, 3378-3384.
- (27) Morrill, P. L.; Sleep, B. E.; Slater, G. F.; Edwards, E. A.; Sherwood Lollar, B. Evaluation of isotopic enrichment factors for the biodegradation of chlorinated ethenes using a parameter estimation model: toward an improved quantification of biodegradation. *Environ. Sci. Technol.* **2006**, *40*, 3886-3892.
- (28) van Breukelen, B. M.; Hunkeler, D.; Volkering, F. Quantification of sequential chlorinated ethene degradation by use of a reactive transport model incorporating isotope fractionation. *Environ. Sci. Technol.* **2005**, *39*, 4189-4197.
- (29) Amt für Umweltschutz Stuttgart, *KORA - TVI: Forschungsbericht, Förderkennzeichen 02WN0353*; Projekt 1.3: Natürlicher Abbau und Rückhalt eines komplexen Schadstoffcocktails in einem Grundwasserleiter am Beispiel des ehemaligen Mineralölwerks Epple; Stuttgart, **2007**.
- (30) Zwank, L.; Berg, M.; Schmidt, T. C.; Haderlein, S. B. Compound-specific carbon isotope analysis of volatile organic compounds in the low-microgram per liter range. *Anal. Chem.* **2003**, *75*, 5575-5583.
- (31) Jochmann, M. A.; Blessing, M.; Haderlein, S. B.; Schmidt, T. C. A new approach to determine method detection limits for compound-specific isotope analysis of volatile organic compounds. *Rapid Commun. Mass Spectrom.* **2006**, *20*, 3639-3648.
- (32) Chen, D. J. Z.; MacQuarrie, K. T. B. Numerical simulation of organic carbon, nitrate, and nitrogen isotope behavior during denitrification in a riparian zone. *J. Hydrol.* **2004**, *293*, 235-254.
- (33) Mariotti, A.; Germon, J. C.; Hubert, P.; Kaiser, P.; Letolle, R.; Tardieux, A.; Tardieux, P. Experimental determination of nitrogen kinetic isotope fractionation: some principles; illustration for the denitrification and nitrification processes. *Plant and Soil* **1981**, *62*, 413-430.
- (34) Prommer, H.; Barry, D. A.; Zheng, C. MODFLOW/MT3DMS-based reactive multicomponent transport modeling. *Ground Water* **2003**, *41*, 247-257.
- (35) Van Breukelen, B. M.; Prommer, H. Beyond the Rayleigh Equation: isotope fractionation reactive transport modeling improves quantification of biodegradation. *Environ. Sci. Technol.* **2008**, *42*, 2457-2463.
- (36) Vogel, T. M.; Criddle, C. S.; McCarty, P. L. Transformations of halogenated aliphatic compounds. *Environ. Sci. Technol.* **1987**, *21*, 722-736.
- (37) Alvarez-Cohen, L.; Gerald E. Speitel, J. Kinetics of aerobic cometabolism of chlorinated solvents. *Biodegradation* **2001**, *12*, 105-126.
- (38) Haston, Z. C.; McCarty, P. L. Chlorinated ethene half-velocity coefficients (Ks) for reductive dehalogenation. *Environ. Sci. Technol.* **1999**, *33*, 223-226.
- (39) Wiedemeier, T. H.; Swanson, M. A.; Wilson, J. T.; Kampbell, D. H.; Miller, R. N.; Hansen, J. E. Approximation of biodegradation rate constants for monoaromatic hydrocarbons (BTEX) in groundwater. *Ground Water Monit. Remediat.* **1996**, *16*, 186-194.
- (40) Barth, J. A. C.; Slater, G.; Schüth, C.; Bill, M.; Downey, A.; Larkin, M.; Kalin, R. M. Carbon isotope fractionation during aerobic biodegradation of trichloroethene by *Burkholderia cepacia* G4: a tool to map degradation mechanisms. *Appl. Environ. Microbiol.* **2002**, *68*, 1728-1734.
- (41) Chu, K. H.; Mahendra, S.; Song, D. L.; Conrad, M. E.; Alvarez-Cohen, L. Stable carbon isotope fractionation during aerobic biodegradation of chlorinated ethenes. *Environ. Sci. Technol.* **2004**, *38*, 3126-3130.
- (42) Gelhar, L. W.; Welty, C.; Rehfeldt, K. R. Critical Review of Data on Field-Scale Dispersion in Aquifers. *Water Resources Research* **1992**, *28*, 1955-1974.



### 6.5. Appendix

**Setup of 1D Reactive Transport Model.** The 1D model has a longitudinal extent of 532 m, discretised into 2 m long columns. A fixed flow rate was defined as the upstream boundary condition while a fixed head of 227.32 m (measured at well B42) forms the boundary at the downstream end. The effective porosity and hydraulic conductivity were set to 0.02 and 2.0 m/d, respectively, based on estimates derived from the 3D groundwater flow model that was more specifically developed for the region located north to the present study site (1). The flow velocity applied in the 1D reactive transport model of 3.93 m/d was determined by particle tracking simulations with the 3D flow model. At this velocity, mechanical dispersion dominates over molecular diffusion.

**Setup of 2D Reactive Transport Model.** The 2D model was discretised in transverse (horizontal) direction (100 m width, 9750 to 10725 cells), creating a uniform 2D flow field. Assumptions were, as before, steady-state flow and stable geochemical conditions. The widths of the model cells ranged between 1 m and 10 m, with refinement near the plume centerline.

**Reaction Kinetics.** The model is appropriate when the microbial mass is not changing with time within the region of interest and for biodegradation at low pollutant levels, and is often applied to field analysis for simplification purposes. In this study, 1st order reaction rates produced a reasonable representation of the observed field data. The reaction models also assumed that biological degradation reactions only occurred in the aqueous phase (conservative assumption).

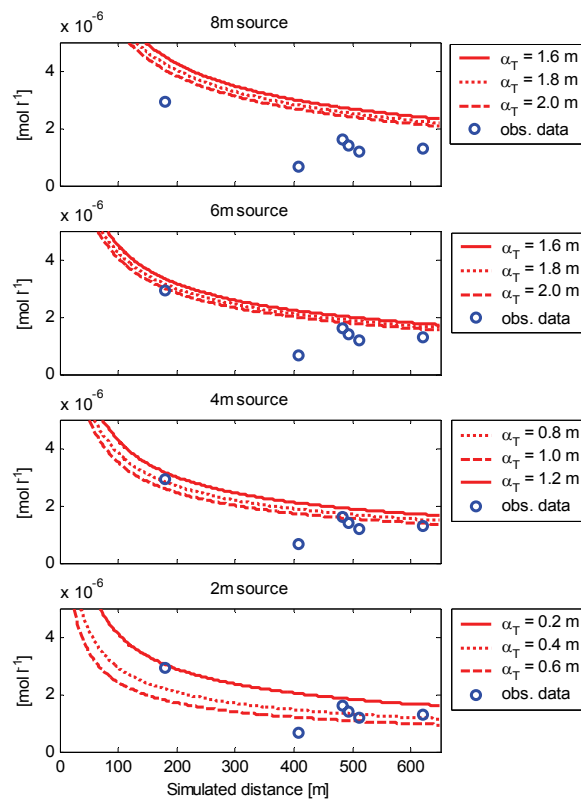
**Table A6-1.** 1D hydraulic model properties; average velocity from particle tracking and porosity/conductivity from 3D model (1).

Cross-sectional area, m <sup>2</sup>	1
Flow velocity, m/d	3.93
Flow rate, m <sup>3</sup> /d	0.0786
K, m/d	2
i	0.0393
n <sub>e</sub>	0.02
h (x=1 m), m	248.11
h (x=531 m), m	227.32
α <sub>L</sub> , m	0.5

**Investigation of Potential Source Widths.** Source widths of 2, 4, 6 and 8 m were investigated in combination with varying  $\alpha_T$  values in order to simulate the observed PCE concentrations, assuming the sampled wells are located at or near the plume centerline. The results of these simulations are shown in Figure A6-1. The results demonstrate that the range of possible plume widths extends to around 6 m at the most, for a reasonable range of transverse dispersivity values. The required dispersion for each case is given in Table A6-2. The 4 m source width most closely matched the measured PCE concentrations for  $\alpha_T$  of 1 m and  $\alpha_L$  of 10 m.

**Table A6-2.** Dispersivity factors required for varying source widths in 2D model in order to simulate observed PCE concentrations under aerobic, PCE-recalcitrant, conditions, assuming a transverse dispersivity,  $\alpha_L = 10 \cdot \alpha_T$

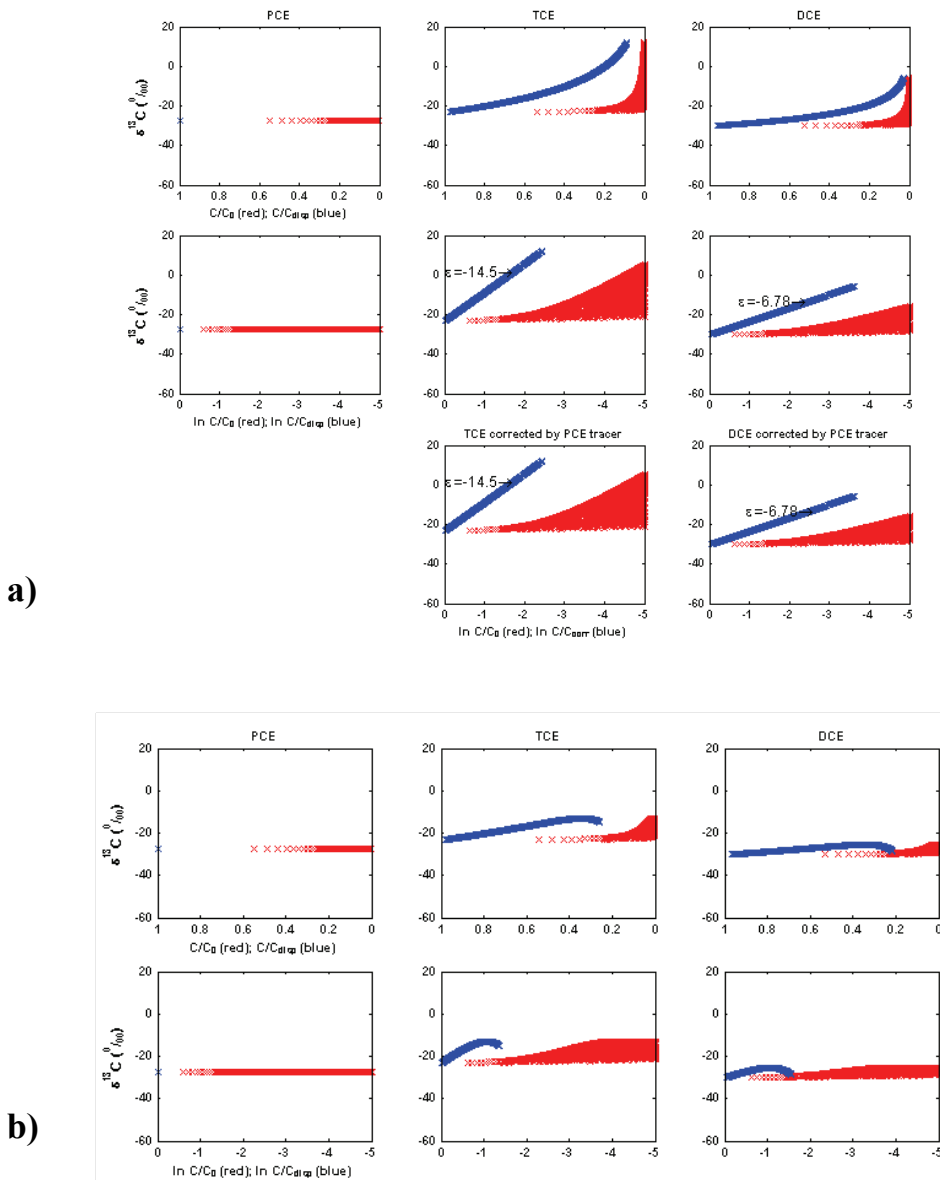
Source width	$\alpha_T$ required to agree with field data (setting $\alpha_L = 10 \cdot \alpha_T$ )
2 m	0.2 m
4 m	1 m
6 m	2 m
8 m	> 2 m



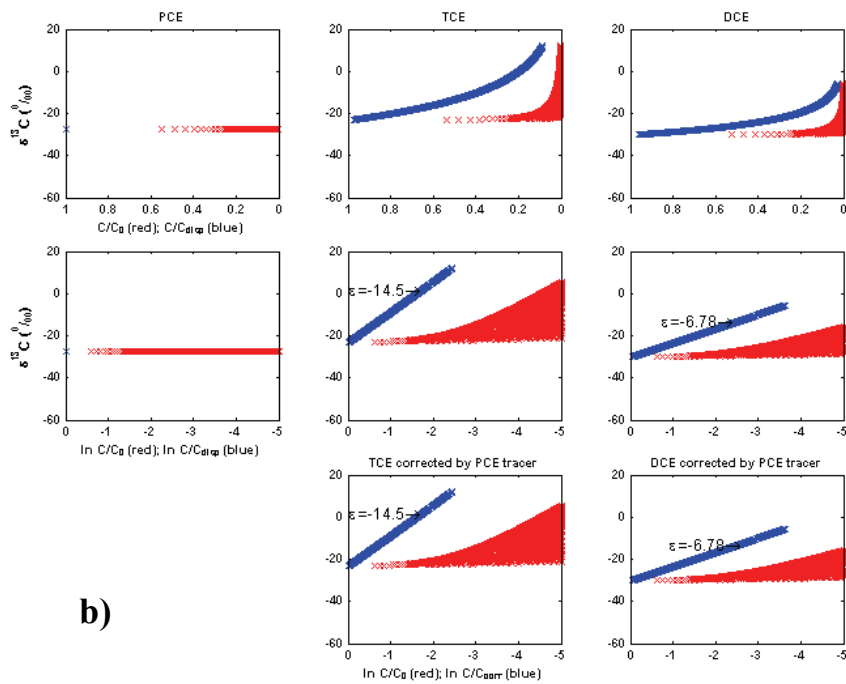
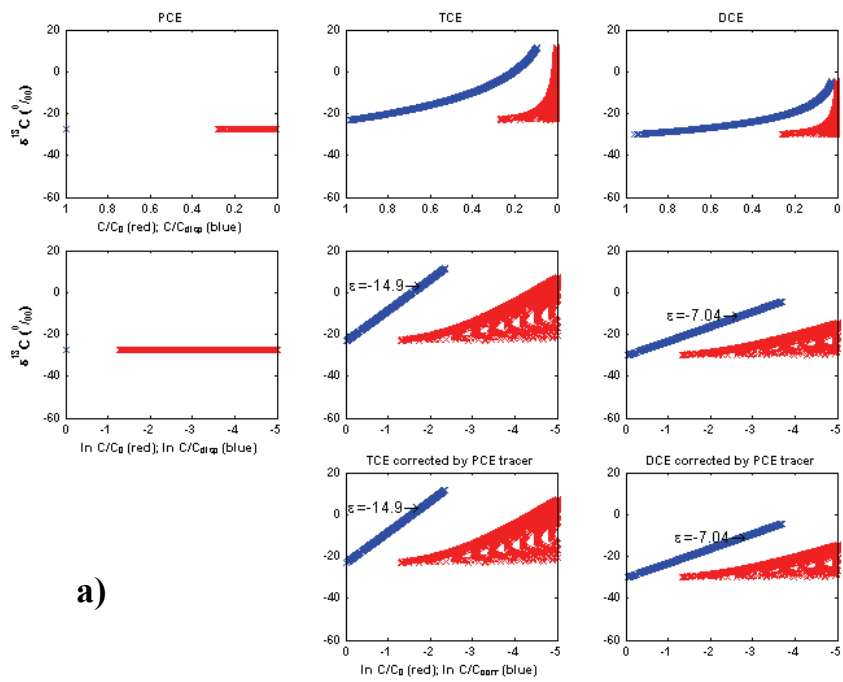
**Figure A6-1.** 2D model results of PCE concentrations along the centerline of a 2D plume with varying transverse dispersion ( $\alpha_T$ ) for different source widths under aerobic, PCE-recalcitrant conditions.

**Comparing Rayleigh to Reactive Transport Models.** The influence on the observed Rayleigh fractionation by a heterogeneous aquifer is illustrated as follows: if an aquifer is 1 m thick and the lower 0.2 m are void of oxygen and therefore not undergoing degradation, while the upper 0.8 m undergo 1st order aerobic degradation, a Rayleigh plot of a 4 m wide source and 1 m transverse dispersivity compared to a non-differentiated aquifer is shown in Figure A6-3b. The calculations for this illustration were made in MATLAB by incorporating, as in a fully screened well, 80% reactive and 20% non-reactive concentrations. However, reaction rates due to dispersion and heterogeneity will always be overestimated (2); therefore, there is a counter-effect. Volatilization, sorption and diffusion did not seem to play a significant role in carbon isotope fractionation based on the consistent PCE isotope data.

During quantification of biodegradation processes through CSIA, the presence of heterogeneous groundwater flow systems will also cause uncertainty (2-4). It would be useful to obtain both concentration and isotope data from multilevel sampling. This would allow investigation on the variability of concentrations over the thickness of the aquifer and to prevent problems that potentially arise from mixing of different water types within fully filtered wells. Nevertheless, this is expected to slightly underestimate the rates of reaction (2) as was the case with increasing longitudinal dispersion in this study. Generally, heterogeneities in microbial activity occurs at the pore scale, orders of magnitude smaller than the fully screened well, and a contaminant plume is orders of magnitude larger still (5). When geochemical parameters are consistent with conditions favourable to aerobic degradation throughout the study length of the plume (as in the case of the wells at this site), anaerobic microenvironments, if they do exist, are present within microenvironments and represent only a relatively small fraction of the volume being sampled (5). A more significant factor affecting CSIA reaction rate quantification is the transport velocity, because it is in direct proportion to the degradation rate estimate. Additionally, when calculating the extent of biodegradation, the initial contaminant concentration estimate has a great influence at a short distance downstream (6). A high standard deviation in some isotope values measured along a flow line induce only minor effects on the estimated mass removed (6).



**Figure A6-2.** Plot of Rayleigh equation in a two-dimensional flow field demonstrating effects of dispersion and heterogeneity. Effect of **a)** dispersion in a homogeneously reactive aquifer, and **b)** in vertically differentiated reaction zones (simulating a fully screened aquifer with 20% non-reactive to 80% reactive vertical aquifer thickness). The red area represents fraction remaining when calculated as  $C/C_0$  where  $C$  is the concentration in the model field and  $C_0$  is the source concentration. The blue data sets represent adjusted fractions remaining, accounting for dispersion either by reactive transport modeling ( $C/C_{disp}$ ) or using the conservative tracer method ( $C/C_{corr}$ ).



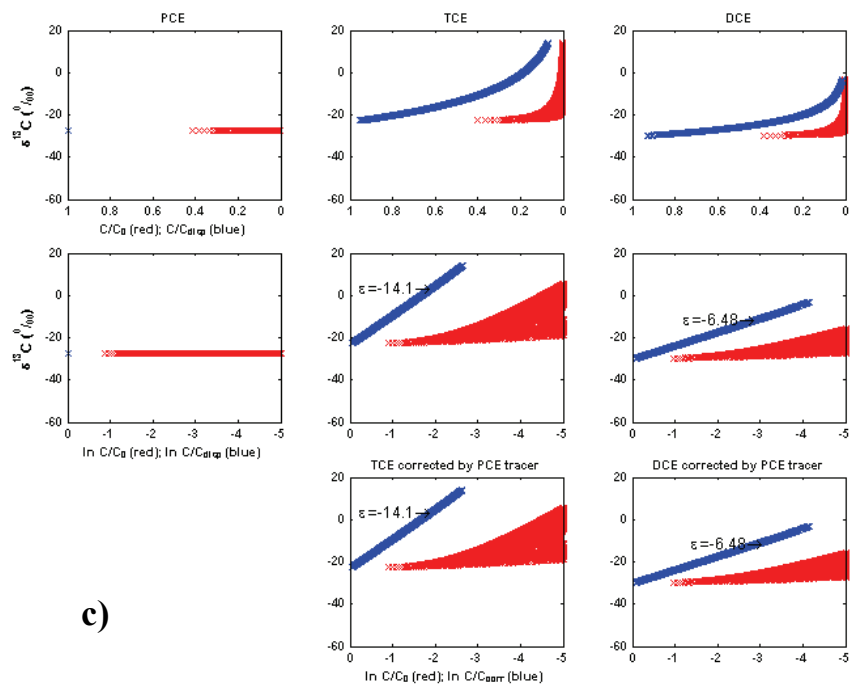


**Figure A6-3 (preceding page).** Plot of Rayleigh equation in a 2D flow field demonstrating effects of dispersion in a homogeneously reactive aquifer for increasing source widths: **a)** 2 m, **b)** 4 m, **c)** 6 m, and correspondingly increasing longitudinal dispersion, as outlined in Table A6-2. The red area represents the fraction remaining when calculated as  $C/C_0$  where  $C$  is the concentration in the model field and  $C_0$  is the source concentration. The blue data sets represent adjusted fractions remaining, accounting for dispersion either by reactive transport modeling ( $C/C_{disp}$ ) or using the conservative tracer method ( $C/C_{corr}$ ).

#### Referenzen:

- (1) Amt für Umweltschutz Stuttgart, *KORA - TV1: Forschungsbericht, Förderkennzeichen 02WN0353*; Projekt 1.3: Natürlicher Abbau und Rückhalt eines komplexen Schadstoffcocktails in einem Grundwasserleiter am Beispiel des ehemaligen Mineralölwerks Epple; Stuttgart, **2007**.
- (2) Abe, Y.; Hunkeler, D. Does the Rayleigh Equation Apply to Evaluate Field Isotope Data in Contaminant Hydrogeology? *Environ. Sci. Technol.* **2006**, 1588-1596.
- (3) Elsner, M.; Zwank, L.; Schwarzenbach, R. P.; Hunkeler, D. A new concept linking observable stable isotope fractionation to transformation pathways of organic pollutants. *Environ. Sci. Technol.* **2005**, 39, 6896-6916.
- (4) Kopinke, F. D.; Georgi, A.; Richnow, H. H. Comment on "New Evaluation Scheme for Two-Dimensional Isotope Analysis to Decipher Biodegradation Processes: Application to Groundwater Contamination by MTBE". *Environ. Sci. Technol.* **2005**, 39, 8541-8542.
- (5) Sturchio, N. C.; Clausen, J. L.; Heraty, L. J.; Huang, L.; Holt, B. D.; Abrajano, T. A. Chlorine isotope investigation of natural attenuation of trichloroethene in an aerobic aquifer. *Environ. Sci. Technol.* **1998**, 32, 3037-3042.
- (6) Meckenstock, R. U.; Morasch, B.; Griebler, C.; Richnow, H. H. Stable isotope fractionation analysis as a tool to monitor biodegradation in contaminated aquifers. *J. Contam. Hydrol.* **2004**, 75, 215-255.

## 7. General Conclusions and Outlook

The main aim of the present work was to demonstrate the potential of compound-specific isotope analysis (CSIA) for studying the source and fate of organic contaminants at heterogeneous and complex aquifer systems. One major drawback in the application of CSIA to field studies, is that current GC/IRMS systems are limited in their sensitivity. To overcome this limitation, various sample extraction and injection techniques were optimized and validated for their use in CSIA field studies. For volatile compounds, a commercially available purge-and-trap sample extractor has been technically improved within this work. Good performance of the system was demonstrated for low-contaminated sites and by a comparison with extraction techniques that are already well-established in CSIA for volatile organics. Overall, the results obtained and discussed within Chapter 2 demonstrate that the sample preconcentration and extraction techniques applied are well suited for the compound-specific carbon isotope analysis of volatile compounds at trace concentrations. For semi-volatile organic compounds, a sample introduction technique, that (until now) has been restricted to quantitative analysis, was applied in the present study to continuous-flow isotope ratio determinations for the first time. The technique, based on the injection of large sample volumes of organic extracts into a programmable temperature vaporizer (PTV) injector with subsequent solvent-venting and trapping of the analytes on a cooled packed liner, was thoroughly validated for the application in GC/IRMS in terms of its accuracy, precision, linearity, reproducibility and limits of detection (Chapter 3). The optimized PTV-LVI method allows to determine accurately and precisely  $\delta^{13}\text{C}$  values of semi-volatile organic contaminants at low  $\mu\text{g/L}$  or  $\mu\text{g/kg}$  concentrations and thus expands the applicability of CSIA considerably in environmental studies. The applicability of the method was validated for  $\delta^{13}\text{C}$  determination of individual PAHs and exemplified by a source apportionment study at a contaminated site. As one of the most important requirements in GC/IRMS is the baseline-separation of peaks (see Chapter 4) sample cleanup before analysis was mandatory.

The combination of the PTV-LVI method with preparative HPLC would offer a time and labour efficient method for the determination of isotopic compositions of semi-volatile organic compounds even in difficult matrices. Due to the method developments attained in the present study, future work could be extended to assess contaminant sources and degradation reactions at larger scales, e.g. in catchment hydrology. The use of CSIA is open to a range of new application areas, e.g. future studies should include other important soil and groundwater contaminants such

as pesticides, herbicides, or polychlorinated biphenyls. Latest developments in hyphenation of liquid chromatography to IRMS systems (LC/IRMS) would allow for compound-specific stable isotope analysis of non-volatile and thermally unstable compounds in the future.

The present work aimed not only to demonstrate the potential of CSIA in NA field site investigation, but also to test the performance at site conditions, typically confronted with in practical contaminated site management. Potential pitfalls of the analytical procedure were critically discussed and strategies to avoid possible sources of error were provided in Chapter 4. In addition, the need for a thorough investigation of compound-specific isotope fractionation effects possibly involved in any step of the overall analytical method by standards with known isotopic composition was emphasized.

To validate the applicability of the CSIA concept for studying the source and fate of organic contaminants and to reliably quantify the rate of *in-situ* degradation in contaminant plumes even at highly complex conditions, extensive site investigations were performed at an urban, heterogeneous bedrock aquifer system. Chapter 5 demonstrates how compound-specific carbon isotope analysis can be used to allocate contaminant sources at a site with multiple and overlapping plumes. A multiple-line-of-evidence approach including evaluation of historical, hydrological, geochemical and isotopic data and statistical analysis unravelled the contamination scenario at the site. In the present work it was shown that careful statistical evaluation and interpretation of highly precise compound specific isotope signatures, geochemical data and site-specific additional information are essential for a comprehensive site assessment under complex boundary conditions. However, in cases where uncertainties remain, two dimensional CSIA (multiple isotope analysis, e.g.  $\delta^{37}\text{Cl}$  or  $\delta^2\text{H}$ ) may further improve the conclusive power for constraining contaminant sources.

A model-based analysis of concentration and isotope data was carried out to assess natural attenuation of chlorinated ethenes in an aerobic fractured bedrock aquifer. The results (Chapter 6) provided strong evidence for the occurrence of aerobic TCE and DCE degradation. As PCE is recalcitrant in aerobic conditions, it could be used as a conservative tracer to estimate the extent of dilution. The dilution-corrected concentrations together with stable carbon isotope data allowed for the reliable assessment of the extent of biodegradation at the site and plume simulations quantitatively linked aerobic biodegradation with isotope signatures in the field. A comparison of isotope analysis only at the field scale to isotope analysis with reactive transport



---

modeling has demonstrated the need, when quantifying natural attenuation processes, for an integrated approach, particularly when similar degradation processes can result in a range of enrichment factors. Prior to this study, fractionation due to aerobic TCE degradation has only been studied for two particular strains of bacteria and never for a mixed culture. Fractionation due to aerobic DCE degradation is even less well documented. In general, there is a range of compounds with no reported fractionation factors available or the laboratory parameters are not representing the prevailing site-specific conditions. Therefore, further work should be addressed to the investigation of enrichment factors for less-studied compounds. Future laboratory experiments should be performed for a set of various redox conditions and microbial cultures to provide enrichment factors for a wide range of environmental conditions. In addition, further research is required to assess the processes that control these enrichment factors.

## List of Figures and Tables

- Figure 1-1.** Set-up of GC/IRMS system for the determination of carbon isotope ratios of individual compounds, figure taken from Schmidt et al. (8)..... 2
- Figure 1-2.** Decreasing concentration associated with enrichment of heavy isotopologues indicating biodegradation (exemplified for benzene degradation at the former military airfield Brand, site-specific details are given in Chapter 2)..... 5
- Figure 1-3.** HPLC-chromatogram for toluene (column: Eurosoil 4; flow 0.1 mL/min) together with corresponding carbon isotope composition along the peak. The horizontal line represents the  $\delta^{13}\text{C}$  value of the non-fractionated toluene. .... 7
- Figure 2-1.** Effect of two different polymer tubings on extraction efficiency. Extraction efficiencies are represented by amplitude height of the mass 44 peak achieved during enhanced-volume P&T-analyses using PTFE- and PEEK- tubings for sample transfer. Error bars represent the standard deviation based on a triplicate measurement..... 19
- Figure 2-2.** Sorptive loss to PTFE (filled squares, given in %-difference of amplitude heights of  $m/z$  44 peaks relative to PEEK) versus experimental equilibrium PTFE-water partitioning constants ( $\log P_{\text{PTFE}}$ , (23)). Open circles represent the theoretical loss for aromatic hydrocarbons according to  $\log P_{\text{PTFE}}$  values given by (23)... 20
- Figure 2-3.** Evaluation of method detection limits (MDLs) for the investigated compounds. Open circles are representing  $\delta^{13}\text{C}$  values; diamonds show the signal size of mass 44 peak. The linear behavior of signal size versus concentration is indicated by correlation coefficients ( $R^2$ ) always better than 0.996. Error bars represent the standard deviation based on triplicate measurements. The horizontal lines represent the mean isotopic value for each compound ( $\pm 0.5\%$ ). .... 21
- Figure 2-4.** Concentration and carbon isotope data for PCE changing with depth of the aquifer. Internal reproducibility based on triplicate injections of samples and standards is generally  $< 0.5\%$ . .... 23
- Figure 2-5.** Concentration and  $\delta^{13}\text{C}$  values for PCE as qualitative evidence for microbial reductive dehalogenation along the water flow path B2 to B5. The most downgradient well of the site shows the lowest concentration associated with significantly enriched  $\delta^{13}\text{C}$  values. The estimates of biodegradation (B) along this flow path range from 59% to 91%..... 24
- Figure 2-6.** Representative GC/IRMS-chromatogram for groundwaters contaminated with kersosene, sampled at Niedergörsdorf TL1, extraction performed with enlarged-volume-P&T (PTFE tubing), concentration of compounds  $\leq 1.5 \mu\text{g/L}$ . The upper trace, representing the ratio of mass 45/44, serves as indicator for good chromatographic performance of the system..... 26
- Figure 2-7. Left:** Map of Niedergörsdorf illustrating concentration distribution and isotopic composition for A) benzene and B) 1,3,5-trimethylbenzene at the site. **Right:** Linear correlation of isotope composition versus concentration indicate *in-situ* biodegradation according to the Rayleigh equation (plotted wells are located along the flow path illustrated as blue arrows in the maps)..... 27
- Figure 2-8.** GC/IRMS-chromatogram obtained for the analysis of a low-contaminated mineral water (Mombachquelle, Stuttgart) using the enhanced-volume P&T-system equipped with a PEEK-tubing as sample transfer loop. Signal intensities for *cis*-DCE, trichloromethane and 1,1,1-trichloroethane (0.1, 0.13 and 0.17

- µg/L, resp.) were below the MDL;  $\delta^{13}\text{C}$  values for TCE (0.36 µg/L) and PCE (2.28 µg/L) could be reliably determined. .... 28
- Figure A2-1.** Biodegradation estimates for kerosene-contamination at KORA-site Niedergörsdorf (in percent). .... 33
- Figure 3-1.** Effect of solvent and PTV initial temperatures on the instrument response for selected 2- to 5-ring compounds. Injections were made at 100 µL each with same analyte concentration, error bars are indicating the standard deviation of a triplicate measurement. .... 39
- Figure 3-2.** Linear correlation of peak area and amount of compound injected illustrated for A) naphthalene and B) perylene. Results are given for various solvents, initial PTV inlet temperatures and solvent levels (SL); error bars represent standard deviations based on three injections (in most cases smaller than the symbol size). .... 40
- Figure 3-3.** Peak areas as a function of sample volume injected exemplarily shown for a) naphthalene and b) perylene. Volumes of samples injected were 50, 100 and 150 µL. .... 40
- Figure 3-4.** Results for PTV-LVI injections measuring  $\delta^{13}\text{C}$  as a function of different concentrations (represented by different signal sizes) illustrated for a) naphthalene and b) perylene. Varying parameters are volume of injection and solvents injected at optimized PTV initial temperatures, with a solvent level (SL) set to 1%. For comparison, results for a conventional 1µL splitless injection are included. Error bars are indicating the standard deviation of a triplicate injection. .... 42
- Figure 3-5.** Comparison of GC/IRMS chromatograms of a) a conventional 1 µL injection of a 75 mg/L and b) a 100 µL large volume injection of a 750 µg/L PAH working standard diluted in *n*-pentane shows good chromatographical peak resolution, PTV inlet temperatures during the injection were a) 300 °C and b) 20 °C, numbers of compounds correspond to the numbers given Table 3-2. .... 46
- Figure 3-6.** Chromatograms of a soil sample extract after conventional 1µL injection and after a LVI-GC/IRMS to ensure peak heights above the method detection limit of 500 mV. .... 48
- Figure 3-7.** Box-whisker-diagram for individual PAH compounds of the soil samples taken at the site compared to reported mean isotopic compositions of creosote (5), petroleum (38), crankcase oil (39) and town gas process tar (40). .... 49
- Figure A3-1.** Effect of solvent evaporation on  $\delta^{13}\text{C}$  values of individual PAH compounds (not significant). .... 53
- Figure 4-1.** Tetrachloroethene (PCE) concentrations in µg/L (squares) and  $\delta^{13}\text{C}$  ratios in ‰ (circles) in groundwater samples taken from different sampling depths by a multilevel sampling well. Dotted vertical lines represent a mean concentration of 2900 µg/L and a concentration-weighted average  $\delta^{13}\text{C}$  value of -25.7‰ that would have been obtained by conventional groundwater sampling of a fully screened well. .... 56
- Figure 4-2.** **A,** GC/IRMS chromatogram of a soil sample after accelerated solvent extraction (ASE) shows a raised baseline due to unresolved complex mixture (UCM) present in the sample. **B,** GC/IRMS chromatogram of the same soil sample after accelerated solvent extraction (ASE) and cleanup on silica gel. Complete removal of UCM hump but the response (amplitude) of the target compounds is below the linear range of the IRMS at ca. 500 mV (horizontal line). **C,** GC/IRMS chromatogram of the same soil sample after ASE, silica gel cleanup and large volume injection (LVI). Baseline separation of all peaks of interest is achieved, and peak amplitudes are within the linear range of the IRMS and allow for an accurate and precise determination of  $\delta^{13}\text{C}$  values... 60
- Figure 4-3.** **A)** illustrates the detrimental effect on chromatographical resolution due to wrong SPME fiber exposure in a GC-injector. Non-ideal thermal desorption results in peak broadening (mass 44 chromatogram in the lower

- part of the figure) and poor isotope swings with secondary fluctuations recognized in the instantaneous ratio signal (upper trace). **B)** shows the same GC/IRMS analysis but with a correctly placed SPME fiber for comparison. As indicated in the upper trace, isotope swings (S-shaped ratio of mass 45/44) can serve as indicator for good chromatographic performance. .... 61
- Figure 4-4.** GC/IRMS chromatogram of a BTEX containing groundwater sample (obtained at *KORA-site former military airfield Brand*) that was not completely screened by GC/MS before analysis. An unexpected high MTBE concentration (signal size 40 Volt) caused severe contamination of the analytical equipment. .... 62
- Figure 4-5.** GC/IRMS chromatogram of a pentane extract containing phthalates (main peaks) leached out of septum material. Coeluting PAH target peaks (as illustrated in the left) could not be resolved and inhibited an isotope analysis. .... 63
- Figure 4-6.** Amount dependency on  $\delta^{13}\text{C}$  measurements for PCE. Square symbols represent the carbon isotope value in ‰, diamonds indicate signal size of the mass 44 peak in mV. The horizontal broken line represents the iteratively calculated mean  $\delta^{13}\text{C}$  value, solid lines indicate the  $\pm 0.5$  ‰ interval. Values outside the linear range of the IRMS are circled. Measurements were performed in triplicates, the standard deviation of each point is indicated by error bars. The major principles illustrated in this figure are described in Jochmann et al. (27). .. 64
- Figure 4-7.** Effect of poor chromatographic resolution on  $\delta^{13}\text{C}$  values of adjacent peaks. Isotope values for single compound injections were:  $-26.0$  ‰ ( $\pm 0.1$ ,  $n=3$ ) for *trans*-1,2-DCE and  $-28.8$  ‰ ( $\pm 0.1$ ,  $n=3$ ) for MTBE. The measured isotope ratio for the smaller peak shown in **a)** deviates significantly from its actual value. Good peak resolution as indicated in **b)** results in almost accurate isotope values for both compounds. .... 65
- Figure 5-1 (preceding page).** **a)** Map with groundwater potential lines and pie chart diagrams illustrating contaminant distribution found at the site. **b)** Map showing locations of groundwater monitoring wells sampled for concentration and isotope analysis, locations of potential polluters, and suggested location of fault system. Areas A to G depict the various parts of the contaminant plume(s) as discussed in the text. Response for  $\delta^{13}\text{C}$  values of PCE was  $>0.5$  Volt, with the exception of B23 ( $\delta^{13}\text{C}$  given in brackets). Top right: Site-specific geochemistry depicted by manganese concentration isolines (as concentration of dissolved manganese at all individual wells correlates very well with the distribution of anaerobic and aerobic environments within the aquifer system, isolines of manganese distribution have been chosen to depict the site-specific geochemistry). For further details refer to Table 5-1. .... 79
- Figure 5-2.** Conceptual model of the contamination scenario observed in source zone F and zone G. DNAPL is spreading along fractures in the contaminated bedrock aquifer system. Anaerobic conditions drive reductive dechlorination and isotopic enrichment of chlorinated compounds in parts of the aquifer. Dissolution of PCE from DNAPL in the aerobic zone creates an input of undegraded material, i.e. not enriched in  $^{13}\text{C}$ . Linear mixing models explain the isotope signature of PCE observed in well B30 ( $-25.4$ ‰) representing a mixture of already degraded material with an isotope value of  $-23$ ‰ (measured in upgradient wells) and of freshly dissolved (undegraded) material with assumed values of  $-30$ ‰ (not likely) and  $-27$ ‰ (more likely). .... 84
- Figure 5-3.** Box-whisker-diagram illustrating the statistical significance of all  $\delta^{13}\text{C}$  measurements for PCE ( $n$  = number of values); the groups represent areas of same geochemical conditions as depicted in Figure 5-1b, the groundwater wells of each group or area are listed in Table 5-S4. The likeliness for the contamination in area C and D being derived from the same source is strongly supported; Area G can be further separated into 3

- different zones: the area of mixing processes (wells B30, B31, B1Eck, B39\*) and two additional CHC source zones (wells B1M and P836\*, respectively)..... 85
- Figure 5-4.** Origin and transport paths of contaminants evidenced by compound-specific carbon isotope signatures combined with geochemical data, concentration analyses, historical and hydrological information. .... 85
- Figure A5-1.** Linearity of  $\delta^{13}\text{C}$  values for PCE standard (mean value  $-27.2\text{‰}$ ) measured by purge-and-trap-GC/IRMS, intensities represent various standard concentrations yielding signal intensities (m/z 44 signals) from 270 to 8400 mV, horizontal lines indicate the mean  $\delta^{13}\text{C}$  value  $\pm 0.5\text{‰}$  accuracy range, error bars represent the standard deviation of duplicate or triplicate measurements, respectively. .... 90
- Figure A5-2.** Representative GC/IRMS chromatograms of sample B8F. Due to high differences in concentrations of each analyte, several runs have been performed with concentrations adjusted to the linear range of the  $\text{CO}_2$  reference gas peaks to ensure reproducible  $\delta^{13}\text{C}$  values. .... 91
- Figure 6-1.** Map illustrating groundwater flow conditions and VOC contamination in the area of focus. The dashed line indicates suggested location of fault system. .... 98
- Figure 6-2.** One-dimensional aerobic degradation scenario. Degradation rates for TCE and *cis*-DCE were  $0.02$  and  $0.025 \text{ d}^{-1}$ , respectively. The corresponding isotope fractionation factors were  $-12.0$  and  $-6.7\text{‰}$ , respectively. PCE was assumed not to degrade. Longitudinal dispersivities of  $0.5 \text{ m}$  and  $10 \text{ m}$  are represented by dark and light green lines, respectively. .... 102
- Figure 6-3.** Quantification of enrichment factors for TCE and *cis*-DCE undergoing aerobic degradation based of field data.  $f_{\text{corr}}$  represents a “corrected” fraction remaining where the concentration at any downgradient location is corrected for dilution using PCE as a conservative tracer. The equations shown are linear regression models where, according to the Rayleigh equation, the slope represents the isotope enrichment factor. The  $R^2$  value represents the coefficient of determination. .... 103
- Figure 6-4.** Concentration and isotope data of TCE simulated for a  $4\text{m}$  source width using reaction rates to suite regression-optimized TCE isotope signatures. Plume is located in the lower left hand corner and half of a symmetric plume is shown. The observed data (dashed lines) for each well is compared with the simulated values (red line) relative to the distance from the plume centerline. .... 105
- Figure 6-5.** Centerline of two-dimensional model based on calculated enrichment factors, adjusting TCE and *cis*-DCE degradation rates to suit regression-optimized **a)** isotope signatures, and **b)** concentrations, where  $\lambda'_{\text{left}} = v \ln(C_{\text{corr}}/C_0)$ ;  $\lambda'_{\text{right}} = -\text{slope} \cdot v/\epsilon$ . .... 106
- Figure A6-1.** 2D model results of PCE concentrations along the centerline of a 2D plume with varying transverse dispersion ( $\alpha_T$ ) for different source widths under aerobic, PCE-recalcitrant conditions. .... 112
- Figure A6-2.** Plot of Rayleigh equation in a two-dimensional flow field demonstrating effects of dispersion and heterogeneity. Effect of **a)** dispersion in a homogeneously reactive aquifer, and **b)** in vertically differentiated reaction zones (simulating a fully screened aquifer with  $20\%$  non-reactive to  $80\%$  reactive vertical aquifer thickness). The red area represents fraction remaining when calculated as  $C/C_0$  where  $C$  is the concentration in the model field and  $C_0$  is the source concentration. The blue data sets represent adjusted fractions remaining, accounting for dispersion either by reactive transport modeling ( $C/C_{\text{disp}}$ ) or using the conservative tracer method ( $C/C_{\text{corr}}$ ). .... 114

<b>Figure A6-3 (preceding page).</b> Plot of Rayleigh equation in a 2D flow field demonstrating effects of dispersion in a homogeneously reactive aquifer for increasing source widths: <b>a)</b> 2 m, <b>b)</b> 4 m, <b>c)</b> 6 m, and correspondingly increasing longitudinal dispersion, as outlined in Table A6-2. The red area represents the fraction remaining when calculated as $C/C_0$ where $C$ is the concentration in the model field and $C_0$ is the source concentration. The blue data sets represent adjusted fractions remaining, accounting for dispersion either by reactive transport modeling ( $C/C_{disp}$ ) or using the conservative tracer method ( $C/C_{corr}$ ).....	116
<b>Table 2-1.</b> Accuracy and reproducibility of VOC extraction methods applied within this study; $\delta^{13}C$ values given in per mill (‰); signal heights $\geq 1000mV$ .....	22
<b>Table A2-1.</b> Purge-and-trap parameters and gas chromatographic conditions. ....	31
<b>Table A2-2.</b> Isotopic mass balance considerations at the site.....	32
<b>Table A2-3.</b> Applied enrichment factors (batch experiments) for biodegradation estimates. ....	33
<b>Table 3-1.</b> Results for a 100 $\mu L$ injection of PAH working standards diluted in cyclohexane and <i>n</i> -pentane at PTV initial temperatures of 60°C and 20 °C, respectively; based on $n=30-40$ for each compound and method applied. ....	43
<b>Table 3-2.</b> Reproducibility and accuracy of the PTV-LVI method. Values are highly reproducible for optimized injection parameters and accurate compared to values of the same working standards measured by off-line EA/IRMS. (Values in light grey represent the results for compounds injected with the ‘wrong’ solvent.) .....	44
<b>Table 3-3.</b> Variance in $\delta^{13}C$ values for different signal size intervals. ....	45
<b>Table 4-1:</b> Effect of $\delta^{13}C$ on storage time for groundwater samples containing perchloroethene (PCE) with concentrations between 1 and 3 mg/L, stored at 4 °C in the dark, without headspace. Each sample was measured in triplicates ( $n = 3$ ). Sampling was performed at <i>KORA-site Rosengarten-Ehestorf</i> (described in Chapter 2).....	58
<b>Table 5-1.</b> Site-specific geochemical parameters and resultant redox conditions; areas depicted in Figure 5-1b; the wells of each area are included in the statistical diagram Figure 5-3; data available in Table A5-3 in the Appendix. ....	80
<b>Table A5-1.</b> Precision and reproducibility of $\delta^{13}C$ values determined by purge-and-trap GC/IRMS (number of replicates $n = 55$ ). ....	90
<b>Table A5-2.</b> $\delta^{13}C$ values (‰) of samples that have been remeasured after different storage times. ....	92
<b>Table A5-3.</b> Data of field measurements, concentration and compound-specific isotope analyses of samples discussed within Chapter 5. ....	93
<b>Table A5-3 (continued).</b> .....	94
<b>Table 6-1.</b> Concentration and isotope data for chlorinated ethenes in the downgradient series wells.....	101
<b>Table A6-1.</b> 1D hydraulic model properties; average velocity from particle tracking and porosity/conductivity from 3D model ( <i>I</i> ). ....	111
<b>Table A6-2.</b> Dispersivity factors required for varying source widths in 2D model in order to simulate observed PCE concentrations under aerobic, PCE-recalcitrant, conditions, assuming a transverse dispersivity, $\alpha_L=10\cdot\alpha_T$ ....	112

---

## List of Abbreviations

‰	per mill (permil)
$\alpha$	Fractionation factor
$\varepsilon$	Enrichment factor
Ace	Acenaphthene
Ant	Anthracene
ASE	Accelerated solvent extraction
Ay	Acenaphthylene
B	Biodegradation (in %)
BaA	Benzo(a)anthracene
BH	Bochinger Horizont (geological/hydrostratigraphic unit)
BTEX	Benzene, toluene, xylenes, ethylbenzene
<i>c</i>	<i>cis</i> -1,2-
C	Concentration
CH	Cyclohexane
CHC	Chlorinated hydrocarbon
CSIA	Compound-specific isotope analysis
Dbf	Dibenzofuran
DCE	Dichloroethene
DNAPL	Dense non-aqueous phase liquid
DRM	Dunkelrote Mergel (geological/hydrostratigraphic unit)
EA	Elemental analyzer
<i>f</i>	Fraction of contaminant remaining
Fl	Fluorene
Fla	Fluoranthene
GC	Gas chromatography
HPLC	High-performance liquid chromatography
IRMS	Isotope ratio mass spectrometry
$K_{ow}$	Octanol-water partitioning constant
KORA	Kontrollierter natürlicher Rückhalt und Abbau (project name)
LC	Liquid chromatography
LVI	Large-volume injection

MDL	Method detection limit
MeN	1-methylnaphthalene
MNA	Monitored natural attenuation
MTBE	Methyl <i>tert</i> -butyl ether
N	Naphthalene
NA	Natural attenuation
P <sub>PTFE</sub>	Water-Teflon partitioning constant
P&T	Purge-and-trap
PAH	Polycyclic aromatic hydrocarbon
PCE	Tetrachloroethene
PDMS	Polydimethylsiloxane
PEEK	Polyetheretherketone
Per	Perylene
PTFE	Polytetrafluoroethylene (Teflon)
PTV	Programmable temperature vaporizer
Pyr	Pyrene
SPME	Solid-phase microextraction
TCE	Trichloroethene
TCM	Trichloromethane (Chloroform)
<i>t</i>	<i>trans</i> -1,2-
UCM	Unresolved complex mixture
US EPA	United States Environmental Protection Agency
VC	Vinyl chloride
VOC	Volatile organic compound
VPDB	Vienna Peedee Belemnite



## Lebenslauf

Name	Michaela Blessing
Geburtsdatum	03. April 1977
Geburtsort	Schwäbisch Gmünd
1983 – 1987	Grundschule in Reichenbach u.R.
1987 – 1993	Geschwister-Scholl-Realschule in Süssen
1993 – 1996	Wirtschaftsgymnasium der Kaufmännischen Schule in Göppingen (Abitur 02. Juli 1996)
1997 – 2003	Studium der Geologie an der Eberhard-Karls-Universität Tübingen mit den Hauptfächern Geochemie und Angewandte Geologie
SS 1999	Praktikantin am Geologischen Landesamt, München
2002 – 2003	Diplomarbeit: "Veränderungen von mineralischen Deponieabdichtungen im Kontakt mit Modellsickerwässern unter Auflast" (Diplom 03. März 2003)
Seit Juli 2004	Promotionsstudium an der Eberhard-Karls-Universität Tübingen, Doktorandin am Zentrum für Angewandte Geowissenschaften
2004 – 2007	Stipendiatin der Deutschen Bundesstiftung Umwelt
Seit Juli 2007	Wissenschaftliche Mitarbeiterin am Zentrum für Angewandte Geowissenschaften, Tübingen